Lead Identification, Optimization and Characterization of Novel Cancer Treatment Strategies Using Repositioned Drugs

by

David Taylor

A Dissertation Presented in Partial Fulfillment
of the Requirements for the Degree
Doctor of Philosophy

Approved April 2013 by the
Graduate Supervisory Committee:

Kaushal Rege, Chair
Arul Jayaraman
David Nielsen
Vikram Kodibagkar
Lenore Dai

ARIZONA STATE UNIVERSITY

May 2013

ABSTRACT

Cancer is the second leading cause of death in the United States and novel methods of treating advanced malignancies are of high importance. Of these deaths, prostate cancer and breast cancer are the second most fatal carcinomas in men and women respectively, while pancreatic cancer is the fourth most fatal in both men and women. Developing new drugs for the treatment of cancer is both a slow and expensive process. It is estimated that it takes an average of 15 years and an expense of $800 million to bring a single new drug to the market. However, it is also estimated that nearly 40% of that cost could be avoided by finding alternative uses for drugs that have already been approved by the Food and Drug Administration (FDA).

The research presented in this document describes the testing, identification, and mechanistic evaluation of novel methods for treating many human carcinomas using drugs previously approved by the FDA. A tissue culture plate-based screening of FDA approved drugs will identify compounds that can be used in combination with the protein TRAIL to induce apoptosis selectively in cancer cells. Identified leads will next be optimized using high-throughput microfluidic devices to determine the most effective treatment conditions. Finally, a rigorous mechanistic analysis will be conducted to understand how the FDA-approved drug mitoxantrone, sensitizes cancer cells to TRAIL-mediated apoptosis.

ACKNOWLEDGMENTS

I would like to start by thanking my mentor Dr. Kaushal Rege, for all of the support and guidance he has given during my time at Arizona State University. I know that his advice has been an integral part of my success, and I am truly grateful.

I would also like to thank Dr. Arul Jayaraman and Dr. Jeongyun Kim for being wonderful hosts and mentors during my visit to Texas A&M University, and for their continued support as collaborators. A very special thanks must also be given to Dr. Lenore Dai, Dr. David Nielsen, and Dr. Vikram Kodibagkar for their willingness to work on my committee. I'd like to acknowledge the individuals who trained me on the various equipment and procedures necessary for the collection of my data and the continued success of my experiments. These individuals include Dr. Page Baluch, Dr. Honor Glenn, Dr. Laura Gonzales, and Seron Eaton also from the ASU Biodesign Institute. This also includes the members of both Dr. Sierks' and the Dr. Nielsen's research groups. I'd like to express my gratitude to Christine Parsons and Celia Barker who both helped me run experiments and to perform the necessary data analysis. Thank you Fred Pena for keeping everything running. I extend my deepest thanks and gratitude to Dr. Sutapa Barua, Dr. Huang-Chiao Huang, and Dr. Rebecca Bullard Linton for helping me get started in the laboratory and for always being there when I needed help with an experiment, procedure, or finding something in the lab. I would also like to thank the rest of my colleagues, James Ramos, Sai Pavan, Matthew Christensen, Karthik Subramaniam, Jennifer Lehrman, Beatrice Tamakloe, Divya Nair, Caesario Sutiyoso, Dr. Thrimoorthy Potta, Dr. Jacob Elmer, Dr. Bhavani Miryala, and all of our undergraduate researchers. I

want to also thank all of the past members of the Rege lab who I had the pleasure of working with. No research is possible without funding and so I must thank the National Institute of Health, the National Cancer Institute, the Arizona State University Dean's Fellowship, and the Phoenix Chapter of the ARCS Foundation.

An important thanks to all of my friends and family who have given their support and love to me through the years; I can only hope to repay a fraction of your affections. Teamwork equals dreamwork.

Thank you Laura Swantek for everything you have done for me! I'd go into a detailed list of ways you've helped me but the list would probably be longer than my dissertation. I'd truly be lost without you.

My final and biggest thanks goes to my mother for reasons too numerous and too complex to put into words.

TABLE OF CONTENTS

Page

LIST OF TABLES vi

LIST OF FIGURES vii

CHAPTER

1 INTRODUCTION 1

Apoptosis 5

Combination Treatments 8

Mitochondrial Depolarization 11

Reactive Oxygen Species 13

Microfluidic Devices 13

2 PARALLEL SCREENING OF FDA-APPROVED ANTINEOPLASTIC DRUGS FOR IDENTIFYING SENSITIZERS OF TRAIL-INDUCED APOPTOSIS IN CANCER CELLS 16

Introduction 16

Methods 19

Results and Discussion 25

Conclusions 57

3 DESIGN AND TESTING OF A PROGRAMMABLE HIGH-THROUGHPUT MICROFLUIDIC CELL ARRAY FOR COMBINATORIAL DRUG SCREENING 58

Introduction 58

CHAPTER Page

Methods 60

Results and Discussion 69

Conclusions 85

4 MECHANISTIC INVESTIGATION OF THE TRAIL-SENSITIZATION ACTIVITY OF MITOXANTRONE 86

Introduction 86

Methods 89

Results and Discussion 95

Conclusions 136

5 FUTURE DIRECTIONS 137

Introduction 137

Future Directions 1 138

Future Directions 2 146

REFERENCES 154

APPENDIX

A Identification of Mitochondria Damaging Agents Using a Parallel Screen of Antineoplastic Drugs 173

B Additional Combination Treatment Experiments in Alternate Cell Lines And Using Alternate Drugs 187

BIOGRAPHICAL SKETCH 202

LIST OF TABLES

Table Page

2.1 Summary of drugs identified as TRAIL sensitizing agents and their previously known activity 31

3.1 Summary of LC_{50} value analysis for microfluidic based treatments 79

3.2 Summary of LC_{50} value analysis for microfluidic device based and 96-well plate based treatments 83

4.1 Summary of Western blot densitometry analysis 134

LIST OF FIGURES

Figure Page

1.1 Intrinsic and extrinsic signaling pathways of apoptosis 4

2.1 Dose response for TRAIL as a single agent treatment in the PC3-TR cell line 25

2.2 Flow chart outlining the screening process of the 55 drugs tested 26

2.3 Single-agent drug toxicity pre-screen (20 μM) with PC3-TR cell line..... 27

2.4 Parallel screening of drugs from the Johns Hopkins Chemical Compound Library as TRAIL sensitizers..... 28

2.5 PC3-TR cells were first incubated with drug treatments (20 μM) for 24 hours after which time the media was removed, refreshed and cells were treated with TRAIL (10 ng/mL) for an additional 24 hrs 29

2.6 Dose response for doxorubicin in malignant cell lines 33

2.7 Dose response for mithramycin (plicamycin) in malignant cell lines..... 35

2.8 Dose response for mitoxantrone in malignant cell lines 37

2.9 Dose response for gemcitabine in malignant cell lines 39

2.10 Dose response for thioTEPA in malignant cell lines 40

2.11 Evaluation of secondary analysis in PC3-TR cells 42

2.12 Evaluation of mitoxantrone and mithramycin in additional malignant lines (pancreatic)..... 43

Figure Page

2.13 Evaluation of mitoxantrone and mithramycin in additional malignant lines (breast) 45
2.14 Evaluation of mitoxantrone in 22Rv1 prostate cancer cells 47
2.15 Evaluation of treatments in non-malignant cell line 49
2.16 Dose response of TRAIL with single mitoxantrone and mithramycin concentrations in PC3-TR cells 51
2.17 Comparison between different treatment methodologies in PC3-TR cells..... 52
2.18 Microscopy images of mitoxantrone treated PC3-TR cells 55
2.19 Microscopy images of mithramycin treated PC3-TR cells 56
3.1 Microfluidic control and gradient generation 64
3.2 Representative images of the microfluidic device and its operation visualized using colored dyes 71
3.3 Representative fluorescent images of Calcein AM stained PC3 cells following sequential treatments 75
3.4 Sequential combination treatments with the microfluidic platform 76
3.5 combination treatments with the microfluidic platform 78
3.6 Comparison between microfludic based results and 96-well plate based results for doxorubicin 81
3.7 Comparison between microfludic based results and 96-well plate based results for mitoxantrone 82

Figure Page

4.1 Kinetic dose response for mitoxantrone in PC3-TR human prostate cancer cells....96

4.2 Kinetic dose response for mitoxantrone in PC3 human prostate cancer cells....98

4.3 Microscopy images of single-agent and combination treatments in PC3-TR cells....100

4.4 Response of PC3-TR cells following treatment with Antimycin A....103

4.5 Response of prostate cancer following treatment with increasing concentrations of mitoxantrone....104

4.6 Response of pancreatic cancer following treatment with increasing concentrations of mitoxantrone....105

4.7 Response of breast cancer following treatment with increasing concentrations of mitoxantrone....107

4.8 Microscopy images of PC3-TR cells for depolarization studies....109

4.9 Reactive oxygen species generation in mitoxantrone treated, PC3-TR prostate cancer cells....111

4.10 Reactive oxygen species generation in mitoxantrone treated, MIAPaCa-2 pancreatic cancer cells....112

4.11 Reactive oxygen species generation in mitoxantrone treated, BXPC-3 pancreatic cancer cells....113

Figure Page

4.12 Reactive oxygen species generation in mitoxantrone treated, MDA-MB-231 breast cancer cells 115

4.13 Kinetic comparison between mitochondrial depolarization and ROS generation 117

4.14 The effect of N-acetylcysteine (NAC) on reactive oxygen species generation in PC3-TR prostate cancer cells 118

4.15 Mitoxantrone dose response (2 h; 0-100 μM) with N-acetylcysteine co-treatments in PC3-TR prostate cancer cells 120

4.16 24 hour mitoxantrone dose response with N-acetylcysteine co-treatments in PC3-TR prostate cancer 121

4.17 Response of PC3 and PC3-TR prostate cancer cells following treatments with increasing concentrations of pixantrone 123

4.18 Reactive oxygen species generation in pixantrone treated, PC3-TR prostate cancer cells 125

4.19 Reactive oxygen species generation in mitoxantrone treated, PC3 human prostate cancer cells 126

4.20 Kinetic dose response for pixantrone in PC3 human prostate cancer cells..... 128

4.21 Western blot analysis following combination experiments with mitoxantrone.. 133

5.1 Microfluidic based, co-culture experiments 150

Figure Page

A.1 50 µM screening of the John Hopkins Clinical Compound Library for mitochondrial depolarization activity 180

A.2 Mitochondrial depolarization studies of mitoxantrone-loaded PEG-PE micelles in PC3-TR prostate cancer 184

B.1 Kinetic dose response for mitoxantrone in MB49 murine bladder cancer cells..... 193

B.2 Kinetic dose response for mithramycin in MB49 murine bladder cancer cells 195

B.3 Dose response for dichloroacetic acid (DCA) in PC3-TR human prostate cancer cells 197

B.4 Dose response for abiraterone in PC3 human prostate cancer cells..... 198

B.5 Dose response for cabazitaxel in PC3 and 22Rv1 human prostate cancer cells 199

CHAPTER 1

INTRODUCTION

In 2012, it is estimated that over 570,000 men and women died of cancer related illnesses in the United States making cancer the second most lethal affliction in the country. Of this total, 28,000 deaths in men were the results of prostate cancer, 39,500 deaths in women were the result of breast cancer, and 37,000 deaths were the result of pancreatic cancer [1]. Patient survival can be greatly improved through the early detection and treatment of these malignances but there still exist many limitations to the treatment of cancer. Difficulties with early diagnosis, tumor metastasis, resistance to chemotherapeutic treatments, and limited specificity of chemotherapeutic treatments are all prevalent and can reduce the efficacy of clinical treatments. Developing novel treatment methodologies that can overcome the limitations of current treatments and aid in the treatment of advanced malignancies are of high importance.

Developing new drugs is both a slow and expensive process. A 2003 analysis of 68 FDA approved drugs found that it takes an average of 15 years and an estimated expense of $800 million to bring a single new drug to market [2]. The FDA approval process is also very stringent and a study done in 2010 showed that over a 10 year period (1999-2008) the number of drugs approved for use by the FDA decreased while the research and development costs doubled [3]. Recently there has been a push to find new uses for drugs that have already been approved for use by the FDA. Researchers from the School

of Medicine at John Hopkins University released a short article summarizing the need to find new uses for old drugs arguing that the current standard for drug discovery is too costly and time consuming to effectively combat disease. They suggest that by finding alternative uses for FDA approved drugs, nearly 40% of the total drug development costs can be reduced. These drugs will also see an accelerated approval process for their alternative uses since they can progress directly to phase II clinical trials since their pharmacological properties have already been determined [4].

The idea of finding alternative uses for existing drugs is not new, and there are several examples of researchers who have identified alternative uses for drugs designed for the treatment of different aliments. The drug ceftriaxone is an antibiotic that can stabilize β-lactam enzymes which can inhibit the synthesis of bacterial cell walls but researchers discovered the drugs could also be used for the treatment of Amyotrophic Lateral Sclerosis (ALS) due to the drug's ability to increase the expression of glutamate transporters [5]. Similarly, the antibiotic minocycline, which inhibits aminoacyl tRNA, was also found to inhibit the release of cytochrome C from the mitochondria which also was important for the treatment of ALS [6]. Dapsone, a drug used to treat leprosy, and fosmidomycin, a drug used to treat urinary tract infections, were both identified as having antimalarial activities when used in combination therapies with other drugs (dapsone/chloroproguanil and fosmidomycin/clindamycin) [7-9]; one of our research strategies involves the use of combination treatments and these studies show how this can be a powerful treatment methodology. Another example that is directly relevant to our line of studies was the identification of the antiamebic, fumagillin as a therapeutic for

brain, breast, cervical, and prostate cancer [10, 11]. Finally, the drug eflornithine was initially developed for the treatment of cancer but failed clinical trials; the drug was later used in the treatment of African trypanosomiasis (African Sleeping Sickness) [12]. These represent only a few of the cases in which new uses have been identified for pre-existing drugs but they demonstrate the power of using this methodology for the treatment of many ailments. These cases also demonstrate the flexibility of the treatment options be it as a single agent treatment, a combination treatment, or as a treatment with a drug that was initially failed clinical trials.

In the studies presented in this document, we will be exploring the use of FDA-approved drugs for the treatment of various cancer types and trying to identify novel treatment methodologies and drug effects that can be exploited to improve these treatments. By looking specifically at FDA approved drugs we hope to limit the amount of time and money spent needed to bring potentially helpful treatments to the public. To this end we are studying two specific treatment options: (1) Identifying FDA-Approved drugs that can be used in combination with the protein TRAIL to induce apoptosis selectively in cancer cells and working to optimize the effect of the combination treatments using high-throughput microfluidic devices. (2) Identifying FDA-Approved drugs that show the ability to induce direct damage to the mitochondria and the subsequent testing of these drugs in delivery vehicles designed to improve the effects of the drugs while limiting damage to healthy tissue.

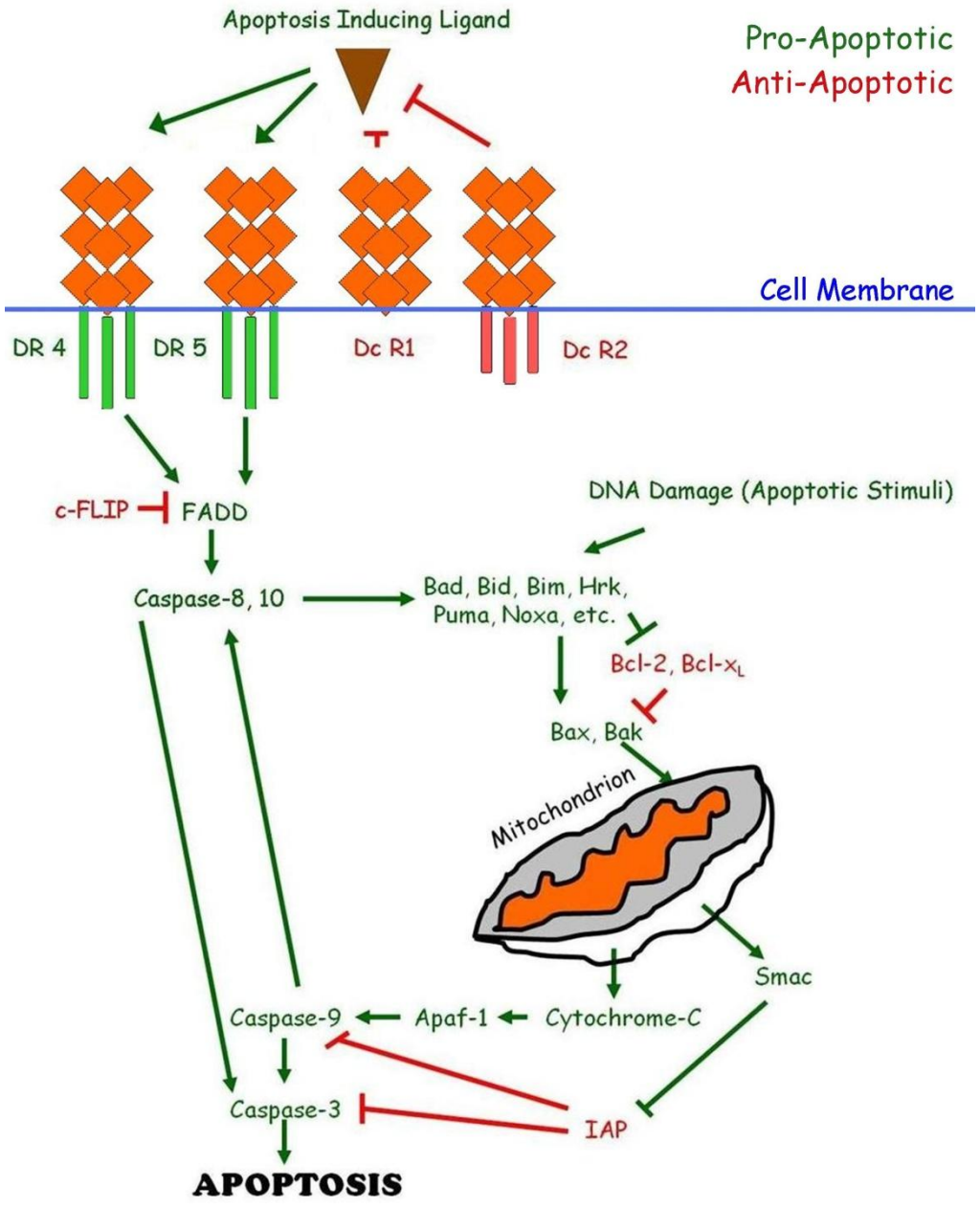


Figure 1.1 Intrinsic and extrinsic signaling pathways of apoptosis. Proteins that contribute to the execution of apoptosis are shown in green while proteins that inhibit the process are shown in red. The mitochondrion is a key regulator of apoptosis and is also shown.

APOPTOSIS

One method of minimizing the harmful drug effects of is identify treatment mechanisms that induce apoptosis instead of necrosis [13]. Apoptosis is a cellular suicide mechanism that is used to eliminate cells that have sustained severe damage or are no longer needed. In healthy cells this process is closely regulated and an equilibrium is maintained between pro-apoptotic proteins and anti-apoptotic proteins. If there is an apoptotic stimulation, the cell will shift the equilibrium to induce apoptosis resulting in the death of the cell [14]. Stimuli that can begin the apoptotic cascade can include developmental cues, the activation of proapoptotic receptors, loss of growth factor signals, heat shock, irradiation, and cytotoxic drugs [15, 16]. However, in many cases breakdowns in the apoptotic process can occur leading to poor regulation of the process. The result of which can be a pro-apoptotic environment where cells undergo apoptosis when they should not, as is the case in many degenerative diseases [17, 18]. The result can also be an anti-apoptotic environment in which damaged/unhealthy cells grow continuously, as is the case in many types of cancer (the relevant case for these studies) [14] [19]. When looking at cells that are exhibiting unchecked cell growth (i.e. cancer), it is important to understand that the breakdown in the apoptotic mechanism can be beneficial for treatment since the damaged cells will not be able to regulate perturbations to the mechanism as well as healthy cells. Essentially, cancer cells acquire an inherent resistance to apoptosis but are continually being pushed to initiate the process because the cells are malfunctioning. By stimulating the apoptotic process it is possible to aid the malignant cells in their attempts to induce apoptosis. Conversely, healthy cells are not trying to initiate apoptosis and so the stimulation of the process in these cells will be

balanced by the anti-apoptotic activity of the cell. This leads to a degree of selectivity when using treatments that attempt to invoke the apoptotic mechanism [20-22].

The feature that distinguishes apoptosis from other types of programmed cell death (e.g. autophagy, paraptosis) is that the mechanism is primarily controlled through the activation of **c**ystein-**asp**artic acid prote**ases** (caspases) that execute the cells [23]. The pathways that are used to activate these caspases form the mechanism of apoptosis (**Figure 1.1**). The induction of apoptosis occurs either through the intrinsic activation of the caspases, or the extrinsic activation of the caspases [15]. The intrinsic pathway is triggered intercellularly by the loss of growth factors or by severe damage to the cell [24]. The intrinsic pathway is mainly controlled through interactions between the members of the Bcl-2 protein family which includes both pro-survival and pro-apoptotic members. In this pathway pro-apoptotic Bcl-2 members like Bax and Bak, permeate the outer membrane of the mitochondria [25, 26]. This causes the release of the soluble proteins cytochrome c and Smac/DIABLO into the cytoplasm. Cytochrome c stimulates the formation of a complex known as an apoptosome, and eventually causes activation of caspase 9. Caspase 9 then cleaves the effector caspases 3, 6, and 7 which send the final signals to induce apoptosis [23]. Smac/DIABLO works to inhibit the pro-survival protein IAP by binding with IAP and reducing its activity [27]. An integral part of regulation in the intrinsic pathway is the expression of tumor suppressing protein p53. Normally, p53 responds to cellular stress by arresting the cell division cycle. In the case of severe cell damage, p53 promotes apoptosis by the expression of genes such as Puma and Noxa that

inhibit pro-survival Bcl-2 members. Additionally, p53 also plays a role in the extrinsic apoptotic pathway by expressing surface death receptors [28].

In the extrinsic pathway, apoptosis occurs through the activation of proapoptotic receptors on the cellular surface by apoptosis inducing ligands. When these receptors are activated, they recruit the adaptor protein Fas-associated death domain (FADD). FADD provides a link between the death receptor and procaspases 8 and 10, which bind to form the death-inducing signaling complex (DISC) [29]. During the formation of the DISC apoptosis can be regulated by the protein c-FLIP. c-FLIP is structurally similar to procaspases 8 and 10 so it can bind to FADD to prevent DISC formation and it can also remove FADD binding sites to caspase 8 [30]. Intercellular signaling can continue in two different ways based on the levels of DISC produced and on the activity, after stimulation, of caspase 8. In type 1 cells high levels of DISC are produced and the stimulation of caspase 8 is large enough to activate the effector caspases 3, 6, and 7 and induce apoptosis. In type 2 cells lower levels of DISC are produced which are insufficient for caspase 8 to activate the effector caspases and instead the signal is amplified by cleavage of the protein Bid. Bid initiates the intrinsic pathway to help activate the effector caspases [31].

In these studies, our research was centered around two different treatment methodologies, both of which employ apoptosis as a means of inducing cell death in cancer cells while limiting death in healthy tissue. The first treatment methodology focuses on combination type therapies using a drug that is known to induce apoptosis selectively in malignant

cells. The second methodology focuses on the induction of apoptosis by applying treatments that directly cause damage to the mitochondria. The following sections will describe these methodologies more fully.

COMBINATION TREATMENTS

Tumor Necrosis Factor-α Related Apoptosis Inducing Ligand (TRAIL) is a member of the Tumor Necrosis Factor (TNF) super-family of cytokines which induces apoptosis upon specific binding to death receptors (DR) 4 and 5 expressed on the outer cellular membrane. TRAIL and agonistic antibodies to DR4 and DR5 are attractive treatment options due to their ability to induce apoptosis selectively in malignant cells while demonstrating minimal cytotoxicity in non-malignant cells [32-36]. Trimeric, soluble TRAIL variants are well tolerated in mice and chimpanzees [37] and show little toxicity towards primary human hepatocytes and endothelial cells in culture [38, 39]. TRAIL has demonstrated significant anti-tumor activity in xenograft models [40-42] and certain TRAIL formulations (non-histidine tagged) are considered safe for in vivo applications [43].

Despite the promise of TRAIL, many tumor cells are naturally resistant or can developed resistance to TRAIL-induced apoptosis [44]. Common resistance developed in PDAC cells include over-expression of anti-apoptotic proteins like XIAP [45, 46], survivin [47], c-Flip [48, 49] and Bcl-2 [50], and down-regulation of pro-apoptotic proteins (e.g. Bid

[51]). The inhibition/down regulation of anti-apoptotic proteins and the promotion of pro-apoptotic proteins can sensitize resistant cells to TRAIL [52-55].

In our research we try to identify drugs that form a synergistic relationship with TRAIL and cause the cancer cells to undergo apoptosis. The idea is that cancer cells are already primed to die but due to defects in the apoptotic pathway they continue to grow and divide. The resistance to TRAIL that many cells have/develop can be overcome using small molecule drugs that are able to suppress and negate the resistances. Since cancer cells are already primed to die, the natural response for regulating apoptosis would be in favor of cell death as opposed to in healthy cells where the response would be for cell survival. The result would be that the combination drug/TRAIL treatment would be more effective in cancer cells then in normal cells leading to fewer side effects of treatment. This is in addition to the selectivity that TRAIL shows toward cancer cells. The hope is that the synergistic effect of the sensitizer drug/TRAIL will allow for low concentration treatments of the drug to be administered (which may not be cancer cell selective) further reducing damage to non-malignant cells. Once drugs that sensitize cancer cells to TRAIL-mediated apoptosis are identified the goal is to determine the concentrations of drug and TRAIL that result in the largest loss of cell viability while maintaining the synergistic effect of the combination treatments and limiting non-specific damage.

Identifying drugs that show a synergistic relationship with TRAIL has been a research pathway that other researchers have previously explored. TRAIL sensitizing activity has been identified for a range of different drugs including daunorubicin [56], doxorubicin

[57], epirubicin [58], cisplatin [59], oxaliplatin [60], camptothesin and its derivative CPT-11 [61], docetaxel [62], paclitaxel [63], iriontecan [64] and gemcitabine [65] all of which are drugs developed specifically for the treatment of cancer. Additionally, compounds like curcumin [66], genistein [67], verticillin A [68], thapsigargin [69], and lanatoside C [70] represent natural products and non-cancer specific drugs that have also been shown to enhance TRAIL sensitization activity. These previous studies are important because they provide a starting point for our research and they also allow for comparisons to be made between our data and previously published work. Additionally, some of these combination therapies with TRAIL (trade name Dulanermin) have proceeded to clinical trials. Phase II trials with TRAIL and rituximab for the treatment of Non-Hodgkin's Lymphoma have been shown to be well tolerated but indicate that combination treatments did not improve the objective response compared to the single agent treatments [71]. Ongoing phase II studies for TRAIL combination treatments with carboplatin, paclitaxel and bevacizumab for the treatment of non-small cell lung cancer have also shown the treatments to be well tolerated [72], while phase I studies for combination treatments of TRAIL with bevacizumab, cetuximab, FOLRIRI, FOLFOX, and irinotecan for the treatment of colorectal cancer have also been well tolerated with no adverse interactions between the treatments [73, 74].

It is clear that the field for identifying TRAIL-sensitizing compound is very active but our work is novel in that it specifically aims to identify compounds that are already approved by the FDA. Although many of the drugs identified as TRAIL-sensitizers are

FDA approved, there has not been a comprehensive screen of FDA approved drugs for their sensitization activity.

MITOCHONDRIAL DEPOLARIZATION

Mitochondria represent a key component in both the intrinsic and extrinsic apoptotic pathways. The an alternative treatment methodology investigated in this research is identifying FDA approved drugs that cause direct damage to the mitochondria. The intrinsic and extrinsic apoptotic pathways both are very well regulated process which maintain a steady balance between pro- and anti-apoptotic mechanisms. However, at the heart of apoptosis are mitochondria which, aside from the Type 1 activation of the extrinsic pathway, are integral to the execution of apoptosis. One of the final steps in the apoptotic process is the permeabilization of the mitochondrial membrane by Bax and Bak and the subsequent release of pro-apoptotic proteins (cytochrome c, SMAC/DIABLO) into the cytoplasm. The mitochondrial permeability transition represents a "point of no return" in the apoptosis signaling cascade [75]. Traditional chemotherapeutics induce genomic DNA damage, which triggers apoptosis signaling in cancer cells from the starting point of the process. While these DNA-damaging treatments can be successful [76], several studies indicate that the overexpression of anti-apoptotic proteins can overcoming the pro-apoptotic signals triggered by these treatments. This leads to an increased survival of cancer cells which can later manifest itself as additional resistance to the treatments [44, 77-79]. It is therefore an attractive therapeutic strategy to induce mitochondrial damage directly in order to facilitate the permeabilization of the

mitochondrial membrane and bypass any pro-survival mechanisms that act upstream of the mitochondria (e.g. Bcl-2 overexpression, p53 inhibition) [80, 81].

Our strategy for attacking the mitochondria involves identifying drugs that can cause a reduction in the mitochondria membrane potential (mitochondrial depolarization). Mitochondria are considered to be the "power generators" of cells; they produce most of the cell's adenosine triphosphate (ATP) via the process of oxidative phosphorylation. During this process a high concentration of protons are pumped into the space between the inner and outer mitochondrial membranes (intermembrane space). Since the concentration of protons is much higher in the intermembrane space as compared to the mitochondrial matrix, a highly negative electrical gradient (-160 mV) is generated across the inner mitochondrial membrane [82]. The electrical potential stored in this gradient is what drives the production of ATP. By finding agents that attack the mitochondria and cause a reduction in the mitochondrial membrane potential we will be severely limiting mitochondrial function which will have an effect on ATP synthesis, ROS generation, pH, as well as other factors [83]. In addition, the loss in membrane potential will cause the mitochondria to swell which can result in both the inner and outer mitochondrial membranes becoming permeable. This in turn leads to the release of pro-apoptotic proteins like cytochrome c into the cytoplasm thereby beginning the apoptotic cascade [84].

By focusing our efforts to induce direct damage to the mitochondria we will be limiting the effect of any inherent apoptotic resistances the cell may have. This damage can

facilitate the induction of apoptosis as well as cause severe damage to the mitochondria and limit its function.

REACTIVE OXYGEN SPECIES

The loss of mitochondrial membrane potential and the generation of reactive oxygen species (ROS) are closely related. During the production of ATP, the mitochondria also generate ROS which, when functioning normally, can be regulated. However, when mitochondria undergo some type of damage (e.g. mitochondrial depolarization) the generation of ROS increases and the capacity of the mitochondria to regulate the ROS decreases. On the other hand, an increase in ROS will cause oxidative stress which will cause damage to the mitochondria. In essence a feed-forward loop is created between oxidative stress and mitochondrial damage [85] and if there is a decrease in the MMP then there is likely an increase in ROS generation.

MICROFLUIDIC DEVICES

Another major component of this research is the design and testing of microfluidic platforms for the optimization of drug treatments. When studying the effect of chemotherapeutic compounds it is important to identify the concentrations of the drug that maximize the chemotherapeutic effect while limiting the amount of drug needed to achieve the effect. This can limit the non-specific effects of the drug and can also reduce the cost associated with the treatment (less material used). In combination therapies, determining the optimum concentration is also of high importance. In order to optimize

treatment effects it is useful to develop systems in which a range of drug concentrations can be developed and tested rapidly. To achieve this goal, microfludic platforms that use a diffusion based mixing structure (dilution modules) to generate concentration gradients are used [86]. These platforms also provide the added benefit of using less material (i.e. the smaller volumes require less drug to be used for a given treatment concentration).

Dilution modules of microfluidic devices operate by taking advantage of the changes in fluid dynamics at the micro-scale to produce a diffusive mixing unit that can be produce nearly linear concentration gradients [87]. The effects of laminar flow, diffusion, and the surface area to volume ratio, become much more important at the micro-scale. Consider the Reynolds number equation:

$$Re = \frac{l_0 v_0 \rho}{\mu} \quad (1.1)$$

If there is a change in scale, the characteristic length (l_0) and the characteristic velocity (v_0) are the variables will dominate since density (ρ) and viscosity (μ) are both properties of the fluid [88]. In the case of microfluidic devices the characteristic length is very small and so the Reynolds number is usually small and the effects of turbulent mixing can be negated. The majority of mixing in microfluidic devices occurs due to diffusion. The amount of time needed for a particle to travel over a distance is proportional to the square of that distance [89]. As a result, this effect becomes significant over very small distances. In microfluidics it is often convenient to use the dimensionless Peclet number to relate the rate of advection of flow to the rate of diffusion via the equation:

$$P\grave{e} = \frac{l_0 v_0}{D} \quad (1.2)$$

where D is the mass diffusion coefficient [88]. The numerator gives the advection term while the denominator gives the diffusion term. In devices with a high Peclet number mixing occurs slowly because the process is controlled by advection. A low Peclet number means mixing will occur faster since the process is dominated by diffusion. Since the streams developed in microfluidics are usually laminar, control of flow velocity and channel geometry can be used to control diffusion and mixing. The gradient generating dilution modules uses a channel geometry that encourages diffusive mixing by keeping a low l_0 and v_0. Keep in mind that in this case the characteristic length is the width of the channel and not the overall length which should indeed be larger to provide more time for diffusion to occur.

The following work will describe the development of a microfluidic screening system that is capable of generating gradients using the diffusive mixing system described above as well as perpendicular to the flow of the device. Using these paired concentrations, the effects of combination treatments can be studied with this system.

CHAPTER 2

PARALLEL SCREENING OF FDA-APPROVED ANTINEOPLASTIC DRUGS FOR IDENTIFYING SENSITIZERS OF TRAIL-INDUCED APOPTOSIS IN CANCER CELLS

INTRODUCTION

Tumor Necrosis Factor-α Related Apoptosis Inducing Ligand (TRAIL) is a member of the Tumor Necrosis Factor (TNF) super-family of cytokines that engages the cellular apoptotic mechanism upon specific binding to death receptors (DRs) 4 and 5 on the cell surface [44]. TRAIL has attracted significant attention in recent years due to its ability to selectively induce apoptosis in transformed (malignant) cells while demonstrating little cytotoxicity in normal cells [32, 34-36, 38, 90]. TRAIL binds cell-surface death receptors (DR4 and DR5) as a homotrimer and triggers the formation of the Death-Inducing Signaling Complex (DISC); the Fas-Associated Death Domain (FADD) and caspases 8 or 10 are recruited to the DISC from the cytoplasm. The proteolytic activation of initiator caspases leads to the subsequent activation of executioner caspases (e.g. caspase-3), which ultimately results in apoptosis in Type I Cells. Activation of caspase-8 engages the mitochondria-amplified apoptosis machinery in Type II cells [38]. The binding of TRAIL to decoy receptors (DcR) 1 and 2 has also been demonstrated; it is hypothesized that these receptors play a role in maintaining the homeostasis of TRAIL activity in vivo [20, 35].

Recombinant TRAIL induces apoptosis in a variety of human cancer cell lines including those of breast, colon, lung, prostate, liver, leukemia, lymphoma, and neuroblastoma [20, 32, 34, 91]. TRAIL has also demonstrated potent anti-tumor activity in a number of xenograft models including those of colon and breast carcinomas [40-42]. Soluble TRAIL variants are well tolerated in mice and chimpanzees [37] and demonstrate minimal cytotoxicity towards primary human hepatocytes and endothelial cells in culture [38, 39]. As a consequence of the selectivity towards malignant cells, certain TRAIL formulations (e.g. non-histidine tagged TRAIL) are considered safe for potential therapeutic applications [43].

Although TRAIL and agonistic antibodies to death receptors 4 and 5 are promising candidates for cancer therapy, many tumor cells are inherently resistant or acquire resistance to TRAIL-mediated apoptosis. Commonly implicated resistance mechanisms include dysfunction of the Fas-Associated Death Domain (FADD) / improper assembly of the Death-Inducing Signaling Complex (DISC) [48], loss of caspase-8 activity [92-94], constitutively active Akt/protein kinase B [95], and over-expression of anti-apoptotic proteins such as c-Flip [48, 49] and Bcl-2 [50]. As a result, therapeutic strategies involving DNA-damaging radiotherapy [96, 97], genotoxins [76] [98], and peptides [99] have been investigated for enhancing cancer cell sensitivity to TRAIL [76] and / or agonistic antibodies against DR4/DR5 [100].

This chapter describes the parallel screening of fifty-five FDA-approved and foreign-approved chemotherapeutic drugs used to identify existing anti-cancer drugs that might act as TRAIL sensitizers in resistant prostate, pancreatic, and breast cancer cells. Drugs were first pre-screened individually (single agent treatment) for toxicity at a concentration of 20 μM using TRAIL-resistant PC3-TR prostate cancer cells; candidates that resulted in greater than 70% reduction in cancer cell viability were screened for TRAIL sensitization activity at a lower concentration of 10 μM. A total of fourteen potential TRAIL sensitizer leads, including six whose TRAIL sensitization activities were previously unknown, were identified from the screen. Five leads were further characterized in prostate, pancreatic, and breast cancer cells.

METHODS

Cell Culture Techniques

Three human prostate cancer cell lines (PC3, PC3-TR, and 22RV1), three human pancreatic cancer lines (Panc-1, MIAPaCa2, and BXPC-3), two human breast cancer lines (MDA-MB-231, and MDA-MB-453) and one immortalized human pancreatic epithelial cell line (HPDE6) were used in the current study. PC3-TR (TR: TRAIL resistant) [101] cells were a generous gift from Dr. Aria Olumi at the Massachusetts General Hospital in Boston, MA. Cells were grown in 75 cm^2 Corning cell culture flasks with RPMI 1640 tissue culture media supplemented with 10% Fetal Bovine Serum and 1% penicillin / streptomycin (10000 units/mL penicillin G and 10000 μg/mL streptomycin) at 37°C with 5% CO_2.

Reagent/Drug Preparation

The Johns Hopkins Chemical Compound Library (JHCCL) [102] was purchased from The Johns Hopkins University School of Medicine. The library contains a total of 1514 FDA- and foreign-approved drugs. The anti-neoplastic plate (plate #1) consists of 55 FDA-approved approved anti-cancer drugs and was employed in the screen for identifying TRAIL sensitizers. All stock solutions of the drugs from the library were supplied at a concentration of 10 mM in either DMSO or water. For expanded dose-response experiments, additional doxorubicin and mitoxantrone were purchased from Sigma while gemcitabine, mithramycin, and thioTEPA were obtained through the NCI/NIH Developmental Therapeutic Program. TRAIL was purchased from R&D

Systems and reconstituted in PBS at a 10 µg/mL stock concentration in 50 µL aliquots to prevent multiple freeze/thaw cycles. All solutions were prepared to ensure that the final solvent (DMSO or water) concentration in cell treatments would be less than 1% (v/v) to limit non-specific activity.

Single Agent and Combination Treatments

Cells were plated in 96 well plates at a density of either 8,400 cells/well (prostate and pancreatic lines) or 20,000 cells/well (breast cancer lines) and incubated at 37°C and 5% CO_2 for approximately 24 hours. For single-agent treatments, cells were exposed to drug candidates at a concentration of 20 µM for 24 hours at which point, cell viability was determined using the MTT (3-(4,5-dimethylthiazolyl-2) -2,5-diphenyltetrazolium bromide) assay. Single-agent TRAIL treatments were carried out similarly; a dose range of 0-100 ng/mL of TRAIL was used. For sequential combination treatments, cells were first treated with a sensitizer drug candidate for 24 hours. The media was then removed, replaced with fresh serum-containing media, and the cells were treated with TRAIL. Cells were incubated for an additional 24 h after which, viability measurements were carried out using the MTT assay. In order to determine if dosing of the combination treatment had an effect on the efficacy, simultaneous combination treatments were carried out by treating cells with the sensitizer drug and TRAIL at the same time for 24 h at which point, cancer cell viability was determined using the MTT assay.

Determination of Cell Viability

Cell viability was assessed using the MTT cell proliferation assay (ATCC CA#30-1010k). Following addition of the MTT reagent (2 h at 37^{o}C), cells were treated with a lysis buffer from the kit and kept at room temperature in the dark for two hours in order to carry out complete lysis and to solubilize the MTT product. The absorbance of each well was measured using a Biotech Synergy 2 Multi-Detection Microplate Reader at 570 nm. Each experiment included a set of blank wells (media only), a live control (no treatment) and a dead control (200 µL of 10 µM H_2O_2 or 1.5 µL of 20 µM Quillaja were employed for inducing death in the cell population). Background absorbance was measured using the blank and subtracted from all absorbance measurements. In the case of drugs that potentially interfered with the assay, a separate set of media-only wells were treated with equivalent volumes of the drug, and the measured absorbance was subtracted as the background. This was carried out to eliminate any bias caused by the natural absorbance of the drug itself. Fractional cell viability was calculated as: (OD of sample – OD of dead control)/(OD of live control – OD of dead control) where OD is the optical density. Percentage cell viability was calculated by multiplying the fractional viability by 100. Data are plotted as percentage reduction in cell viability compared to control (untreated cells) in which, a 0% value on the graph means 100% viability and 100% value on the graph means 0% viability.

Statistical Analyses

Screening experiments were carried out in duplicate and expanded dose responses with identified leads were performed at least in triplicate. Data are presented as the mean ± one standard deviation. The standard deviation of each set was calculated based on the variation between experiments. ANOVA was performed using the t-test function in Microsoft Excel. Analysis of the single-agent treatment was performed in order to determine whether or not a drug had a significant effect when compared to the live (untreated) control. Efficacies of sensitization were determined by comparing the decrease in cell viability following combination treatments (i.e. drug in combination with TRAIL) to the reduction in cell viability as a consequence of the additive effect of single-agent treatments (drug alone + 10 ng/mL TRAIL alone).

Live/Dead Analysis

As an alternate assessment of cell viability, a calcein AM /ethidium homodimer-1 viability/cytotoxicity kit (Invitrogen L3224) was used to measure treatment efficacy for a select set of combination treatments. Briefly, a working solution of 2 μM calcien AM and 4 μM ethidium homodimer-1 (EthD-1) was prepared in a solution of sterile 1X PBS. The working solution was then added to each well of the cell culture plate and incubated at 37°C with 5% CO_2 for 30-45 minutes. Fluorescence imaging was then carried out using a Zeiss Observer D1 fluorescent microscope. A 38 HE filter set (Excitation: 470/40; Emission: 525/50) was used to image the fluorescence of the calcein AM (green fluorescence) while a 43 HE filter set (Excitation: 550/25; Emission: 605/70) was used to measure the fluorescence of the EthD-1 (red fluorescence).

Annexin V and Propidium Iodide Analysis

An annexin V / propidium iodide assay (Invitrogen L3224) was carried out to determine if combination treatments induced apoptosis in cells. Briefly, a working solution of 2% annexin V and 1 μg/mL propidium iodide (PI) was prepared in a solution of 1X annexin binding buffer. The working solution was added to each well of the cell culture plate and incubated at room temperature for 15-20 minutes. Fluorescence imaging was then performed using a Zeiss Observer D1 fluorescent microscope. A 38 HE filter set (Excitation: 470/40; Emission: 525/50) was used to measure the fluorescence of the annexin V (green fluorescence) while a 43 HE filter set (Excitation: 550/25; Emission: 605/70) was used to measure the fluorescence of the propidium iodide (red fluorescence).

Image Analysis

All image processing was performed using ImageJ [103] image processing software. For the live/dead analysis the threshold of the fluorescent image was adjusted so that any background noise was removed and that the boundary between individual cells was well defined. The image was then converted to a binary format. In some cases, it was difficult to differentiate between cell boundaries in which case the Watershed process was used to distinguish between individual cells while ensuring that any cells that were incorrectly divided were accounted for [104]. The "Analyze Particles" function was then used to obtain a final cell count. The live cell count was then normalized against the live control cell count to give an indication of the cell viability. The brightness of the images was adjusted so that the background had zero pixel intensity value in case of annexin

V/PI analyses. Next, false color was applied to the image; green was applied for the annexin V stains and red was applied to the PI stains.

RESULTS AND DISCUSSION

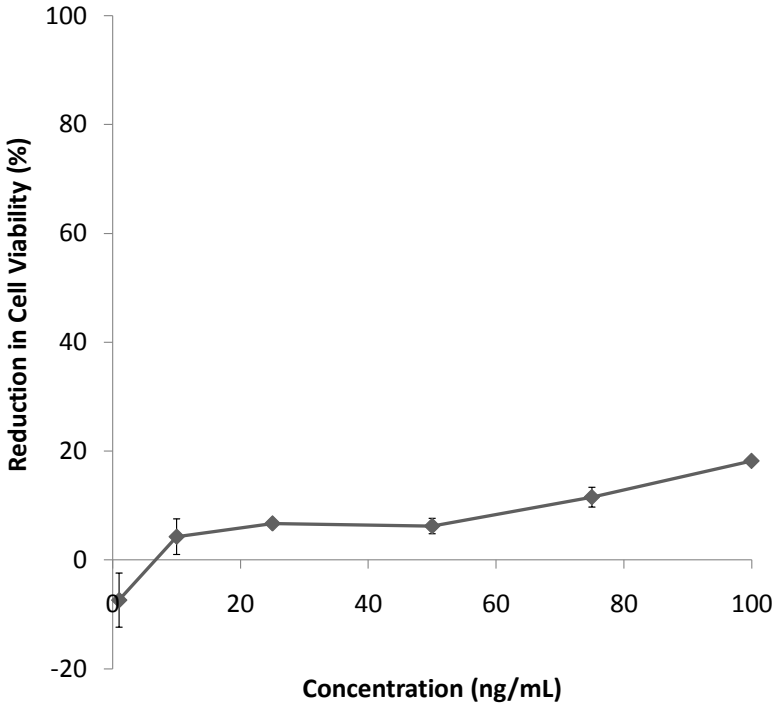


Figure 2.1 Dose response for TRAIL as a single agent treatment in the PC3-TR cell line. Cells were incubated with TRAIL for a 24-hour period followed by analysis with MTT. TRAIL at 10 ng/mL concentration causes a 4.3% (+/- 3.2%) increase in viability reduction compared to the live control.

In the current study, we screened a small library of fifty-five FDA- and foreign-approved antineoplastic drugs from the Johns Hopkins Clinical Compound Library (JHCCL) in order to identify chemotherapeutics that sensitize prostate, pancreatic and breast cancer cells to TRAIL-induced apoptosis. Identification of FDA-approved drugs as TRAIL sensitizers is an attractive discovery strategy since it is possible to rapidly translate these novel combinations to the clinic. PC3-TR (TR: TRAIL resistant) human prostate cancer cells were used in the primary screening, since it was hypothesized that lead candidates discovered for this resistant cell line might be relevant to clinical phenotypes that develop

resistance to TRAIL. The cell line demonstrated low susceptibility to single-agent TRAIL treatments; a 20% loss of viability reduction was observed in PC3-TR cells at concentrations as high as 100 ng/mL (**Figure 2.1**). We employed a TRAIL concentration of 10 ng/mL in subsequent combination treatment experiments in order to keep the TRAIL dose at a minimum; under these conditions, single-agent TRAIL induced a loss of viability in approximately 4% of the PC3-TR cell population.

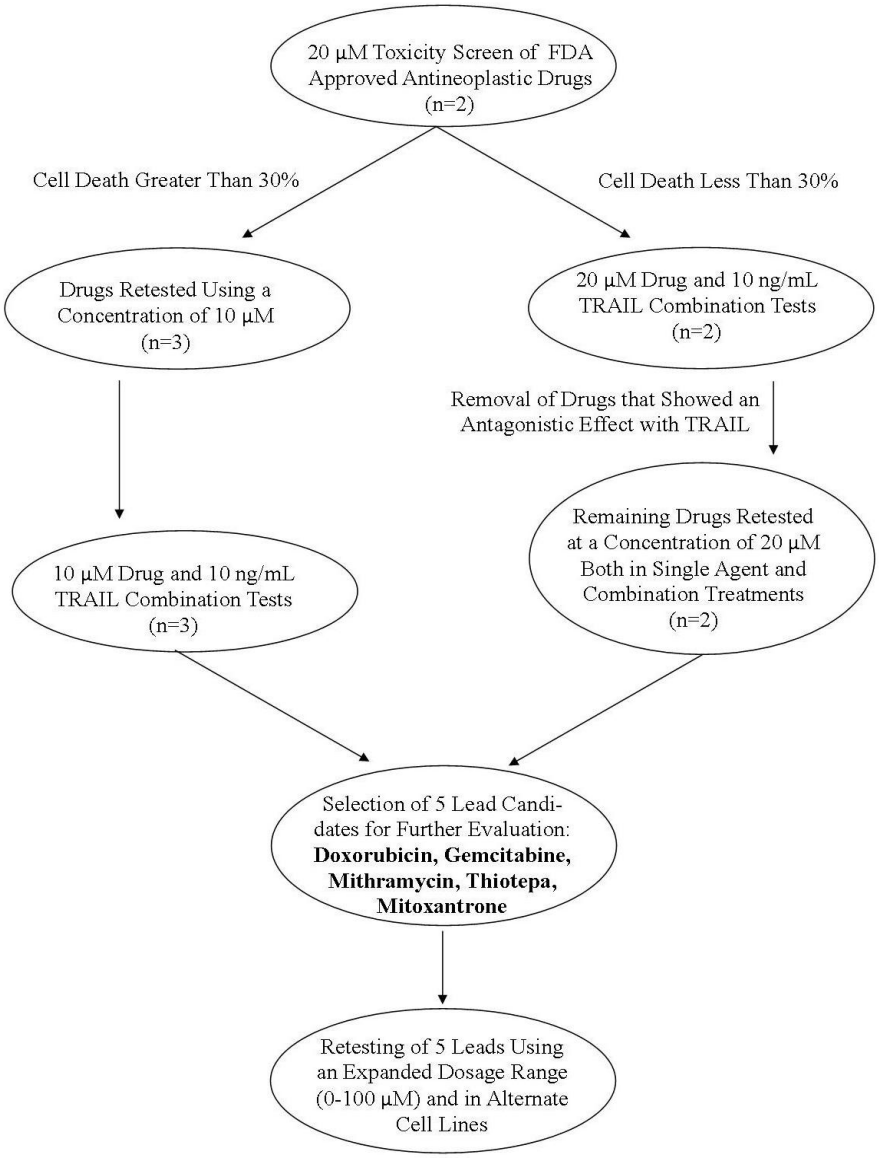


Figure 2.2 Flow chart outlining the screening process of the 55 drugs tested.

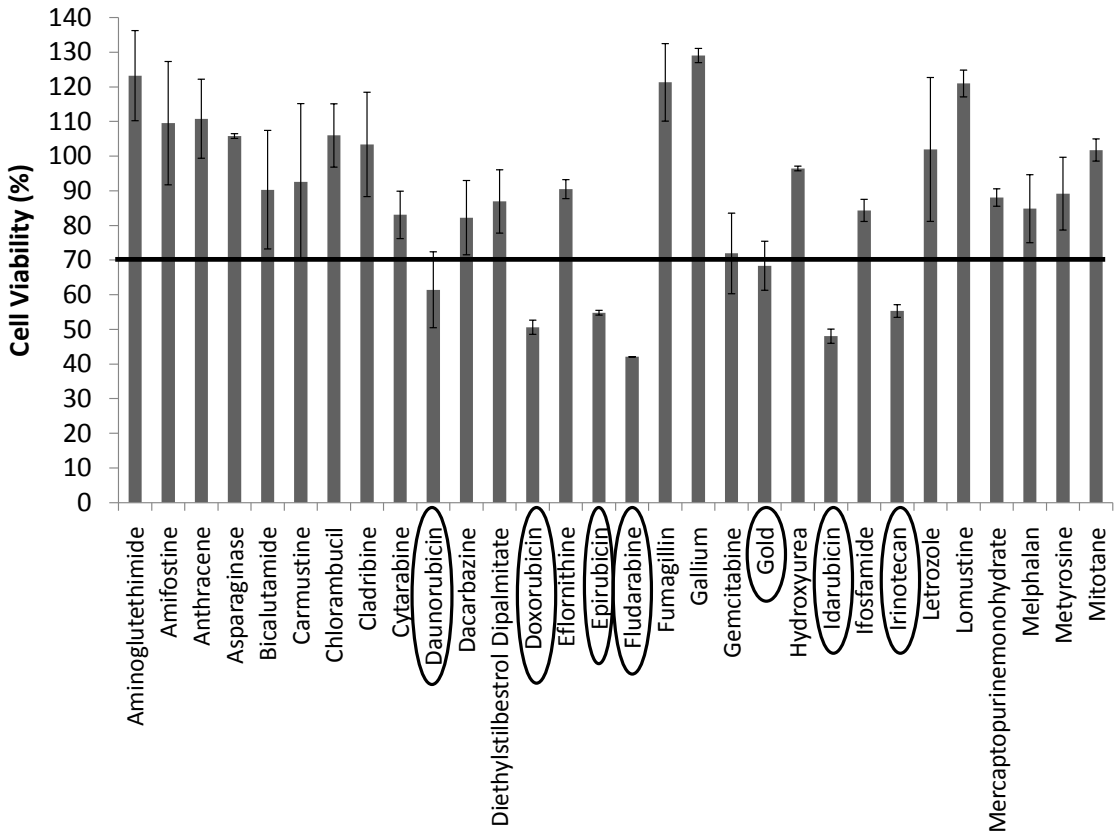


Figure 2.3 Single-agent drug toxicity pre-screen (20 µM) with PC3-TR cell line. Drugs found to induce a decrease in cell viability greater than 30% were retested at an alternate drug concentration of 10 µM (drugs circled). Drugs were incubated with the cells for a 24-hour period after which an MTT analysis was performed.

Identification of FDA-Approved Drugs as TRAIL Sensitizers in Prostate, Pancreatic, and Breast Cancer Cell Lines using Parallel Screening. The overall screening schematic is shown in **Figure 2.2.** PC3-TR cells were initially treated with 20 µM of each drug in order to carry out an initial screen for drug toxicity. Eleven drugs (arsenic, daunorubicin, doxorubicin, epirubicin, fludarabine, idarubicin, irinotecan, docetaxel, mithramycin, gold, mitoxantrone) resulted in > 30% loss in PC3-TR cell viability at 20 µM in the initial toxicity screen (**Figure 2.3**) and were screened for their TRAIL sensitization activities at a lower concentration of 10 µM (**Figure 2.4**). Use of

lower drug concentrations (10 μM) limits the single agent toxicity, which can also allow for identification of synergistic interactions with TRAIL. Forty-four drugs from the library demonstrated cell viabilities higher than 70% at a concentration of 20 μM and were screened for their ability to sensitize PC3-TR cells to TRAIL under these conditions (**Figure 2.5**).

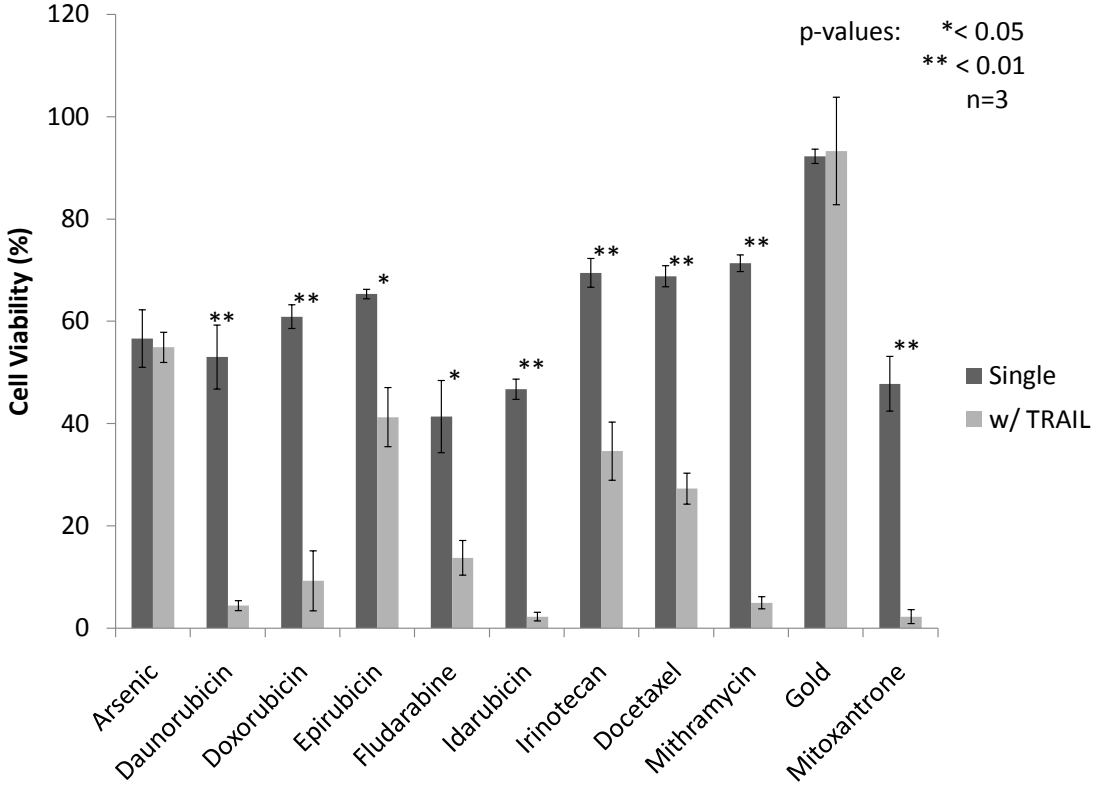


Figure 2.4 Parallel screening of drugs from the Johns Hopkins Chemical Compound Library as TRAIL sensitizers. PC3-TR human prostate cancer cells were first incubated with drug treatments (10 μM) for 24 hours after which time the media was removed, refreshed and cells were treated with TRAIL (10 ng/mL) for an additional 24 hrs.

Combination treatments with sensitizer drugs (24h) followed by TRAIL (24h) were carried out in a sequential treatment format to identify candidates that sensitized PC3-TR cells to TRAIL-induced apoptosis. Combination treatments that induced statistically

significant ($p < 0.05$) reduction in the viability of PC3-TR cells, compared to the sum of the individual treatments (i.e. additive effects of TRAIL alone + chemosensitizer drug alone), were identified as leads. Nine drugs, daunorubicn, doxorubicin, fludarabine, idarubicin, irinotecan, docetaxel, mithramycin, mitoxantrone and epirubicin, were identified as lead sensitizers of TRAIL induced apoptosis from the 10 μM screen (**Figure 2.4**). Of these, seven have been previously identified as TRAIL sensitizers for different malignancies, but only five have been reported for prostate cancer (**Table 2.1**) [56, 57, 105-107].

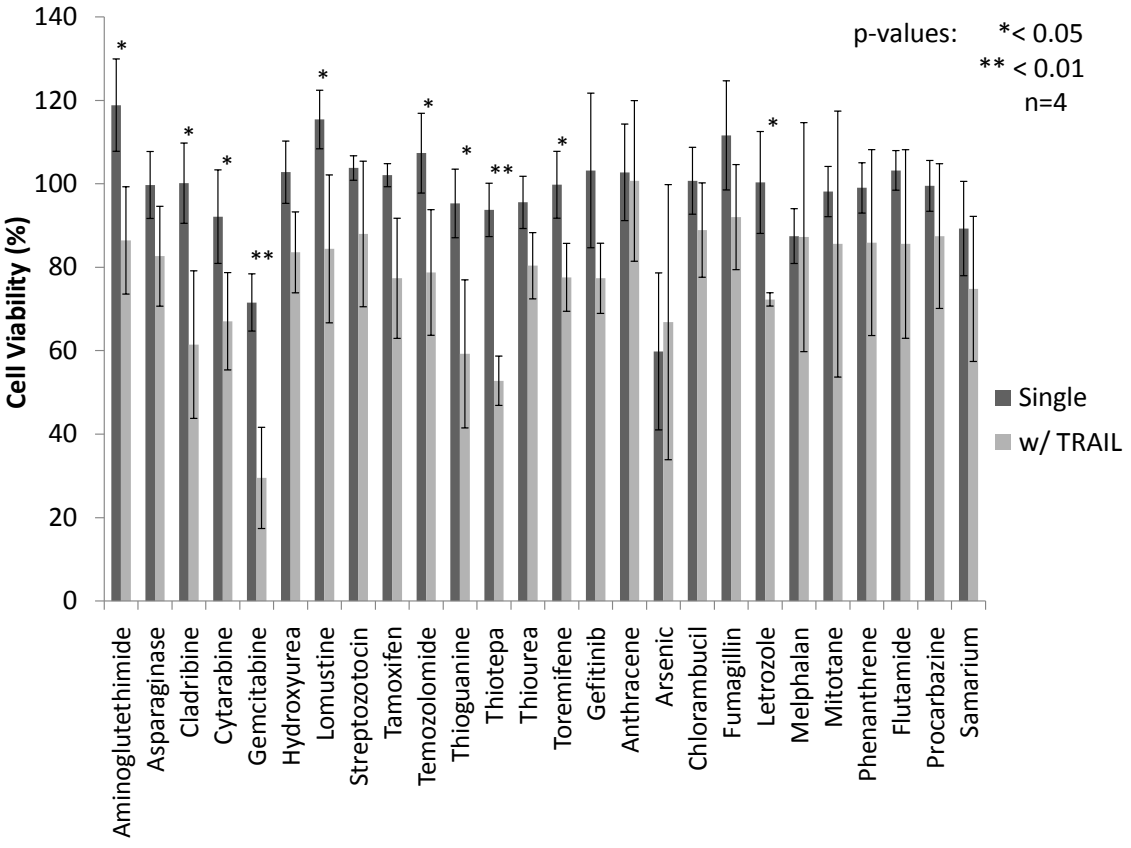


Figure 2.5 PC3-TR cells were first incubated with drug treatments (20 μM) for 24 hours after which time the media was removed, refreshed and cells were treated with TRAIL (10 ng/mL) for an additional 24 hrs.

To our knowledge, two drugs, idarubicin and mitoxantrone, have not been previously described as TRAIL sensitizers for any cancer cell type and are therefore new candidates that can be used in combination with TRAIL. The screen with 20 μM drug concentration identified the following drugs as TRAIL sensitizer leads: cladribine, cytarabine, gemcitabine, thioguanine and thioTEPA (**Figure 2.5**). Of these drugs, gemcitabine has been previously shown as a TRAIL sensitizer in different malignant cells, including prostate and pancreatic cancers [98]. Taken together, the two screens led to the identification of fourteen chemotherapeutic drug leads that sensitize PC3-TR prostate cancer cells to TRAIL-induced apoptosis; other candidates that demonstrated moderate efficacies (for example, toremifene, lomustine, temozolomide, aminoglutethimide, and letrozole) were also identified but not pursued further due to the presence of more promising leads. These results indicate that the screen accurately identified both, existing as well as new TRAIL sensitizers from the drug library. A summary of effective TRAIL sensitizers from the screen, along with their corresponding efficacies for reducing cancer cell viability, is provided in **Table 2.1**.

From the TRAIL chemosensitizer leads identified above, five drugs - doxorubicin, gemcitabine, mithramycin, mitoxantrone, and thioTEPA were chosen for additional evaluation. These drugs have been approved by the FDA for chemotherapeutic administration in different malignancies. Doxorubicin and gemcitabine were selected since both have been previously characterized as TRAIL-sensitizing agents in prostate and / or pancreatic cancer cells [49, 65, 108-110]. Mithramycin has also been shown to sensitize prostate cancer cells to TRAIL [107] but to our knowledge, the drug has not

been previously demonstrated to possess TRAIL sensitization activity in pancreatic cancer cells. Neither mitoxantrone nor thioTEPA has previously been shown to act as TRAIL sensitizers in cancer cells to the best of our knowledge. Additional factors that were used to determine candidates for subsequent characterization included single-agent drug toxicities in the PC3-TR cell line (drugs with lower toxicities were given preference), the total loss of cancer cell viability induced by the combination treatment compared to the single agent treatments, and prior knowledge of the drugs as TRAIL sensitizers.

Table 2.1 Summary of drugs identified as TRAIL sensitizing agents and their previously known activity.

Drug Name	Drug Alone	Drug Alone + TRAIL Alone (Additive)	Combination Treatment	p-Value	Known TRAIL Sensitizer?	Known TRAIL Sensitizer in Prostate Cancer?	Known TRAIL Sensitizer in Pancreatic Cancer?
10 μM							
Daunorubicin	47	51.3	95.6	< 0.01	Yes	No	No
Docetaxel	31.2	35.5	72.7	< 0.01	Yes	Yes	No
Doxorubicin	**39**	**43.3**	**90.8**	**< 0.01**	**Yes**	**Yes**	**Yes**
Epirubicin	34.7	39	58.7	< 0.05	Yes	Yes	No
Fludarabine	58.6	62.9	86.2	< 0.05	Yes	No	No
Idarubicin	53.3	57.6	97.7	< 0.01	No	No	No
Irinotecan	30.6	34.9	65.4	< 0.01	Yes	Yes	No
Mithramycin	**28.6**	**32.9**	**95**	**< 0.01**	**Yes**	**Yes**	**No**
Mitoxantrone	**52.2**	**56.5**	**97.7**	**< 0.01**	**No**	**No**	**No**
20 μM							
Cladribine	0	4.1	38.5	< 0.05	No	No	No
Cytarabine	7.9	12.2	32.9	< 0.05	No	No	No
Gemcitabine	**28.4**	**32.7**	**70.5**	**< 0.01**	**Yes**	**Yes**	**Yes**
Thioguanine	4.7	9	40.8	< 0.05	No	No	No
Thiotepa	**6.2**	**10.5**	**47.2**	**< 0.01**	**No**	**No**	**No**

Additional evaluation involved expanding the range of the drug dose from 0 to 20 µM for doxorubicin and 0 to 100 µM for the other drugs in PC3-TR and PC3 human prostate cancer cells, and the Panc-1 human pancreatic cell cancer line. It is important to note that the screening experiments employed drugs from the JHCCL (frozen 10 mM aliquots), while the lead characterization experiments employed drugs obtained from Sigma (doxorubicin, mitoxantrone) and the NCI/NIH Developmental Therapeutic Program (gemcitabine, mithramycin, thioTEPA) which were reconstituted in either DMSO or water, based on the solvent that was used for the respective drugs supplied in the JHCCL.

Combination treatments were carried out with 10 ng/mL TRAIL, which induced a loss of viability of 4.3% (+/- 3.2%) in PC3-TR cells, 8.4% (+/- 4.2%) in PC3 cells, and 1.4% (+/- 7.4%) in Panc-1 cells, when administered alone. Such low levels of viability loss are demonstrative of the resistance of these cancer cells to TRAIL-induced apoptosis. It is important to note that while PC3-TR cells are derived from PC3 cells, the two lines are inherently different and therefore, it can be expected that the two cell lines respond differently to drug treatments. For example, we have previously shown that closely related prostate cancer cell lines, PC3 and PC3-PSMA cells, demonstrate markedly different behavior in response to nanoparticle treatment [111].

The expanded dose range of the lead candidates in the PC3-TR cell line showed trends similar to those seen in the primary screen; all lead candidates induced significant losses in cancer cell viability when used in combination with TRAIL (**Figures 2.6-2.10**). Doxorubicin, mithramycin, and mitoxantrone demonstrated synergistic efficacies in

combination with TRAIL in PC3 and Panc-1 cells (**Figures 2.6-2.8)**. Conversely, neither gemcitabine nor thioTEPA demonstrated significant synergy in these cells (**Figures 2.9 & 2.10)**.

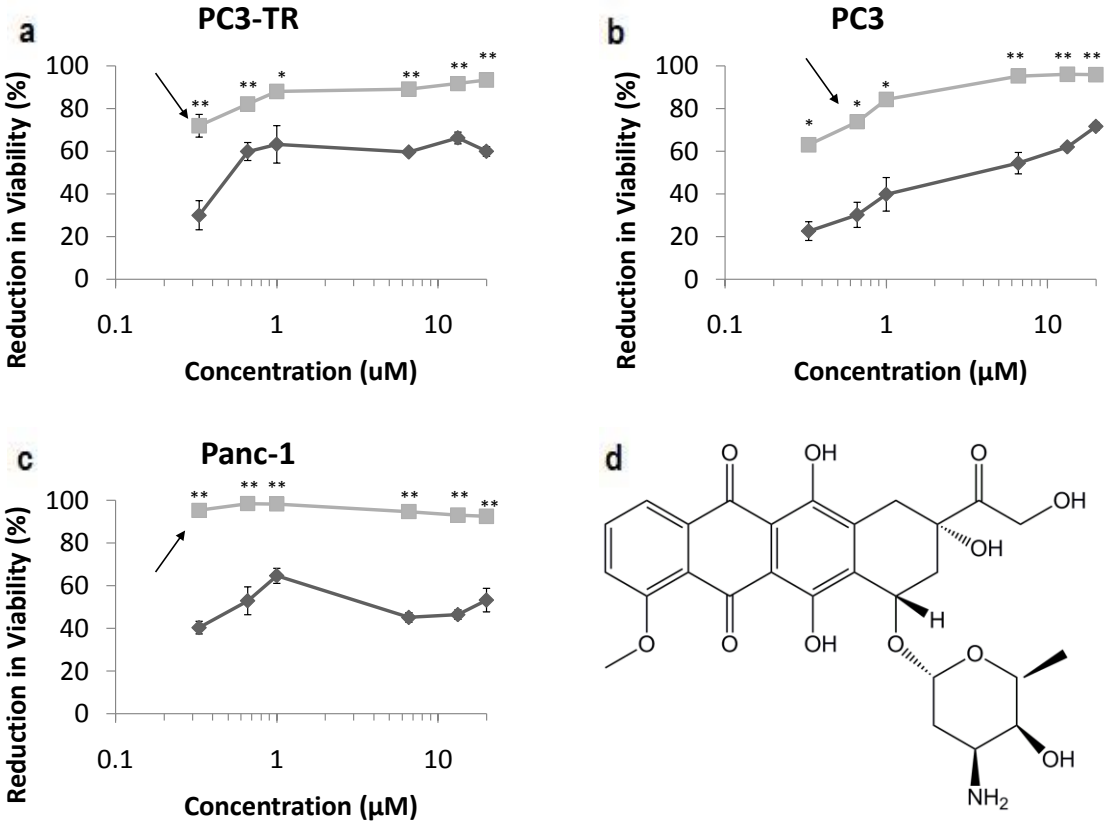


Figure 2.6 Dose response for doxorubicin in malignant cell lines. (a) PC3-TR, (b) PC3 human prostate cancer cells, and (c) Panc-1 pancreatic cancer cells. Single-agent treatments are shown as "dark grey diamonds" and combination treatments with 10 ng/mL of TRAIL are shown as "light grey squares". Comparisons were made between the single agent and combination treatments; asterisks (*) and (**) indicate p-values < 0.05 and < 0.01, respectively. (d) molecular structure of doxorubicin. Arrows indicate the concentrations at which the enhancement in viability reduction is the greatest. Data are presented on a logarithmic scale for x-axes in the plots. Lines connecting data points are for visualization only.

The median concentrations of single-agent doxorubicin (**Figure 2.6**) that resulted in 50% loss of viability in the cancer cell population compared to the untreated control (LC_{50}) were approximately 0.6 µM, 6 µM and 0.6 µM in PC3-TR, PC3, and Panc-1 cells, respectively. However, in combination with 10 ng/mL TRAIL, the LC_{50} values for doxorubicin were 0.25 µM for PC3-TR and PC3 cells, and 0.1 µM (100 nM) for Panc-1 cells, all of which are substantially lower than the single-agent concentrations (**Figure 2.6)**. The greatest loss of cancer cell viability for the doxorubicin-TRAIL combination treatment compared to single-agent doxorubicin treatment was observed at 0.33 µM (42%), 1 µM (44.4%), and 0.33 µM (55%) for PC3-TR, PC3, and Panc-1 cells, respectively (**Figure 2.6)**. The cytotoxic effect of doxorubicin is attributed to its DNA intercalation as well as its disruption of cellular functions upon cell membrane binding. Intercalation inhibits nucleotide replication via the stabilization of type II topoisomerase [112]. Doxorubicin is currently approved for the treatment of acute lymphoblastic leukemia, acute myeloblastic leukemia, Wilms' tumor, neuroblastoma, soft tissue and bone sarcomas, breast cancer, ovarian cancer, transitional cell bladder cancer, thyroid cancer, gastric cancer, Hodgkin's disease, malignant lymphoma, bronchogenic cancer, ovarian cancer, AIDS-Related Kaposi's sarcoma, and multiple myeloma. The TRAIL sensitization activities of doxorubicin are due to the ability of the drug to down-regulate the anti-apoptotic protein c-FLIP [108, 113], activate pro-apoptotic caspases [114, 115] and induce reactive oxygen species (ROS) formation in cancer cells [116]. Thus, the genotoxic activity of doxorubicin activates the internal apoptosis pathway, while simultaneously sensitizing the cell to external, receptor-mediated apoptosis by the TRAIL ligand.

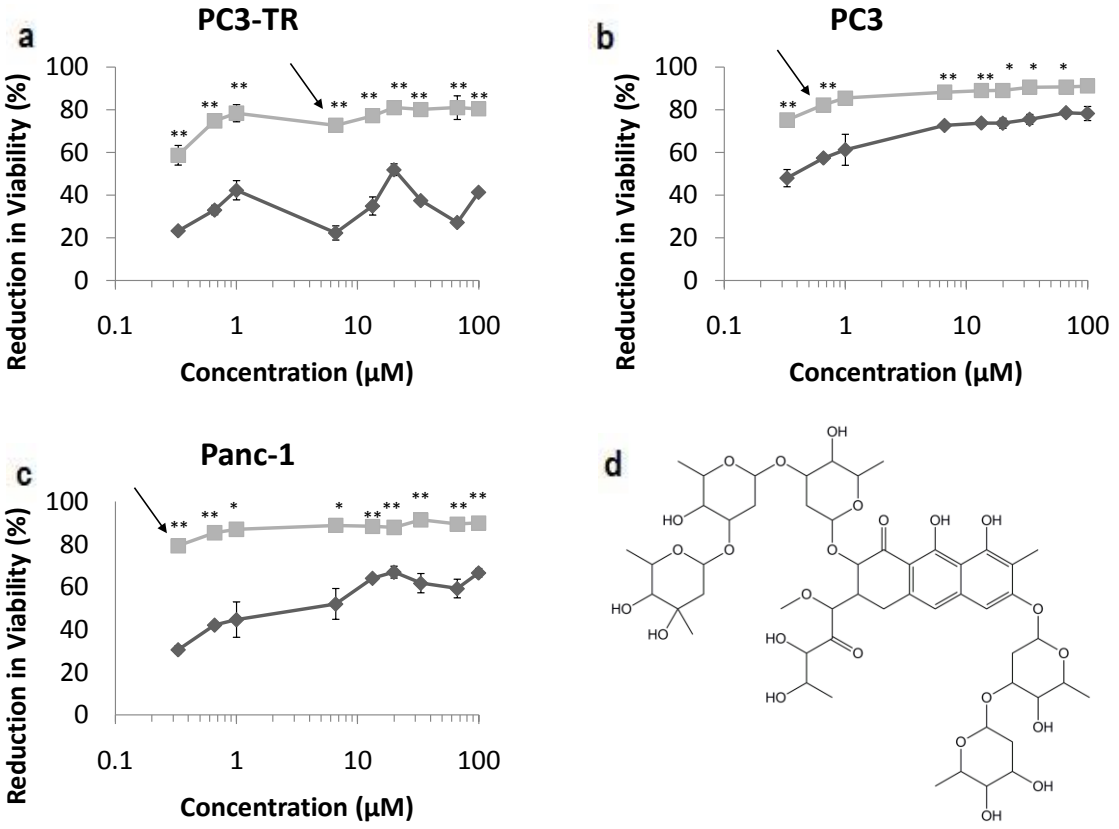


Figure 2.7 Dose response for mithramycin (plicamycin) in malignant cell lines. (a) PC3-TR, (b) PC3 human prostate cancer cells, and (c) Panc-1 pancreatic cancer cells. Single-agent treatments are shown as "dark grey diamonds" and combination treatments with 10 ng/mL of TRAIL are shown as "light grey squares". Comparisons were made between the single agent and combination treatments; asterisks (*) and (**) indicate p-values < 0.05 and < 0.01, respectively. (d) molecular structure of mithramycin. Arrows indicate the concentrations at which the enhancement in viability reduction is the greatest. Data are presented on a logarithmic scale for x-axes in the plots. Lines connecting data points are for visualization only.

The LC_{50} values for single-agent mithramycin were 20 µM, 0.5 µM and 6 µM for PC3-TR, PC3, and Panc-1 respectively. However, in combination with 10 ng/mL TRAIL, the LC_{50} values for mithramycin were approximately 0.2 µM for PC3-TR and PC3 cells, and 0.1 µM for Panc-1 cells, respectively (**Figure 2.7**). Combination treatments with

mithramycin (plicamycin) demonstrated the greatest enhancement in loss of cancer cell viability at 6.6 µM (50.5%), 0.66 µM (24.9%) and 0.33 µM (48.6%) in PC3-TR, PC3, and Panc-1 cells respectively, compared to single-agent mithramycin treatment (**Figure 2.7**). Importantly, mithramycin demonstrated one of the highest efficacies in combination with TRAIL; a difference of 67% in loss of cancer cell viability was seen for the combination treatment compared to the additive effect of the single-agent treatments (67% increase; **Figure 2.4**). Mithramycin is an antineoplastic antibiotic derived from Streptomyces and is approved by the FDA for the treatment of testicular cancer and hypercalcaemia [117]. The antineoplastic properties of mithramycin are likely linked to the binding of mithramycin to GC-rich section of DNA and the subsequent inhibition of RNA synthesis and regulation of transcription [118]. The TRAIL-sensitization activity of mithramycin is not very well characterized, but one study suggests that this activity is caused by the down regulation of X-linked Inhibitor of Apoptosis Protein (XIAP) [107]. XIAP inhibits apoptosis by binding to and inhibiting caspases 3, 7 and 9. Mithramycin is able to prevent the transcription of XIAP through its binding activity to DNA [107, 117]. This action would sensitize cancer cells to both, intrinsic and extrinsic apoptosis pathways. However, the extent to which mithramycin activated the intrinsic pathway has not been elucidated.

LC_{50} values for single-agent mitoxantrone were approximately 10 µM for PC3-TR and PC3 cells, and 5 µM for Panc-1 cells. However, in combination with 10 ng/mL TRAIL, the LC_{50} values for mitoxantrone were significantly reduced to 0.6 µM, 0.1 µM and 1 µM for PC3-TR, PC3 and Panc-1 cells, respectively (**Figure 2.8**). In the case of

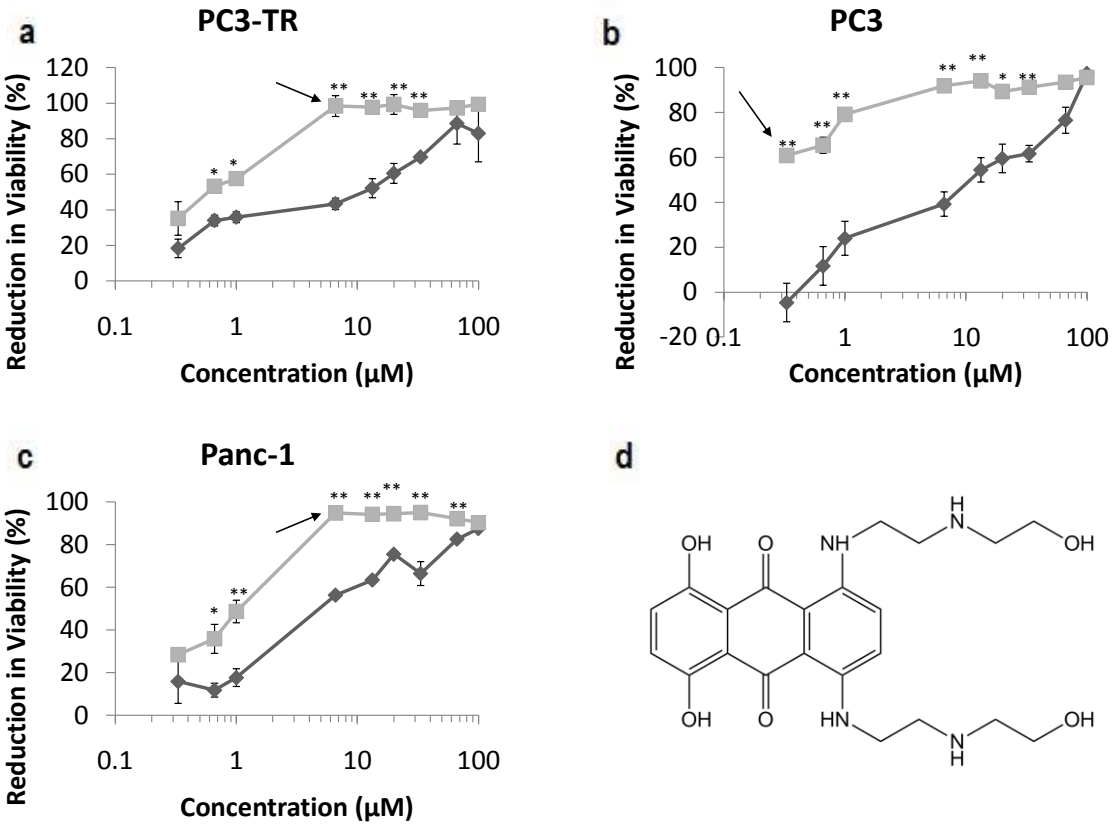


Figure 2.8 Dose response for mitoxantrone in malignant cell lines. (a) PC3-TR, (b) PC3 human prostate cancer cells, and (c) Panc-1 pancreatic cancer cells. Single-agent treatments are shown as "dark grey diamonds" and combination treatments with 10 ng/mL of TRAIL are shown as "light grey squares". Comparisons were made between the single agent and combination treatments; asterisks (*) and (**) indicate p-values < 0.05 and < 0.01, respectively. (d) molecular structure of mitoxantrone. Arrows indicate the concentrations at which the enhancement in viability reduction is the greatest. Data are presented on a logarithmic scale for x-axes in the plots. Lines connecting data points are for visualization only.

mitoxantrone-TRAIL combination treatment, the greatest enhancement in loss of viability was observed at 6.6 µM (55.0%) in PC3-TR, 0.33 µM (60.8%) in PC3, and 6.6 µM (38.5%) in Panc-1 cells (**Figure 2.8**), compared to mitoxantrone alone. The chemotherapeutic activity of mitoxantrone is attributed to its ability to intercalate into DNA, resulting in cross-links and strand breaks. Additionally, mitoxantrone also

interferes with RNA synthesis and inhibits topoisomerase II [119]. Mitoxantrone has been approved by the FDA for palliative treatment of prostate cancer and curative treatment of acute nonlymphocytic leukemia; the drug has also been recently approved for the treatment of multiple sclerosis. Although we did not find reports that describe the use of mitoxantrone as a TRAIL sensitizer, mitoxantrone has been demonstrated to possess synergistic relationship with Tumor Necrosis Factor (TNF) for inducing apoptosis in cells [120, 121]. A detailed evaluation that describes the mechanisms behind the TRAIL-sensitization activity of mitoxantrone is currently under investigation in our laboratory.

In the case of gemcitabine, statistically significant enhancement of viability reduction occurred in PC3-TR at concentrations above 6.6 μM (**Figure 2.9**). Further increase in concentration to 100 μM resulted in an enhancement of cell viability loss up to a maximal value of 29% for the combination treatment over the single drug treatment. Gemcitabine is currently approved for the treatment of ovarian cancer (with carboplatin), breast cancer (with paclitaxel), non-small cell lung cancer (with cisplatin), and pancreatic cancer. Gemcitabine is metabolized intercellularly to active diphosphate and triphosphate nucleosides which work via two mechanisms to inhibit DNA synthesis. First, gemcitabine diphosphate inhibits the enzyme ribonucleotide reductase, which is a catalyst of reactions to form deoxynecleoside triphosphates. Second, gemcitabine triphosphate competes with other deoxynecleoside triphosphates for incorporation into DNA, which is enhanced by the action of gemcitabine diphosphate. Although the TRAIL sensitization activity of gemcitabine is not fully understood, it is hypothesized that the response is

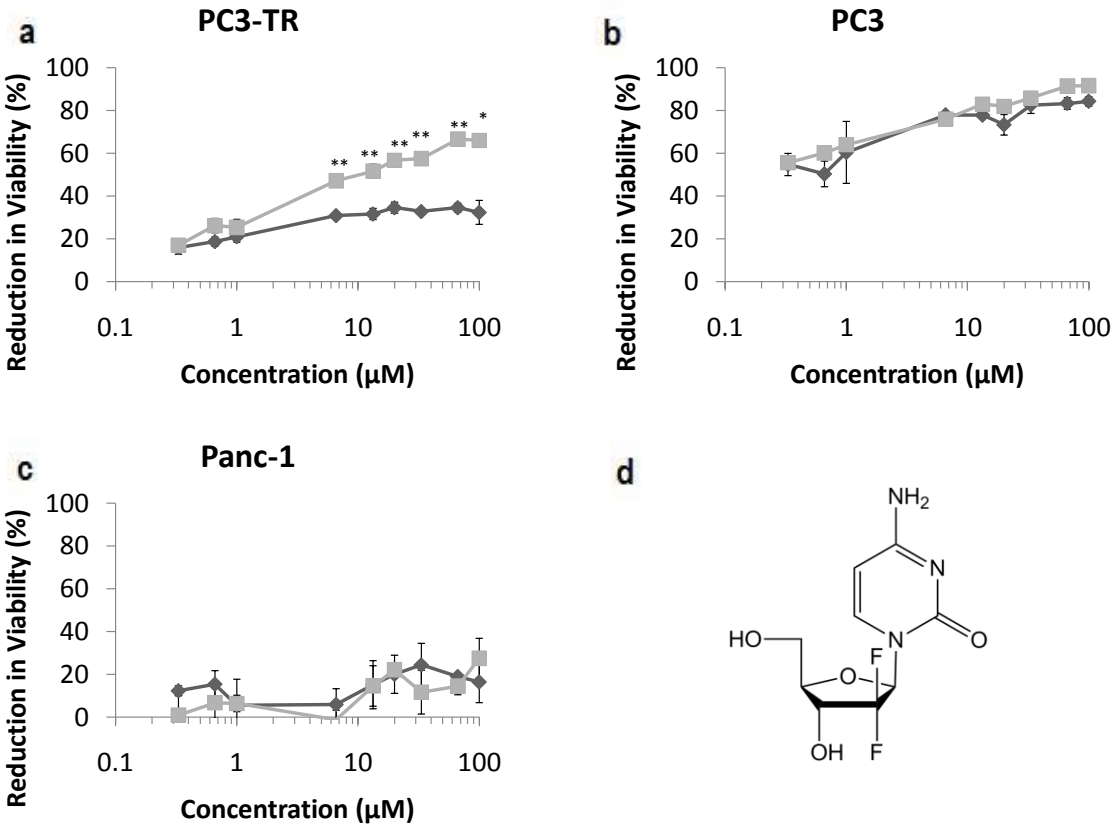


Figure 2.9 Dose response for gemcitabine in malignant cell lines. (a) PC3-TR, (b) PC3 human prostate cancer cells, and (c) Panc-1 pancreatic cancer cells. Single-agent treatments are shown as "dark grey diamonds" and combination treatments with 10 ng/mL of TRAIL are shown as "light grey squares". Comparisons were made between the single agent and combination treatments; asterisks (*) and (**) indicate p-values < 0.05 and < 0.01, respectively. (d) molecular structure of gemcitabine. Arrows indicate the concentrations at which the enhancement in viability reduction is the greatest. Data are presented on a logarithmic scale for x-axes in the plots. Lines connecting data points are for visualization only.

related to the activation of pro-apoptotic caspases [65, 98]. Previous results have shown that the combination treatment of gemcitabine and TRAIL increases the activation of caspases 8 and 3, while a single agent treatment of gemcitabine increases the activation of only caspase 3 [65]. Although synergy was observed in PC3-TR cells with gemcitabine, we did not see synergy between gemcitabine and TRAIL in PC3 and Panc-1

cells, which differs from other reports in the literature [65, 98]. This is likely due to differences in the concentrations of both drug and TRAIL conditions that were employed in these other studies; for example, other studies have employed 100 ng/mL TRAIL, which is ten-fold higher than the concentration used in our study [65, 98].

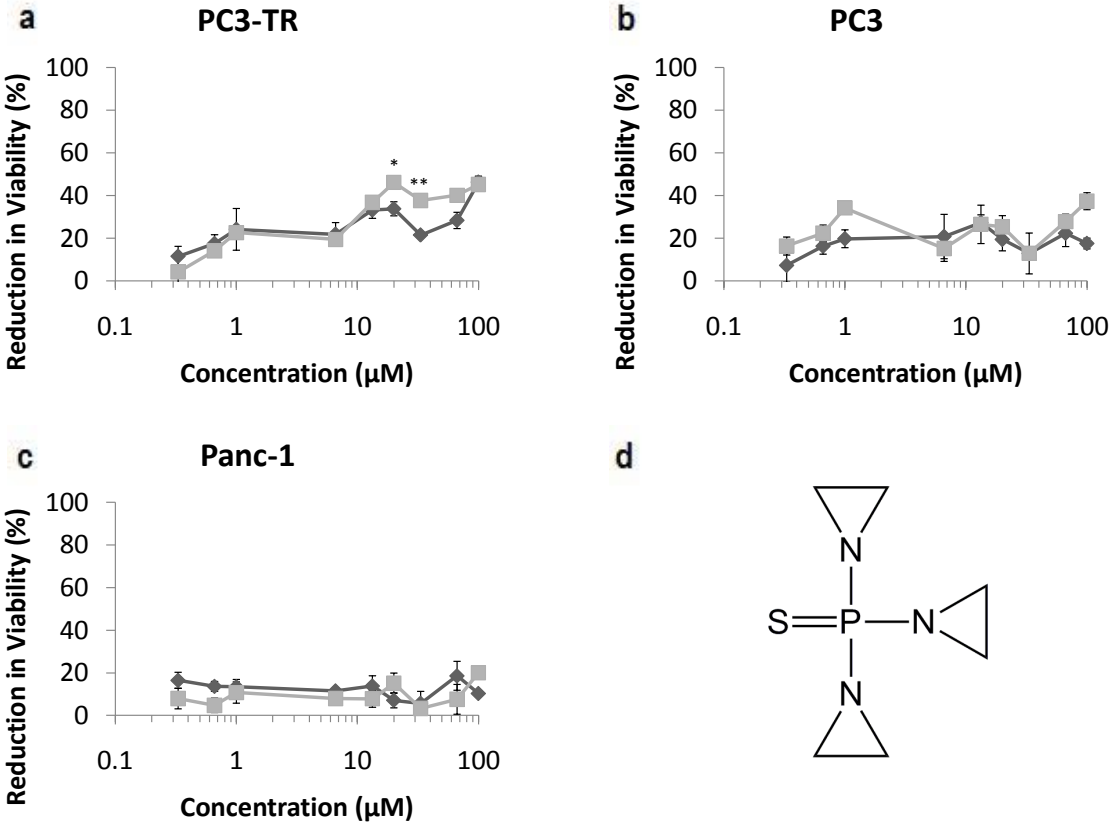


Figure 2.10 Dose response for thioTEPA in malignant cell lines. (a) PC3-TR, (b) PC3 human prostate cancer cells, and (c) Panc-1 pancreatic cancer cells. Single-agent treatments are shown as "dark grey diamonds" and combination treatments with 10 ng/mL of TRAIL are shown as "light grey squares". Comparisons were made between the single agent and combination treatments; asterisks (*) and (**) indicate p-values < 0.05 and < 0.01, respectively. (d) molecular structure of thioTEPA. Data are presented on a logarithmic scale for x-axes in the plots. Lines connecting data points are for visualization only.

ThioTEPA has been approved by the FDA for the treatment of breast cancer, ovarian cancer, superficial papillary carcinoma of urinary bladder, lymphosarcoma, and Hodgkin's disease. ThioTEPA is a radiomimetic drug that can produce ethylenimine radicals, which disrupt DNA. ThioTEPA showed a 40% difference in viability reduction between the combination treatments and the additive effect of the single agent treatments in the initial screen with PC3-TR; however, only an 8% increase was observed in case of the combination treatment compared to individual treatments in the subsequent experiments (**Figure 2.5 & 2.10**). This might be due to the different sources of the drug employed in the screening and characterization experiments.

In order to confirm the above results obtained using the MTT assay, a secondary analysis method using Live/Dead® fluorescence staining was employed to count living cell populations following single-agent mitoxantrone/mithramycin treatments as well as TRAIL-based combination treatments in the PC3-TR cell line. Image analysis showed that single-agent TRAIL caused a 6% (+/- 4%) decrease in cell viability (not shown). **Figure 2.11** compares cell viability calculated using the MTT assay to the normalized live cell count. The greatest deviation between the MTT and live/dead analysis occurs in the combination mitoxantrone and TRAIL experiments. Deviation is greatest at lower concentrations of mitoxantrone but diminishes as the concentration increases. The average difference between cell viability data for single-agent mitoxantrone is 12.9% between the two methods, while the average difference is 15% for the mitoxantrone-TRAIL combinations. The single-agent and combination treatments with mithramycin show excellent agreement between the two cell viability analysis methods. The average

difference between analysis methods is 10.4% for mithramycin alone and only 5.6% for the mithramycin-TRAIL combination treatment. These results indicate that the MTT and the live/dead methods are comparable for these systems, which is an indication that the MTT assay is a reliable method for screening and rapidly identifying synergistic combination treatments.

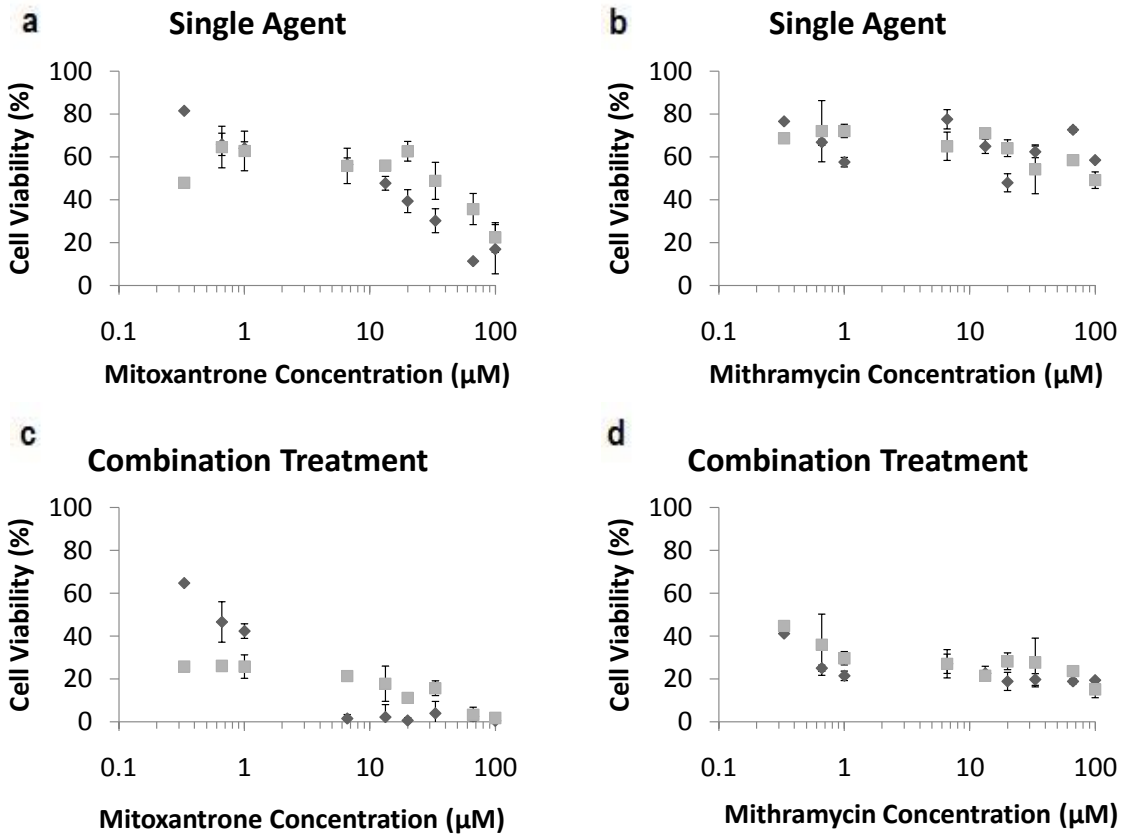


Figure 2.11 Evaluation of secondary analysis in PC3-TR cells. (a) Single-agent mitoxantrone, (b) single-agent mithramycin, (c) combination treatment with mitoxantrone and 10 ng/mL TRAIL and (d) combination treatment with mithramycin and 10 ng/mL TRAIL. Analysis results performed using the MTT assay are shown as "dark grey diamonds" and analysis results performed using the live/dead stain are shown as "light grey squares". Data are presented on a logarithmic scale for x-axes in the plots.

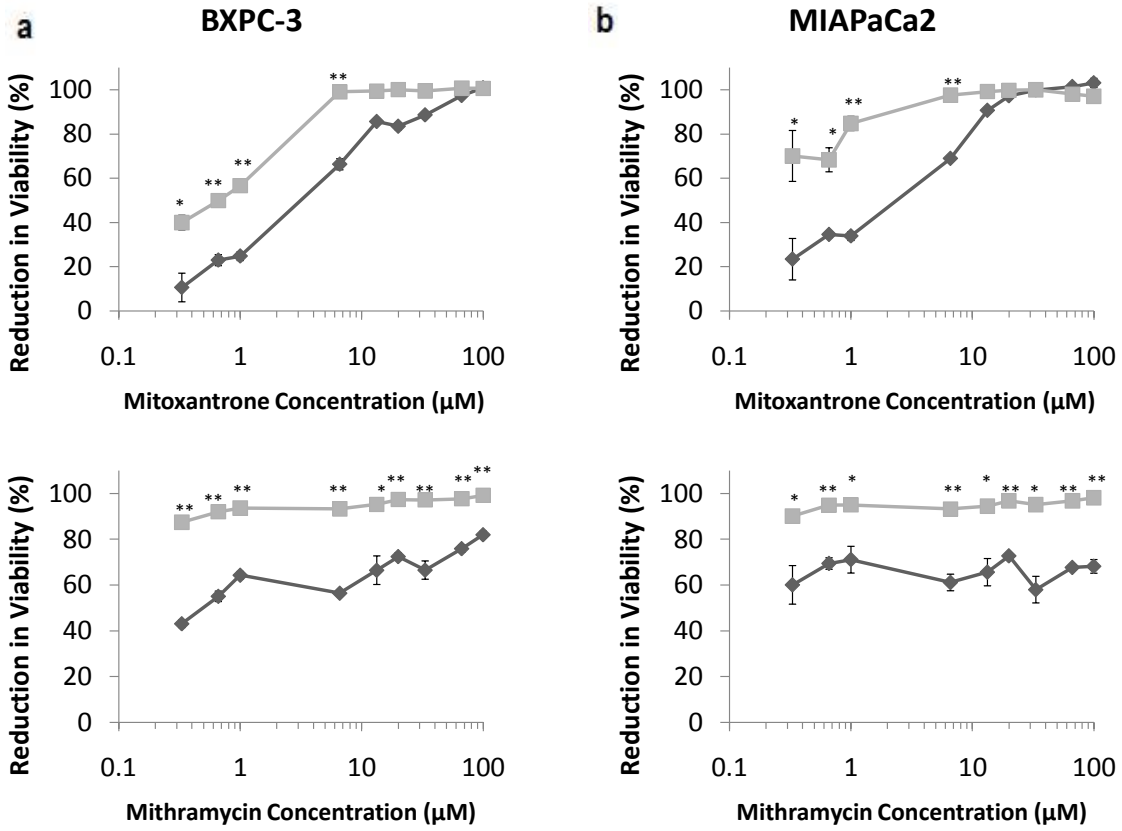


Figure 2.12 Evaluation of mitoxantrone and mithramycin in additional malignant lines. (a) BXPC-3, and (b) MIAPaCa2 human pancreatic cancer cells. Single-agent treatments are shown as "dark grey diamonds" and combination treatments with 10 ng/mL of TRAIL are shown as "light grey squares". Comparisons were made between the single agent and combination treatments; asterisks (*) and (**) indicate p-values < 0.05 and < 0.01, respectively. Data are presented on a logarithmic scale for x-axes in the plots. Lines connecting data points are for visualization only.

Following the identification of mitoxatrone and mithramycin as potent sensitizers of TRAIL-induced apoptosis in cancer cells above, we further evaluated the activities of these drugs in two additional human pancreatic cancer cell lines, BXPC-3 and MIAPaCa2 (**Figure 2.12**). Single-agent TRAIL treatments resulted in a loss of viability in 14.3% (+/- 9.8%) in BXPC-3, and 9.2% (+/-3.8%) in MIAPaCa2 cells. The LC_{50} value for single-agent mitoxantrone was approximately 4 μM for BXPC-3 and 3 μM for

MIAPaCa2 cells. In comparison, the LC_{50} values for the mitoxantrone-TRAIL combination treatments were 0.66 µM for BXPC-3 and 0.1 µM for MIAPaCa2 cells. Similarly, LC_{50} values for single-agent mithramycin were 0.3 µM for BXPC-3 and 0.2 µM for MIAPaCa2 cells. The LC_{50} values for the mithramycin-TRAIL combination treatments were less than 0.1 µM (100 nM) for both, BXPC-3 and MIAPaCa2 cells.

In BXPC-3 cells, the largest difference in loss of viability induced by the drug-TRAIL combination compared to single-agent drug treatment were observed at 6.6 µM (18.5%) and 0.33 µM (42.0%) for mitoxantrone and mithramycin, respectively. In MIAPaCa2 cells, the largest enhancements in viability reduction following combination treatments were observed with mitoxantrone and mithramycin doses of 0.33 µM (37.5%) and 33.3 µM (28.0%), respectively. In case of mitoxantrone, the TRAIL sensitization activity was most effective at lower concentrations of the drug; extensive reduction in cancer cell viability was observed with high concentrations of mitoxatrone in these cells. In contrast, the response was largely invariant as a function of concentration for mithramycin in these cells. These results are similar to those observed with other cancer cell lines (**Figure 2.7 & 2.8**). Taken together, the significant reduction in the LC_{50} values observed in case of combination treatments, compared to the additive effects of single-agent treatments of chemotherapeutic drugs and TRAIL, further demonstrates the efficacy this approach for the ablation of pancreatic cancer cells.

In addition to the two pancreatic cancer cell lines, we also tested the efficacy of mitoxantrone and mithramycin in two human breast cancer cell lines, MDA-MB-231 and

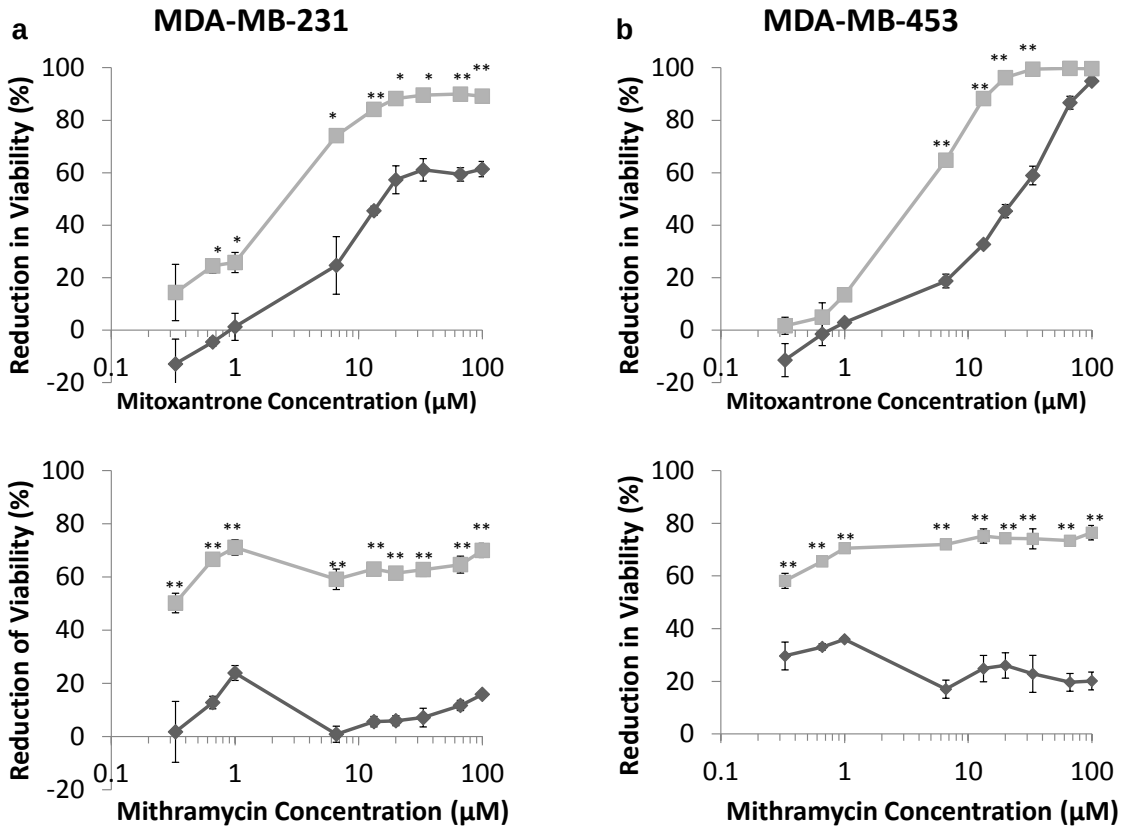


Figure 2.13 Evaluation of mitoxantrone and mithramycin in additional malignant lines. (a) MDA-MB-231, and (b) MDA-MB-453 human breast cancer cells. Single-agent treatments are shown as "dark grey diamonds" and combination treatments with 10 ng/mL of TRAIL are shown as "light grey squares". Comparisons were made between the single agent and combination treatments; asterisks (*) and (**) indicate p-values < 0.05 and < 0.01, respectively. Data are presented on a logarithmic scale for x-axes in the plots. Lines connecting data points are for visualization only.

MDA-MB-453 (**Figure 2.13**). Single-agent TRAIL treatments resulted in a loss of viability in 8.8% (+/- 5.7%) in MDA-MB-231, and 8.0% (+/-10.0%) in MDA-MD-453 cells. For single-agent mitoxantrone, the LC_{50} value was approximately 15 µM for MDA-MB-231 cells and 25 µM for MDA-MB-453 cells. In comparison, the LC_{50} values for the mitoxantrone-TRAIL combination treatments were approximately 5 µM for both MDA-MB-231 and MDA-MB-453 cell lines. Over the concentrations tested (0-100 µM),

single-agent mithramycin did not cause a reduction in viability of 50% or less which suggests that the LC_{50} value of single mithramycin is greater than 100 µM. The LC_{50} values for the mithramycin-TRAIL combination treatments were 0.33 µM for MDA-MB-231 and 0.2 µM for MDA-MB-453. In MDA-MB-231 cells, the largest difference in loss of viability induced by the drug-TRAIL combination compared to single-agent drug treatment were observed at 6.6 µM for both mitoxantrone (49.7%) and mithramycin (58.3%). In MDA-MB-453 cells, the largest reductions in viability following combination treatments were observed with mitoxantrone and mithramycin doses of 13.3 µM (55.6%) and 100 µM (56.3%), respectively. In the case of mitoxantrone, the TRAIL sensitization activity was most effective at moderate to high concentrations of the drug. There is a complete loss of viability at the three highest mitoxantrone combination treatment conditions (33.3, 66.6, and 100 µM) in MDA-MD-453, but even the high concentration combination treatments do not fully reduce cell viability in the MDA-MB-231 cells. This suggests that the MDA-MB-231 cell line may have some inherent resistance to mitoxantrone. In both breast cancer lines we again saw the response to mithramycin was largely concentration independent. Although the largest difference in viability reduction was at 6.6 µM (58.3%) and 100 µM (56.3%) in MDA-MB-231 and MDA-MB-453 respectively, in both cases the viability reduction was between 50% and 60% for almost all the concentrations investigated. As was demonstrated in the pancreatic cancer cells, there is a significant reduction in the LC_{50} values observed in the combination treatments as compared to the additive effects of single-agent treatments of the chemotherapeutic drugs and TRAIL. This provides evidence that the chemotheraputic

drug/TRAIL combination treatments are additionally effective at treating breast cancer in addition to the malignancies previously described.

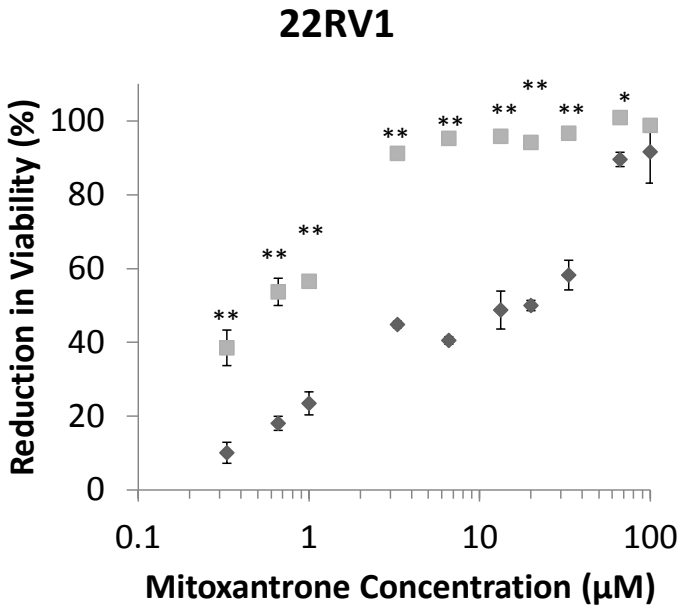


Figure 2.14 Evaluation of mitoxantrone in 22Rv1 prostate cancer cells. Single-agent treatments are shown as "dark grey diamonds" and combination treatments with 10 ng/mL of TRAIL are shown as "light grey squares". Comparisons were made between the single agent and combination treatments; asterisks (*) and (**) indicate p-values < 0.05 and < 0.01, respectively. Data are presented on a logarithmic scale for x-axes in the plots.

In addition to the PC3 and PC3-TR cells tested during the initial screening experiments, dose response experiments were also conducted using 22Rv1 prostate cancer cells (**Figure 2.14**). Single-agent TRAIL treatments resulted in a loss of viability in 4.3% (+/- 2.3%) in 22Rv1 cells. Single-agent mitoxantrone gave an LC_{50} value approximately equal to 13.3 µM and an LC_{50} value of 0.5 µM for the mitoxantrone-TRAIL combination treatments. In these cells, the largest difference in loss of viability induced by the mitoxantrone-TRAIL combination was 54.8% observed at 6.6 µM. In case of the 22Rv1

cells, the TRAIL sensitization activity was highly effective at all concentrations tested with the exception of the two highest concentrations (66.6 and 100 μM). Taken together these results suggests that the 22Rv1 cell line is also sensitized to TRAIL by mitoxantrone treatments.

The Combination Treatment of Low-dose Mitoxantrone and TRAIL is Selective towards Malignant Pancreatic Cells Compared to Normal Pancreatic Epithelial Cells. With the exception of gemcitabine and thioTEPA, the largest enhancements in viability reduction occurred at sub-micromolar or low micromolar concentrations for the other drugs. This is significant since the use of lower concentrations of these genotoxins can reduce damage to healthy tissue during therapy. This was demonstrated further by comparing single-agent verses the combination treatment LC_{50} values for each of the chemotherapeutic drugs. In the case of doxorubicin, mithramycin and mitoxantrone, the LC_{50} values decreased when each of these drugs was used in combination with TRAIL regardless of the cell line. With doxorubicin, this decrease in the LC_{50} value was relatively small in PC3-TR (0.6 μM to 0.25 μM) and Panc-1 (0.6 μM to 0.1 μM) cells, but significant in PC3 cells (6 μM to 0.25 μM). Mithramycin exhibited a relatively small change in the LC_{50} value for PC3 cells (0.5 μM to 0.2 μM), a moderate change for Panc-1 cells (6 μM to 0.1 μM), and the largest total change for PC3-TR cells (20 μM to 0.2 μM). Mitoxantrone demonstrated a moderate decrease in the LC_{50} value for Panc-1 cells (5 μM to 1 μM) and significantly larger decreases in LC_{50} values for the drug in combination with TRAIL in both, PC3-TR (10 μM to 0.6 μM) and PC3 (10 μM to 0.1 μM) cells.

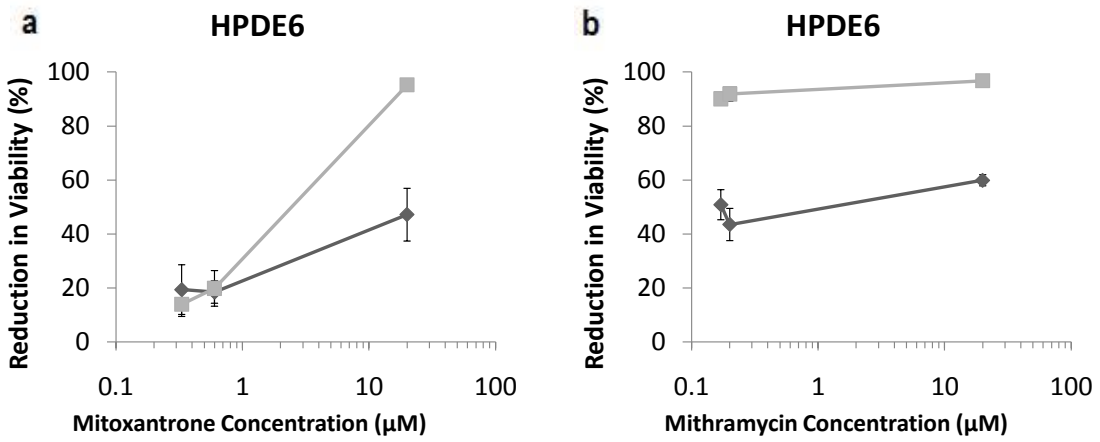


Figure 2.15 Evaluation of treatments in non-malignant cell line. Mitoxantrone (a) and mithramycin (b) in HPDE6 human pancreatic duct epithelial cells. Single-agent treatments are shown as "dark grey diamonds" and combination treatments with 10 ng/mL of TRAIL are shown as "light grey squares". Data are presented on a logarithmic scale for x-axes in the plots. Lines connecting data points are for visualization only.

The effects of mitoxantrone and mithramycin in the non-malignant HPDE6 [122, 123] pancreatic cells were tested in order to determine the selectivity of these two drugs and their combination with TRAIL for malignant cells compared to normal cells (**Figure 2.15**). Single-agent TRAIL showed a viability loss of 3.3% (+/- 12.4%) in HDPE6 cells compared to untreated cell control, suggesting that TRAIL shows little to no activity in these cells. Low concentrations (0.33 and 0.6 μM) of single-agent mitoxantrone also exhibited minimal loss in HPDE6 cell viability, while the 20 μM treatment resulted in a loss of viability of approximately 50% cells. Single-agent mithramycin treatment, however, resulted in a loss of viability in 40%-60% of the cell population even at the lower concentrations, which was considerably higher than that observed with mitoxantrone (**Figure 2.15**). A comparison of the single agent treatments and the combination treatments for mitoxantrone indicated selectivity of the drug at lower concentrations. In HDPE cells, 0.33 and 0.6 μM mitoxantrone in combination with 10

ng/mL TRAIL induced a 13.9% (+/- 4.5%) and 19.8% (+/-6.6%) loss of viability respectively, while mitoxantrone alone resulted in 19.3% (+/- 9.2%) and 18.4% (4.1%) at these doses. Importantly, single-agent mitoxantrone and mitoxantrone + TRAIL induced a respective loss of cell viability of 16% and 28.4% in Panc-1 cells, 10.6% and 40% in BXPC3 cells, 23.4% and 70% in MIAPaCa2 (0.33 μM mitoxantrone). These conditions indicate that the combination of low-dose mitoxantrone with TRAIL is selective towards malignant pancreatic cells compared to normal cells. As may be expected, this selectivity is lost at higher concentrations of mitoxantrone. We did not observe significant selectivity for cancer cells compared to non-malignant cells in case of mithramycin. While the results with mitoxantrone are promising due to the observed selectivity, an effective chemotherapeutic window of operation may be available for the mithramycin-TRAIL combination in vivo.

Higher Concentrations of TRAIL in Combination Treatments do not Demonstrate Increased Efficacies. The previous studies were carried out with different concentrations of the chemosensitizer drug followed by a single dose of TRAIL (**Figure 2.1**). Following identification of mitoxantrone and mithramycin as potential TRAIL sensitizers, we investigated the effect of different TRAIL concentrations in combination with a single dose of these sensitizer drugs. LC_{50} values for mitoxantrone-TRAIL and mithramycin-TRAIL combination treatments were 0.6 and 0.2 μM, respectively, for PC3-TR cells. The single-agent 0.6 μM mitoxantrone treatment, resulted in a loss of viability of 31.4% (+/- 2.0%) in PC3-TR cells compared to the untreated control (**Figure 2.16**), which is in good agreement with the data trend shown in **Figure 2.8**.

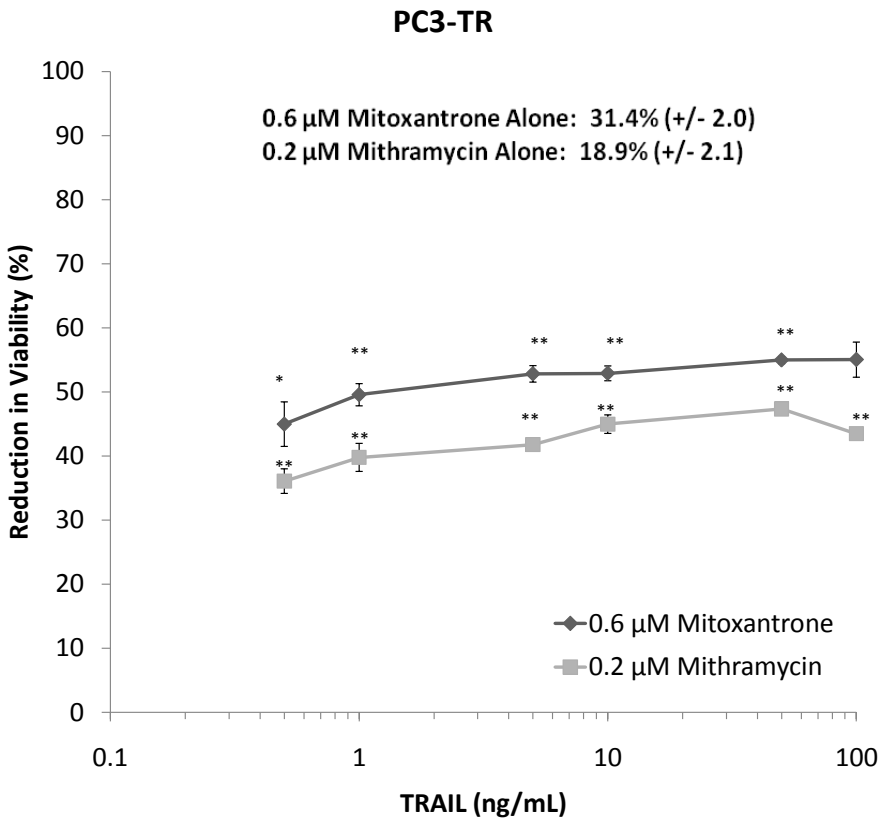


Figure 2.16 Dose response of TRAIL with single mitoxantrone and mithramycin concentrations in PC3-TR cells. Mitoxantrone treatments are shown as "dark grey diamonds" and mithramycin treatments are shown as "light grey squares". Comparisons were made between the single agent and combination treatments; asterisks (*) and (**) indicate p-values < 0.05 and < 0.01, respectively. Data are presented on a logarithmic scale for x-axis in the plot. Lines connecting data points are for visualization only.

The single agent treatment of 0.2 µM mithramycin resulted in a loss of viability of 18.9% (+/- 2.1%) of cells compared to untreated cells (**Figure 2.16**), which is also in good agreement with data shown in **Figure 2.7**. As expected, the loss of cancer cell viability upon treatment with single-agent 0.6 µM mitoxantrone and 0.2 µM mithramycin was less than 50%, since these are less efficacious than the combination treatments. These single-agent concentrations were chosen to investigate the efficacy of different TRAIL doses,

which were varied from 0-100 ng/mL (**Figure 2.16**). Over the concentration range studied for TRAIL, the overall reduction in cell viability between the lowest (0.5 ng/mL) and highest (100 ng/mL) TRAIL concentrations increases by only 10% for both drug treatments, indicating that lower TRAIL doses (e.g. 10 ng/mL) may possess sufficient activity in the current combination treatments.

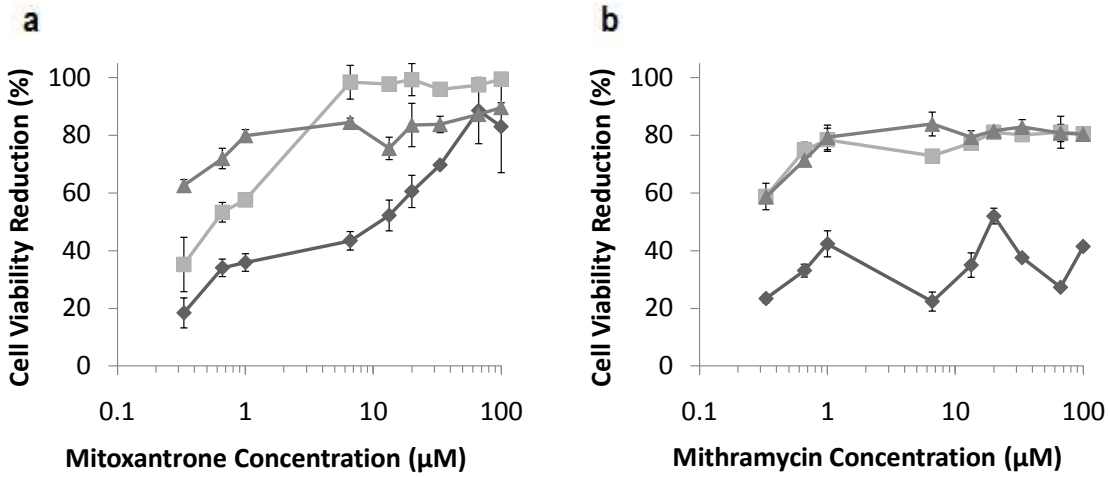


Figure 2.17 Comparison between different treatment methodologies in PC3-TR cells. (a) Mitoxantrone (b) and mithramycin in PC3-TR prostate cancer cells. Single-agent treatments are shown as "dark grey diamonds", sequential combination treatments with 10 ng/mL of TRAIL are shown as "light grey squares" and simultaneous combination treatments with 10 ng/mL of TRAIL are shown as "grey triangles". Data are presented on a logarithmic scale for x-axis in the plots Lines connecting data points are for visualization only.

Sequential vs. Simultaneous Combination Treatments. In the previous experiments, combination treatments were performed in a sequential format by first treating cells with a sensitizing drug for 24 hours, removing the drug from the cells, and then applying a TRAIL treatment for an additional 24 hours. An alternate combination treatment methodology is to apply both the sensitizing drug and TRAIL "simultaneously" in which

both, the drug and TRAIL are administered together. In our hands, simultaneous treatments with mitoxantrone demonstrated a higher loss of PC3-TR cell viability for low concentrations of the drug compared to the sequential treatments (**Figure 2.17**). However, this trend is reversed at higher drug concentrations.

The overall increase in loss of cancer cell viability between the lowest concentration of mitoxantrone (0.33 μM) and the highest concentration of mitoxantrone (100 μM) for the simultaneous treatments is about 25% (**Figure 2.17**), compared to 65% for sequential treatments. Interestingly, mithramycin did not show large differences in the loss of cell viability between the sequential and the simultaneous combination treatments. The difference between the two drugs and their dependence on treatment order is likely most closely related to the kinetics of how each drug is processed and how quickly the sensitization effect is achieved. In the case of mithramycin it is likely that the kinetics of sensitization are rapid and that even when the drugs are co-administered, there is sufficient time for the drug to sensitize the cells to TRAIL mediated apoptosis. On the other hand, it is possible that the kinetics of sensitization are slower for mitoxantrone and that the synergy between mitoxantrone and TRAIL is highest when the drug has sufficient time to overcome cellular resistances to TRAIL. We are currently following up on these observations in our laboratory.

Mitoxantrone-TRAIL and Mithramycin-TRAIL Combinations induce Apoptosis in PC3-TR Cells. In order to verify the induction of apoptosis, cells were treated with an annexin V and propidium iodide (PI) stain following incubation with single-agent and

combination drug treatment. The annexin V/PI stain distinguishes between apoptotic and necrotic cells based on fluorescence. In this assay, live cells will not fluoresce, early apoptotic cells fluoresce green, while late apoptotic and necrotic cells can fluoresce either red or demonstrate both red and green fluorescence. Images were acquired for single agent and combination treatments of mitoxantrone (**Figure 2.18**) and mithramycin (**Figure 2.19**) in PC3-TR cells. As expected, the live cell control and the 10 ng/mL TRAIL-alone treatment control demonstrated little to no fluorescence. Single agent treatment with mitoxantrone (0.33 μM) resulted in both apoptotic and necrotic cell populations, although the majority of the cell population consisted of live cells. The corresponding mitoxantrone-TRAIL simultaneous combination treatment results in a large population of apoptotic and necrotic cells (**Figure 2.18**), which also demonstrate changes in cell. Mithramycin treatments demonstrated similar trends and showed a clear decrease in cell population between single agent and combination treatments. This validates results shown in **Figure 2.7**. Overall, these results indicate that TRAIL-based combination treatments with mitoxantrone and mithramycin induce apoptosis in PC3-TR cells.

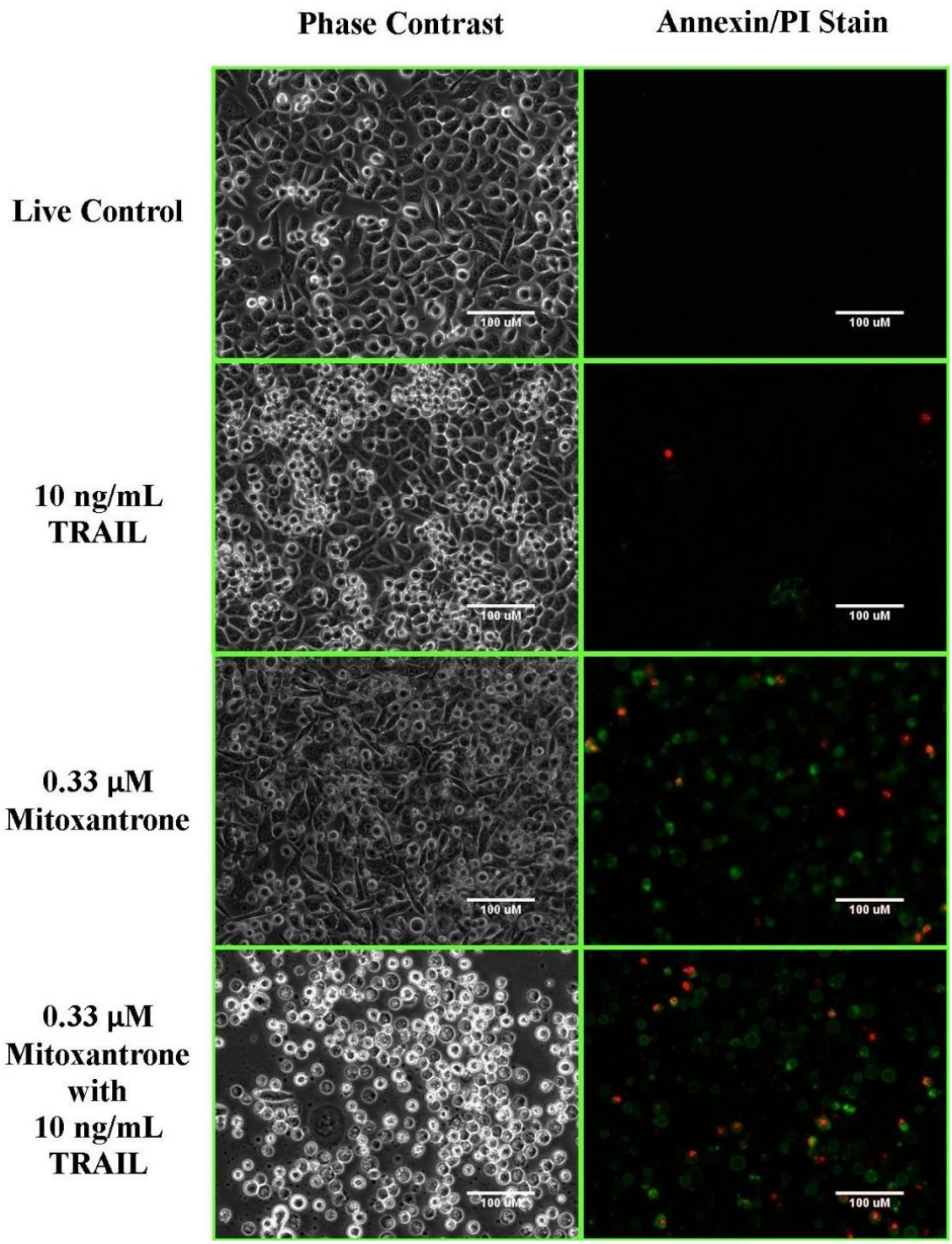


Figure 2.18 Microscopy images of mitoxantrone treated PC3-TR cells. Left panels are phase contrast images and right panels are fluorescence images visualized with an annexin V and propidium iodide stain. Apoptotic cells exhibit green fluorescence only. Dead cells can exhibit either lone red fluorescence or red and green fluorescence simultaneously. Live cells are non-fluorescent.

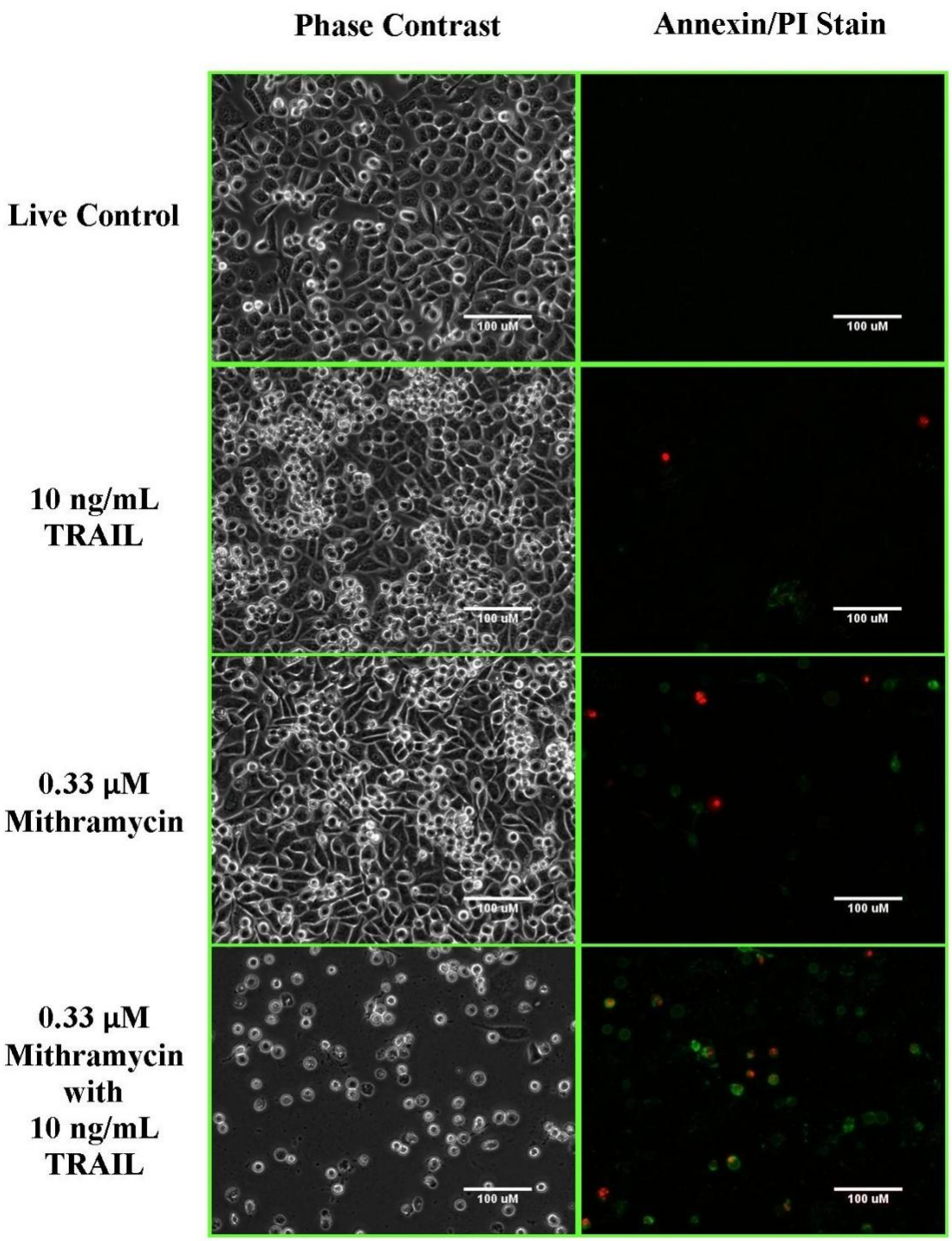


Figure 2.19. Microscopy images of mithramycin treated PC3-TR cells. Left panels are phase contrast images and right panels are fluorescence images visualized with an annexin V and propidium iodide stain. Apoptotic cells exhibit green fluorescence only. Dead cells can exhibit either lone red fluorescence or red and green fluorescence simultaneously. Live cells are non-fluorescent.

CONCLUSIONS

In the current study, fifty-five FDA- and foreign-approved antineoplastic drugs were screened in order to identify chemotherapeutic candidates that sensitized malignant prostate and pancreatic cells to TRAIL-induced apoptosis. The initial screen was performed using a TRAIL resistant prostate cancer cell line (PC3-TR) and several drugs were identified as potential sensitizing agents. The screen was able to identify drugs with previously unknown TRAIL sensitization activities in prostate as well as pancreatic and breast cancer cells, which can lead to the identification of new chemotherapeutic drug combinations and therefore potentially increase therapeutic options against these malignancies.

CHAPTER 3

DESIGN AND TESTING OF A PROGRAMMABLE HIGH-THROUGHPUT MICROFLUIDIC CELL ARRAY FOR COMBINATORIAL DRUG SCREENING

INTRODUCTION

As described in the previous chapter, using a sensitizing drug in combination with TRAIL can lead to an enhancement in the treatment of cancer cells in-vitro. When identifying drugs that can potentially sensitize cells to TRAIL-mediated apoptosis it is necessary to have screening system that can quickly and accurately identify drug candidates that demonstrate the desired effect. Additionally, the efficacy of chemotherapeutic drugs, as well as interaction between different drugs, is dose-dependent [124, 125]. The number of experiments that are necessary to identify and optimize lead drug candidates is quite large and so it is advantageous to have a system in which the experimental space can be covered rapidly. Traditionally, this need is met through the use of high-throughput screening equipment (e.g. high-throughput liquid handling systems [126]) but these systems are quite expensive and also still require large quantities of experimental material, most notably the drug solutions. One novel way of overcoming these limitations is through the use of high-throughput microfluidic devices [127, 128].

For the identification and optimization of effective combination treatments, a microfluidic platform that allows for the rapid generation of combinatorial concentration

gradients is necessary. It is also necessary that such treatments can be administered to cells and the effect of the treatments measured. Several groups have reported the development of microfluidic platforms capable of maintain cell cultures which allow for the investigation of cell responses and gene expression profiling [87, 129-131]. Additionally, other groups have also developed combinatorial mixing systems that accept multiple inputs and are able to generate combination gradients based on diffusive mixing [132, 133]. This chapter will describe the development and testing of a programmable microfluidic cell array that combines on-chip cell culture with on-chip generation of drug concentrations for combination drug treatment studies. This microfluidic device has 64 individual cell culture chambers in which, cells can be cultured and exposed to either sequentially or simultaneous combination treatments. Each of the 64 culture chambers is exposed to a different treatment thus creating a matrix of varying treatment conditions. Testing of this platform is first demonstrated by sensitizing PC3 prostate cancer cells to TRAIL-induced death using both doxorubicin and mitoxantrone which were both described in the previous chapter to be TRAIL sensitizing agents. Additionally, the performance of the device will be compared to that of the combinatorial drug treatments in a well-plate based experiment. These studies were done in collaboration with Texas A&M University. All experimental data collected using the microfluidic platforms was done by our collaborators at Texas A&M and data collected for well-plate based comparisons was done by our lab at Arizona State University.

METHODS

Cells Culture and Reagents

Human prostate cancer PC3 cells were cultured and propagated in RPMI medium with 10% fetal bovine serum and 1% penicillin/streptomycin (10000 units/mL penicillin, 10000 μg/μL streptomycin). Doxorubicin was purchased from MP Biomedicals and stored at a stock concentration of 3 mM. TRAIL was purchased from R&D Systems and reconstituted in PBS at a 10 μg/mL stock concentration in 50 μL aliquots to prevent multiple freeze/thaw cycles. Mitoxantrone was purchased from Sigma and stored at a stock concentration of 10 mM.

Design and Fabrication of Microfluidic Devices

Microfluidic devices were fabricated at Texas A&M University in the Materials Characterization Facility using routine soft lithography methods as previously described [134, 135]. The device consists of an upstream concentration generation module connected to an array of downstream cell culture chambers (**Figure 3.1**). The cell culture module consists of eight rows of chambers, each containing eight distinct culture chambers, for a total of 64 chambers. Access to each row of eight cell culture chambers is individually controlled using a valve array through a pneumatic channel allowing a specific drug concentration to be delivered to each row.

The microfluidic device consists of two PDMS layers: 1) a fluidic layer containing the micro-channels required for generating different concentrations of the drug and the cell

culture chambers, and 2) a pneumatic layer for controlling fluid access to cell culture chambers. The PDMS layer for the fluidic layer was 150 µm thick and was fabricated by casting the pre-polymer on a master mold, spinning at 1200 rpm for 1 minute, followed by curing the pre-polymer. The pneumatic layer for controlling the micro-chamber was 4 mm in thickness. The channel height for fluidic channels and cell culture micro-chambers was 100 µm, and the height of pneumatic layer for controlling the micro-chamber was 200 µm. Prior to replicating, the SU-8 mold was treated with tridecafluoro-1,2,2,2-tetrahydrooctyl-1-trichlorosilane so that PDMS membranes could be peeled from the SU-8 mold without damaging the membrane or the mold.

Microfluidic devices were assembled by exposing the different PDMS layers and glass slides to oxygen plasma (150 mTorr, 100 W, 40 sec) in a reactive ion etcher. Then, the fluidic layer membrane was aligned and bonded to the pneumatic layer. In order to enable actuation of the PDMS micro-chamber, tubing was connected to the pneumatic layer and vacuum was applied when the PDMS structure was bonded to glass to prevent irreversible bonding between the PDMS micro-chamber and the glass. Access ports were punched into the pneumatic layer prior to bonding to the fluidic layer. Holes for access to the fluidic layer were punched prior to bonding to the glass slide.

The valve array consisted of eight independently controllable valve groups, with each group containing eight valves that are operated simultaneously. The chamber regions can be isolated (or exposed) from fluid by lowering (or raising) a ~ 25 nL volume micro-chamber using a pneumatic source. The chamber valve system was designed such that the

center of the valve is fixed and only the boundary wall moves during operation. This is important because it minimizes the volume (~ 8 nL) of liquid lost during operation of the valve and alleviates pressure on cells.

Generation of Drug Concentrations in the Microfluidic Array

Different concentrations of drugs were generated in the array using a diffusive mixer in conjunction with a syringe pump and automatic valve synchronization system, depending on the specific experiment (**Figure 3.1**). For experiments involving the sequential exposure of cells to two drugs, a stock solution of the first drug (A) and a buffer solution were introduced into the inlets of a diffusive mixer to generate eight different drug concentrations ("horizontal gradient"). After a stable concentration gradient was attained (~60 sec), a valve set that control a row of eight cell culture chambers was opened for 10 sec and closed, capturing the drug containing solution in the culture chambers. Valves that control different rows of cell culture chambers were sequentially operated from row #1 to #8. After 24 hours of exposure to drug A, concentration gradients of the second drug (B) were generated by mixing a stock solution of drug B with a buffer solution at a specific flow rate to generate a single concentration of drug B. This stream of drug B was introduced upstream into both streams entering the diffusive mixer thereby making the mixer ineffectual. A single valve set that controls access to a row of eight cell culture chambers was opened for 10 sec and closed capturing the single concentration of drug B. By applying positive pressure to lower a PDMS barrier, pneumatically controlled chambers (i.e., a small area isolated from the surrounding regions) are formed and only the specified row of cell culture chambers is exposed to the drug combination. Different

concentrations of drug B are generated by changing the flow rate of the buffer and thereby diluting drug B to different levels. As a new concentration of drug B is fed into the device, a different valve set is operated to capture the new drug dilution. This process is continued until rows #1 through #8 are exposed to treatments. The concentrations of doxorubicin generated in the diffusive mixer for this study were 0.0, 0.9, 1.7, 2.6, 3.5, 4.2, 5.2, and 6.0 μM. The concentrations of mitoxantrone generated were 0.0, 1.4, 2.9, 4.3, 5.7, 7.1, 8.6, and 10 μM. The concentration range for TRAIL was 0.0, 2.9, 5.7, 8.6, 11.4, 14.3, 17.1, and 20.0 ng /mL. In these experiments doxorubicin and mitoxantrone individually represent drug A while TRAIL represents drug B.

For experiments where cells were simultaneously exposed to pair-wise combinations of two drugs, the diffusive mixer was used along with the syringe pump and automatic valve synchronization system (**Figure 3.1**). In this case, the diffusive mixer was used as described above to first generate eight concentrations of the drug A. Next, a single concentration of drug B was generated as described above and introduced upstream into both inlet streams of the diffusive mixer used for generating the concentration range of the first drug A (i.e., into streams containing the stock solution of drug A and its buffer). This combined solution (i.e., containing a stock concentration of A and a fixed concentration of B) was diluted in the diffusive mixer to generate 8 pair-wise concentrations. Since drug B is present at the same concentration in both inlet streams, its concentration is the same in all the streams exiting the diffusive mixer whereas drug A forms a gradient of eight concentrations. This arrangement generates eight pair-wise combinations (i.e., eight concentrations of drug A (A_1 to A_8), each with a single

concentration of drug B, ΔB_1) used to expose cells cultured in one row of culture chambers to the treatments (**Figure 3.1**). Valve sets are controlled as described above in order to isolate a single row of culture chambers to the pair-wise combination.

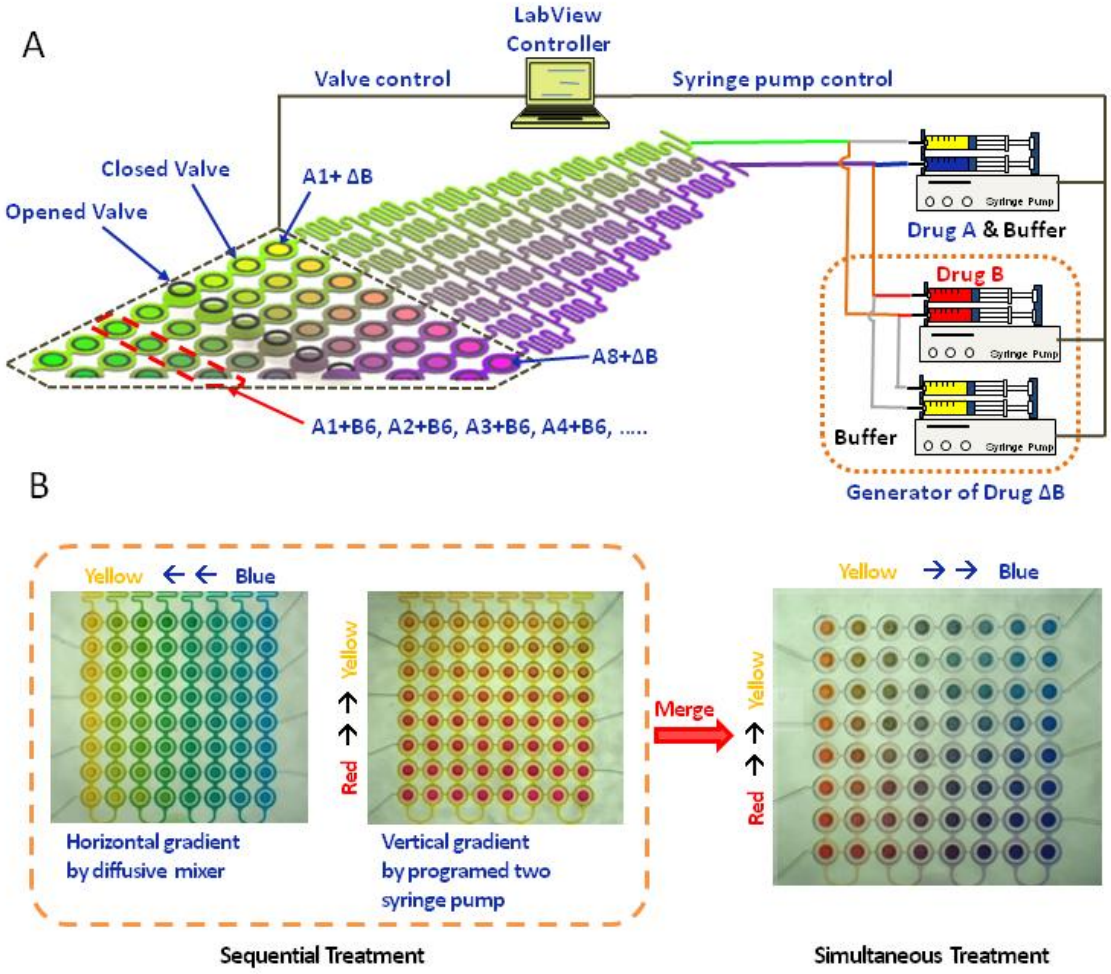


Figure 3.1 Microfluidic control and gradient generation. A) Schematic of the microfluidic device, valve control, and syringe pump control systems. A concentration gradient for Drug A is generated using the on-chip diffusive mixer. The concentration gradient for Drug B is controlled using LabView through the manipulation of both the syringe pump and valve control systems. B) Representative images of dye-based concentration gradients and the combinatorial treatment methodologies associated with each gradient.

Different concentrations of drug B are generated by changing the flow rate of the buffer and thereby diluting drug B to different levels (ΔB_1 through ΔB_8). A stream containing a second concentration of drug B (e.g. ΔB_2) is mixed with eight concentrations of drug A (A_1 to A_8) to generate a second set of eight pair-wise concentrations ($A_1 + \Delta B_2$, $A_2 + \Delta B_2$, etc) and used to expose a second row of cell culture chambers to a unique pair-wise drug combination. As a new pair-wise concentration is generated, a different valve set is operated to capture the new treatment. This process is continued until to generate eight different concentrations of drug B (ΔB_1 to ΔB_8), with each concentration of drug B being mixed with eight concentrations of drug A. Thus, this scheme resulted in the generation of 64 pair-wise concentrations of drugs A and B. The concentrations of doxorubicin, mitoxantrone, and TRAIL used for generating the pair-wise combinations are as given above.

Operation of the syringe pumps and the valve array was carried out using a programmable LabView (Austin, TX) interface (**Figure 3.1A**). Each group of valves (controlling a single row of eight cell culture chambers) in the valve array was individually opened or closed by applying vacuum and compressed air through a single port on the pneumatic controller. Since different valve groups were connected to different ports on the pneumatic controller, each valve group could be operated without affecting other valve groups. This facilitated exposing cells in only a specific row to a given drug combination.

Cell culture in microfluidic devices

The glass slides (bottom) in all devices were coated with 50 μg/mL collagen I (BD Biosciences, San Jose, CA) for 16 h at 4ºC and excess collagen I was removed by rinsing with 500 μL of RPMI medium. PC3 cells were seeded in each chamber using the LabView controlled syringe pump and pneumatic controller. The pneumatically controlled chambers were formed as described above by applying positive pressure to lower a PDMS barrier which resulted in a small area being isolated from the surrounding regions. When this operation was performed with a cell suspension (~ 5 x 10^6 cells/mL) flowing through the device, cells were trapped in specific locations (i.e., in a single row). Cells were captured in each chamber sequentially from bottom to top (row #8 to row #1) for ~ 2 sec each at a total flow rate of 2 mL/h (or a flow rate of 0.25 mL/h) to ensure uniform cell seeding. Cells that were excluded from the culture chamber were washed out. Seeded cells were allowed to attach onto the collagen-coated glass surface and proliferate for 24 h. To support growth of PC3 cells, RPMI medium was refreshed in each chamber every 3 h using the procedure described above. After 24 h, cells were exposed to different drugs either sequentially or simultaneously as described. The growth medium in each chamber (containing a specific drug combination treatment) was replenished every 3 h for the duration of the experiment. Prior to each round of media refreshment, the channels were washed with buffer for 30 sec to remove any residual drug in the media present outside the cell culture chambers. The entire set of operations – generation of drug combinations, trapping of cells in the culture chambers, and perfusing cells with drug-containing medium –was carried out over several days by automatically

controlling the opening/closing of valves through the LabView interface without any manual intervention.

At the end of drug treatment, cells in each of the drug-treated cell culture chambers were stained with calcein AM and green-fluorescent cells were counted. The cell viability after treatment was determined as the ratio of number of live cells in each drug-treated chamber to the number of live cells in the untreated control. Since dead cells are likely to be washed away with the periodic media change, the number of dead cells was not enumerated. Thus, this approach provides an indicator of loss of viability of cancer cells in the device.

The efficacy of sequential and simultaneous treatments were compared analytically using LC_{50} value analysis. The LC_{50} values were approximated by drawing a best fit curve between data points on a concentration versus cell viability graph; the LC_{50} value is the concentration at which the curve intersected 50% viability.

Cell experiments in well plates

Well plates (96 wells/plate) were pretreated with 50 μg/mL of collagen I per well for 12 h at 4°C and excess collagen was removed. Cells were plated at a density of 8,400 cells/well and incubated at 37°C and 5% CO_2 for approximately 24 h. For sequential exposure treatments, cells were first treated with a sensitizer drug for 24 h. The media was then removed, replaced with fresh serum-containing media, and the cells were treated with TRAIL. Cells were incubated for an additional 24 h after which cell viability

was assessed using the calcein AM stain as described above. Simultaneous exposure treatments were carried out by treating cells with the sensitizer drug and TRAIL at the same time for 24 h at which point, calcein AM was used to determine viability.

RESULTS AND DISCUSSION

Characterization of concentration gradients in the device. Using colored dyes, two types of concentration gradients can be generated in the microfluidic device as shown in **Figure 3.1B**. The most basic concentration gradient is generated by mixing two streams in a standard diffusive mixer [136]. This is demonstrated in **Figure 3.1B (left panel)** where yellow and blue color dye solutions (representing the minimum and maximum concentrations of a drug) were injected through the two inlets of a diffusive mixer and resulted in eight outlet concentrations ("horizontal gradient" of colors between yellow and blue) were generated. In this arrangement, each cell in a row of culture chambers has a different drug concentration and this pattern is repeated in all the rows. This arrangement represents the gradient used in experiments where cells were exposed to the first chemotherapeutic agent of a sequential treatment (i.e. exposure to eight concentrations of drug A).

The second type of concentration gradient was generated through control of the syringe pump and automatic valve synchronization system as described in Methods. This is shown in **Figure 3.1B (middle panel)** where yellow and red streams (representing the minimum and maximum concentrations of the second drug) were mixed together to generate a "vertical gradient" of colors between yellow and red. In this arrangement, each cell in a row of culture chambers has the same drug concentration which varies between rows. This arrangement represents the gradient used in experiments where cells were

exposed to the second chemotherapeutic agent of a sequential treatment (i.e. exposure to eight concentrations of drug B).

The final concentration gradient was generated by merging the two color gradients (vertical direction concentration gradient: yellow to blue; horizontal direction concentration gradient: yellow to red) as described in Methods to yield an array of pair-wise combinations. This arrangement represents the gradient used in experiments where cells were simultaneously exposed to two chemotherapeutic drugs at eight concentrations each, for a total of 64 pair-wise concentrations (**Figure 3.1B right panel**).

The sequence of steps involved in operation of the microfluidic device is shown in **Figure 3.2**. Violet dye was initially flowed through the channels with the cell chambers closed so that no violet dye was captured in the cell culture chambers and only present outside the cell chamber area (**Figure 3.2A**). Next, the cell culture chambers were opened to trap violet dye as described in Methods (**Figure 3.2B**) in a manner that emulates cell seeding in the device. A concentration gradient between yellow and blue dyes was established in the diffusive mixer and the solution was trapped in the cell culture chambers by opening the valve that controls a specific set of chambers for 10 sec. This is shown in **Figure 3.2C** where the top three rows have a dye solution trapped inside the chambers, and in the fourth row where the violet dye is being replaced with the dye solution gradient; the four lower rows still have violet dye in them.

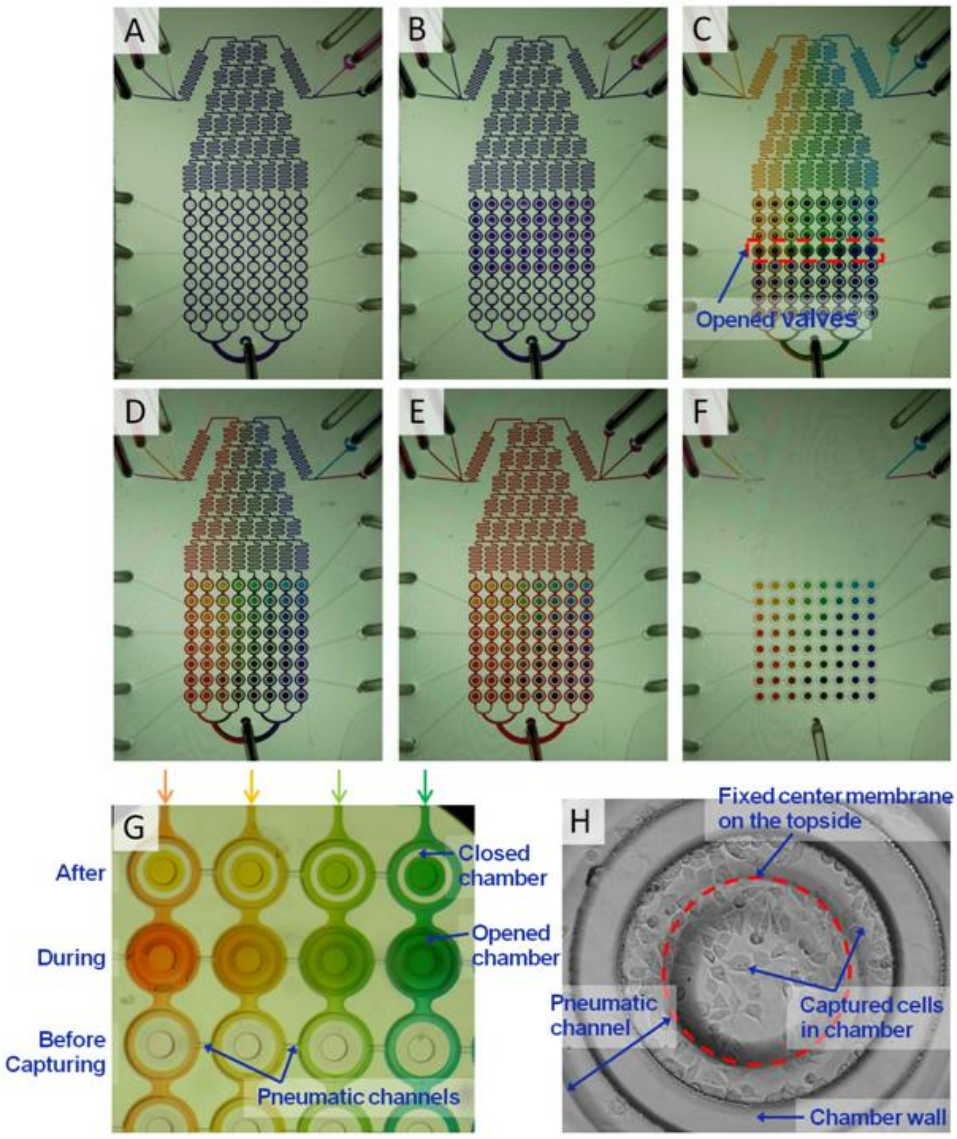


Figure 3.2 Representative images of the microfluidic device and its operation visualized using colored dyes. A) A single concentration of violet dye is pumped into both inlets of the microfluidic device. The valve system holds the culture chambers closed isolating the chambers from the dye. B) The top five culture chamber rows are individually opened, given time to fill, and closed thereby capturing and isolating the dye. C) Yellow and blue dyes are fed into opposite inlets of the device forming a horizontal gradient. This gradient is then trapped in each of the eight rows of cell culture chambers where the fourth row shows an open valve set. D) "Merging" of horizontal and vertical concentration gradients. A single concentration of pre-diluted orange dye is mixed with yellow and blue dyes at both inlets. One row of culture chambers is opened and the gradient mixture is captured. The inlet concentration of the orange dye is changed and the process is repeated until all chamber rows are filled. Captured treatments remain isolated and unaffected by E) flowing orange dye and F) empty channels. G) Operation of the pneumatic valve control system demonstrating chambers before, after, and during trapping. H) A representative chamber with cultured PC3 cells.

The “merging” of horizontal and vertical gradients to generate an array of pair-wise concentrations was carried out as described below. Red and yellow dyes were mixed at a ratio of 7:1 (i.e., mimics generation of a single concentration of drug B) (**Figure 3.1A**) and the resultant orange dye stream was added to the blue and yellow streams upstream of the gradient mixer. The color (ranging from violet to orange) was used to replace the blue-yellow color solution in a single row of the cell culture chambers as described in Methods. This step was repeated with a range of red and yellow dye mixtures until each row of culture chambers was filled. **Figure 3.2D** shows the resultant array of colors trapped in the device, with each color representing a single pair-wise concentration of two drugs automatically generated using the LabView-controlled system. Next, the entire channel was filled with orange dye to mimic the media flowing around the cell culture chamber. No mixing between the outside orange solution and the solution trapped inside the chambers was observed after 24 h (**Figure 3.2E)**. The color dyes trapped in the chamber without any liquid surrounding it is shown in **Figure 3.2F**. The operation of the pneumatically controlled trapping system is demonstrated in **Figure 3.2G** using color dyes. Three sets of chambers are shown: empty chambers prior to trapping of color dye solution, chambers during trapping, and chambers after trapping of solution. Before trapping, each chamber is empty and liquid flows around the closed chamber without entering. This demonstrates the fidelity of the valve system in trapping liquid and maintaining it separate from the surrounding liquid.

Most microfluidic systems [129, 137] using a diffusive mixer need continuous perfusion of two components to generate and maintain concentration gradients. However, the

pneumatically-controlled system in our device does not require continuous perfusion for keeping cells exposed to concentration gradients. This approach has several advantages. First, it minimizes the amount of drug used per experiment, which is significant considering that the compound libraries used for screening typically contain limited amounts of material and are expensive. Second, cells cultured in the chamber are not exposed to significant shear stress continuously as the time required for trapping solutions inside the cell culture chamber is only ~10 sec. Therefore, this system would be especially advantageous when working with cells (e.g. primary cells) that are sensitive to shear stress. Moreover, different concentration gradients (e.g., non-linear or exponential concentration gradient) can be easily generated by programming the Labview interface which gives the system flexibility in designing drug screening experiments.

Cell culture in the microfluidic device. The prostate cancer cell line PC3 was used for these studies. PC3 cells were captured in the array of cell culture chambers and maintained for 24 h (with media refreshed every 3 h) in a 5% CO_2 incubator at 37°C for adaptation to the microfluidic environment prior to drug exposure. PC3 cells proliferated in the device and were not adversely affected by the microfluidic environment for 5 days (not shown). **Figure 3.2H** shows a representative cell culture chamber with PC3 cells grown for 24 h.

Sequential treatment with TRAIL sensitizer drugs and TRAIL. The microfluidic cell array was used to investigate the effect of the combinatorial treatment of chemotherapeutic drugs and TRAIL on the viability of PC3 human prostate cancer cells.

PC3 cells were cultured on-chip and exposed sequentially to different concentrations of doxorubicin and TRAIL or mitoxantrone and TRAIL. In these treatments, the second drug treatment (e.g. TRAIL) is administered after a 24 h treatment of a first drug dose (e.g. doxorubicin or mitoxantrone). In order to carry out sequential treatments, PC3 cells were first exposed to different concentrations of doxorubicin or mitoxantrone as listed in Methods. These concentrations were chosen based on their effect on PC3 cells [138] and were chosen such that they spanned both sides of the previously identified optimum concentration (3 μM for doxorubicin and 5 μM for mitoxantrone).

Different concentrations of drugs were generated by mixing two streams containing 0 and 6 μM doxorubicin or 0 and 10 μM mitoxantrone using the diffusive mixer described in **Figure 3.1**. After 24 h exposure to doxorubicin or mitoxantrone, a gradient of 0 – 20 ng/mL TRAIL was generated and sensitized cells were exposed for an additional 24 h. The cell viability after 24 h exposure to TRAIL was determined as described in Methods. **Figure 3.3** shows representative fluorescent images from the array of cells chambers in a single experiment. The data in the insets (**Figure 3.3B**) show that cells not exposed to either doxorubicin or TRAIL have proliferated and are confluent in the cell culture chamber (top left). Exposure to 6 μM of either doxorubicin (top right) or 20 ng/mL of TRAIL (bottom left) alone demonstrate a small loss of viability whereas cells that were exposed sequentially to 6 μM doxorubicin followed by exposure to 20 ng/mL TRAIL have very few live cells. Images for only the doxorubicin/TRAIL combination are shown, and similar results were obtained with the mitoxantrone/TRAIL combination as well.

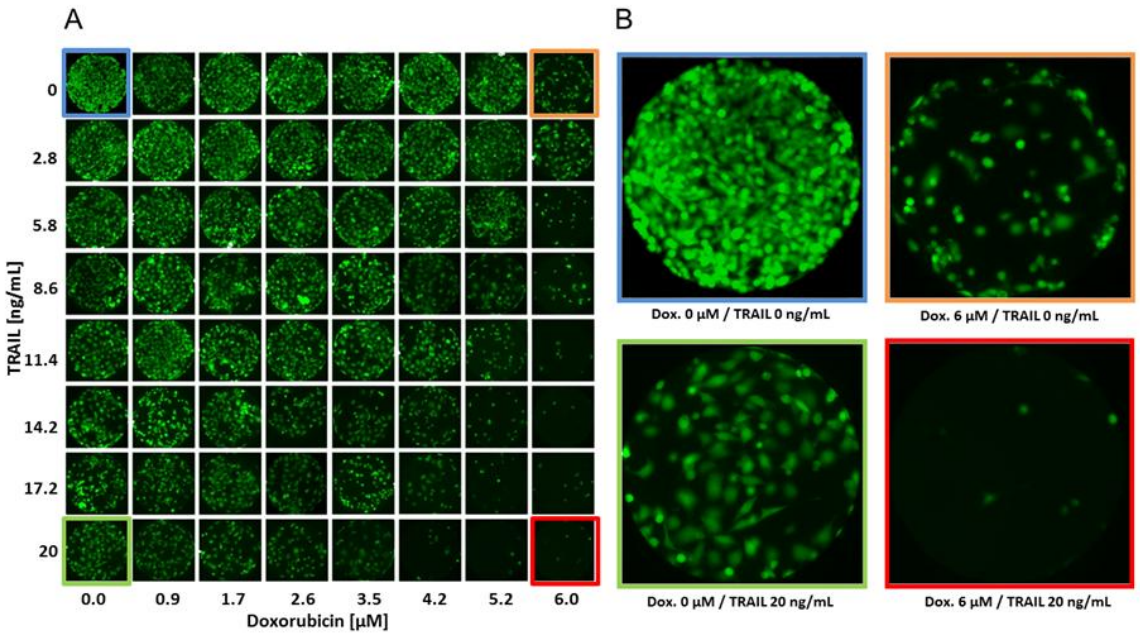


Figure 3.3 Representative fluorescent images of Calcein AM stained PC3 cells following sequential treatments. A) Cells were treated with 64 unique treatment combinations of doxorubicin (0-6 μM) and TRAIL (0-20 ng/mL). B) Enlarged images of selected treatment conditions including: No Treatment (top left), 6 μM single-agent doxorubicin (top right), 20 ng/mL TRAIL single agent (bottom left), and the combination treatment of 6 μM doxorubicin and 20 ng/mL TRAIL (bottom right).

The fraction of live cells in the different cell chambers was determined as described in Methods. **Figure 3.4A** shows that exposure to TRAIL alone without doxorubicin sensitization led to a dose-dependent decrease in cell viability, with ~40% decrease in viability at the highest concentration tested (20 ng/mL). Doxorubicin by itself also induces a loss in PC3 cell viability as seen from a dose-dependent decrease in cell viability even in the absence of TRAIL (**Figure 3.4A**). The effect of sensitization is evident from the data on PC3 cell exposure to 2.6 μM of doxorubicin. The cell viability decreases from ~ 60% in the absence of TRAIL to ~5% with an increase in the concentration of TRAIL. This extent of decrease is smaller at lower and higher doxorubicin concentrations, as may be expected. In the former case, the concentration of

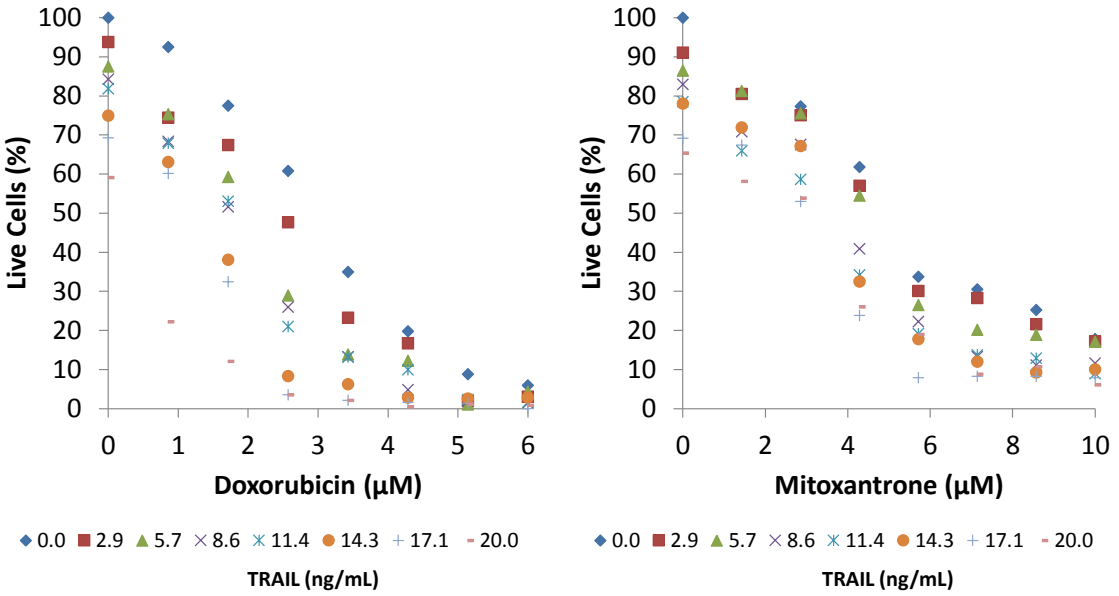


Figure 3.4 Sequential combination treatments with the microfluidic platform. Cells were culture in the microfluidic device and exposed to A) doxorubicin and B) mitoxantrone for 24 hours. After this period, the initial drug treatments were removed and the cells were treated with TRAIL for an additional 24 hours. Fluorescent microscopy was then used to count cells labeled with Calcein AM.

doxorubicin used is not sufficient to fully sensitize cells to TRAIL-mediated cell death whereas in the latter case, doxorubicin by itself decreases cell viability (**Figure 3.4A**). Since the objective of combination therapy is to achieve maximum possible decrease in cell viability with the lowest concentration of sensitizer or chemotherapeutic molecule, sensitizing PC3 cells with ~3 μM doxorubicin followed by exposure to ~14 ng/mL of TRAIL is sufficient to reduce cell viability by ~95%. Sensitization with mitoxantrone prior to TRAIL exposure was somewhat less effective than doxorubicin, with a maximum decrease from ~65% to 20% cell viability when PC3 cells were sensitized with 4.3 μM of mitoxantrone (**Figure 3.4B**). This indicates that doxorubicin was a marginally more effective sensitizer than mitoxantrone in these *in vitro* investigations. These results are

along the lines of what is anticipated, since different drugs will possess differential activities depending on the cancer cell lines investigated [138].

Simultaneous treatment with TRAIL sensitizer drugs and TRAIL. PC3 cells were also simultaneously exposed to 64 pair-wise concentrations of doxorubicin and TRAIL or mitoxantrone and TRAIL in the microfluidic device. Pair-wise concentrations were generated as described in Methods and as demonstrated in **Figure 3.3** with color dyes. PC3 cells were exposed to different concentration pairs for 24 h. The media in the cell chambers was replenished with fresh media with a specific pair-wise combination of the two drugs (doxorubicin or mitoxantrone, along with TRAIL). **Figure 3.5A** shows that PC3 cells exposed simultaneously to pair-wise combinations of doxorubicin and TRAIL for 24 h demonstrate a dose-dependent decrease in cell viability. However, the decrease in cell viability observed with this treatment was less than that observed with sequential exposure to doxorubicin and TRAIL. The decrease in cell viability upon simultaneous exposure to 2.6 μM of doxorubicin and 20 ng/mL of TRAIL was only 50% (**Figure 3.5A**), compared to the 95% decrease observed with the sequential exposure to the two drugs at the same concentrations (**Figure 3.4A**). Similar results were also observed with simultaneous exposure of PC3 cells to mitoxantrone and TRAIL (**Figure 3.5B**); for example, the decrease in cell viability with 4.3 μM of mitoxantrone and 20 ng/mL of TRAIL was only ~ 40% as compared to the 80% decrease seen with sequential treatments (**Figure 3.4B**). However, a higher decrease in PC3 cell viability was observed at the higher concentrations of both doxorubicin and mitoxantrone although this is undesirable

since the goal is to achieve the highest level of cell death while minimizing the overall treatment concentrations.

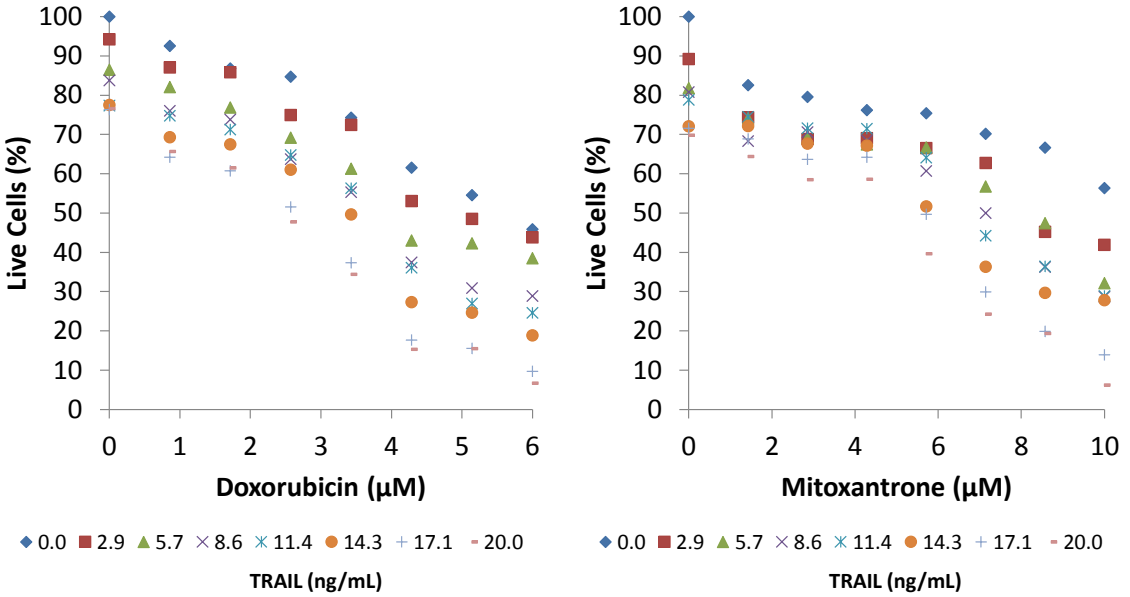


Figure 3.5 Simultaneous combination treatments with the microfluidic platform. Cells were culture in the microfluidic device and exposed to A) doxorubicin and B) mitoxantrone mixed with TRAIL for a total of 24 hours. Fluorescent microscopy was then used to count cells labeled with Calcein AM.

We performed an LC_{50} analysis in order to further compare simultaneous and sequential treatments in the microfluidic device (**Table 3.1**). In this analysis, the dose of chemosensitizer drug (either doxorubicin or mitoxantrone) required for inducing death in 50% of the PC3 cell population was determined for each concentration of TRAIL employed. As expected, the LC_{50} value decreases for both sensitizer drugs as the TRAIL concentration increases both for simultaneous and sequential treatments. In all cases, the LC_{50} value of doxorubicin is marginally higher than that of mitoxantrone, although they are in the same order of magnitude (low micromolar range). As seen in **Table 3.1**, LC_{50}

values for both drugs are lower in the case of sequential treatments compared to simultaneous treatments, as discussed previously.

Table 3.1 Summary of LC_{50} value analysis for microfluidic based treatments.

	Sequential Treatment		***Simultaneous Treatment***	
TRAIL (ng/mL)	**Doxorubicin (μM)**	**Mitoxantrone (μM)**	**Doxorubicin (μM)**	**Mitoxantrone (μM)**
0	3.2	5	5.6	11
2.9	2.5	5	5	8
5.7	2.2	4.6	4.2	8
8.6	1.9	3.8	3.8	7.1
11.4	1.9	3.5	3.8	6.8
14.3	1.5	3.4	3.4	5.8
17.1	1.4	3.4	2.8	5.7
20	0.4	3.5	2.6	5.2

Taken together, these results are consistent with our previous findings in well-plate screens, which indicated that sequential treatments of mitoxantrone resulted in higher efficacies of TRAIL sensitization compared to those observed with simultaneous treatments [138]. It is possible that mitoxantrone needs a long time for sensitization activity and that it is necessary to treat cells with the drug for 24 hours, and also with TRAIL for an additional 24 h. It is still important to note that the microfludic device can be operated in a sequential as well as simultaneous drug treatment format, which makes this a powerful platform for screening as well as end-point and transient dosing studies. The fact that there are significant differences in drug efficacy depending on how the drug combinations are applied shows that both concentration gradients and combination

methods have to be investigated to test the full potential of drugs. While this significantly increasing the number of experiments that needs to be conducted, it further underscores the necessity of a high-throughput screening platform such as the presented microfluidic array.

The utility of the microfluidic array is clearly evident from the PC3 viability data. While a maximum decrease in cell viability can be achieved by simply using high concentrations of doxorubicin, mitoxantrone, or TRAIL, this is undesirable as the side effects observed with use of high drug concentration often outweigh the benefits. Since combination therapy seeks to identify the lowest concentrations where maximum possible cancer cell death is achieved, the ability to generate different dose-response curves in a high-throughput manner is of significant interest.

Comparison of microfluidic device and well plate cultures. The results obtained with the microfluidic device were compared against those obtained from exposing PC3 cells to the different drugs under the two treatment regimes (sequential and simultaneous) in a 96-well plate. **Figure 3.6** and **Figure 3.**7 show the results of these comparisons with doxorubicin and mitoxantrone respectively. In general, the combination treatments in the device lead to a smaller losses of PC3 cell viability than those in well plates. While sequential treatment efficacies were more comparable between the two formats, the differences were more pronounced for simultaneous exposure to a sensitizer drug and TRAIL. Similar observations can be made for LC_{50} values of the two drugs determined in

96-well plates and the microfluidic device (**Table 3.2**). For the two conditions tested, the values were in the low micromolar range in the device.

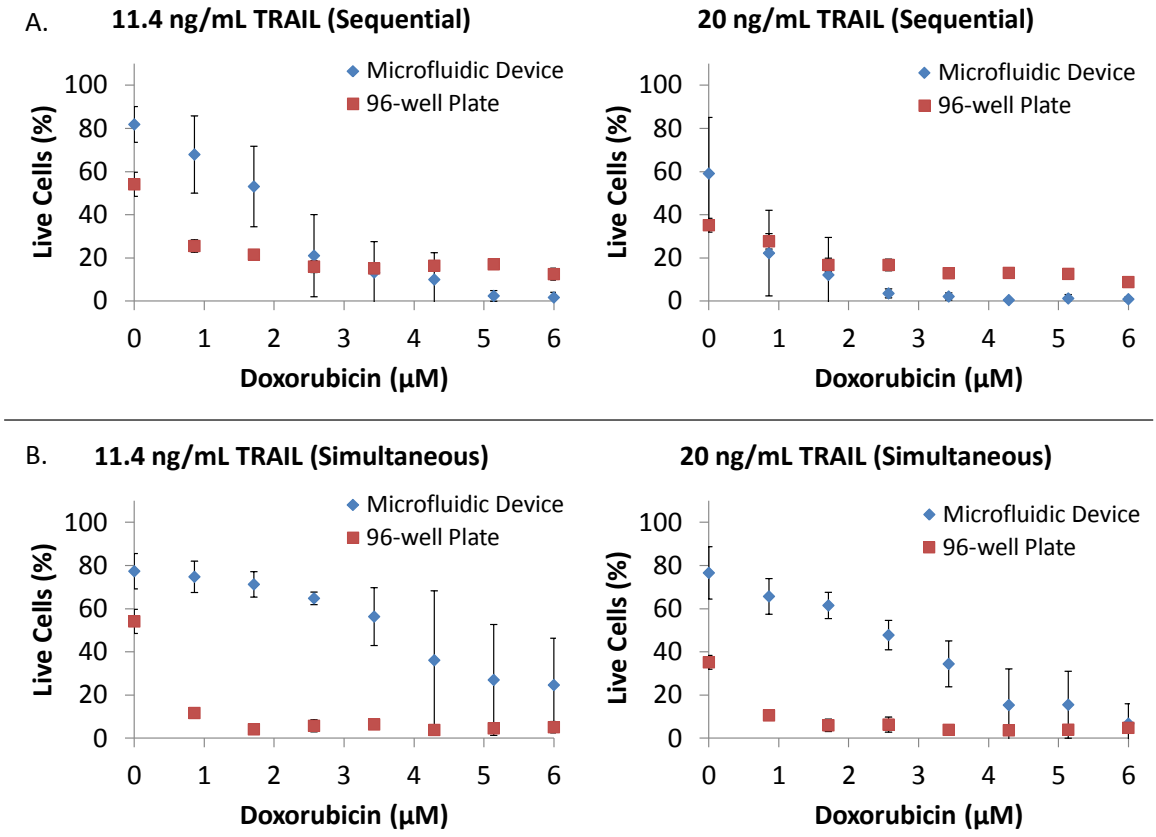


Figure 3.6 Comparison between microfludic based results and 96-well plate based results for doxorubicin. Cells were treated with equivalent doses of doxorubicin for two concentrations of TRAIL in both A) sequential and B) simultaneous combination treatments.

Several factors could possibly contribute to the difference in drug efficacy between the two formats. First, the microfluidic device was operated with periodic media replenishment every 3 h (i.e. in a fed-batch mode) and removal of waste products whereas nutrients were not replenished and waste product levels build up for the duration of the experiment in the well plate cultures. Given that these treatments typically occur

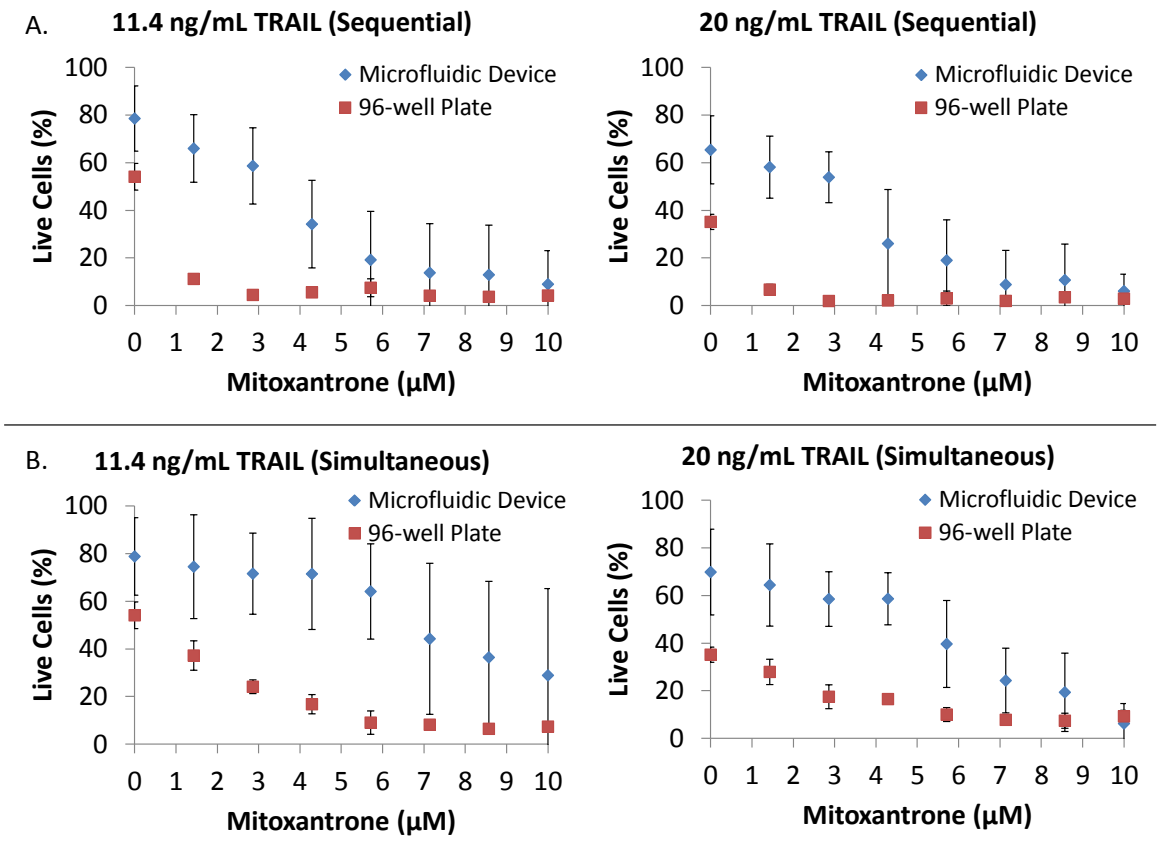


Figure 3.7 Comparison between microfludic based results and 96-well plate based results for mitoxantrone. Cells were treated with equivalent doses of mitoxantrone for two concentrations of TRAIL in both A) sequential and B) simultaneous combination treatments.

over a period of 24-48 hours, it is possible that the addition of fresh nutrients and/or removal of waste products lead to the lower drug efficacy (or higher cancer cell viability) seen in microfluidic devices. Second, the high local concentrations of growth factors present in the microchannel environment could also lead to an increase in cell viability as compared to the macro-scale well plate cultures [139]. Third, the cell density (number of cells per unit area) is different between the two systems (higher in the device compared to the well plate system), which can potentially contribute to the higher growth rate and cell viability observed in the device. It is also possible that the absorption of drug molecules

Table 3.2 Summary of LC_{50} value analysis for microfluidic device based and 96-well plate based treatments.

	LC_{50} Values (Sequential Treatment)			
	Microfluidic Device		***96 Well Plate***	
TRAIL (ng/mL)	**Doxorubicin (μM)**	**Mitoxantrone (μM)**	**Doxorubicin (μM)**	**Mitoxantrone (μM)**
11.4	1.9	3.5	< 0.9	< 1.4
20	0.4	3.5	NA	NA

	LC_{50} Values (Simultaneous Treatment)			
	Microfluidic Device		***96 Well Plate***	
TRAIL (ng/mL)	**Doxorubicin (μM)**	**Mitoxantrone (μM)**	**Doxorubicin (μM)**	**Mitoxantrone (μM)**
11.4	3.8	6.8	< 0.9	0.7
20	2.6	5.2	NA	NA

into PDMS [140] leads to the difference between the two systems. However, this effect is likely to be minimal as we perfused collagen through the channels prior to seeding, which would reduce absorption of drugs into the PDMS [141]. Secondly, fresh medium containing the drug molecule was perfused through the channels every 3 h over the duration of the experiment, which would be expected to saturate the PDMS and minimize absorption at later time points. Nevertheless, it is not possible to completely eliminate the possibility that absorption of drugs in the PDMS leads to decreased drug efficacy. It is important to note that despite the differences between the microfluidic device and the well plate culture, the microfluidic device does capture the synergy between doxorubicin and TRAIL and mitoxantrone and TRAIL combination treatments, indicating the utility of this approach, for both screening and dosing studies. As with any screening

methodology, additional lead validation methods will be necessary when selecting leads from microfluidic device based studies.

CONCLUSIONS

We developed a microfluidic cell array capable of generating different concentrations and 64 pair-wise combinations on-chip in a fully automated process while exposing cells cultured on the device to the generated combinations. The cell culture array was used to screen and optimize combinatorial drug treatments against PC3 prostate cancer cells. While the utility of this device has been described and characterized using chemotherapeutic drugs as sensitizer for TRAIL-induced cell death, this work can be extended to identifying combinatorial drug treatments for a variety of diseases. The ability to carry out sequential and simultaneous combination treatments also facilitates exploration of diverse toxicological and biological dosing studies.

CHAPTER 4

MECHANISTIC INVESTIGATION OF THE TRAIL-SENSITIZATION ACTIVITY OF MITOXANTRONE

INTRODUCTION

Up to this point, the work presented has primary focused on the identification and optimization of treatment methodologies designed to incorporate repositioned drugs. Through screening of the JHCCL and the design/testing of the high-throughput microfluidic cell array, the effect of several drugs in novel treatment strategies has been shown. However, these previous studies have not focused on understanding the underlying biological mechanism of these treatment strategies. Understanding these mechanisms is of high importance since it gives a fuller understanding of the therapeutic process which can facilitate the identification of ways the treatment can be improved and enhanced [14, 142-144]. For example, the identification of biological markers specific to malignant cells can provide researchers a therapeutic targets that help limit damage to healthy tissue [145, 146]. Similarly, by understanding the mechanisms behind a drug's effect, it is possible to develop strategies that help enhance the efficacy of the drug [147]. These mechanisms can also provide a more directed approach to the identification of new therapies by providing insight into what drug activities are important. This information can be used to identify drugs that have similar activities which can then be tested for their efficacy [148-150]. Although our studies focus on the repositioning of old drugs, the mechanistic effects of specific functional groups can also be determined and this

information can used to synthesize new drugs designed to enhance positive (or reduce negative) drug effects [151, 152]

This chapter describes the mechanistic evaluation of mitoxantrone's TRAIL sensitization activity. In chapter 2 mitoxantrone was identified as a potent TRAIL sensitizing agent during a screen of several FDA-approved compounds. This chapter will being with an initial mechanistic characterization of the drug, and include measuring the ability of the drug to induce mitochondrial depolarization and generate reactive oxygen species (ROS) in several different cell lines using a range of treatment concentrations. The results from these studies suggested that the loss in mitochondrial membrane potential occurs prior to the generation of ROS but that both events occurred within 6 hours of the initial treatment. The information presented in this chapter will then expand on these initial mechanistic and kinetic experiments in an effort to fully elucidate the cellular mechanism responsible for mitoxantrone's TRAIL sensitization activity. Cell viability, following treatments of mitoxantrone/TRAIL, was evaluated at 30 mins, 2, 6, and 24 hours to determine how early mitoxantrone mediated, TRAIL sensitization would occur. These results suggested that the sensitization event occurred very early (30 mins- 2 hrs). Based on our and other's results, it likely that mitoxantrone facilitates the generation of ROS, which are known to have TRAIL-sensitizing activities including the up-regulation of pro-apoptotic proteins (cytochrome C [153], DR5 [154]) and the down regulation of anti-apoptotic proteins (c-FLIP [155], XIAP [116]). Experiments designed to implicate ROS in the sensitization activity represent the latter body of work in this chapter. These studies will attempt to demonstrate the importance of ROS in mitoxantrone's TRAIL-

sensitizing activity by limiting the concentration of ROS using the ROS scavenger N-acetylcysteine (NAC). Additionally, the drug pixantrone, a mitoxantrone analog shown to be less cardiotoxic due to a lower production of ROS [156, 157], will be used in combination with TRAIL to determine how effective the drug is compared to mitoxantrone. Finally, Western Blot Analysis will be used to evaluate the concentration of apoptosis related proteins, specifically those known to be influenced by ROS.

METHODS

Cell Culture Techniques

Two human prostate cancer cell lines (PC3, and PC3-TR), two human pancreatic cancer lines (MIAPaCa2, and BXPC-3), and one human breast cancer line (MDA-MB-231) were used in the current study. PC3-TR (TR: TRAIL resistant) [101] cells were a generous gift from Dr. Aria Olumi at the Massachusetts General Hospital in Boston, MA. Cells were grown in 75 cm^2 and 175 cm^2 Corning cell culture flasks with RPMI 1640 tissue culture media supplemented with 10% Fetal Bovine Serum and 1% penicillin / streptomycin (10000 units/mL penicillin G and 10000 μg/mL streptomycin) at 37°C with 5% CO_2.

Reagent/Drug Preparation

All reagents and drugs used in this study were reconstituted in either deionized water, ethanol, or DMSO depending on solubility. Solutions were prepared to ensure that the final solvent concentration in cell treatments would be less than 1% (v/v) to limit non-specific activity.

Single Agent and Combination Treatments

Cells were plated in 96 well plates at a density of 10,000 cells/well and incubated at 37°C and 5% CO_2 for approximately 24 hours. For single-agent drug treatments, cells were exposed to a range of drug concentrations (0-100 μM) for 30 mins, 2, 6, and 24 hours at which point the media was refreshed, and cell viability was determined using the MTT

(3-(4,5-dimethylthiazolyl-2) -2,5-diphenyltetrazolium bromide) assay. For sequential combination treatments, cells were first treated with the sensitizer drug for 30 mins, 2, 6, or 24 hours. The media was then removed, replaced with fresh serum-containing media, and the cells were treated with TRAIL. Cells were incubated for an additional 24 h after which, viability measurements were carried out using the MTT assay.

Determination of Cell Viability

Cell viability was assessed using the MTT cell proliferation assay (ATCC CA#30-1010k). Following addition of the MTT reagent (3 h at 37^{o}C), cells were treated with a lysis buffer from the kit and kept at room temperature in the dark for at least two hours in order to carry out complete lysis and to solubilize the MTT product. The absorbance of each well was measured using a Biotech Synergy 2 Multi-Detection Microplate Reader at 570 nm. Each experiment included a set of blank wells (media only), a live control (no treatment) and a dead control (0.5 μL of MTT lysis buffer). Fractional cell viability was calculated as: (OD of sample – OD of dead control)/(OD of live control – OD of dead control) where OD is the optical density. Percentage cell viability was calculated by multiplying the fractional viability by 100. Data are plotted as percentage reduction in cell viability compared to control (untreated cells) in which, a 0% value on the graph means 100% viability and 100% value on the graph means 0% viability.

Mitochondrial Depolarization Experiments

Cells were plated in black, clear-bottom 96 well plates at a density of 10,000 cells/well and incubated at 37°C with 5% CO_2 for approximately 24 hours. Cells were then

incubated with 6.39 μM of JC-1 dye (Sigma) for 1-1.5 hours after which the cell culture media was removed and refreshed. 1-100 μM concentrations of mitoxantrone/pixantrone were then added to the dye-treated cells. After the final treatment, fluorescent measurements were immediately taken using the Biotech Synergy 2 Multi-Detection Microplate Reader for green fluorescence (Ex. 485/40, Em. 528/20) and red fluorescence (Ex. 485/40, Em. 590/35). Following the fluorescence measurement, cells were incubated at 37°C with 5% CO_2 and were periodically removed to take readings at various time points.

Analysis of the JC-1 fluorescent data was carried out in order to determine changes in the mitochondrial membrane potential of the treated cells compared to the live control cells. First the ratio of red fluorescent intensity/green fluorescent intensity was calculated for each well. The average R/G ratio for the live control cells was calculated and the remaining R/G ratios were normalized against this value. This is done in order to account for the decrease in the R/G ratio caused by the dye. A second normalization was then performed for each treatment against itself at the 0 hour reading (i.e. all R/G ratios measured in a given well were divided by the R/G ratio in that well at the 0 hour time point). This normalization is done so comparisons between data can be easily made since at the 0 hour time point, all wells will give a normalized value of 100%.

Reactive Oxygen Species Experiments

The production of reactive oxygen species was accessed using the fluorescent dye 2',7'-dichlorfluorescein-diacetate (DCFH-DA) (Sigma). Cells were plated in black, clear-

bottom 96 well plates at a density of 8,400 cells/well and incubated at 37°C with 5% CO_2 for 24 hours. Cells were then treated with 100 µM of DCFH-DA and incubated for 45-60 mins. The dye-containing media was removed and refreshed and drug treatments were added. Hydrogen peroxide was used as a positive control and the live control consisted of cells only treated with DCFH-DA. Fluorescent measurements were made using the Biotech Synergy 2 Multi-Detection Microplate Reader with an excitation of 485/40 and emission of 528/20. After the fluorescence measurements were made, cells were incubated at 37°C with 5% CO_2 and were removed only when taking measurements at additional time points.

The reactive oxygen species scavenger, N-acetylcysteine (NAC) (Sigma), was used to protect cells from the effects of reactive oxygen species generated following treatments of mitoxantrone. Cells were pretreated with a 5 mM solution of NAC 1 hour prior to treatment with mitoxantrone. This NAC concentration was maintained following the addition of mitoxantrone as the single agent/combination treatments methodologies were completed.

Statistical Analyses

All experiments were performed in at least triplicate. Data are presented as the mean ± one standard deviation. Standard deviation of a data set was calculated based on experimental variation. ANOVA was performed using the t-test function in Microsoft Excel.

Annexin V and Propidium Iodide Analysis

An annexin V / propidium iodide assay (Invitrogen L3224) was carried out to determine if combination treatments induced apoptosis in cells. Briefly, a working solution of 2% annexin V and 1 μg/mL propidium iodide (PI) was prepared in a solution of 1X annexin binding buffer. The working solution was added to each well of the cell culture plate and incubated at room temperature for 15-20 minutes. Fluorescence imaging was then performed using a Zeiss Observer D1 fluorescent microscope. A 38 HE filter set (Excitation: 470/40; Emission: 525/50) was used to measure the fluorescence of the annexin V (green fluorescence) while a 43 HE filter set (Excitation: 550/25; Emission: 605/70) was used to measure the fluorescence of the propidium iodide (red fluorescence).

Western Blot Analysis

Cells were seeded in 6-well plates at a concentration of 250,000 cells per well and incubated for 24 hours. Cells were then treated according to the different experimental conditions. Treated cells were collected and washed three times with ice-cold phosphate buffered saline (PBS) then centrifuged at 1000xg for 5 minutes. Cellular lysates were suspended in 50-200 μL of ice-cold RIPA Buffer (10 mL RIPA base, 1 protease inhibitor cocktail tablet (Roche #0469312001), 1 mM sodium orthovanadate, and 1 mM sodium fluoride) and rocked for 15 minutes at 4 °C. The extracts were centrifuged at 14,000xg for 10 minutes after which any remaining cell debris was removed. Protein concentrations were measured using the Pierce BCA Protein Assay Kit (Thermo Scientific #23225) according to manufacturer's instructions. Protein lysates were mixed with 6X SDS-loading buffer and denatured at 100 °C for 5 minutes. Samples were

applied on an SDS polyacrylamide gel for electrophoresis. Proteins were transferred to PVDF membranes (GE Healthcare RPN2020F). Blots were then blocked in Tris-buffered saline and Tween 20 (TBST) with 5% milk for 1-2 hours. Blots were rinsed in TBST (15 minutes; x4) then incubated with primary antibody in 5% milk/TBST overnight at 4 °C. Blots were rinsed in TBST (15 minutes; x4) and incubated with secondary antibody in 5% milk/TBST for 1-2 hours. Blots were rinsed in TBST (15 minutes; x4) then dried. SuperSignal West Femto Maximum Sensitivity Substrate (Thermo Scientific #34095) was used according to manufacturer's instruction for detection.

RESULTS AND DISCUSSION

Previous reports have shown that mitoxantrone has the effect of generating losses in mitochondrial membrane potential (MMP) and increasing the generation of reactive oxygen species (ROS) [158]. These activities are important because when determining the mechanisms behind the TRAIL-sensitization activity of the drug, it is important to consider any biological changes mitoxantrone is causing since these changes can be related to the sensitization activity. With this in mind, it becomes important to evaluate what changes were occurring, when they were occurring, and the effect of these changes on the TRAIL-sensitizing activity of mitoxantrone.

Kinetic Evaluation of Mitoxantrone's TRAIL-Sensitization Activity in Prostate Cancer. Previous studies have almost exclusively examined the TRAIL-sensitization activity of drugs after treatment of said drugs for 24 hours (and an additional 24 hours for TRAIL combinations). However it is possible that pre-treating the cells for periods less than 24 hours could be sufficient to induce TRAIL sensitization in the malignant cells. With this in mind experiments were set up to evaluate the kinetics of TRAIL-sensitization following treatments of mitoxantrone. PC3-TR cells were treated with single-agent mitoxantrone (0-100 μM) for 30 mins, 2, 6, and 24 hours after which time MTT analysis was carried out directly (single-agent treatment) or the mitoxantrone-containing media was removed and refreshed with media containing 10 ng/mL TRAIL for 24 hours (combination treatment). The results of these experiments are shown in **Figure 4.1**. These results indicate that there is a significant loss of viable cells when comparing single-agent mitoxantrone to combination treatments of mitoxantrone and

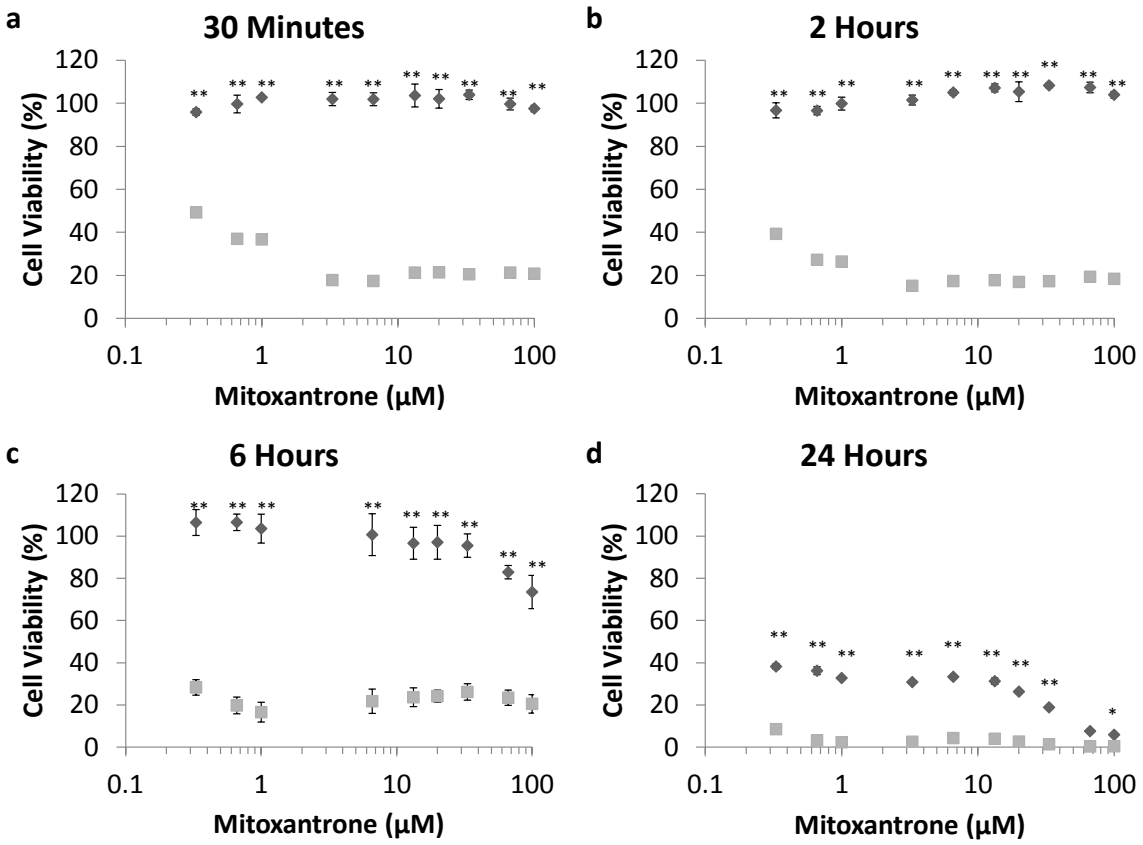


Figure 4.1 Kinetic dose response for mitoxantrone in PC3-TR human prostate cancer cells. Cells were treated with mitoxantrone for (a) 30 minutes, (b) 2 hours, (c) 6 hours, and (d) 24 hours. For single-agent treatments (dark grey diamonds) the cell viability was assessed following the mitoxantrone treatments. For combination treatments (light grey squares), 10 ng/mL of TRAIL was applied for 24 hours following the initial mitoxantrone treatments. Comparisons were made between the single agent and combination treatments; asterisks (*) and (**) indicate p-values < 0.05 and <0.01, respectively. Data are presented on a logarithmic scale for x-axes in the plots.

TRAIL for all of the treatment times tested. In the case of the 30 minute treatment (**Figure 4.1a**), the single agent treatments have little to no effect on cell viability with the LC_{50} value being difficult to determine since the highest concentration treatment (100 μM) gives no loss of viability. Following the combination treatments with TRAIL, the LC_{50} value drops to about 0.33 μM as the viability continues to decrease to about 20% with the highest concentration treatments. The 2 hour treatment results (**Figure 4.1b**)

exhibit similar trends to the 30 minute treatments with the LC_{50} value for the single agent treatment being difficult to determine while the LC_{50} for the combination treatment is less than 0.33 μM. After 6 hours (**Figure 4.1c**), the highest concentrations of mitoxantrone begin to start reducing viability with the 100 μM treatment causing a reduction to about 75% (though it is still not clear what the LC_{50} value is). The 6 hour combination treatments reduce the viability to 15-25% for all combinations tested. Combination treatment studies at 24 hours had previously been conducted during the initial JHCCL screening studies (**Figure 2.8a**). The results from this experimental set (**Figure 4.1d**) showed a much larger loss of cell viability for both single agent and combination treatments. However, additional investigations concluded that this difference in performance of the drug can be attributed to a difference in the cell stocks used to collect the data. Results from these experiments suggest that the cellular changes that sensitize cells to TRAIL occur within 6 hours of the initial treatment with mitoxantrone.

To confirm these results, similar experiments were carried out in an alternate prostate cancer cell line, PC3 (**Figure 4.2**). Unlike in PC3-TR, the 30 minute and 2 hour, low concentration treatments (> 3.3 μM) did not show a significant reduction in viability when comparing single agent and combination treatments (**Figure 4.2a & b)**. However, the 30 minute combination treatments showed a significant reduction in cell viability at concentrations above 20 μM, while 2 hour combination treatments showed synergy at concentrations above 6.6 μM. Similar to PC3-TR, the single agent treatments of the drug at 30 minutes and 2 hours showed little to no effect on cell viability, resulting in LC_{50}

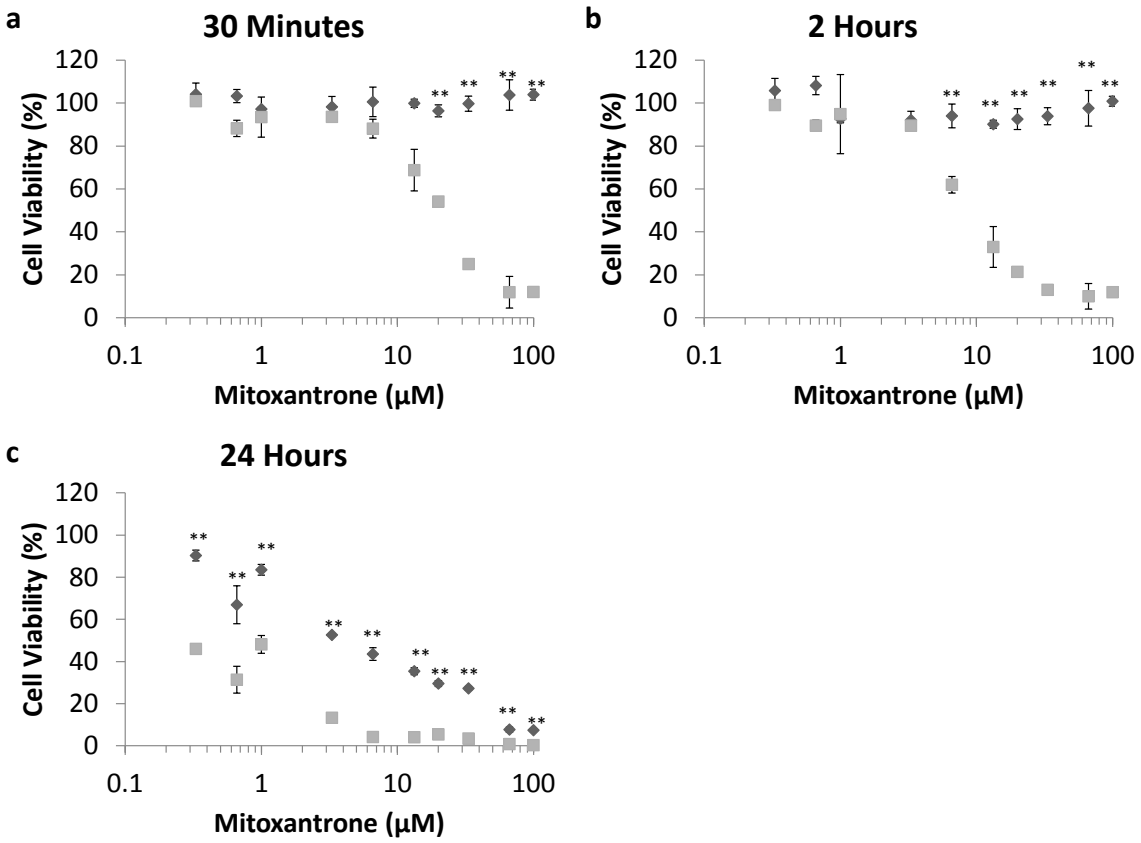


Figure 4.2 Kinetic dose response for mitoxantrone in PC3 human prostate cancer cells. Malignant cells were treated with mitoxantrone for (a) 30 minutes, (b) 2 hours, and (c) 24 hours. For single-agent treatments (dark grey diamonds) the cell viability was assessed following the mitoxantrone treatments. For combination treatments (light grey squares), 10 ng/mL of TRAIL was applied for 24 hours following the initial mitoxantrone treatments. Comparisons were made between the single agent and combination treatments; asterisks (*) and (**) indicate p-values < 0.05 and <0.01, respectively. Data are presented on a logarithmic scale for x-axes in plots.

values greater than 100 μM. The LC_{50} value for the 30 minute and 2 hour combination treatments were approximately 20 and 9 μM respectively. Twenty-four hour combination experiments with PC3 cells were also conducted during the initial JHCCL screening studies (**Figure 2.8b**) but unlike the PC3-TR cells, there was good agreement between those studies and the results shown in **Figure 4.2c**. As seen previously, the 24 hour combination treatments show a significant reduction in cell viability as compared to the

single agent treatments. The LC_{50} value for the 24 hour single agent treatments is 5 μM while the LC_{50} for the combination treatments is about 0.1 μM. The results of these studies confirm the observations made in the PC3-TR line and add credence to the notion that the cellular event that leads to mitoxantrone sensitizing cells to TRAIL occurs within the first few hours of treatment.

An increase in ROS generation is known to occur within the first few hours of treatment and because ROS is known to have proapoptotic activities [116, 159] it was hypothesized that the generation of ROS by mitoxantrone could explain the drug's TRAIL-sensitizing activities. In both of experimental sets, it is important to note that the 10 ng/mL TRAIL alone treatment showed a 0-10% reduction in cell viability and this effect was taken into account when determining statistically significance.

In order to verify the importance of kinetics in TRAIL-sensitization activity of mitoxantrone, cells were treated with an annexin V and propidium iodide (PI) stain. In these experiments, single-agent treatments were treated with mitoxantrone for 2 hours and then incubated with a buffer only control for an additional 24 hours. Combination treatments were treated with mitoxantrone for 2 hours followed by treatment with 10 ng/mL TRAIL for another 24 hours. Analysis of these images indicate that treatments of single-agent mitoxantrone and single-agent TRAIL have little effect on the cell viability; neither treatment produces a large amount of green or red fluorescing cells (**Figure 4.3**). However, it is clear that the combination treatments with mitoxantrone and TRAIL produce a large number of cells that are undergoing apoptosis or dying. These results can

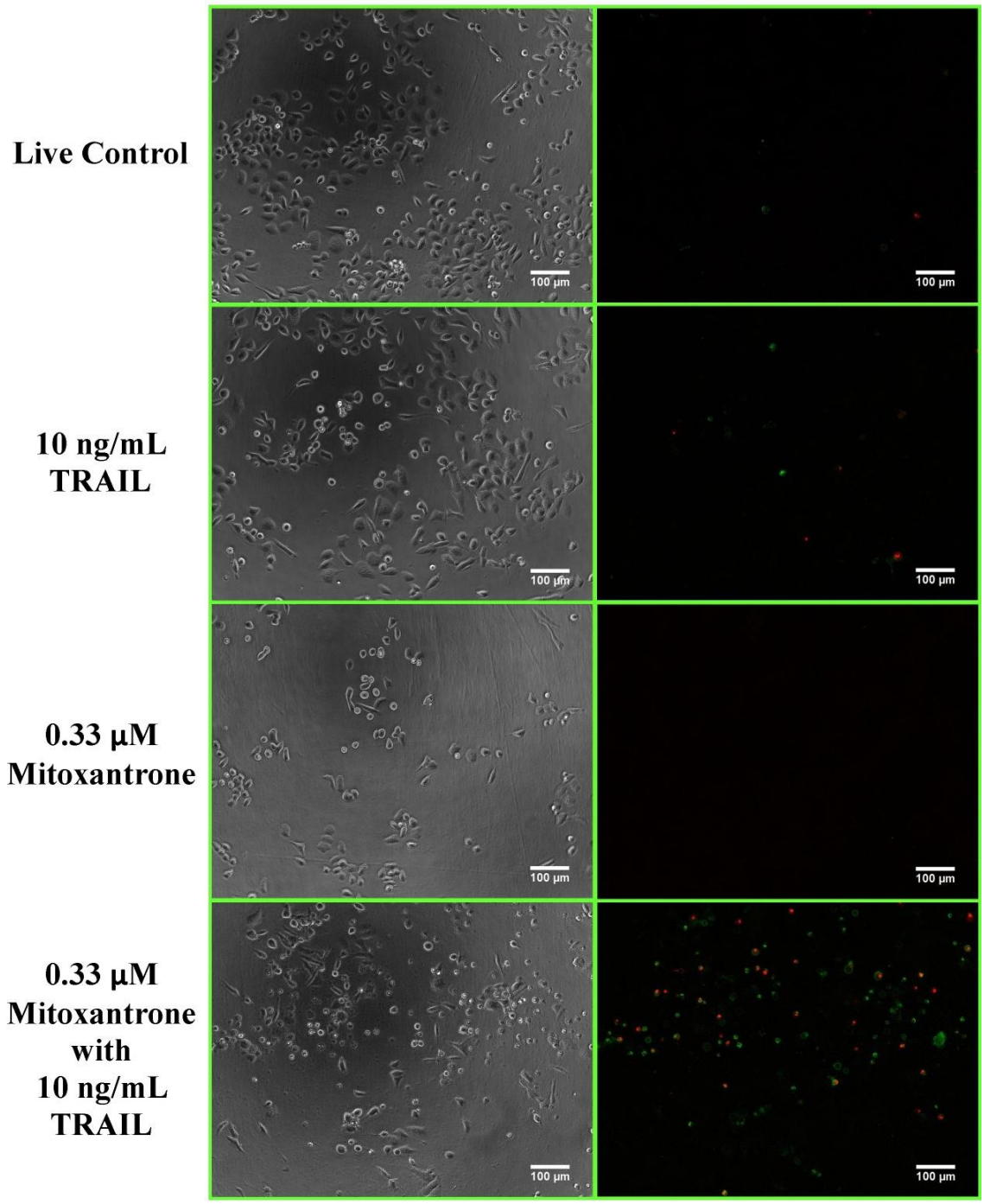


Figure 4.3 Microscopy images of single-agent and combination treatments in PC3-TR cells; mitoxantrone treatments were for 2 h, while TRAIL treatments were for 24 h. Left column shows phase contrast images and right column shows fluorescence images visualized with an annexin V and propidium iodide stain. Apoptotic cells exhibit green fluorescence only. Dead cells can exhibit either lone red fluorescence or red and green fluorescence simultaneously. Live cells are non-fluorescent.

be compared to those shown in **Figure 2.18** where the same experiment was carried out for 24 hour mitoxantrone treatments. In both cases the live control, single-agent TRAIL, and the combination treatments show similar behavior, but a key difference is seen when comparing the single-agent mitoxantrone treatments. The 24 hour single-agent mitoxantrone treatments are shown to cause the cells to die or become apoptotic while the 2 hour treatments do not have this effect. This is significant since mitoxantrone is an antineoplastic drug and its primary, DNA intercalating, activity is expected to reduce cell viability. However, these results confirm that combination treatments are still effective after only a 2 hour treatment with mitoxantrone while the single agent treatment has little to no effect. Because TRAIL is known to be selective toward malignant cells it is possible that shorter treatments of mitoxantrone can reduce the primary, non-specific, effect of the drug without sacrificing the efficacy of the combination treatment. Additionally, this information also indicates that important cellular changes occur during the first few hours of treatment which have the effect of sensitizing the cells to TRAIL treatments. This means that by identifying what changes occur during this period, it will become easier to narrow down the mechanisms responsible for mitoxantrone's TRAIL-sensitization activity.

Dose Response Studies with Mitoxantrone in Prostate and Pancreatic Cancer: Mitochondrial Membrane Potential. To begin we looked into mitoxantrone's ability to depolarizes the mitochondria of malignant cells. As described in Chapter 1, mitochondria serve as key checkpoints in the induction of apoptosis. The release of pro-apoptotic proteins from the mitochondria is though as the "point of no return" in the apoptotic

mechanism [83]. Therefore, it is important to understand if mitoxantrone actively damages the mitochondria because this mechanism might be related to the TRAIL-sensitization activity of the drug. Prior to testing mitoxantrone, a dose response experiment using a known mitochondrial depolarizer, antimycin A [160], was conducted to ensure the experimental conditions were optimized and were relevant to the chosen system. PC3-TR cells were cultured and changes in MMP were measured by tracking the fluorescent activity of the cationic dye, 5,5',6,6'-tetrachloro-1,1',3,3'-tetraethylbenzimidazolylcarbocyanine iodide (JC-1). JC-1 in its monomeric form emits at approximately 527 nm after a 488 nm excitation while the aggregate form emits at 590 nm with the same excitation. The largely negative mitochondrial membrane potential causes the dye to form aggregate at the mitochondrial membrane but if the membrane potential decreases the dye aggregates revert to their monomeric form in the cytoplasm [161]. Therefore, changes in the MMP can be tracked by measuring the fluorescent activity of the dye at both emission wavelengths. The red fluorescence/green fluorescence ratio is calculated and normalized as described in the Methods and plotted against the time each reading was collected. For the antimycin experiment, measurements of the MMP were taken every 15 minutes during the first hour of treatment followed by readings every hour until 5 hours of treatment with a final reading at 24 hours (data point not shown). These results, shown in **Figure 4.4**, indicate that as the concentration of antimycin A increased, the R/G fluorescent ratio (representative of MMP) showed an equivalent decrease. These results are consistent with the fact that antimycin A is a known mitochondrial depolarizer and serves as validation that the experimental conditions are suitable for a screening experiment. This experiment also

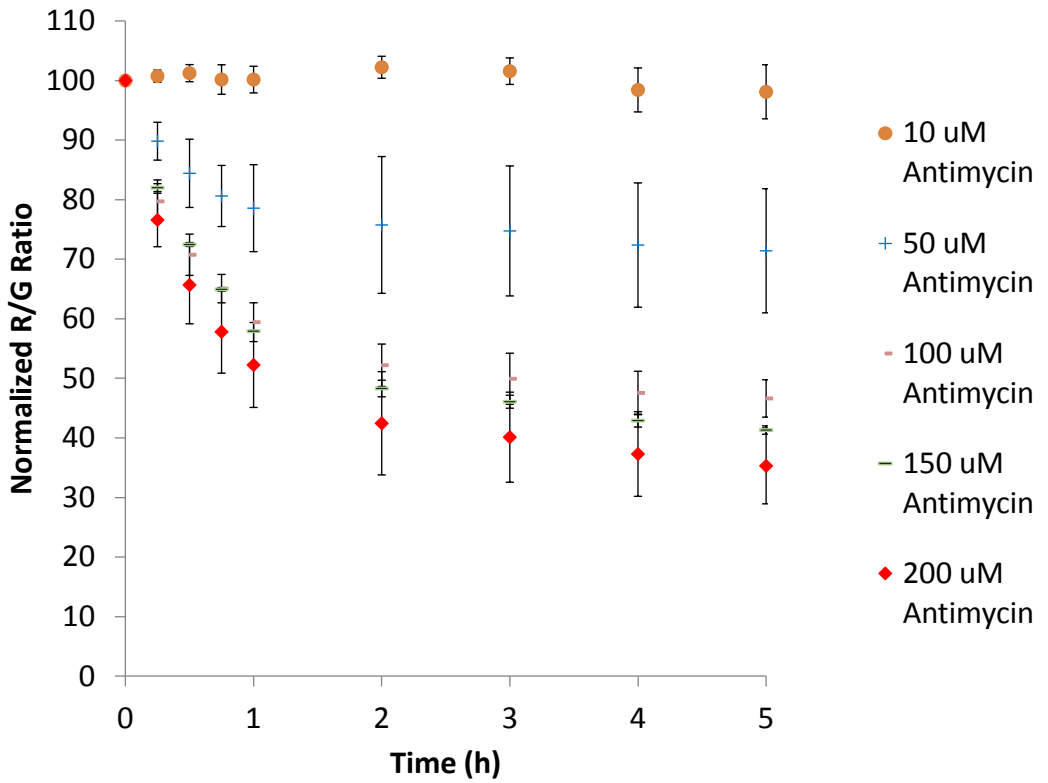


Figure 4.4 Response of PC3-TR cells following treatment with Antimycin A. Mitochondrial membrane potential (MMP) was measured using the fluorescent dye JC-1 following treatments with a known mitochondrial depolarizing agent, Antimycin A. The fluorescent emission of JC-1 changes based on the MMP and will emit red at high membrane potentials and green at low membrane potentials. Data is presented as the change in the normalized red fluorescent/green fluorescent ratio.

provided some insight into the time scale over which depolarization occurs in which it is clear that during the first hour there is a large decrease in the MMP and that, as time progresses, this effect begins to stabilize. Additionally, these results also provide a positive control for all future experiments since it is clear that antimycin A at concentrations of 50 µM and higher is able to induce depolarization.

Since the method for measuring changes in MMP was found to be effective experiments measuring the effect of mitoxantrone on MMP was evaluated. The depolarizing activity

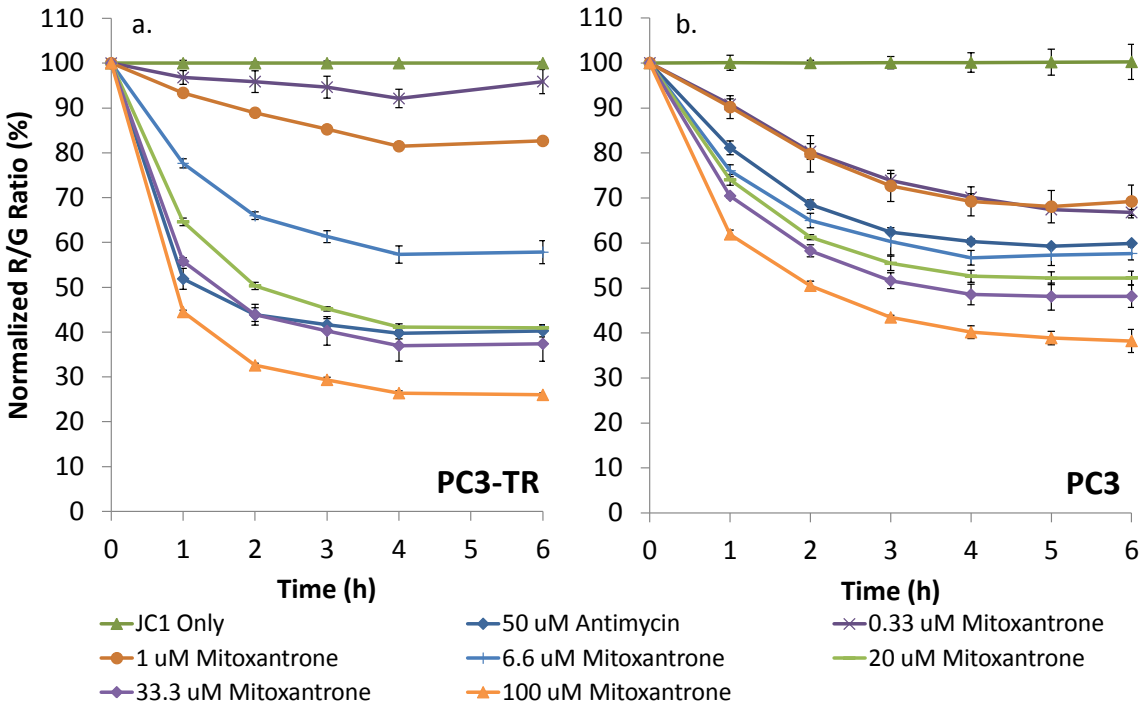


Figure 4.5 Response of prostate cancer following treatment with increasing concentrations of mitoxantrone. The change in membrane potential in the cell lines a) PC3-TR and b) PC3 shows dose dependence. Lines connecting data are for visualization only.

of mitoxantrone was determined by testing a concentration range from 0 to 100 µM. **Figure 4.5** gives a kinetic dose response for (**a**) PC3-TR and (**b**) PC3 prostate cancer cell lines. As expected, both cell lines show a dose dependant response to the mitoxantrone treatments and the speed and extent of the depolarization increases as concentration increases. Some interesting differences arise when comparing the PC3-TR results and the PC3 results. Most notably is that the PC3 cell line seems to be more resistant to the depolarization induced by mitoxantrone at higher concentrations, but more susceptible to depolarization induced by the drug at lower concentrations when compared to the PC3-TR line. Over 6 hours, PC3-TR shows a very small decrease in the R/G ratio (> 5%) using a concentration of 0.33 µM and about a 75% decrease with a 100 µM

concentration. Alternatively, PC3 shows a 30% reduction in the R/G ratio with a 0.33 µM concentration and a 60% reduction with 100 µM after the same 6 hour period. Additionally, there is also a clear different in the efficacy of the antimycin control in these two cell lines. In the PC3-TR line, antimycin causes a 60% decrease in the R/G ratio over six hours, but it only causes a 40% decrease in PC3. PC3-TR cells are derived from a PC3 parent line, and resistance to the protein TRAIL has been attributed to the over expression of the anti-apototic protein, c-FLIP. However, it is unclear if the different responses these two lines exhibit can be attributed to the effect of c-FLIP, or if additional factors play a role. Regardless, in both lines our studies show a significant loss of membrane potential over a period of six hours following treatment with mitoxantrone.

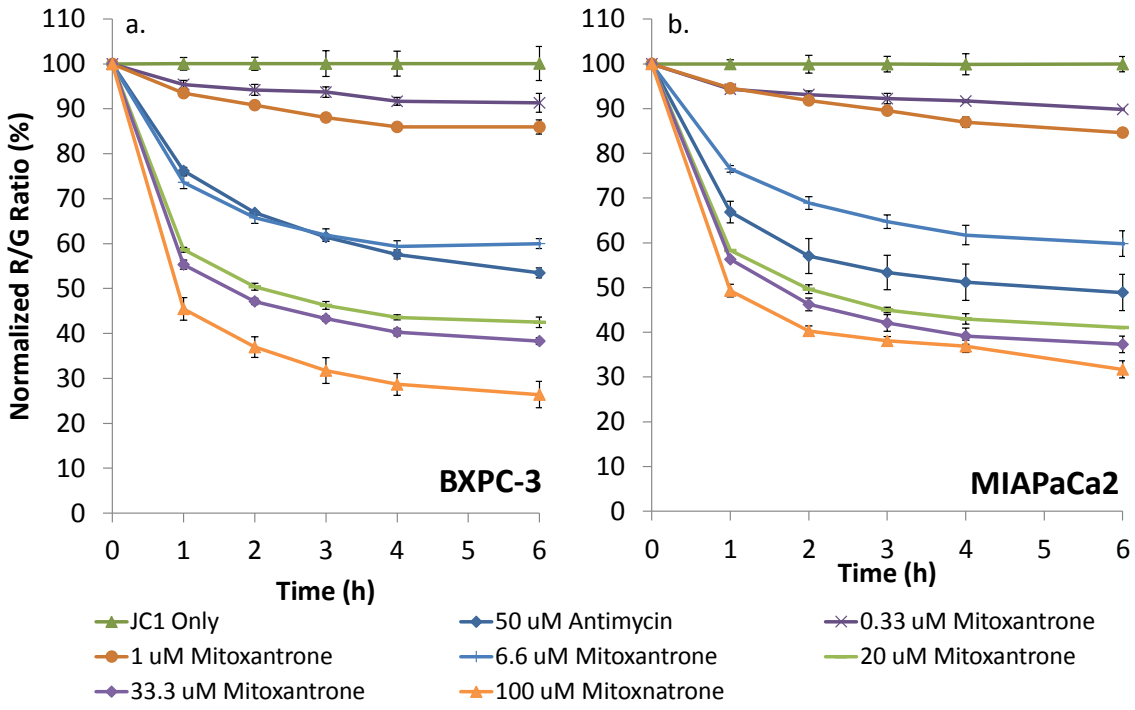


Figure 4.6 Response of pancreatic cancer following treatment with increasing concentrations of mitoxantrone. The change in membrane potential in the cell lines a) BXPC-3 and b) MIAPaCa-1 shows dose dependence. Lines connecting data are for visualization only.

In addition to the prostate cancer lines tested, dose response studies were also carried out in two human pancreatic cancer lines. **Figure 4.6** shows the change in the MMP over a six hour period in (**a**) BXPC-3 and (**b**) MIAPaCa2, following treatments with mitoxantrone. In these two cell lines there is also a dose dependant response to the mitoxantrone treatments. 0.33 µM mitoxantrone causes a 10% decrease in the R/G ratio over a six hour period in both cell lines, while a 100 µM treatment causes a 75% decrease in BXPC-3 and a 70% decrease in MIAPaCa2. The antimycin control reduces the R/G ratio by approximately 50% in both cell lines. These results indicate that the two pancreatic cancer lines exhibit nearly identical responses to the mitoxantrone treatments. These responses are also very similar to what is seen in the PC3-TR prostate cancer line (**Figure 4.5a**). This suggests that the mechanisms of depolarization are likely similar in both pancreatic cancer lines and in the PC3-TR line.

Additionally, the depolarizing effect of mitoxantrone was also tested in the MDA-MB-231 breast cancer cell line shown in **Figure 4.7**. As previously seen with the prostate and pancreatic cancer cell lines, the MDA-MB-231 cells also show a does dependant response to the mitoxantrone treatments. One of the key differences between treatments in this cell line and the other tested lines is that the kinetics of depolarization seem to take place almost exclusively during the first hour of treatment. At the 100 µM treatment concentration, the R/G ratio decrease by almost 60% during the first hour and after six hours of treatment there is little additional depolarization caused by the drug. These results are interesting since in the four other lines tested, there was a large initial decrease

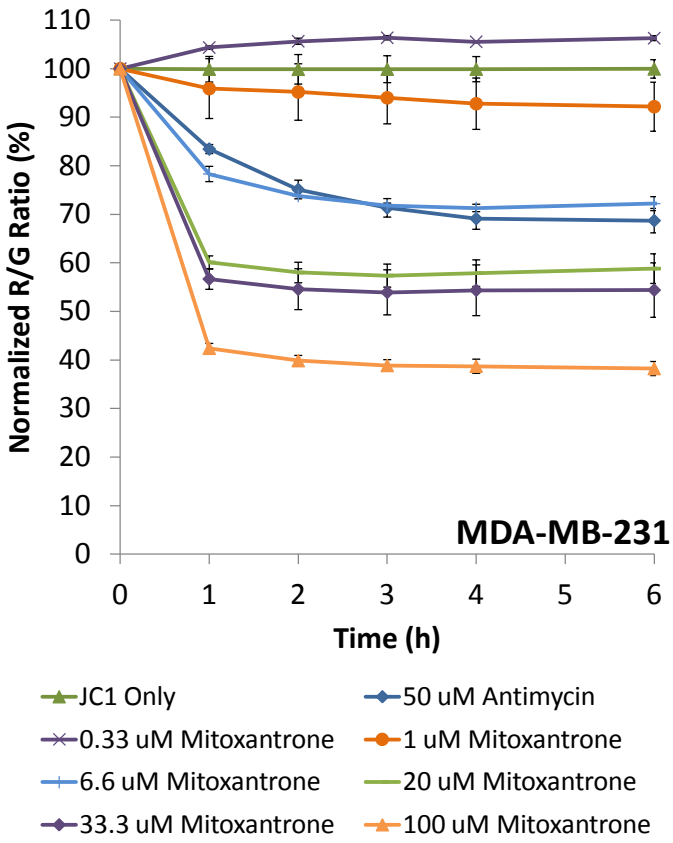


Figure 4.7 Response of breast cancer following treatment with increasing concentrations of mitoxantrone. Change in membrane potential in the MDA-MB-231 cell line shows dose dependence. Lines connecting data are for visualization only.

in the R/G ratio and the ratio continued to steadily decrease for a few hours after the initial hour. It is only after an approximate 4 hour treatment time that the change in the ratio begins to equilibrate. Furthermore, low concentration treatments of mitoxantrone, in the MDA-MB-231 cell line, seem to be ineffective; after a 6 hour treatment with 0.33 µM mitoxantrone, there is a very slight increase in the R/G ratio of the cells (5%). Overall it does appear that the breast cancer line shows a higher resistance to the depolarization activity of mitoxantrone than lines like PC3-TR and BXPC-3 although the difference is small.

All previous results have been obtained by taking measurements of fluorescent intensity using a microplate reader. However, in order to confirm the microplate reader results, fluorescent microscopy was employed to visualize the effects of mitoxantrone in JC-1 stained, PC3-TR cells. **Figure 4.8** shows microscopy images at 0 and 4 hours for cells treated with (**a**) the JC-1 dye alone (live control) and (**b**) 20 μM mitoxantrone. Average R/G ratios for each treatment condition are also given for each fluorescent image. In **Figure 4.8a** there is an increase in the amount of green fluorescence when comparing the 0 h and 4 h live controls, which is attributed to the fact the that JC-1 dye by itself has some depolarizing activity. In order to make meaningful comparisons of other drug treatments, this effect is accounted for by normalization the data against the live control and standardizing the measurements. This sets the R/G ratio of the live control to 100% for all time points as is demonstrated in the figure. **Figure 4.8b** shows the effects of mitoxantrone treatments in which there is a clear increase in the intensity of the green fluorescence when comparing the 0 h and 4 h treatments. Importantly these studies show that the relative fluorescence for the 0 h live control and the 0 h mitoxantrone treatment are nearly equal which is expected since at the initial treatment point the effects of the drug are not expected to be acting. The microscopy results confirm the results obtained using the fluorescent plate reader. The only notable different between the two measurements is that, after 4 hours, the plate reader shows a 60% decrease in the R/G ratio with a 20 μM mitoxantrone treatment and the microscopy measurements only shows a 25% decrease. However, some variation in the measurements taken is expected since different systems are being used to measure and collect the data. In the plate reader the fluorescent signal is measured directly while in the microscopy experiments the

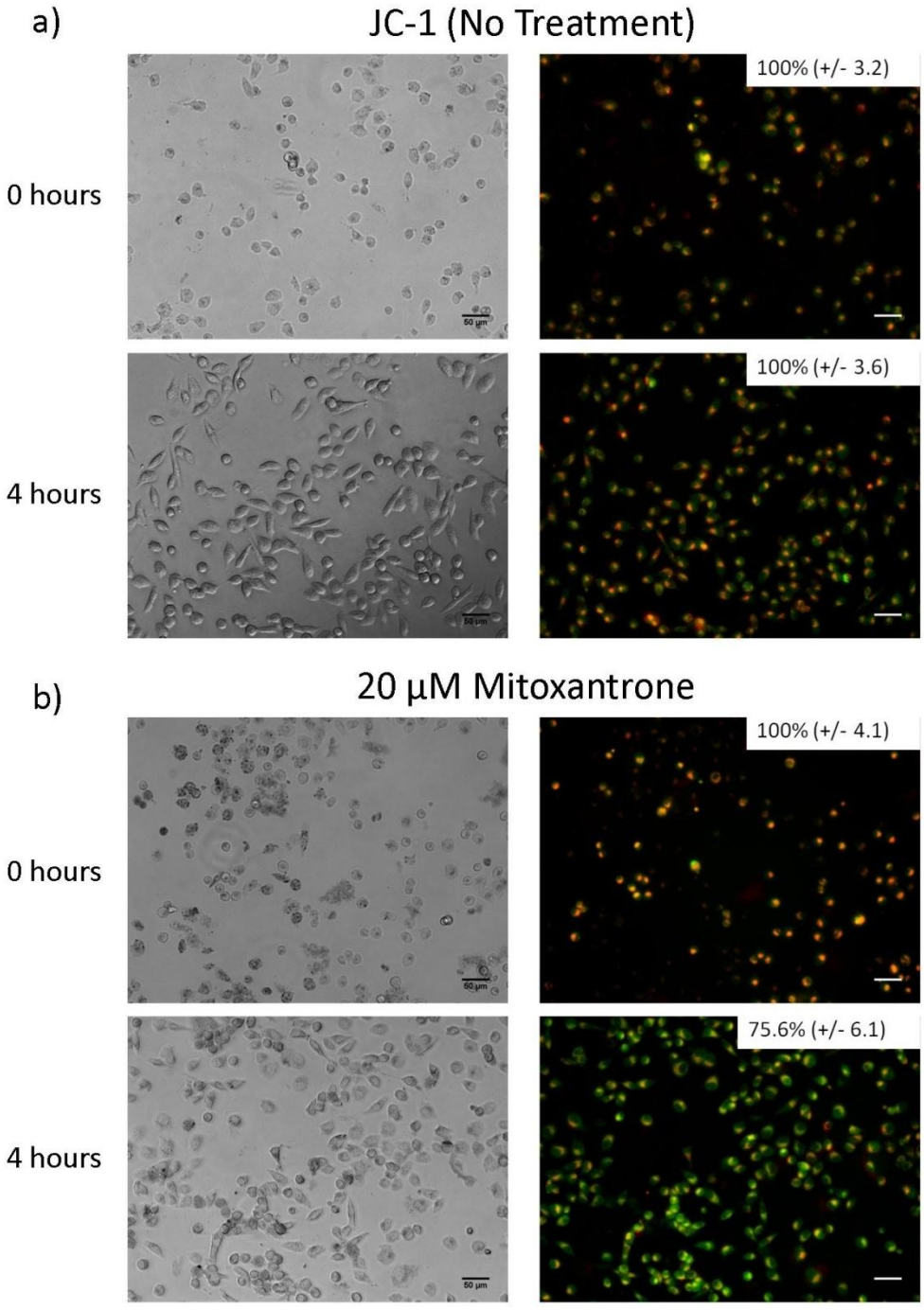


Figure 4.8 Microscopy images of PC3-TR cells for depolarization studies. Images were captured for a) live control cells (dye only) and b) mitoxantrone treated cells at 0 and 4 hours. Fluorescent images are presented as an overlay of red and green fluorescent images in which the JC-1 dye fluoresces red when it aggregates near mitochondria and fluoresces green when the dye dissociates into the cytoplasm. Normalized ratios of the fluorescent intensity (R/G) in each image are also presented.

fluorescent signal is determined though image analysis. Another important difference is that, in the plate reader, the dye is excited at 485/40 nm and emission measurements are taken at 528/20 and 590/35 nm. However, in the microscopy experiments, the dye is first excited at 470/40 nm with emissions taken at 525/50 nm (green fluorescence) and then excited at 550/25 nm with emissions taken at 605/70 nm (red fluorescence). Since the red fluorescent measurements are not taken using the same excitation wavelengths, it makes sense that there would be difference in the intensity measurements taken and could account for the difference in measurements observed. Regardless, both the microplate results and the microscopy results demonstrate the ability of mitoxantrone to depolarize mitochondria in prostate and pancreatic cancer cell lines and that the kinetics of this activity occur within the first few hours of treatment.

Dose Response Studies with Mitoxantrone in Prostate and Pancreatic Cancer: Reactive Oxygen Species. Loss of MMP and the generation of reactive oxygen species (ROS) are closely related processes as described in Chapter 1. Mitochondria consistently generate ROS, but the organelles are equipped with the mechanisms necessary to control the concentrations of these species. However, damaged mitochondria will not be able to effectively control ROS concentrations. Similarly, high concentrations of ROS can cause an otherwise healthy mitochondrion to being to malfunction. Since the loss of MMP and the generation of ROS are coupled it became important to know how treatments of mitoxantrone were changing ROS concentrations. The kinetics of the change in these levels will vary from system to system and so an important question that we will be trying to answer is if a decrease in MMP leads to an increase in ROS or vice-versa.

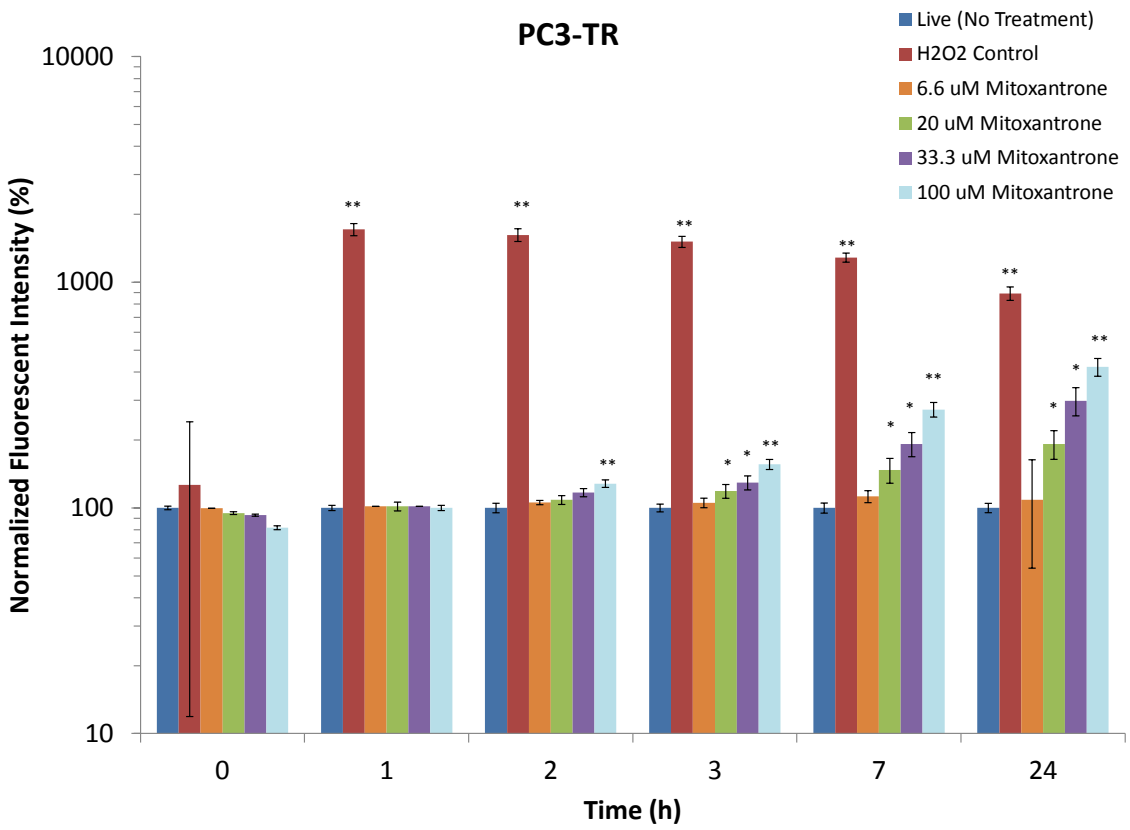


Figure 4.9 Reactive oxygen species generation in mitoxantrone treated, PC3-TR prostate cancer cells. Time point measurements of ROS generation were made over a 24 hour period based on the fluorescent intensity of the DCFH-DA dye. Comparisons were made against the live control; asterisks (*) and (**) indicate p-values < 0.05 and < 0.01, respectively. Data are presented as the normalized fluorescent intensity based on the live control measurements. Data are presented on a logarithmic scale for y-axes in the plots.

DCFH-DA was used to measure ROS levels as described in Methods. DCFH-DA is a non-fluorescent, cell permeable molecule. When the compound permeates the cell, it is deacetylated by cellular esterases to form non-fluorescent DCFH. DCFH is then oxidized by ROS to form the fluorescent molecule, 2',7'-Dichlorofluorescin (DCF) (i.e. as ROS levels increase, fluorescent intensity increases). **Figure 4.9** shows a dose response experiment with mitoxantrone in the PC3-TR cell line. The hydrogen peroxide control rapidly increases the fluorescent signal, as expected, and over time the signal steadily

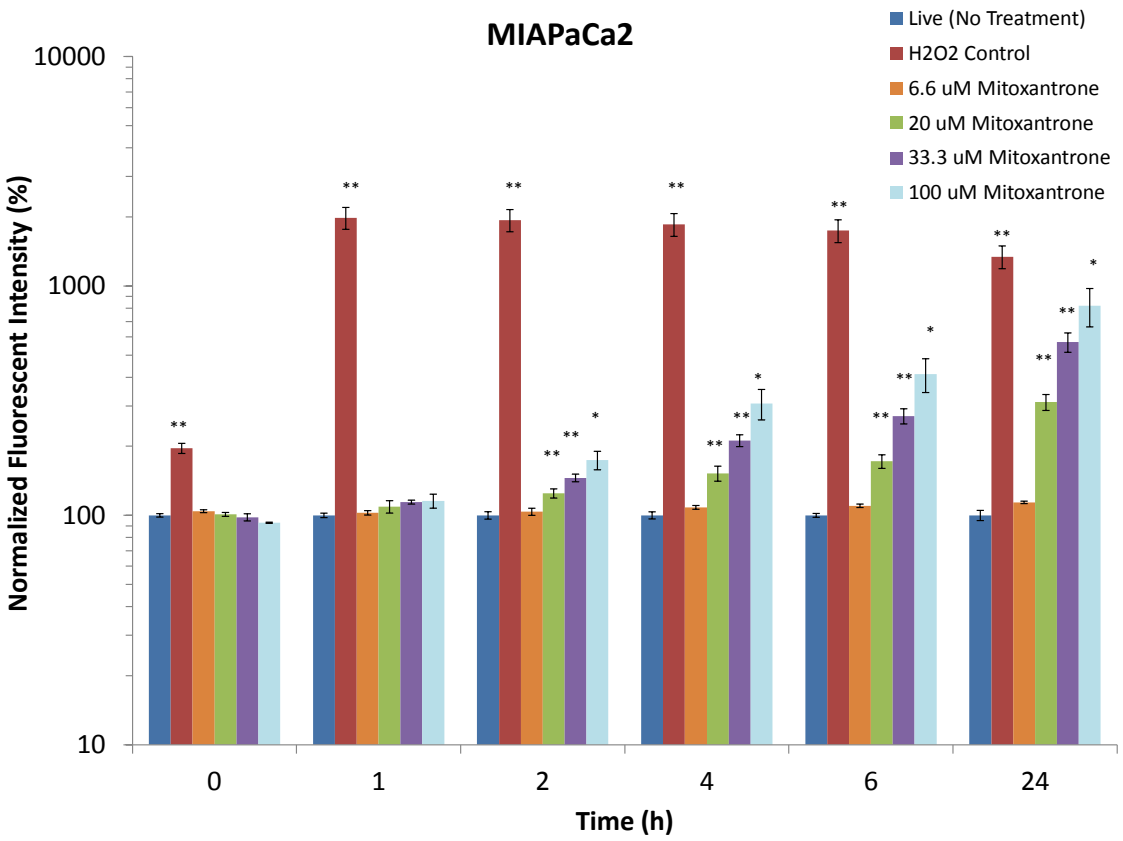


Figure 4.10 Reactive oxygen species generation in mitoxantrone treated, MIAPaCa-2 pancreatic cancer cells. Time point measurements of ROS generation were made over a 24 hour period based on the fluorescent intensity of the DCFH-DA dye. Comparisons were made against the live control; asterisks (*) and (**) indicate p-values < 0.05 and < 0.01, respectively. Data are presented as the normalized fluorescent intensity based on the live control measurements. Data are presented on a logarithmic scale for y-axes in the plots.

weakens. This suggests that the positive control is working and that this system is sensitive enough to track changes in ROS generation. The results show that after 3 hours of mitoxantrone treatments at concentrations above 20 µM, there is a significant increase in the concentration of intracellular ROS. The ROS levels then continue to increase until the 24 hour time point when measurements were ceased. After 24 hours, the 100 µM treatment shows an approximate 300% increase in the fluorescent intensity, while 100% and 200% enhancements are seen for 20 and 33.3 µM treatments respectively. From

these results it also appears that low concentrations of mitoxantrone (6.6 µM and below) do not results in a significant increase in the ROS concentration even after 24 hours of treatment (only a 10% increase in fluorescent intensity). This is interesting because at a concentration of 6.6 µM, the treated cells showed a significant decrease in the R/G ratio compared to the untreated controls (**Figure 4.5a**).

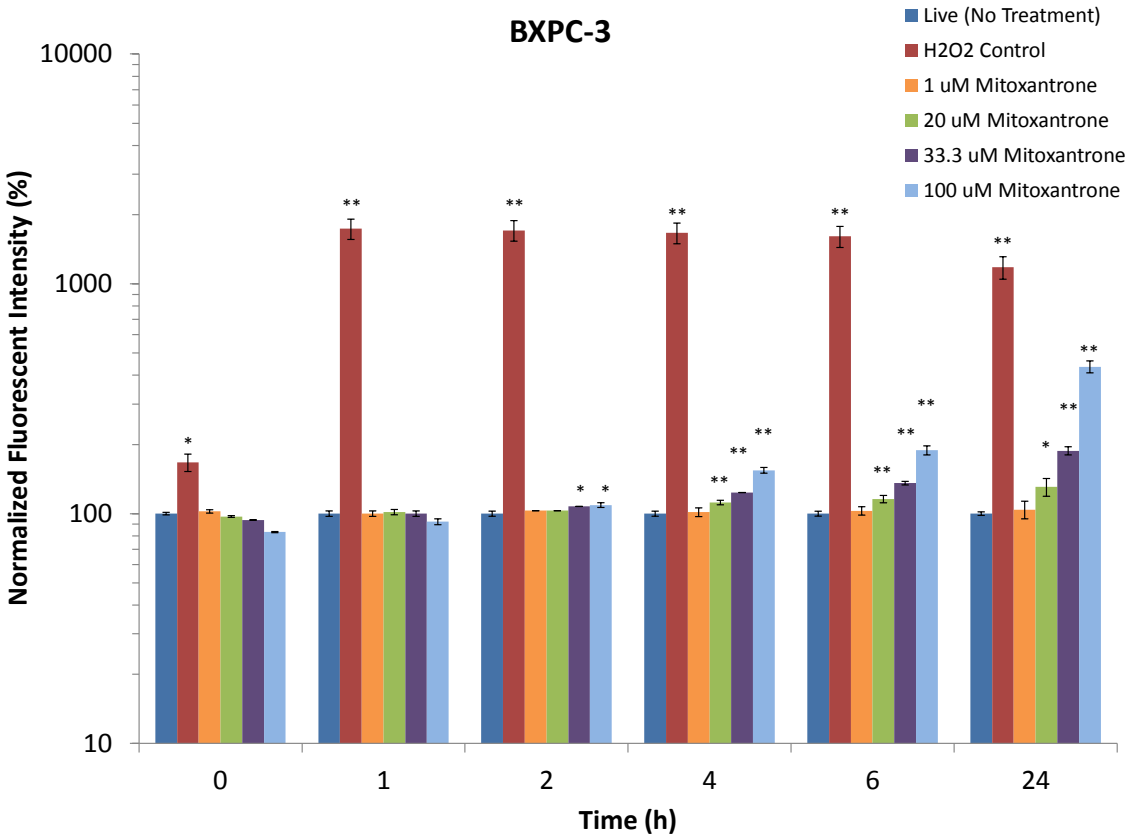


Figure 4.11 Reactive oxygen species generation in mitoxantrone treated, BXPC-3 pancreatic cancer cells. Time point measurements of ROS generation were made over a 24 hour period based on the fluorescent intensity of the DCFH-DA dye. Comparisons were made against the live control; asterisks (*) and (**) indicate p-values < 0.05 and < 0.01, respectively. Data are presented as the normalized fluorescent intensity based on the live control measurements. Data are presented on a logarithmic scale for y-axes in the plots.

A dose response study of ROS generation in the pancreatic cancer line MIAPaCa-2 (**Figure 4.10**) was also performed. The trend of these results mimics that of the PC3-TR cells except, in this cell line, the effects happen more quickly and with greater intensity. MIAPaCa-2 cells show that after 2 hours, ROS levels significantly increase after treatment with mitoxantrone at and above 20 μM. This can be compared to the PC3-TR data where only the 100 μM treatment showed a significant increase in ROS levels after 2 hours. Additionally, the level of ROS production is much greater than in the prostate cancer cell line; after 24 hours the 100 μM mitoxantrone treatment showed an approximate 700% increase in the fluorescent intensity, while 200% and 500% enhancements were seen for 20 and 33.3 μM treatments respectively.

These experiments were also carried out in the BXPC-3 pancreatic cancer line (**Figure 4.11**) where the trend of ROS production shows a significant increase in the 20 and 33.3 μM concentrations after only 2 hours which is similar to the rate at which MIAPaCa-2 cells showed significant increases in ROS concentrations. However, the level of ROS production seems to be less than in the PC3-TR and MIAPaCa-2 cell lines. After 24 hours the 100 μM treatment shows an approximate 300% increase in the fluorescent intensity signal which is comparable to the PC3-TR experiments but the 20 and 33.3 μM treatments only show 50% and 100% increases respectively. In measuring changes in the MMP, PC3-TR, MIAPaCa-2, and BXPC-3 all showed similar responses to the mitoxantrone treatments (**Figures 4.5a and 4.6**) yet the three different cell lines showed varying levels of ROS production. It stands to reason that the production of ROS is not

solely dependent on the magnitude of the change in MMP since the response can vary between cell lines when the change in MMP is mostly constant.

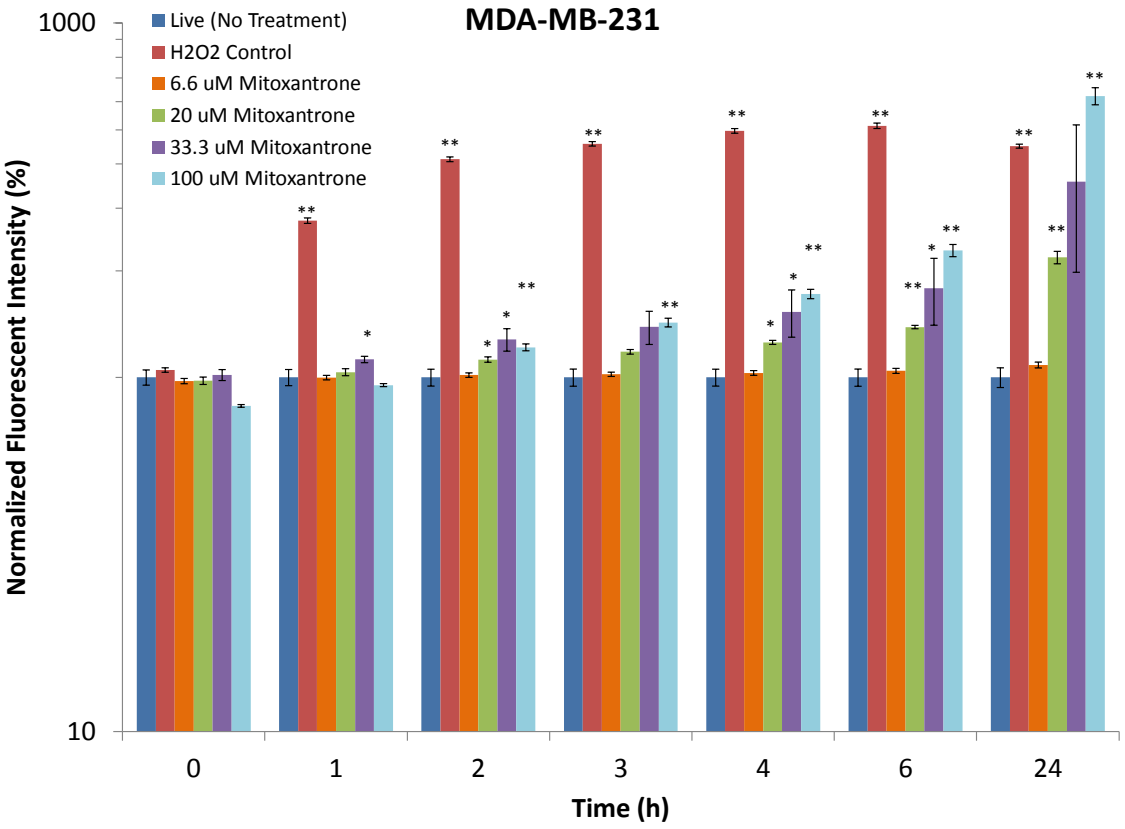


Figure 4.12 Reactive oxygen species generation in mitoxantrone treated, MDA-MB-231 breast cancer cells. Time point measurements of ROS generation were made over a 24 hour period based on the fluorescent intensity of the DCFH-DA dye. Comparisons were made against the live control; asterisks (*) and (**) indicate p-values < 0.05 and < 0.01, respectively. Data are presented as the normalized fluorescent intensity based on the live control measurements. Data are presented on a logarithmic scale for y-axes in the plots.

The effect of mitoxantrone on ROS levels in MDA-MB-231 cells was also evaluated as shown in **Figure 4.12**. In this experiment the treatment concentration of the H_2O_2 control was reduced in order to provide a better an improved scale over which to view the treatment data but all other conditions were kept constant. After 2 hours, mitoxantrone

treatments greater than 20 µM start to show a significant increase in the ROS concentrations. After 24 hours of treatment, the 100 µM condition shows a 5.5-fold increase in the ROS concentration while the 20 µM and 33.3 µM conditions show 1.5 and 2.5-fold increases respectively. Compared to the other cell lines tested, the ability and extent of mitoxantrone to generate ROS in MDA-MB-231 falls between the highest efficacy in the MIAPaCa-2 pancreatic cancer line and the lower efficacy in the PC3-TR prostate cancer cell line. The kinetics of the ROS production also appear to be quite rapid since there it only takes 2 hours for the ROS concentration to be significantly higher than the no treatment controls.

The manner in which ROS are generated appears to be different from the manner in which the MMP decreases. As the time of treatment increases the ROS levels continue to increase, but the loss in MMP occurs within the first few hours of treatment and there is no significant change in the potential at later time points. **Figure 4.13** compares the rate of mitochondrial depolarization to the rate of ROS generation in the MIAPaCa-2 pancreatic cancer cell line following treatment with 20 µM of mitoxantrone. When comparing the data sets in this manner, it is easy to visualize the rate at which the two phenomena occur. By comparing the slope of the line connecting data points it is clear that in the first hour there is a much greater loss of MMP than an increase in ROS production; the MMP decreases by approximately 40% of its initial value while the fluorescent signal generated by the ROS has only increased by 10%. The figure also demonstrates that while the initial loss of membrane potential is high, the subsequent reading do not show depolarization and the response seems to stabilize over time.

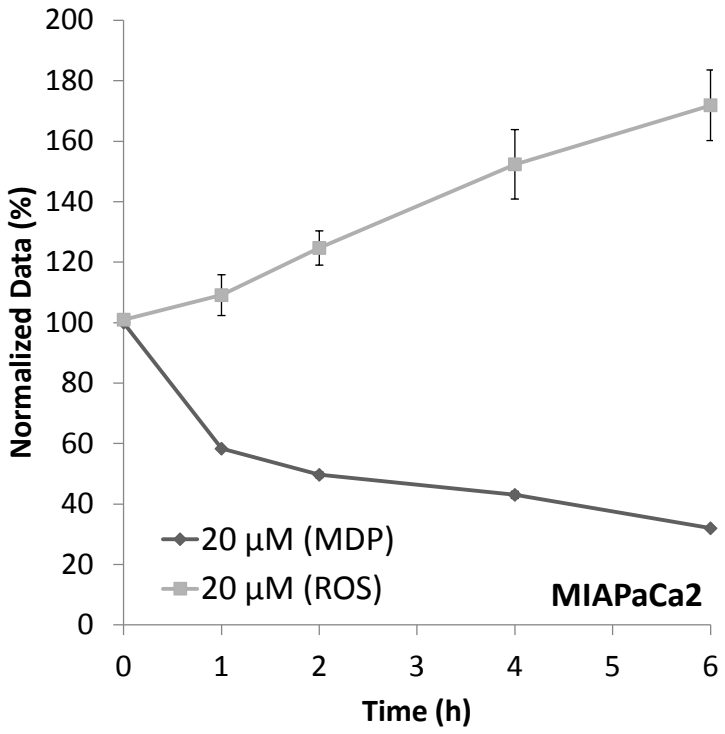


Figure 4.13 Kinetic comparison between mitochondrial depolarization and ROS generation. Normalized data are compared over a 6 hour time period in the MIAPaCa-2 human pancreatic cancer cell line.

However, the rate of ROS generation steadily increases during the initial 6 hours and continues to increase up to the the 24 hour time point. What this seems to indicate is that a loss of MMP facilitates the increased production of ROS. This is an important distinction since the two phenomena are part of a feed-forward loop and there is the potential that the increase in ROS could cause a change in MMP due to oxidative stress.

Evaluating the Effect of N-acetylcysteine on the TRAIL-Sensitizing Activity of Mitoxantrone. In order to evaluate the effect ROS had on the TRAIL-sensitizing activity of mitoxantrone, the ROS scavenger N-acetylcysteine (NAC) was used to reduce ROS concentrations. Dose response studies with mitoxantrone where carried out in PC3-

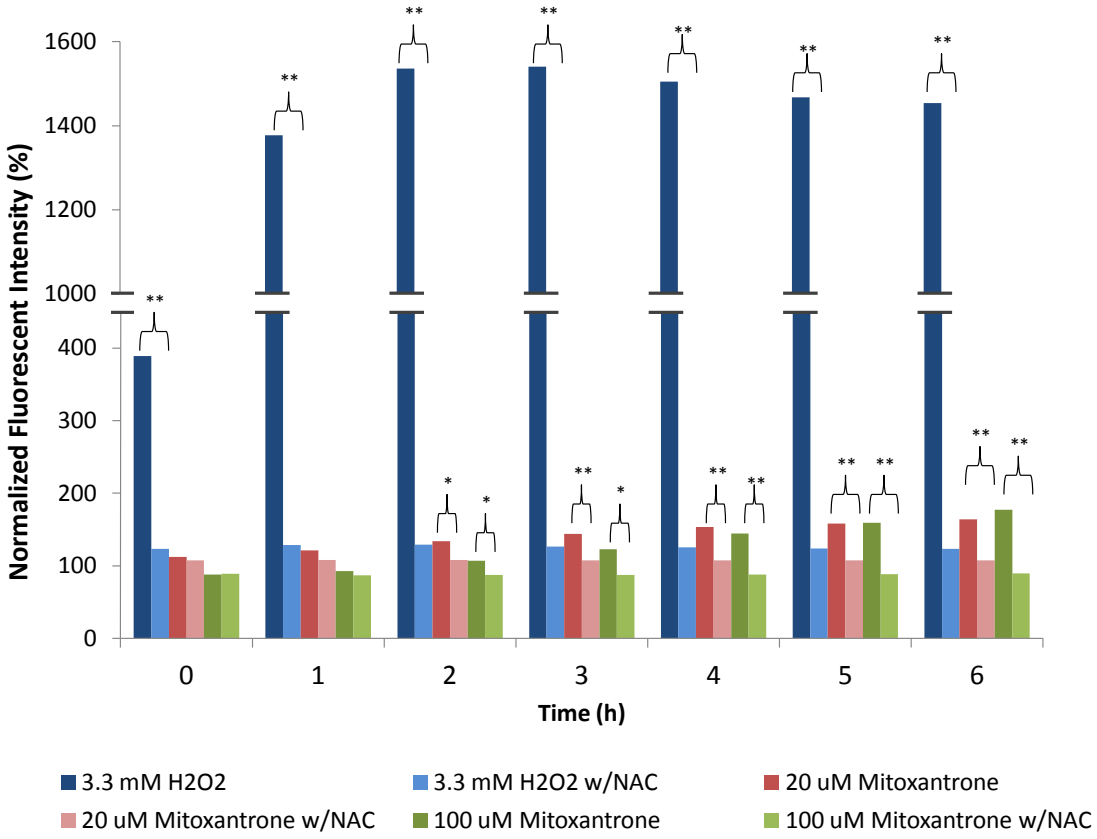


Figure 4.14 The effect of N-acetylcysteine (NAC) on reactive oxygen species generation in PC3-TR prostate cancer cells. Time point measurements of ROS generation were made over a 6 hour period based on the fluorescent intensity of the DCFH-DA dye. Asterisks (*) and (**) indicate p-values < 0.05 and < 0.01, respectively. Data are presented as the normalized fluorescent intensity based on the live control measurements.

TR cells with and without co-treatments of NAC (**Figure 4.14**). In these studies hydrogen peroxide was used as a positive control and the effect of the treatments was evaluated over a 6 hour period. The positive controls showed an immediate increase in fluorescent intensity for the cells not treated with NAC but the cells treated with NAC showed only a slightly elevated fluorescent intensity (compared to the live control). Between 1 and 6 hours this difference between the cells with and without NAC and treated with hydrogen peroxide showed a 13-fold increase between the two conditions.

Mitoxantrone treatments did not generate the same high levels of ROS as the positive control but the treatments containing no NAC did increase significantly. The ROS levels of the mitoxantrone and NAC co-treated cells did not exhibit a significant increase over the live control cells. The difference between the mitoxantrone treated cells with and without NAC became statistically significant after the 2nd hour of treatment. These results indicate that the ROS-scavenger NAC is able to significantly reduce the intracellular concentrations of the ROS generated both by hydrogen peroxide and by mitoxantrone. Upon verification that NAC could limit the production of ROS by mitoxantrone, it was hypothesized that if ROS were contributing to the TRAIL-sensitizing activity of mitoxantrone then limiting the ROS concentration should protect the mitoxantrone treated cells from TRAIL-mediated apoptosis. Cell viability was measured following single agent and combination treatments with mitoxantrone in cases with and without NAC. 2 hour single agent treatments of 0-100 μM mitoxantrone showed no statistical difference between the viability of cells with and without NAC (**Figure 4.15a**). These results are important because they indicate that the NAC treatments do not reduce the cell viability and will not contribute to the toxic effects of mitoxantrone. Results from the 2 hour combination mitoxantrone/TRAIL treatments show that for all concentrations tested, cell viability was higher for the cells treated with the ROS scavenger NAC (**Figure 4.15b**). These data also shows that at several concentrations (0.33, 3.3, 6.6, 13.3, 33.3, and 100 μM) the difference between the cells with and without NAC was statistically significant. On average cells treated with NAC show approximately 12.2% (+/- 5.8%) higher viability than those without NAC.

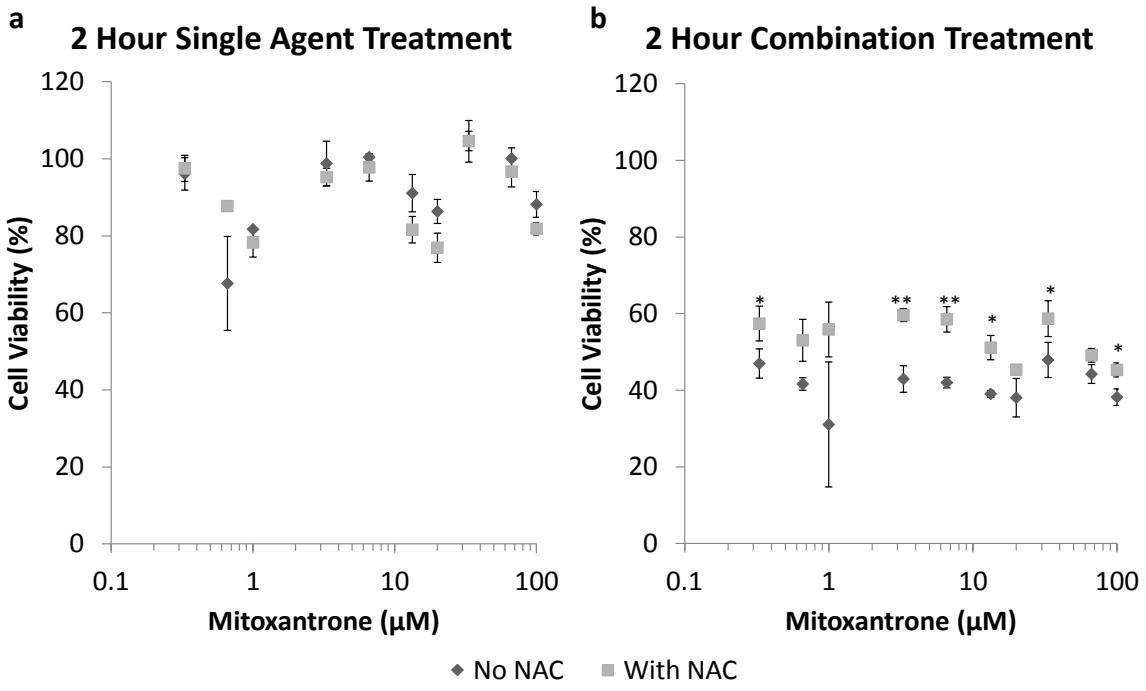


Figure 4.15 Mitoxantrone dose response (2 h; 0-100 μM) with N-acetylcysteine co-treatments in PC3-TR prostate cancer cells. (a) Single agent and (b) sequential combination treatments with 10 ng/mL TRAIL. Comparisons were made between treatments with and without NAC; asterisks (*) and (**) indicate p-values < 0.05 and <0.01, respectively. Data are presented on a logarithmic scale for x-axes in the plots.

This experiment was also performed for 24 hour treatments of mitoxantrone. For the 24 hour single agent treatments it is apparent that there is a significant difference between the NAC treatments (**Figure 4.16a**). For all concentrations tested, cells treated with NAC so less loss of viability than those without the treatment, and only in two cases was the difference between those treatments not statistically significant (1 and 100 μM). On average cells treated with NAC show an 8.2% (+/- 3.6%) increase in viability as compared to cells without NAC. These results add credence to the assertion that mitoxantrone generates ROS and that the effect of ROS contributes to the drug's antineoplastic activities. Examination of the 24 hour mitoxantrone/TRAIL combination

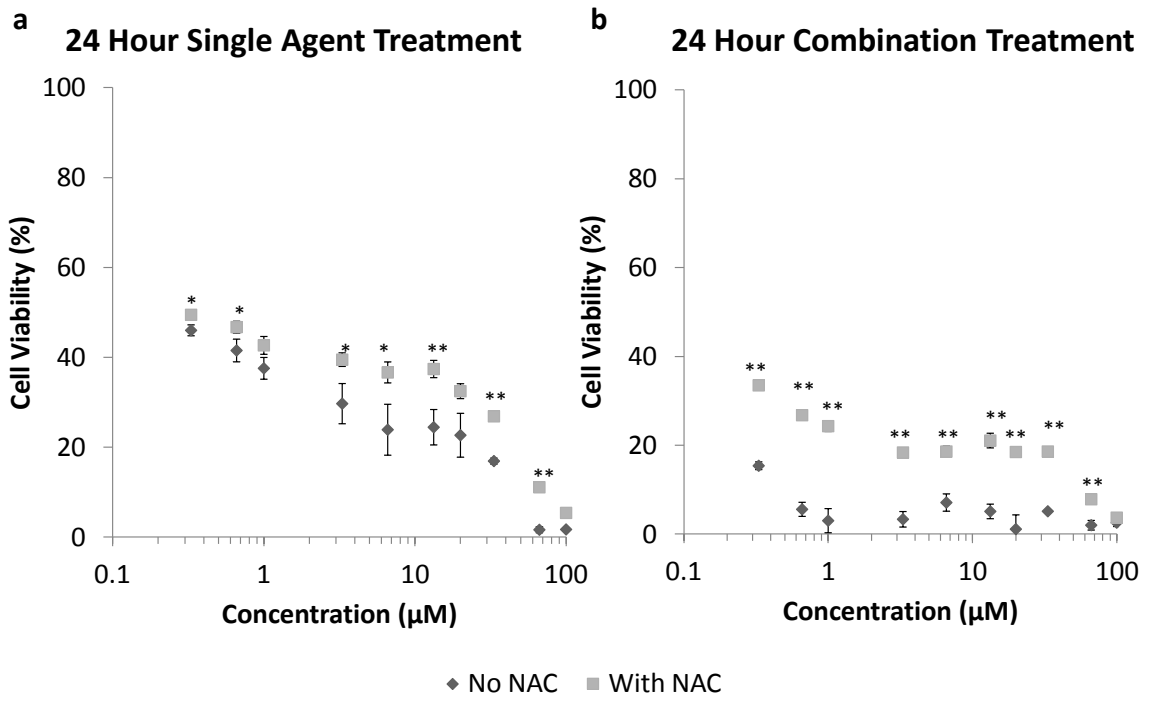


Figure 4.16 24 hour mitoxantrone dose response with N-acetylcysteine co-treatments in PC3-TR prostate cancer. 0-100 μM (a) single agent and (b) sequential combination treatments with 10 ng/mL TRAIL. Comparisons were made between treatments with and without NAC; asterisks (*) and (**) indicate p-values < 0.05 and <0.01, respectively. Data are presented on a logarithmic scale for x-axes in the plots.

treatments indicates that NAC treatments reduce the efficacy of the treatments (**Figure 4.16b**). For all concentrations tested, the difference between the treatments with and without NAC is statistically significant ($p > 0.01$) with the exception of the highest concentration tested (100 μM). Cells treated with NAC show an average 14% (+/- 6.5%) increase in viability. These results further confirm that reducing the intracellular ROS concentrations, reduces the efficacy of mitoxantrone and TRAIL combination treatments. In fact, the results from these combination treatments indicate that the cell viability for single-agent mitoxantrone without NAC, and the viability for combination treatments

with NAC are not statistically different when taking the effect of TRAIL into consideration (8.8% reduction in viability).

The results from the 2 hour mitoxantrone treatments (**Figure 4.15**) show that treatments of NAC do not have an effect on viability when considering the single agent treatments but cells treated with NAC are protected from the combination treatment of mitoxantrone and TRAIL. The 24 hour mitoxantrone treatments (**Figure 4.16**) indicate NAC protects cells from mitoxantrone as a single agent treatment and as a combination treatment with TRAIL. The results also show that single-agent mitoxantrone treatments and combination treatments with NAC are equivalent. These results strongly suggest that ROS play an integral part in mitoxantrone's TRAIL sensitization activity. Cells with lower concentrations of ROS show significant increases in cell viability when undergoing combination treatments.

Comparison of the Efficacy of Mitoxantrone and the Mitoxantrone-Analog, Pixantrone. Pixantrone is an aza-anthracenedione that, similar to mitoxantrone, acts as a topoisomerase II inhibitor and DNA intercalating agent [157, 162, 163]. The drug is undergoing FDA approval trials for the treatment of lymphoma, leukemia, breast cancer and has recently completed Phase III clinical trials for Non-Hodgkins Lymphoma [164, 165]. The drug has attracted significant attention as a chemotherapeutic agent because the drug has been shown to be less cardiotoxic than other antineoplastic drugs like mitoxantrone without reducing overall efficacy [156, 166]. Importantly, the drug generates fewer reactive oxygen species, which is thought to be the reason for the drug's

lower cardiotoxicity [157]. This mitoxantrone analog serves as an important control to mitoxantrone since the drug has similar activity to mitoxantrone with a key difference being the generation of ROS. If the TRAIL-sensitizing activity of mitoxantrone is dependent on the generation of ROS, then combination treatments with pixantrone should show lower efficacies.

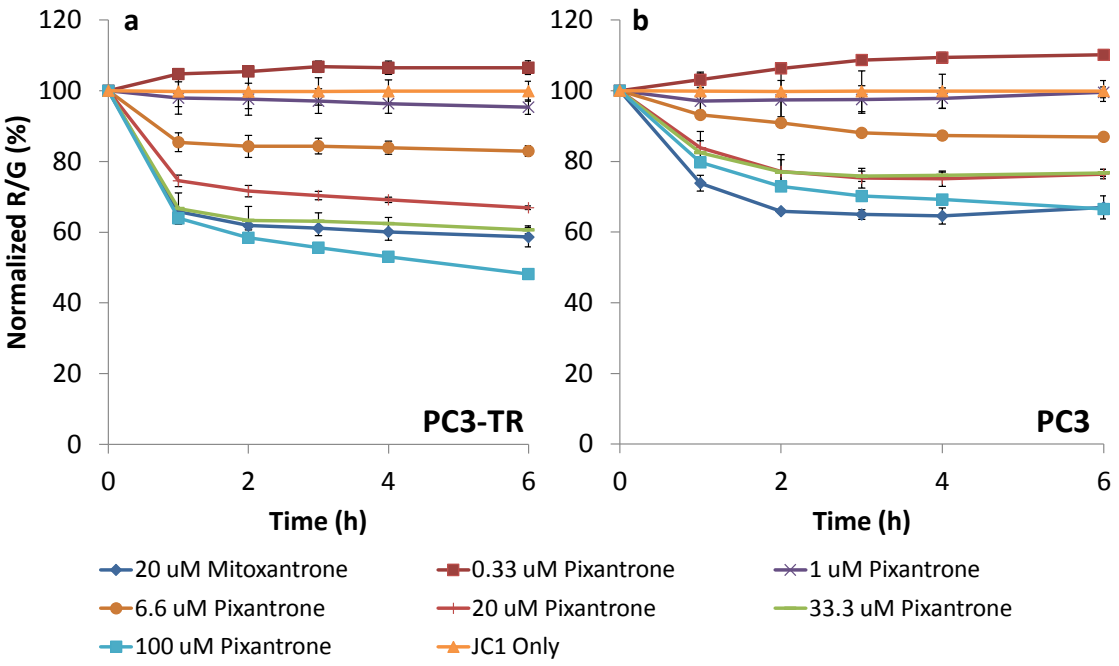


Figure 4.17 Response of PC3 and PC3-TR prostate cancer cells following treatments with increasing concentrations of pixantrone. The change in mitochondrial membrane potential in the cell lines (a) PC3-TR and (b) PC3 shows dose dependence. Lines connecting data are for visualization only.

In order to confirm that pixantrone did result in generation of lower concentrations of ROS, experiments were performed using the same probes and experimental conditions as previously used for mitoxantrone (Detailed in Chapter 4). In these experiments, cellular changes during the first 6 hours of treatment were tracked in the two prostate cancer cell

lines, PC3-TR and PC3. The JC-1 dye was used to track changes in MMP following the treatment of the two cell lines with pixantrone (**Figure 4.17**). In these experiments a positive control of 20 μM mitoxantrone was used to confirm the assay was working and to serve as a basis for comparison between the two drugs. These studies show a dose dependant response to the pixantrone treatments since the calculated R/G ratio decreases with increasing pixantrone concentration. Another interesting trend is that like the same experiment run with mitoxantrone (**Figure 4.5**), PC3 cells appear to be more resistant to the depolarization induced by pixantrone than PC3-TR cells. Over 6 hours, PC3-TR shows a very small increase in the R/G ratio (6%) using a concentration of 0.33 μM and a 50% reduction with a 100 μM concentration. Most importantly, during this 6 hour period the 20 μM mitoxantrone treatment gives a 40% reduction in the normalized R/G ratio. This indicates that at one fifth of the concentration, 20 μM of mitoxantrone is nearly as effective as 100 μM of pixantrone (**Figure 4.17a**). PC3 cells show an approximate 10% increase in the R/G ratio following a 0.33 μM treatment of pixantrone over a 6 hour period. During this time, 100 μM of the drug results in a 34% decrease in the R/G ratio. Following treatments of 20 μM mitoxantrone the PC3 cells also show a 34% decrease in the R/G ratio. This suggests that in this line, 20 μM of mitoxantrone and 100 μM of pixantrone depolarizes the mitochondria to the same extent (**Figure 4.17b**). Results from both cell lines indicate that pixantrone is less effective at inducing the loss of MMP than mitoxantrone. As discussed previously, the loss of MMP and the generation of ROS are closely related and so it is expected that pixantrone would cause less disruption to the membrane potential if the drug does generated fewer ROS than its analog, mitoxantrone. DCFH-DA was used to measure ROS levels in the same manner as when measurements

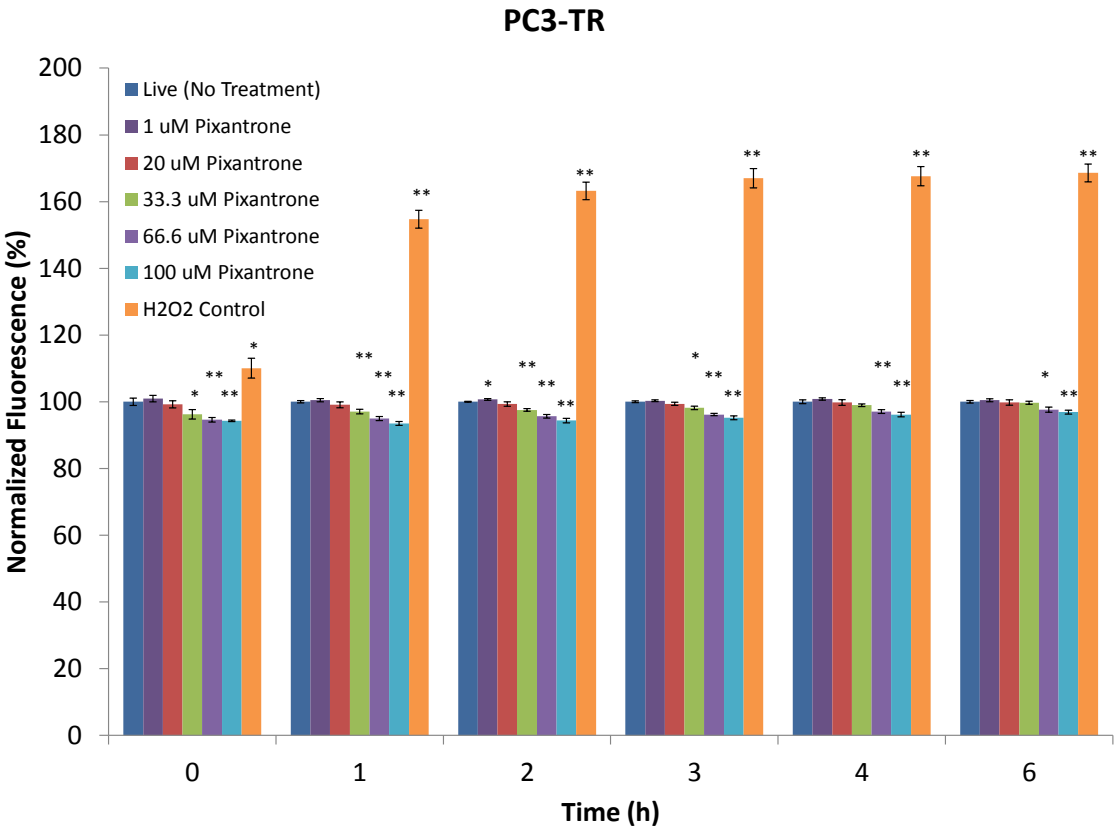


Figure 4.18 Reactive oxygen species generation in pixantrone treated, PC3-TR prostate cancer cells. ROS concentrations measurements were made over a 6 hour period based on the fluorescent intensity of the DCFH-DA dye. Comparisons were made against the live control; asterisks (*) and (**) indicate p-values < 0.05 and < 0.01, respectively. Data are presented as the normalized fluorescent intensity based on the live control measurements.

were taken with mitoxantrone. In these experiments an increase in fluorescent signal corresponds to an increase in ROS concentrations. **Figure 4.18** shows a dose response experiment with pixantrone in the PC3-TR cell line. Hydrogen Peroxide is used as a positive control and as expected it shows the largest and fastest increase in fluorescent intensity as previously shown in the H_2O_2 treatments without NAC shown in **Figure 4.14**. An important distinction between this experiment and the earlier experiment is that the H_2O_2 concentration was reduced significantly from 3.3 mM to 0.33 mM so that the

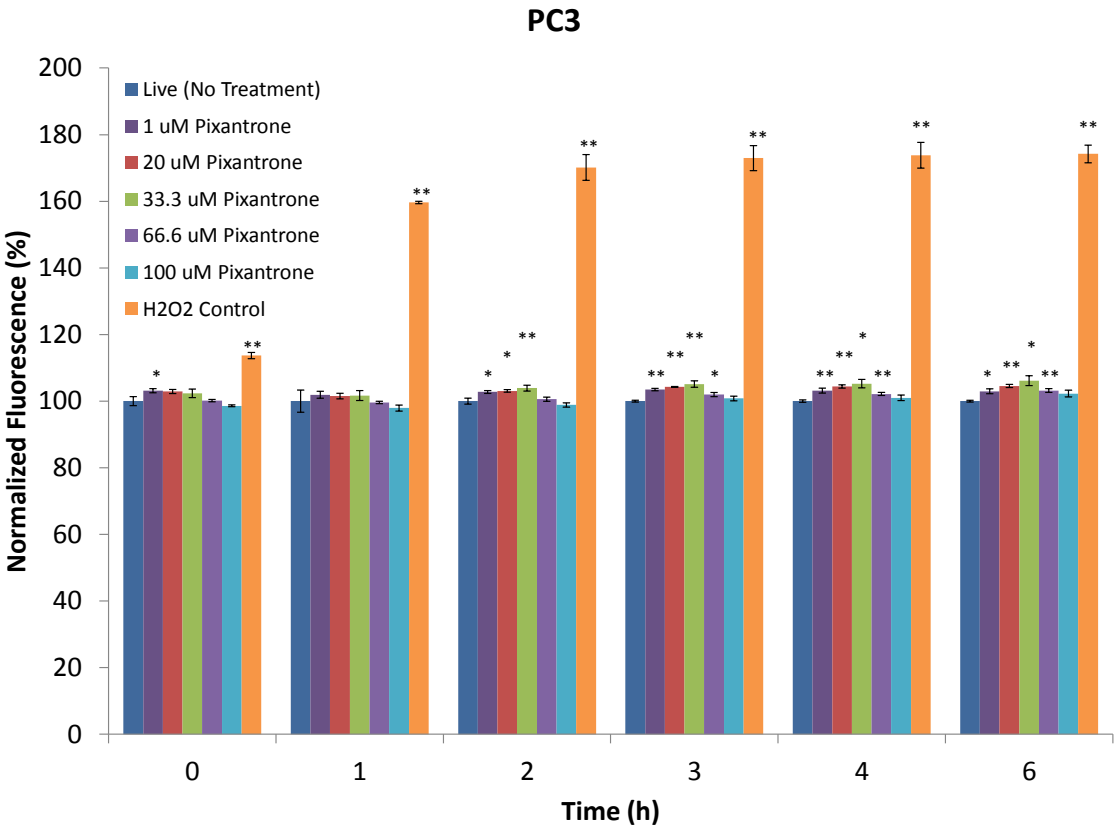


Figure 4.19 Reactive oxygen species generation in mitoxantrone treated, PC3 human prostate cancer cells. ROS concentrations measurements were carried out over a 6 hour period based on the fluorescent intensity of the DCFH-DA dye. Comparisons were made against the live control; asterisks (*) and (**) indicate p-values < 0.05 and < 0.01, respectively. Data are presented as the normalized fluorescent intensity based on the live control measurements.

effect of the positive control didn't dwarf the more subtle changes of the drug treatments. **Figure 4.18** shows a low concentration treatment of pixantrone (1 μM) and the four highest treatment concentrations (20, 33.3, 66.6, and 100 μM) of the drug. Interestingly, the high concentration treatments are shown to significantly reduce the fluorescent intensity as compared to the live control. This is very unexpected since although the drug is known to generate fewer ROS than mitoxantrone there have been no indications that the drug has ROS scavenging activity. However, there is only a 6.5% difference between

the live control and treatment of pixantrone that showed the greatest decrease in fluorescence (100 μM, 1 hour) indicating that while the difference is significant, the effect is small considering the H_2O_2 treatments cause show an approximately 60% increase in the normalized fluorescent intensity. Similarly when comparing these values to the mitoxantrone treatments in the same cell line (**Figure 4.14**), there is an approximate 160-180% increase in the normalized fluorescence when looking at 6 hour treatments of 20-100 μM mitoxantrone (without NAC treatments).

The ROS studies were also performed in PC3 cells (**Figure 4.19**). These results contrast those seen in the PC3-TR cell line since none of the pixantrone treatments show statistically significant reductions in the fluorescence intensity. Treatments of pixantrone start to show significant increases in the fluorescent signal at the initial time point (1 μM) but it is only after 2-3 hours that the increased fluorescence remains consistent. During this 2-3 hour time 1, 20, 33.3, and 66.6 μM treatments of pixantrone all show a significant increase in the normalized fluorescent signal as compared to the live control.

At 6 hours the 33.3 μM pixantrone treatment gives a 6% increase in the normalized fluorescence, the highest increase observed in any of the pixantrone treatments. However, this 6% is inconsequential when compared to the 70% increase caused by H_2O_2. ROS studies for mitoxantrone were not performed in PC3 cells but 20-100 μM treatments of mitoxantrone in MIAPaCa-2 pancreatic cancer cells showed a 100-300% increase in normalized fluorescent intensity after 6 hours (**Figure 4.10**) , and MDA-MB-231 breast cancer cells showed a 50-150% increase after 6 hours (**Figure 4.12**). Taken

together these results all indicate that pixantrone treatments produce minuscule ROS concentrations when compared to the mitoxantrone treatments. These results support the findings found in the literature and provide experimental proof that pixantrone can suitably be used to study whether or not the TRAIL-sensitization activity of mitoxantrone depends on the generation of ROS.

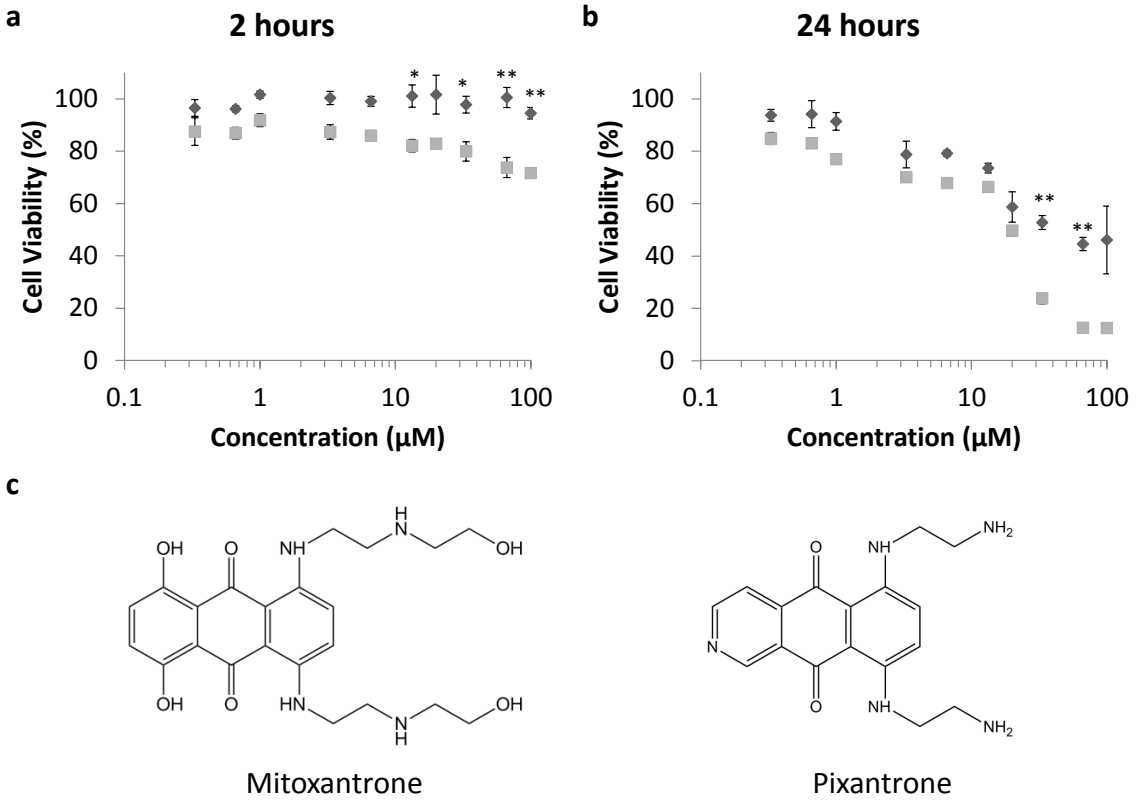


Figure 4.20 Kinetic dose response for pixantrone in PC3 human prostate cancer cells. Malignant cells were treated with mitoxantrone for (a) 2 hours, and (b) 24 hours. For single-agent treatments (dark grey diamonds) the cell viability was assessed following the mitoxantrone treatments. For combination treatments (light grey squares), 10 ng/mL of TRAIL was applied for 24 hours following the initial mitoxantrone treatments. Comparisons were made between the single agent and combination treatments; asterisks (*) and (**) indicate p-values < 0.05 and <0.01, respectively. Data are presented on a logarithmic scale for x-axes in plots. (c) Chemical structures for mitoxantrone (left) and pixantrone (right).

Single agent and combination treatment studies were conducted in the PC3 prostate cancer cell line with treatments of pixantrone and 10 ng/mL of TRAIL (**Figure 4.20**). In these studies, single-agent TRAIL treatments induced an approximate 10% loss in cell viability. The expanded dose range of pixantrone showed a dose dependant response after both 2 and 24 hours of treatment. While the pixantrone/TRAIL combination treatments consistently showed higher efficacies than the single agent treatments, statistically significant sensitization only occurred for the high concentration drug treatments. The 2 hour pixantrone treatment (**Figure 4.20a**) showed significant differences in cell viability after 13.3, 33.3, 66.6, and 100 μM treatments of TRAIL; the greatest difference in cell viability between the single agent and combination treatments was 27% (66.6 μM) which is then adjusted to 17% to account for the effect of single agent TRAIL. This is in contrast to the 2 hour combinatorial studies performed in the same cell line with mitoxantrone (**Figure 4.2b**) where 6.6-100 μM treatments all showed a highly significant difference in the cell viability when comparing single agent and combination treatments. These studies indicated that the largest difference in cell viability between the treatments to be 83% (66.6 μM) after taking the effect of TRAIL into consideration. The LC_{50} analysis between the pixantrone and mitoxantrone treatments indicate that it is not possible to compare the value for the single agent drug treatments, but when looking at the combination treatments the LC_{50} value for pixantrone is greater than 100 μM while the value for mitoxantrone is approximately 9 μM. These results indicate that pixantrone is a poor TRAIL sensitizer when compared to its analog mitoxantrone. Although statistically pixantrone seems to have some synergy with

TRAIL, the overall effectiveness of the treatments is less than that of mitoxantrone, and requires significantly larger concentrations to achieve those effects.

The 24 hour pixantrone treatments (**Figure 4.20b**) showed a significant difference in viability at 33.3 and 66.6 μM concentrations; the greatest difference in cell viability between the single agent and combination treatments was 22% (66.6 μM) after the adjustment made for the effect of single-agent TRAIL. These results can be compared to the 24 hour combinatorial studies performed with mitoxantrone in PC3 cells (**Figure 4.2c**). These studies showed all treatments (0.33-100 μM) gave highly significant differences in the cell viability when comparing single agent and combination treatments. In the mitoxantrone studies, the greatest enhancement in drug activity occurred at the 0.33 μM concentration where there was a 40% difference (the effect of TRAIL accounted for) in the cell viability between single agent and combination treatments. By comparing the single agent LC_{50} values we see that pixantrone gives an LC_{50} value of approximately 45 μM while mitoxantrone gives a value of 5 μM. The LC_{50} values for the combination treatments are 20 μM and 0.1 μM for pixantrone and mitoxantrone respectively. This suggest that a pixantrone dose is 200 time higher than an equivalent mitoxantrone dose when considering combination treatments. These results confirm that, while it does appear to have some TRAIL-sensitization activity, the overall effect of pixantrone is significantly less than that of mitoxantrone. The TRAIL-sensitization activity of mitoxantrone occurs following lower concentrations of treatment and is also more highly effective. Additionally, these results indicate that single agent pixantrone is also less effective than single agent mitoxantrone. The LC_{50} value for pixantrone is 9 times higher

than mitoxantrone. This is not fully unexpected since the 24 hour, single agent, NAC viability experiments (**Figure 4.16a**) showed the ROS scavenging activity of NAC was able to reduce the effectiveness of single agent mitoxantrone which indicates that some of the toxicity of the drug is related to the generation of ROS; in the case of pixantrone this ROS generation is significantly reduced.

Analysis of the pixantrone, a mitoxantrone analog, have shown that the drug is less effective at inducing mitochondrial depolarization, and generates lower concentrations of ROS. It was hypothesized that the ROS mitoxantrone generates were primarily responsible for the TRAIL-sensitization activity of the drug and that since pixantrone generates fewer ROS, it should be less effective at sensitizing the cells to TRAIL. These results confirm this hypothesis and provide additional evidence that ROS are key in the mitoxantrone sensitization mechanism.

Western Blot Analysis of Pro-Apoptotic Mechanisms Influenced by Reactive Oxygen Species. As mentioned previously, ROS are known to have a wide range of pro-apoptotic activities. As discussed in the previous chapter, excessive production of ROS can disrupt the electron transport chain and as a result the mitochondria can become damaged. The resulting loss of mitochondrial membrane integrity can then facilitate the release of pro-apoptotic proteins like cytochrome C and SMAC/DIABLO [153]. Additionally, ROS can also induce pro-apoptotic changes earlier in the apoptotic mechanism. Elongation factors are a family of enzymatic proteins responsible for facilitating the movement of mRNA through the ribosome during protein synthesis [167].

One of these proteins called elongation factor 2 (EF-2) is known to be susceptible to oxidative phosphorylation caused by ROS; the phosphorylation of EF-2 deactivates the enzyme thereby decreasing overall protein synthesis [168]. As a result, the concentration of proteins with short half-lives begins to decrease and the effect of such proteins is attenuated [116]. Several anti-apoptotic proteins like cFLIP [169], XIAP [170], and survivin [171] are known to have short half-lives and as a result ROS are able to decrease resistance to apoptosis through this mechanism. Additionally, ROS can also induce stresses in the endoplasmic reticulum leading to the activation of the CCAAT/ehnancer binding protein homologous protein (CHOP) [172]. Transcriptional DR5 expression can be regulated by CHOP as the protein binds to promoter regions of the DR5 gene [172, 173]. As a result, expression of the death receptors increase, thereby making the cells more susceptible to extrinsically activated apoptosis.

Our previous results indicated that ROS play a role in the TRAIL-sensitization activity of mitoxantrone and based on the known effects ROS can have on apoptotic functions, we targeted three specific proteins (DR5, CHOP, and c-FLIP) to understand what effects mitoxantrone-generated ROS were having. Combination treatment experiments were carried out and analyzed using Western blot techniques (**Figure 4.21**). The results of this analysis indicated that mitoxantrone had apparent effects on each of the proteins screened. Using the live control (no treatment) as a basis for comparison, DR5 concentrations all seemed to increase with the exception of the 6 hour single agent treatment. The combination treatments at 6 and 24 hours showed 70% to 90% increases in DR5 concentration as summarized in **Table 4.1**. The analysis suggests that CHOP

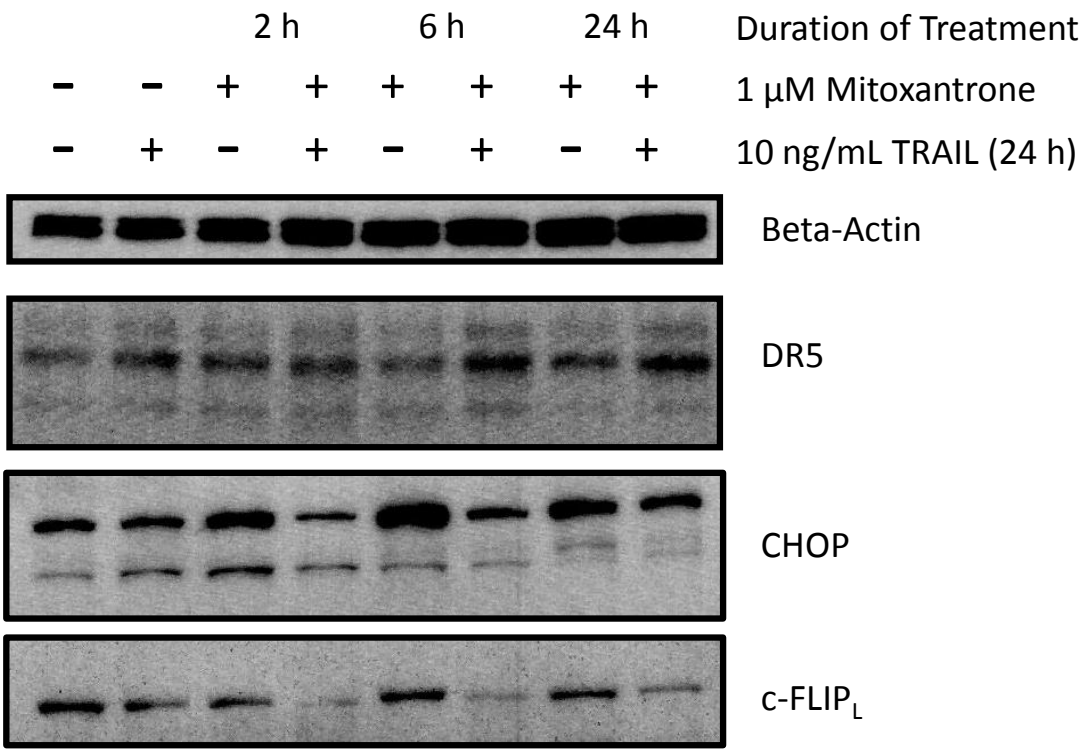


Figure 4.21 Western blot analysis following combination experiments with mitoxantrone. PC3-TR prostate cancer cells were treated with 1 μM mitoxantrone for 2, 6, and 24 hours. For single agent treatments cell lysates were immediately collected (cell death was equal to 0%, 0%, and 70% for 2, 6, and 24 hours respectively); for combination treatments mitoxantrone was removed and treatments continued with 10 ng/mL TRAIL for an additional 24 hours (cell death was equal to 75%, 85%, and 98% for 2, 6, and 24 hours respectively. Quantification of these results is provided in **Table 4.1** below.

concentrations are highest for the single agent treatments with 70%, 210%, and 60% increases at 2, 6, and 24 hours respectively. The combination treatment tend to slightly decrease CHOP concentrations. The c-FLIP concentrations all appear to decrease for all treatment conditions tested with the combination treatments all producing 50% decreases in the concentration as compared to the live control.

Table 4.1 Summary of Western blot densitometry analysis. Values are first normalized against the house-keeper protein (beta-actin) and then against the live control. SA: Single Agent, CT: Combination Treatment.

			2 Hours		6 Hours		24 Hours	
	Live Control	TRAIL Alone	SA	CT	SA	CT	SA	CT
DR5	1.0	1.3 ±0.3	1.2 ±0.1	1.2 ±0.0	1.0 ±0.0	1.7 ±0.3	1.3 ±0.2	1.9 ±0.2
CHOP	1.0	0.9 ±0.1	1.7 ±0.1	0.8 ±0.0	3.1 ±0.8	0.8 ±0.0	1.6 ±0.2	1.0 ±0.0
c-FLIP	1.0	0.8	0.7	0.5	0.9	0.5	0.8	0.5

Taken together, the results from the Western blot protein analysis seem to follow the expected trends and provide confirmation that the generation of ROS is responsible for the TRAIL-sensitization activity of mitoxantrone. The concentrations of DR5 and CHOP are related since excessive ROS leads to endoplasmic reticulum stress which cause an up-regulation of CHOP followed by DR5. The analysis shows that DR5 concentrations increase with the most significant of these increases occurring following the combination treatments at 6 and 24 hours. The CHOP concentrations appear to greatly increase following the single agent treatments but then decrease during the combination treatments. These results are somewhat surprising because the effect of the ROS should drive the concentrations of CHOP up much in the same manner DR5 concentrations increase. To understand why this may be occurring it is important to identify how the timing of the experiment is set up. For single agent treatments, protein lysates are collected after 2, 6, and 24 hours. For combination treatments, the lysates are collected after 26, 30 and 48 hours due to the additional 24 hours added to each treatment (due to TRAIL). Previous studies have shown CHOP mRNA to have a half-life of less than 4

hours [174]. The Western blot analysis seems to suggest that there is an initial increase in the CHOP expression between 2 and 6 hours but as the treatment time progresses to 24, 26, 30, and 48 hours, CHOP expressions decrease significantly. Because ROS also influence translational activity, the half-life of CHOP may be low enough that less of the protein is synthesized at the longer treatment times. Analysis of the c-FLIP results indicate that concentrations of the protein decrease for each of the conditions tested. This is in agreement with the expected trends since the ROS should reduce translational activity, leading to a decrease in the levels of c-FLIP (40 minute half-life [169]). Since the combination treatments have the highest total treatment times, they show the greatest reduction in c-FLIP concentrations.

The results of this analysis indicate that the TRAIL-sensitization activity of mitoxantrone is related to the generation of ROS. The Western blot analysis has shown that mitoxantrone facilitates the CHOP-mediated, up-regulation of DR5 while simultaneously limiting translational activity resulting in the down-regulation of c-FLIP. Both of these activities have pro-apoptotic effects and make the induction of apoptosis by TRAIL less difficult.

CONCLUSIONS

Kinetic and mechanistic studies were used to identify the mechanisms responsible for mitoxantrone's TRAIL-sensitization activity. These studies identified mitoxantrone as a mitochondrial depolarizing agent and confirmation studies showed that the drug consistently decreased the mitochondrial membrane potential over a wide variety of concentrations in different prostate, pancreatic, and breast cancer cell lines. The concentrations of reactive oxygen species were also measured and shown to increase following treatments of mitoxantrone. Results indicated that these cellular changes occurred during the first 6 hours of treatment with mitoxantrone and further kinetic studies indicated that the changes occurring during this time are sufficient to sensitize treated cells to TRAIL-mediated apoptosis. Since ROS have been shown to have pro-apoptotic activities, the ROS-scavenger NAC was characterized and shown to limit the TRAIL-sensitization activity of mitoxantrone. The mitoxantrone analog, pixantrone was shown to produce few ROS than mitoxantrone and was also shown to be a comparatively poor TRAIL-sensitizer. These results further implicated ROS as a major factor in TRAIL-sensitization. Finally, Western blot analyses were conducted to determine what effects mitoxantrone treatments were having on apoptosis-related proteins. Knowing that ROS appeared to play a role in the sensitization activity, a small screen of these proteins showed that mitoxantrone treatments limit the generation of the anti-apoptotic protein c-FLIP, and increase the expression of the pro-apoptotic proteins CHOP and DR5.

CHAPTER 5

FUTURE DIRECTIONS

INTRODUCTION

The primary objective of the research presented to this point has revolved around the identification of FDA-approved drugs that can be used in novel chemotherapeutic treatment methodologies and how these methodologies can be improved and enhanced. To this end we have: 1) described the screening and identification of drugs that act synergistically with the pro-apoptotic protein TRAIL, 2) worked to design, build, and test a microfluidic device that can be used to optimize the experimental conditions to make the combination treatments more effective, 3) and identified the mechanism responsible for the TRAIL sensitization activity of the antineoplastic drug, mitoxantrone. In this outline the work that I believe to be the next steps in the evolution of this work.

FUTURE DIRECTION 1: Screen the remaining drugs in the John Hopkins Clinical Compound Library for TRAIL-sensitization activity and identify the mechanism of action of identified leads.

Introduction

Chapter 2 describes how we screened a small set of FDA-approved antineoplastic drugs for their ability to work synergistically with TRAIL to induce cell death in various cancer cell lines. This selective screen was done with antineoplastic agents since some of the antineoplastic drugs from the library had previously been shown to work in combination with TRAIL and we could verify the results of our screen by comparing the drugs we identified with those in the literature. It was also beneficial to study antineoplastic drugs since the majority of these drugs are nucleosides and their activities are closely coupled with the apoptotic machinery used by TRAIL. During this screen we identified several drug candidates which showed an enhanced effect when used in combination with TRAIL and we further characterized the activity in additional cell lines while confirming our results. Additionally, we also looked at how the combination treatment methodologies could be changed and what effect that would have on cell viability. In order to expand these studies it will be necessary to perform a rigorous mechanistic evaluation of the identified leads in order to understand why TRAIL-sensitization is occurring like the one completed for mitoxantrone. It is also desirable to complete the screening studies with the remaining compounds in the drug library to see if there are drugs that fall outside of the antineoplastic class that also show synergy with TRAIL.

Hypothesis

Our previous research has already identified several chemotherapeutic drugs that sensitize various types of cancer cells to TRAIL-mediated apoptosis. Future research should expand the screen outside of the antineoplastic drug class in an attempt to indentify addition FDA and foreign approved drugs that exhibit TRAIL-sensitization activity. By developing a detailed understanding of how the sensitization activity occurs it will be possible to develop treatment strategies with these drugs that can be rapidly translated from benchtop to patient bedsides. Additionally, an understanding of these mechanisms can lead to the identification/development of other drugs useful for combination treatments with TRAIL.

Experimental Design

The previous screening of the antineoplastic agents was manually done in 96-well plates with an initial screen conducted at 20 μM followed by a screening at 10 μM for drugs that showed a decrease in cell viability greater than 30%. Drug concentrations were kept low in these experiments in order to limit the toxicity of the drugs since their primary activity was specific to the treatment of cancer. The activities of the single-agent drug treatments were then compared to the activity of the drugs used in combination with TRAIL (sequential treatment). Leads were identified as drugs that showed a decrease in cell viability that was significantly greater than the loss of viability induced by the sum of the single-agent drug and single-agent TRAIL treatments. Screening of the remaining compounds should be carried out using the same process but in the case of the treatment concentrations, it may be necessary to screen at concentrations above 20 μM since it may

be difficult to determine what concentrations of these drugs will be effective for treating cancer when the majority of the remaining drugs are not used for this purpose. In order to rapidly screen the remaining compounds in the drug library it would be advantageous to use a high-throughput liquid handling system (LHS). In order to a LHS it will be necessary to generate a working protocol that mimics the studies performed in the well plate but that is amenable to use by the screening robot. Drugs from the compound library are provided as 10 µM aliquots and distributed among several 96-well plates. The first step in preparing the drugs for treatment would be making 2000 µM drug dilutions for the initial 20 µM treatment. 2000 µM stock concentrations are necessary so the total treatment volume is not below the working range of the machine (< 1 µL) and that the total solvent concentration is less than 1% (v/v) when the drug is applied to the cells. By providing a 96 well plate prefilled with the solvents for each drug, it will be possible to use a LHS to mix the drug dilutions thereby creating a 96 well plate of 2000 µM drug dilutions. These 2000 µM drug plates can then be used to treat plates of adherent cells directly. For single agent treatments, following the incubation of drug treated cells for 24 hours, the LHS will remove and refresh the culture media and then the LHS will be used to treat cells using the MTT assay. The conversion of the MTT reagent to MTT can be measured using the microplate reader as previously described. For combination treatments, the cells should be incubated with 10 ng/mL of TRAIL following the initial drug treatment. In this case, the TRAIL can be premixed with the cell culture media and applied when the LHS refreshes the media after the first 24 hour treatment. An MTT analysis should then be carried out after an additional 24 hour TRAIL treatments. In all experimental cases, replicate experiments should be set up across different 96 well plates

since the LHS is not able to apply the same drug treatment to adjacent wells. For example, the screening of one 2000 μM drug plate will require three separate 96 well plates with adherent cells for triplicate data.

When running the experiments using the liquid handling system the rate determining step will be how fast cells can be grown to confluence and the number of 96 well plates the cells will be able to fill; making drug dilutions and doing drug treatments should only take a few minutes to run using the LHS. There are a total of 24 drug plates in the JHCCL and assuming that all results will only need to be run at a single concentration in triplicate, the single agent treatments will require 72 plates with adherent cells and the combination treatments will require an additional 72 plates. The rate of cell growth is dependent on the line, but a conservative estimate would be that 18 plates can be made in a week which means that the total screening project could be finished in as little as 2 months but it would likely take closer to 3 months since it is unlikely that 20 μM will be the optimum concentration for all 24 drug plates.

Along with screening the remaining compounds in the JHCCL, the second part of this study should be the rigorous mechanistic evaluation of the lead compounds that showed TRAIL sensitizing activity. Such an analysis would be similar to that described in Chapter 4 of this document although since different drugs will have different activities, the exact progression of the evaluations will vary, but a general outline will be described. The ability of TRAIL to induce cell death in malignant cells is a result of the drug activating the extrinsic apoptotic mechanism. As previously described, TRAIL binds to

death receptors on the outer membrane of the cell which leads to the eventual formation of the death-inducing signaling complex (DISC) which can either induce apoptosis directly or can use the intrinsic pathway as an amplification loop and induce apoptosis in that manner. In order to evaluate the mechanism of action of the TRAIL sensitizing drugs it will be necessary to monitor the levels of proteins that are involved in TRAIL-induced apoptosis. Specifically we will monitor the levels of pro-apoptotic proteins (e.g. DR 4 and 5, caspase 3, cytochorme c) and anti-apoptotic proteins (Decoy Receptors 1 and 2, c-FLIP, Bcl-2) to determine if combination treatments show any changes in the protein expression levels and if so which ones. These studies will be carried out using Western blots. Since the activity of TRAIL is rooted in apoptosis, monitoring the levels of apoptotic proteins provides an excellent starting point for the mechanistic evaluation. It is expected that in most cases there will be some change in the apoptotic machinery that makes TRAIL-induced apoptosis more effective. The TRAIL sensitizing activity of doxorubicin is well characterized and is partially attributed to the down-regulation of c-FLIP [108, 113] and the up-regulation of pro-apoptotic caspases [114, 115]. Using information such as this, we can form hypotheses based on the results we see and the treatments we are using as to why a particular drug treatment works synergistically with TRAIL.

The results from the antineoplastic drug screen identified several drugs that showed the ability to sensitize cells to TRAIL. This is expected since the activity of these drugs is related to their ability to cause DNA damage and is therefore closely related to the induction of apoptosis. The mechanisms of action of many of these drugs have been

described while the mechanisms for many others have not. By monitoring changes in the protein levels and comparing our results to the activity of other drugs described in the literature it should be possible to evaluate why the lead candidates in this screen (e.g. mitoxantrone and mithramycin) are effective with TRAIL. Following the complete screening of the JHCCL it is possible that additional TRAIL sensitizers that fall outside of the antineoplastic drug class will be identified. Describing the mechanism of sensitization of such drugs will be potentially more difficult since the activity may fall outside of the apoptotic pathway. However, by using the known activity of TRAIL as a starting point and monitoring cellular changes the drugs induce, it should be possible to elucidate these types of mechanism as well.

Evaluating a large library of FDA-approved drugs has both short-term and long-term advantages. On the short-term side, identifying alternative uses for FDA-approved drugs provides a means of reducing the costs associated with the research and development of drugs as well as the costs associated with the FDA testing and approval of the drugs; the drugs are already made and a portion of the FDA testing is already completed so time and money are saved. This means that the transition between the lab findings and patient treatments could be significantly reduced. The future trajectory of these short-term studies should be centered around the testing of these different combination treatments in-vivo. Before any type of transition to patients occurs it is necessary to confirm that the combination treatments are effective outside of plate based experiments and that such treatments are not overly harmful to healthy tissue.

In addition to in-vivo experiments, future work with these drugs/TRAIL should include a strategy for the delivery. Although the effect of TRAIL is cancer cell specific, the effect of many other drugs is not. It may be possible to mitigate this effect by using relatively low concentrations of the sensitizer drugs but non-specific effects are always a concern. Developing a cancer-targeting delivery system should not only reduce damage to non-malignant cells but can also enhance the efficacy of the treatment. In addition to targeting functionality, the delivery systems could potentially incorporate both the drug and TRAIL on a single carrier making it possible to apply a single treatment instead of multiple ones. One limitation of any delivery system is that the system itself has to be approved for use by the FDA and while the focus of our work is to limit the cost associated with the FDA approval, delivery systems may be necessary to limit the non-specific effects of a given treatment.

The long-term advantages of screening the library and identifying the mechanism of action of the drugs is that it may be possible to determine what functionality the drugs have and how it relates to their TRAIL sensitizing activity. From this information it may be possible to model the effect of specific TRAIL sensitizing activities and using this information to identify compounds outside of the JHCCL that may also have this activity. Although our research is mainly concerned with identifying leads that have already been approved by the FDA, this strategy could also be applied to designing new drugs with a specific TRAIL sensitization functionality. Essentially, the complete screening and understanding of this library will provide specific information about the chemical characteristics that help these drugs work synergistically with TRAIL and so the directed

synthesis of compounds that take advantage of these characteristics could should enhanced efficacy and specificity.

FUTURE DIRECTION 2: Design and testing of in-vitro systems that emulate the tumor microenvironment of pancreatic cancer.

Introduction

The objective of this proposed research is to develop an in-vitro model of the desmoplastic reaction associated with pancreatic cancer in order to maximize the treatment efficacy of chemotherapeutic treatments. The study described in Chapter 2 identified several FDA-approved chemotherapeutic drugs that sensitize pancreatic cancer cells to TRAIL-mediated apoptosis in-vitro. The proposed research will test the efficacy of these drugs in an environment in which pancreatic cancer are co-cultured with pancreatic stellate cells and fibroblasts in order to rapidly identify drugs that retain their TRAIL sensitizing effect in the pro-survival microenvironment while simultaneously developing a platform that can be used for the testing of other treatment methodologies.

Pancreatic cancer is the fourth most lethal cancer in the United States. Every year, approximately 44,000 individuals are diagnosed with pancreatic cancer and over 37,000 people die from the disease [175]. The most common type of pancreatic cancer is pancreatic ductal adenocarcinoma (PDAC), accounting for more than 85% of occurrences [176]. PDAC has a 5-year survival rate between 3-5% and a median survival of less than 6 months [177]. The extreme lethality of pancreatic cancer demands new and effective ways to combat the disease and to improve the quality of life of patients. The poor efficacy of chemotherapeutic drugs can be partially attributed to the fibrotic (desmoplastic) response in PDAC [178-180]. Specifically, pancreatic cancer cells can recruit other cell types, like fibroblasts and stellate cells, to create an environment that

promotes proliferation of the cancer cells [181]. Components of the extracellular matrix form and help protect malignant cells by limiting the access of chemotherapeutic drugs, thereby decreasing the overall effect [180]. The fibrotic response and its associated microenvironment present a key challenge in the effective treatment of pancreatic cancer.

The median survival of patients with PDAC is six months with a 5-year survival rate of 3-5% [177]. Surgical options are available if the disease is diagnosed early, increasing the median survival to 18 months and the 5-year survival to approximately 25 percent [182, 183]. However, only 10-15% of PDAC cases are eligible for surgery upon diagnosis [184]. The fibrotic (desmoplastic) response [178-180] in PDAC is largely responsible for the low efficacy of chemotherapeutic drugs. Pancreatic cancer cells will recruit other types of cells, including stellate cells and fibroblasts, to promote cell survival. Formation of an extracellular matrix (collagen) promotes pancreatic cancer survival through the expression of genes that promote proliferation, while simultaneously limiting drug penetration [185, 186]. Effective PDAC treatment methods need to be developed in order to improve the prognosis of the individuals afflicted with this disease.

The expression levels of Death Receptors 4 and 5 (DR4 and DR5) are significantly elevated in PDAC compared to non-malignant pancreatic cells [187, 188]. Although PDAC cells express death receptors, they are resistant to low concentration treatments of TRAIL (1-100 ng/mL) as shown in our initial finding. At higher concentrations (> 200 ng/mL) investors report increased cell death with TRAIL treatment [189]. In-vitro studies have also shown the sensitivity of PDAC cells to TRAIL treatments correlate with their

levels of DR4 and DR5 expression [190] and K-Ras status [191]. In-vivo studies have shown that patient primary tumor xenografts included a mix of TRAIL-sensitive and TRAIL-resistant pancreatic tumors [192]. Furthermore, death receptors antagonist antibodies have demonstrated antitumor activities in PDAC cell lines and animal models [61, 193]. These results all indicate that TRAIL-based therapies are a viable treatment option for PDAC.

Hypothesis

By co-culturing pancreatic cancer with pancreatic stellate cells and fibroblasts in collagen and Matrigel, it should be possible to create an in-vitro screening model that better emulates the tumor microenvironment associated with PDAC. It will also be interesting to examine how the co-cultures will react when grown on top of amikacin hydrogels developed in our lab; these hydrogels shown that a large number of cell lines cultured on these hydrogels have the propensity to aggregate and for spheroids. These platforms will be useful for the design and testing of chemotherapeutic options, potentially leading to lowered failure rates and higher probability of translation. In addition, the in-vitro systems developed in this research can be used to develop targeted treatments and delivery vehicles that exploit the characteristic properties of the microenvironment aiding in the treatment and prevention of the disease.

Experimental Design

Previous investigations (described in Chapter 2) identified several chemotherapeutic drugs that exhibited the ability to sensitize pancreatic cancer to TRAIL-mediated cell death. The immediate studies can be used to determine if these chemotherapeutic treatments are effective in systems that are more representative of the pancreatic tumor microenvironment. To replicate these environments we it will be interesting to study both well-plate based, and microfluidic based experiments (as described in Chapter 4). Research should focus on looking at co-cultures of pancreatic cancer cells and pancreatic stellate cells/fibroblasts and how collagen, Matrigel, and the amikacin hydrogels can be used to make more representative, in-vitro models.

Well plate based experiments should primarily focus on growing co-cultures in collagen/Matrigel [185, 194, 195] and using amikacin hydrogels to form spheroids. Cultures of cells can be plated in a variety of different manners in order to test as many different geometries as possible in order to determine the limitations associated with different geometries. Some geometries that can be considered are: cultured cells grown on a plate bottom with collagen/Matrigel on top of the cells; cells grown on top of collagen/Matrigel; cells cultured between a sandwich of collagen/Matrigel; and three-dimensional geometries in which cells are cultured within a collagen/Matrigel support structure; importantly, the amikacin hydrogels are shown to be able to form three-dimensional spheroids without the need for collagen/Matrigel support structures. These systems are of particular interest because they create a physical barrier that will need to be overcome in order to effectively treat the pancreatic cancer. Cells will be treated with

the sensitizing drug/TRAIL treatment as previously described but in addition to analyzing cell-viability, it will be important to identify how the treatments diffuse into the different geometries.

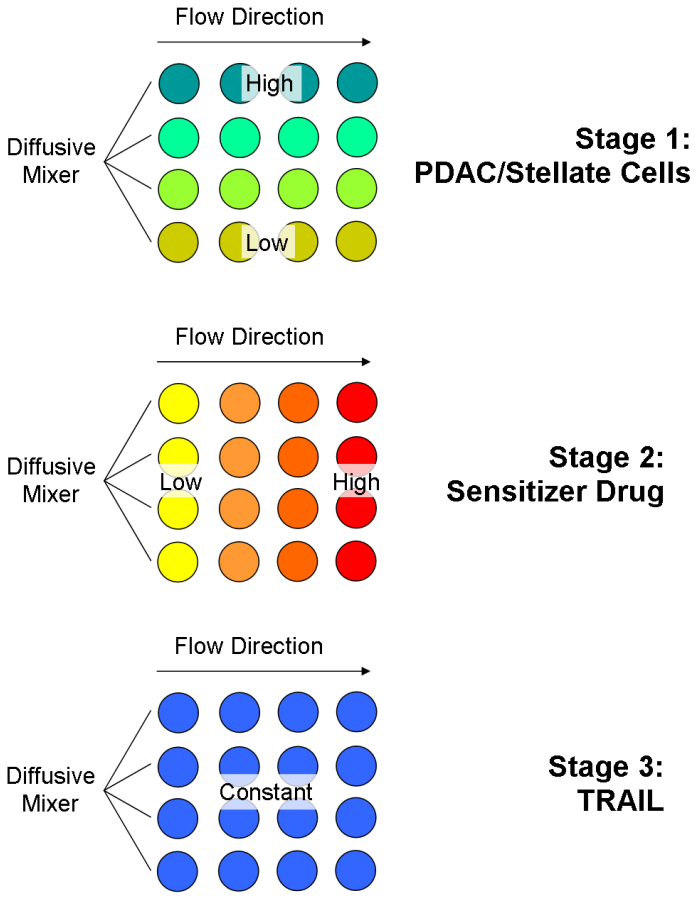


Figure 5.1 Microfluidic based, co-culture experiments. The experimental set-up for these experiments is divided into 3 stages. The first stage is the seeding of the PDAC and stellate/fibroblasts. The second stage is treatment with the TRAIL-sensitizing drug and the final stage is treatment with TRAIL.

Microfluidic based experiments will focus on identifying how the efficacy of chemotherapeutic drugs change when malignant cell lines are co-cultured with cells that promote a pro-survival environment. It will be important to also investigate how the composition of these co-cultures will effect chemotherapeutic options. To do this we will

use the microfluidic device described in Chapter 2. The methodology of how we will set up and test the experiments is shown in **Figure 5.1**. In the **first stage** of the experiment a cell solution of PDAC cells will be injected into one of the inlets of the microfluidic device while a cell solution of pancreatic stellate/fibroblasts will be injected into the other. This will create a gradient of different cell mixtures in the microfluidic device. For example 100% PDAC/0% Stellate cells to 0% PDAC/100% Stellate cells. The **second stage** of the experiment will be the treatment of the co-cultures with a TRAIL-sensitizing drug for 24 hours (although it is possible to apply the drug for any period of time). In this case the drug gradient will be produced via LabView and manipulation of the pneumatic valves. For single agent analysis the experiment should conclude after the second stage at which point the cells are stained for fluorescent image analysis. In the case of combination treatments, the **third stage** is the treatment of the co-cultures with TRAIL for an additional 24 hours. In this stage a single concentration of TRAIL is injected into both microfluidic inlets. This is the limiting step in our experiment since we can only test one concentration of TRAIL at a time but the speed with which experiments can be run on the microfluidic platform should prevent this from being a problem.

In order to better understand the interactions between the pancreatic cancer and the stellate cells it will be important to monitor molecular mechanisms. By monitoring the levels of proteins that have been implicated in the recruitment of stellate cells by malignant pancreatic cancer cells (e.g. interleukin (IL)-1, (IL)-6, transforming growth factor (TGF)-β1) [181, 196, 197] and the levels of proteins expressed in an environment that is favorable to cancer cell growth (e.g. α-SMA, collagen) [181] it will be possible to

determine if the co-culture systems we are developing are better models for the tumor microenvironment than systems where only pancreatic cancer cells are present. In addition, it is also important to understand the behavior of cells after drug treatments since we are interested in measuring the efficacy of our sensitizer drug/TRAIL treatments. This information can then be used to understand why a particular treatment is effective and potentially suggest/develop better treatment methodologies.

The first set of mechanistic evaluations will compare protein levels of the pancreatic cancer cells grown alone, pancreatic stellate/fibroblasts grown alone, and the cells grown in co-culture. The levels of proteins that relate to the tumor microenvironment and of apoptotic related proteins, specifically those involved in the execution/inhibition of TRAIL-mediated apoptosis (e.g. DR 4 and 5, XIAP, c-FLIP, Bcl-2) should all be monitored. This can be done with a variety of different co-culture ratios in order to determine how protein levels in these systems change based on the concentration of different cells in co-culture. Protein levels can be evaluated using Western Blots in plate-based experiments. In addition to the mechanistic studies, it will be necessary to understand if/how the cell viability will change in these experiments. It should be noted that although the primary studies on viability changes in cells grown as co-culture will be explored using the microfluidic system, it will be important to document these changes in the well plate experiments as well. This will also allow for a comparison between the two experimental set ups.

The second set of mechanistic evaluations should examine how cancer cells react when grown in the presence of collagen/Matrigel or when grown on amikacin hydrogels. Using these results we will be able to compare the protein levels in co-culture with and without collegen/Matrigel and protein levels of spheroids formed on amikacin gels. Additionally, the cell viability in these systems should also be evaluated.

Additional mechanistic evaluations will focus on the health of cells following treatments with TRAIL-sensitizing drugs and TRAIL. These results can be compared to cell treatments carried out in non-co-culture experiments. This can help identify the reason for any discrepancies in efficacy between the single cell type and co-culture systems. These evaluations are important in developing treatment methodologies that are more effective in a pro-survival type of microenvironment.

Successful completion of this aim will result in the development of an in-vitro system that better emulates the tumor microenvironment associated with pancreatic cancer. Such a platform would be of extreme value for the design and testing of chemotherapeutic treatment options. While our studies are mainly focused on combinatorial treatments with TRAIL, this is only a single treatment methodology and the system could potentially be used for any pancreatic cancer therapies. Being able to mimic the physiological conditions associated with pancreatic cancer would certainly be of high value and it could lead to improved treatment methodologies. Such a system would also provide the opportunity to exploit the characteristic properties of the microenvironment for targeting and delivery purposes.

REFERENCES

1. Society, A.C. *Cancer Facts & Figures - 2012 - acspc-031941.pdf.* 2013/04/05/21:13:29; Available from: http://www.cancer.org/acs/groups/content/@epidemiologysurveilance/documents/document/acspc-031941.pdf.

2. DiMasi, J.A., R.W. Hansen, and H.G. Grabowski, *The price of innovation: new estimates of drug development costs.* Journal of Health Economics, 2003. **22**(2): p. 151-185.

3. Sleigh, S.H. and C.L. Barton, *Repurposing Strategies for Therapeutics.* Pharmaceutical Medicine, 2010. **24**(3): p. 151-159 10.2165/11536770-000000000-00000.

4. Chong, C.R. and D.J. Sullivan, *New uses for old drugs.* Nature, 2007. **448**(7154): p. 645-646.

5. Rothstein, J.D., et al., *beta-Lactam antibiotics offer neuroprotection by increasing glutamate transporter expression.* Nature, 2005. **433**(7021): p. 73-77.

6. Zhu, S., et al., *Minocycline inhibits cytochrome c release and delays progression of amyotrophic lateral sclerosis in mice.* Nature, 2002. **417**(6884): p. 74-78.

7. Jomaa, H., et al., *Inhibitors of the nonmevalonate pathway of isoprenoid biosynthesis as antimalarial drugs.* Science, 1999. **285**(5433): p. 1573-1576.

8. Shigi, Y., *INHIBITION OF BACTERIAL ISOPRENOID SYNTHESIS BY FOSMIDOMYCIN, A PHOSPHONIC ACID-CONTAINING ANTIBIOTIC.* Journal of Antimicrobial Chemotherapy, 1989. **24**(2): p. 131-145.

9. Missinou, M.A., et al., *Fosmidomycin for malaria.* Lancet, 2002. **360**(9349): p. 1941-1942.

10. Kruger, E.A. and W.D. Figg, *TNP-470: an angiogenesis inhibitor in clinical development for cancer.* Expert Opinion on Investigational Drugs, 2000. **9**(6): p. 1383-1396.

11. Griffith, E.C., et al., *Methionine aminopeptidase (type 2) is the common target for angiogenesis inhibitors AGM-1470 and ovalicin.* Chemistry & Biology, 1997. **4**(6): p. 461-471.

12. Marton, L.J. and A.E. Pegg, *POLYAMINES AS TARGETS FOR THERAPEUTIC INTERVENTION.* Annual Review of Pharmacology and Toxicology, 1995. **35**: p. 55-91.

13. Ghobrial, I.M., T.E. Witzig, and A.A. Adjei, *Targeting apoptosis pathways in cancer therapy.* Ca-a Cancer Journal for Clinicians, 2005. **55**(3): p. 178-194.

14. Ashkenazi, A. and R.S. Herbst, *To kill a tumor cell: the potential of proapoptotic receptor agonists.* Journal of Clinical Investigation, 2008. **118**(6): p. 1979-1990.

15. Fulda, S. and K.M. Debatin, *Extrinsic versus intrinsic apoptosis pathways in anticancer chemotherapy.* Oncogene, 2006. **25**(34): p. 4798-4811.

16. Gulbins, E., et al., *Physiology of apoptosis.* American Journal of Physiology-Renal Physiology, 2000. **279**(4): p. F605-F615.

17. Wong, R.S.Y., *Apoptosis in cancer: from pathogenesis to treatment.* Journal of Experimental & Clinical Cancer Research, 2011. **30**: p. 14.

18. Strasser, A., L. O'Connor, and V.M. Dixit, *Apoptosis signaling.* Annual Review of Biochemistry, 2000. **69**: p. 217-245.

19. Kerr, J.F.R., C.M. Winterford, and B.V. Harmon, *APOPTOSIS - ITS SIGNIFICANCE IN CANCER AND CANCER-THERAPY.* Cancer, 1994. **73**(8): p. 2013-2026.

20. Sheikh, M.S. and A.J. Fornace, Jr., *Death and decoy receptors and p53-mediated apoptosis.* Leukemia, 2000. **14**(8): p. 1509-13.

21. Kaufmann, S.H. and D.L. Vaux, *Alterations in the apoptotic machinery and their potential role in anticancer drug resistance.* Oncogene, 2003. **22**(47): p. 7414-7430.

22. Pommier, Y., et al., *Apoptosis defects and chemotherapy resistance: molecular interaction maps and networks.* Oncogene, 2004. **23**(16): p. 2934-2949.

23. Broker, L.E., F.A.E. Kruyt, and G. Giaccone, *Cell death independent of caspases: A review.* Clinical Cancer Research, 2005. **11**(9): p. 3155-3162.

24. Letai, A., *Pharmacological manipulation of Bcl-2 family members to control cell death.* Journal of Clinical Investigation, 2005. **115**(10): p. 2648-2655.

25. Coultas, L. and A. Strasser, *The role of the Bcl-2 protein family in cancer.* Seminars in Cancer Biology, 2003. **13**(2): p. 115-123.

26. Henry-Mowatt, J., et al., *Role of mitochondrial membrane permeabilization in apoptosis and cancer.* Oncogene, 2004. **23**(16): p. 2850-2860.

27. Kandasamy, K., et al., *Involvement of proapoptotic molecules Bax and Bak in tumor necrosis factor-related apoptosis-inducing ligand (TRAIL)-induced mitochondrial disruption and apoptosis: Differential regulation of cytochrome c and Smac/DIABLO release.* Cancer Research, 2003. **63**(7): p. 1712-1721.

28. Vousden, K.H. and X. Lu, *Live or let die: The cell's response to p53.* Nature Reviews Cancer, 2002. **2**(8): p. 594-604.

29. Ashkenazi, A., *Targeting death and decoy receptors of the tumour-necrosis factor superfamily.* Nature Reviews Cancer, 2002. **2**(6): p. 420-430.

30. Tschopp, J., M. Irmler, and M. Thome, *Inhibition of Fas death signals by FLIPs.* Current Opinion in Immunology, 1998. **10**(5): p. 552-558.

31. Ozoren, N. and W.S. El-Deiry, *Defining characteristics of Types I and II apoptotic cells in response to TRAIL.* Neoplasia, 2002. **4**(6): p. 551-557.

32. Bouralexis, S., D.M. Findlay, and A. Evdokiou, *Death to the bad guys: targeting cancer via Apo2L/TRAIL.* Apoptosis, 2005. **10**(1): p. 35-51.

33. Kim, Y. and D.W. Seol, *TRAIL, a mighty apoptosis inducer.* Mol Cells, 2003. **15**(3): p. 283-93.

34. Kelley, S.K. and A. Ashkenazi, *Targeting death receptors in cancer with Apo2L/TRAIL.* Curr Opin Pharmacol, 2004. **4**(4): p. 333-9.

35. Almasan, A. and A. Ashkenazi, *Apo2L/TRAIL: apoptosis signaling, biology, and potential for cancer therapy.* Cytokine Growth Factor Rev, 2003. **14**(3-4): p. 337-48.

36. Baetu, T.M. and J. Hiscott, *On the TRAIL to apoptosis.* Cytokine Growth Factor Rev, 2002. **13**(3): p. 199-207.

37. Kelley, S.K., et al., *Preclinical studies to predict the disposition of Apo2L/tumor necrosis factor-related apoptosis-inducing ligand in humans: characterization of in vivo efficacy, pharmacokinetics, and safety.* J Pharmacol Exp Ther, 2001. **299**(1): p. 31-8.

38. Thorburn, A., *Death receptor-induced cell killing.* Cell Signal, 2004. **16**(2): p. 139-44.

39. Lawrence, D., et al., *Differential hepatocyte toxicity of recombinant Apo2L/TRAIL versions.* Nat Med, 2001. **7**(4): p. 383-5.

40. Naka, T., et al., *Effects of tumor necrosis factor-related apoptosis-inducing ligand alone and in combination with chemotherapeutic agents on patients' colon tumors grown in SCID mice.* Cancer Res, 2002. **62**(20): p. 5800-6.

41. Singh, T.R., et al., *Synergistic interactions of chemotherapeutic drugs and tumor necrosis factor-related apoptosis-inducing ligand/Apo-2 ligand on apoptosis and on regression of breast carcinoma in vivo.* Cancer Res, 2003. **63**(17): p. 5390-400.

42. Thai le, M., et al., *Apo2l/Tumor necrosis factor-related apoptosis-inducing ligand prevents breast cancer-induced bone destruction in a mouse model.* Cancer Res, 2006. **66**(10): p. 5363-70.

43. Ganten, T.M., et al., *Preclinical differentiation between apparently safe and potentially hepatotoxic applications of TRAIL either alone or in combination with chemotherapeutic drugs.* Clin Cancer Res, 2006. **12**(8): p. 2640-6.

44. Zhang, L. and B. Fang, *Mechanisms of resistance to TRAIL-induced apoptosis in cancer.* Cancer Gene Ther, 2005. **12**(3): p. 228-37.

45. Vogler, M., et al., *Regulation of TRAIL-induced apoptosis by XIAP in pancreatic carcinoma cells.* Oncogene, 2006. **26**(2): p. 248-257.

46. Vogler, M., et al., *Small Molecule XIAP Inhibitors Enhance TRAIL-Induced Apoptosis and Antitumor Activity in Preclinical Models of Pancreatic Carcinoma.* Cancer Research, 2009. **69**(6): p. 2425-2434.

47. Retzer-Lidl, M., R.M. Schmid, and G. Schneider, *Inhibition of CDK4 impairs proliferation of pancreatic cancer cells and sensitizes towards TRAIL-induced apoptosis via downregulation of survivin.* International Journal of Cancer, 2007. **121**(1): p. 66-75.

48. Zhang, X.D., et al., *Relation of TNF-related apoptosis-inducing ligand (TRAIL) receptor and FLICE-inhibitory protein expression to TRAIL-induced apoptosis of melanoma.* Cancer Res, 1999. **59**(11): p. 2747-53.

49. White, S.J., et al., *Targeting the Short Form of cFLIP by RNA Interference is Sufficient to Enhance TRAIL Sensitivity in PC3 Prostate Carcinoma Cells.* Cancer Biol Ther, 2006. **5**(12): p. 1618-23.

50. Fulda, S., E. Meyer, and K.M. Debatin, *Inhibition of TRAIL-induced apoptosis by Bcl-2 overexpression.* Oncogene, 2002. **21**(15): p. 2283-94.

51. Trauzold, A., et al., *Multiple and synergistic deregulations of apoptosis-controlling genes in pancreatic carcinoma cells.* Br J Cancer. **89**(9): p. 1714-1721.

52. Stadel, D., et al., *TRAIL-Induced Apoptosis Is Preferentially Mediated via TRAIL Receptor 1 in Pancreatic Carcinoma Cells and Profoundly Enhanced by XIAP Inhibitors.* Clinical Cancer Research. **16**(23): p. 5734-5749.

53. Kauh, J., et al., *c-FLIP Degradation Mediates Sensitization of Pancreatic Cancer Cells to TRAIL-Induced Apoptosis by the Histone Deacetylase Inhibitor LBH589.* PLoS ONE. **5**(4): p. e10376.

54. Huang, S. and F.A. Sinicrope, *Sorafenib Inhibits STAT3 Activation to Enhance TRAIL-Mediated Apoptosis in Human Pancreatic Cancer Cells.* Molecular Cancer Therapeutics. **9**(3): p. 742-750.

55. Thomas, R.P., et al., *Selective targeting of the nuclear factor-Œ∫B pathway enhances tumor necrosis factor, Ätrelated apoptosis-inducing ligand-mediated pancreatic cancer cell death.* Surgery, 2002. **132**(2): p. 127-134.

56. Jones, D.T., et al., *Cytotoxic drugs enhance the ex vivo sensitivity of malignant cells from a subset of acute myeloid leukaemia patients to apoptosis induction by tumour necrosis factor receptor-related apoptosis-inducing ligand.* British journal of haematology, 2003. **121**(5): p. 713-720.

57. Wu, X.X., et al., *Doxorubicin enhances TRAIL-induced apoptosis in prostate cancer.* International journal of oncology, 2002. **20**(5): p. 949-954.

58. Xu, L., et al., *Epirubicin enhances TRAIL-induced apoptosis in gastric cancer cells by promoting death receptor clustering in lipid rafts.* Molecular Medicine Reports, 2011. **4**(3): p. 407-411.

59. Yin, S., et al., *Cisplatin and TRAIL enhance breast cancer stem cell death.* International Journal of Oncology, 2011. **39**(4): p. 891-898.

60. Xu, L., et al., *Oxaliplatin enhances TRAIL-induced apoptosis in gastric cancer cells by CBL-regulated death receptor redistribution in lipid rafts.* FEBS letters, 2009. **583**(5): p. 943-948.

61. DeRosier, L.C., et al., *Combination treatment with TRA-8 anti death receptor 5 antibody and CPT-11 induces tumor regression in an orthotopic model of pancreatic cancer.* Clin Cancer Res, 2007. **13**(18 Pt 2): p. 5535s-5543s.

62. Yoo, J., S.-S. Park, and Y.J. Lee, *Pretreatment of docetaxel enhances TRAIL-mediated apoptosis in prostate cancer cells.* Journal of cellular biochemistry, 2008. **104**(5): p. 1636-1646.

63. Hunter, T.B., et al., *Paclitaxel and TRAIL Synergize to Kill Paclitaxel-resistant Small Cell Lung Cancer Cells through a Caspase-independent Mechanism Mediated through AIF.* Anticancer Research, 2011. **31**(10): p. 3193-3204.

64. Ray, S. and A. Almasan, *Apoptosis induction in prostate cancer cells and xenografts by combined treatment with Apo2 ligand/tumor necrosis factor-related apoptosis-inducing ligand and CPT-11.* Cancer research, 2003. **63**(15): p. 4713-4723.

65. Xu, Z.W., et al., *Synergistic cytotoxic effect of TRAIL and gemcitabine in pancreatic cancer cells.* Anticancer Research, 2003. **23**(1A): p. 251-258.

66. Jung, E.M., et al., *Curcumin sensitizes tumor necrosis factor-related apoptosis-inducing ligand (TRAIL)-induced apoptosis through reactive oxygen species-mediated upregulation of death receptor 5 (DR5).* Carcinogenesis, 2005. **26**(11): p. 1905-1913.

67. Jin, C.Y., et al., *Genistein sensitizes human hepatocellular carcinoma cells to TRAIL-mediated apoptosis by enhancing Bid cleavage.* Anti-Cancer Drugs, 2009. **20**(8): p. 713-722.

68. Liu, F.Y., et al., *Verticillin A Overcomes Apoptosis Resistance in Human Colon Carcinoma through DNA Methylation-Dependent Upregulation of BNIP3.* Cancer Research, 2011. **71**(21): p. 6807-6816.

69. Huang, L., et al., *Thapsigargin potentiates TRAIL-induced apoptosis in giant cell tumor of bone.* Bone, 2004. **34**(6): p. 971-981.

70. Badr, C.E., et al., *Lanatoside C sensitizes glioblastoma cells to tumor necrosis factor-related apoptosis-inducing ligand and induces an alternative cell death pathway.* Neuro-Oncology, 2011. **13**(11): p. 1213-1224.

71. *A Study of Dulanermin in Combination With Rituximab in Subjects With Follicular and Other Low Grade, CD20+, Non-Hodgkin's Lymphomas - Full Text View - ClinicalTrials.gov*. 2013/04/05/22:55:53; Available from: http://clinicaltrials.gov/ct2/show/NCT00400764?term=Dulanermin&rank=1.

72. Soria, J.C., et al., *Phase 1b Study of Dulanermin (recombinant human Apo2L/TRAIL) in Combination With Paclitaxel, Carboplatin, and Bevacizumab in Patients With Advanced Non-Squamous Non-Small-Cell Lung Cancer.* Journal of Clinical Oncology, 2010. **28**(9): p. 1527-1533.

73. *A Study of Dulanermin Administered in Combination With Camptosar®/Erbitux® Chemotherapy or FOLFIRI (With or Without Bevacizumab) in Subjects With Previously Treated Metastatic Colorectal Cancer - Full Text View - ClinicalTrials.gov*. 2013/04/05/22:56:19; Available from: http://clinicaltrials.gov/ct2/show/NCT00671372?term=Dulanermin&rank=2.

74. *A Study of Dulanermin Administered in Combination With the FOLFOX Regimen and Bevacizumab in Patients With Previously Untreated, Locally Advanced, Recurrent, or Metastatic Colorectal Cancer - Full Text View - ClinicalTrials.gov*. 2013/04/05/22:56:33; Available from: http://clinicaltrials.gov/ct2/show/NCT00873756?term=Dulanermin&rank=3.

75. Brenner, C. and S. Grimm, *The permeability transition pore complex in cancer cell death.* Oncogene, 2006. **25**(50): p. 6678.

76. Ohtsuka, T., et al., *Synergistic induction of tumor cell apoptosis by death receptor antibody and chemotherapy agent through JNK/p38 and mitochondrial death pathway.* Oncogene, 2003. **22**(13): p. 2034-44.

77. Mohapatra, S., et al., *Accumulation of p53 and reductions in XIAP abundance promote the apoptosis of prostate cancer cells.* Cancer Res, 2005. **65**(17): p. 7717-23.

78. Mackey, T.J., et al., *bcl-2/bax ratio as a predictive marker for therapeutic response to radiotherapy in patients with prostate cancer.* Urology, 1998. **52**(6): p. 1085-90.

79. An, J., et al., *Overcoming the radioresistance of prostate cancer cells with a novel Bcl-2 inhibitor*. Oncogene, 2007. **26**(5): p. 652-61.

80. Galluzzi, L., et al., *Mitochondria as therapeutic targets for cancer chemotherapy.* Oncogene, 2006. **25**(34): p. 4812-30.

81. Fantin, V.R. and P. Leder, *Mitochondriotoxic compounds for cancer therapy.* Oncogene, 2006. **25**(34): p. 4787-97.

82. Trapp, S. and R.W. Horobin, *A predictive model for the selective accumulation of chemicals in tumor cells.* Eur Biophys J, 2005. **34**(7): p. 959-66.

83. Costantini, P., et al., *Mitochondrion as a novel target of anticancer chemotherapy.* J Natl Cancer Inst, 2000. **92**(13): p. 1042-53.

84. Pastorino, J.G., et al., *The overexpression of Bax produces cell death upon induction of the mitochondrial permeability transition.* Journal of Biological Chemistry, 1998. **273**(13): p. 7770-7775.

85. Szeto, H.H., *Development of Mitochondria-targeted Aromatic-cationic Peptides for Neurodegenerative Diseases.* Mitochondria and Oxidative Stress in Neurodegenerative Disorders, 2008. **1147**: p. 112-121.

86. Jeon, N.L., et al., *Generation of solution and surface gradients using microfluidic systems.* Langmuir, 2000. **16**(22): p. 8311-8316.

87. Thompson, D.M., et al., *Dynamic gene expression profiling using a microfabricated living cell array.* Analytical Chemistry, 2004. **76**(14): p. 4098-4103.

88. Bird, R.B., W.E. Stewart, and E.N. Lightfoot, *Transport Phenomena*. 2nd ed. 2006, New York: John Wiley & Sons, Inc. 905.

89. Breslauer, D.N., P.J. Lee, and L.P. Lee, *Microfluidics-based systems biology.* Molecular Biosystems, 2006. **2**(2): p. 97-112.

90. Fiorucci, G., et al., *TNF-related apoptosis-inducing ligand (TRAIL) as a pro-apoptotic signal transducer with cancer therapeutic potential.* Curr Pharm Des, 2005. **11**(7): p. 933-44.

91. Yagita, H., et al., *TRAIL and its receptors as targets for cancer therapy.* Cancer Sci, 2004. **95**(10): p. 777-83.

92. Grotzer, M.A., et al., *Resistance to TRAIL-induced apoptosis in primitive neuroectodermal brain tumor cells correlates with a loss of caspase-8 expression.* Oncogene, 2000. **19**(40): p. 4604-10.

93. Hopkins-Donaldson, S., et al., *Loss of caspase-8 expression in neuroblastoma is related to malignancy and resistance to TRAIL-induced apoptosis.* Med Pediatr Oncol, 2000. **35**(6): p. 608-11.

94. Hopkins-Donaldson, S., et al., *Loss of caspase-8 expression in highly malignant human neuroblastoma cells correlates with resistance to tumor necrosis factor-related apoptosis-inducing ligand-induced apoptosis.* Cancer Res, 2000. **60**(16): p. 4315-9.

95. Chen, X., et al., *Constitutively active Akt is an important regulator of TRAIL sensitivity in prostate cancer.* Oncogene, 2001. **20**(42): p. 6073-83.

96. Kim, M.R., et al., *Ionizing radiation can overcome resistance to TRAIL in TRAIL-resistant cancer cells.* FEBS Lett, 2001. **505**(1): p. 179-84.

97. Shankar, S., T.R. Singh, and R.K. Srivastava, *Ionizing radiation enhances the therapeutic potential of TRAIL in prostate cancer in vitro and in vivo: Intracellular mechanisms.* Prostate, 2004. **61**(1): p. 35-49.

98. Zisman, A., et al., *Actinomycin D and gemcitabine synergistically sensitize androgen-independent prostate cancer cells to Apo2L/TRAIL-mediated apoptosis.* J Immunother, 2001. **24**(6): p. 459-71.

99. Barua, S., et al., *Lytic peptide-mediated sensitization of TRAIL-resistant prostate cancer cells to death receptor agonists.* Cancer Lett, 2010. **293**(2): p. 240-53.

100. Sun, S.Y., P. Yue, and R. Lotan, *Implication of multiple mechanisms in apoptosis induced by the synthetic retinoid CD437 in human prostate carcinoma cells.* Oncogene, 2000. **19**(39): p. 4513-22.

101. Zhang, X., et al., *Persistent c-FLIP(L) expression is necessary and sufficient to maintain resistance to tumor necrosis factor-related apoptosis-inducing ligand-mediated apoptosis in prostate cancer.* Cancer Res, 2004. **64**(19): p. 7086-91.

102. Chong, C.R., et al., *A clinical drug library screen identifies astemizole as an antimalarial agent.* Nat Chem Biol, 2006. **2**(8): p. 415-416.

103. Abramoff, M.D., P.J. Magalhães, and S.J. Ram, *Image processing with ImageJ.* Biophotonics International, 2004. **11**(7): p. 36-42.

104. Papadopulos, F., et al., *Common tasks in microscopic and ultrastructural image analysis using ImageJ.* Ultrastructural Pathology, 2007. **31**(4-6): p. 401-407.

105. Gliniak, B. and T. Le, *Tumor necrosis factor-related apoptosis-inducing ligand's antitumor activity in vivo is enhanced by the chemotherapeutic agent CPT-11.* Cancer research, 1999. **59**(24): p. 6153-6158.

106. Meinhold-Heerlein, I., et al., *TRAIL-induced apoptosis of ovarian cancer cell lines with selective drug resistance.* Geburtshilfe und Frauenheilkunde, 2005. **65**(11): p. 1064-1073.

107. Lee, T.J., et al., *Mithramycin A sensitizes cancer cells to TRAIL-mediated apoptosis by down-regulation of XIAP gene promoter through Sp1 sites.* Mol Cancer Ther, 2006. **5**(11): p. 2737-46.

108. El-Zawahry, A., J. McKillop, and C. Voelkel-Johnson, *Doxorubicin increases the effectiveness of Apo2L/TRAIL for tumor growth inhibition of prostate cancer xenografts.* BMC Cancer, 2005. **5**: p. 2.

109. Voelkel-Johnson, C., *An antibody against DR4 (TRAIL-R1) in combination with doxorubicin selectively kills malignant but not normal prostate cells.* Cancer Biol Ther, 2003. **2**(3): p. 283-90.

110. Bai, J., et al., *Predominant Bcl-XL Knockdown Disables Antiapoptotic Mechanisms: Tumor Necrosis Factor, ÄìRelated Apoptosis-Inducing Ligand, ÄìBased Triple Chemotherapy Overcomes Chemoresistance in Pancreatic Cancer Cells In vitro.* Cancer Research, 2005. **65**(6): p. 2344-2352.

111. Barua, S. and K. Rege, *Cancer-cell-phenotype-dependent differential intracellular trafficking of unconjugated quantum dots.* Small, 2009. **5**(3): p. 370-6.

112. Bodley, A., et al., *Dna Topoisomerase Ii-Mediated Interaction of Doxorubicin and Daunorubicin Congeners with Dna.* Cancer research, 1989. **49**(21): p. 5969-5978.

113. Kelly, M.M., B.D. Hoel, and C. Voelkel-Johnson, *Doxorubicin pretreatment sensitizes prostate cancer cell lines to TRAIL induced apoptosis which correlates with the loss of c-FLIP expression.* Cancer Biol Ther, 2002. **1**(5): p. 520-7.

114. Kim, K.H., et al., *Molecular determinants of response to TRAIL in killing of normal and cancer cells.* Clinical Cancer Research, 2000. **6**(2): p. 335-346.

115. Keane, M.M., et al., *Chemotherapy augments TRAIL-induced apoptosis in breast cell lines.* Cancer research, 1999. **59**(3): p. 734-741.

116. White, S.J., et al., *Doxorubicin generates a proapoptotic phenotype by phosphorylation of elongation factor 2.* Free Radical Biology and Medicine, 2007. **43**(9): p. 1313-1321.

117. Northrop, G., S.G. Taylor, and R.L. Northrop, *Biochemical Effects of Mithramycin on Cultured Cells.* Cancer research, 1969. **29**(11): p. 1916-&.

118. Miller, D.M., et al., *Mithramycin selectively inhibits transcription of G-C containing DNA.* Am J Med Sci, 1987. **294**(5): p. 388-94.

119. Fox, E.J., *Mechanism of action of mitoxantrone.* Neurology, 2004. **63**(12): p. S15-S18.

120. Valenti, M., et al., *Potentiation of Tnf-Mediated Cell-Killing by Mitoxantrone - Relationship to Dna Single-Strand Break Formation.* Biochemical pharmacology, 1993. **46**(7): p. 1199-1206.

121. Noviello, E., et al., *Tumour necrosis factor enhances the therapeutic effect of mitoxantrone in human ovarian cancer xenograft.* Cytokine, 1996. **8**(4): p. 330-333.

122. Warner, S.L., et al., *Validation of TPX2 as a Potential Therapeutic Target in Pancreatic Cancer Cells.* Clinical Cancer Research, 2009. **15**(21): p. 6519-6528.

123. Ouyang, H., et al., *Immortal human pancreatic duct epithelial cell lines with near normal genotype and phenotype.* Am J Pathol, 2000. **157**(5): p. 1623-31.

124. Naka, T., et al., *Effects of tumor necrosis factor-related apoptosis-inducing ligand alone and in combination with chemotherapeutic agents on patients' colon tumors grown in SCID mice.* Cancer Res, 2002. **62**: p. 5800-6.

125. Ohgami, T., et al., *Low-dose mithramycin exerts its anticancer effect via the p53 signaling pathway and synergizes with nutlin-3 in gynecologic cancers.* Cancer Sci, 2010. **101**(1387-95).

126. Booth, N.L., et al., *A cell-based high-throughput screen to identify synergistic TRAIL sensitizers.* Cancer Immunol Immunother, 2009. **58**: p. 1229-44.

127. Sugiura, S., et al., *Pressure-driven perfusion culture microchamber array for a parallel drug cytotoxicity assay.* Biotechnol Bioeng, 2008. **100**: p. 1156-65.

128. Wu, M.H., S.B. Huang, and G.B. Lee, *Microfluidic cell culture systems for drug research.* Lab Chip, 2010. **10**: p. 939-56.

129. Lee, P.J., et al., *Nanoliter scale microbioreactor array for quantitative cell biology.* Biotech Bioeng, 2006. **94**: p. 5-14.

130. King, K.R., et al., *A high-throughput microfluidic real-time gene expression living cell array.* Lab Chip, 2007. **7**(1): p. 77-85.

131. Wieder, K.J., et al., *Optimization of reporter cells for expression profiling in a microfluidic device.* Biomed Microdevices, 2005. **7**: p. 213-22.

132. Neils, C., et al., *Combinatorial mixing of microfluidic streams.* Lab Chip, 2004. **4**: p. 342-50.

133. Jang, Y.H., et al., *An integrated microfluidic device for two-dimensional combinatorial dilution.* Lab Chip, 2011. **11**: p. 3277-86.

134. Whitesides, G.M., et al., *Soft lithography in biology and biochemistry.* Annu Rev Biomed Eng, 2001. **3**: p. 335-73.

135. Kim, J., M. Hegde, and A. Jayaraman, *Co-culture of epithelial cells and bacteria for investigating host-pathogen interactions.* Lab Chip. **10**(1): p. 43-50.

136. Jeon, N.L., et al., *Neutrophil Chemotaxis in Linear and Complex Gradients of Interleukin-8 Formed in a Microfabricated Device.* Nature Biotechnology, 2002. **20**: p. 826-830.

137. Neils, C., et al., *Combinatorial Mixing of Microfluidic Streams.* Lab Chip, 2004. **4**: p. 342-350.

138. Taylor, D.J., et al., *Parallel screening of FDA-approved antineoplastic drugs for identifying sensitizers of TRAIL-induced apoptosis in cancer cells.* Bmc Cancer, 2011. **11**: p. 18.

139. Walkers, G.M., M.S. Ozers, and D.J. Beebe, *Insect cell culture in microfluidic channels.* Biomed Microdevices, 2002. **4**: p. 161-66.

140. Toepke, M.W. and D.J. Beebe, *PDMS absorption of small molecules and consequences in microfluidic applications.* Lab Chip, 2006. **6**(12): p. 1484-6.

141. Ostuni, E., et al., *Selective deposition of proteins and cells in arrays of microwells.* Langmuir, 2001. **17**: p. 2828-34.

142. O'Brien, M.A. and R. Kirby, *Apoptosis: A review of pro-apoptotic and anti-apoptotic pathways and dysregulation in disease.* Journal of Veterinary Emergency and Critical Care, 2008. **18**(6): p. 572-585.

143. Bhandary, B., et al., *Mitochondria in relation to cancer metastasis.* Journal of Bioenergetics and Biomembranes, 2012. **44**(6): p. 623-627.

144. Thorburn, A., *Death receptor-induced cell killing.* Cellular Signalling, 2004. **16**(2): p. 139-144.

145. Liu, P.Y., A.K. Death, and D.J. Handelsman, *Androgens and cardiovascular disease.* Endocrine Reviews, 2003. **24**(3): p. 313-340.

146. Reis-Filho, J.S. and A.N.J. Tutt, *Triple negative tumours: a critical review.* Histopathology, 2008. **52**(1): p. 108-118.

147. Parhi, P., C. Mohanty, and S.K. Sahoo, *Nanotechnology-based combinational drug delivery: an emerging approach for cancer therapy.* Drug Discovery Today, 2012. **17**(17-18): p. 1044-1052.

148. Fulbright, J.M., et al., *Can Anthracycline Therapy for Pediatric Malignancies Be Less Cardiotoxic?* Current Oncology Reports, 2010. **12**(6): p. 411-419.

149. Mukherji, D. and R. Pettengell, *Pixantrone for the treatment of aggressive non-Hodgkin lymphoma.* Expert Opinion on Pharmacotherapy, 2010. **11**(11): p. 1915-1923.

150. Hacker, M.P., et al., *Pixantrone is chemically and mechanistically related to mitoxantrone (Mito) and doxorubicin (Dox) but lacks their iron binding properties and myocyte toxicity in vitro.* Proceedings of the American Association for Cancer Research Annual Meeting, 2010. **51**: p. 867-868.

151. Borchmann, P., et al., *Evaluation of cardiac events in patients treated with pixantrone, a novel anthracycline derived drug.* Blood, 2003. **102**(11): p. 291B-292B.

152. Petrioli, R., et al., *The role of doxorubicin and epirubicin in the treatment of patients with metastatic hormone-refractory prostate cancer.* Cancer Treatment Reviews, 2008. **34**(8): p. 710-718.

153. Lemasters, J.J., et al., *The mitochondrial permeability transition in cell death: a common mechanism in necrosis, apoptosis and autophagy.* Biochimica Et Biophysica Acta-Bioenergetics, 1998. **1366**(1-2): p. 177-196.

154. Prasad, S., et al., *ROS and CHOP Are Critical for Dibenzylideneacetone to Sensitize Tumor Cells to TRAIL through Induction of Death Receptors and Downregulation of Cell Survival Proteins.* Cancer Research, 2011. **71**(2): p. 538-549.

155. Nitobe, J., et al., *Reactive oxygen species regulate FLICE inhibitory protein (FLIP) and susceptibility to Fas-mediated apoptosis in cardiac myocytes.* Cardiovascular Research, 2003. **57**(1): p. 119-128.

156. Cavaletti, G., et al., *Pixantrone (BBR2778) reduces the severity of experimental allergic encephalomyelitis.* Journal of Neuroimmunology, 2004. **151**(1-2): p. 55-65.

157. Jamal-Hanjani, M. and R. Pettengell, *Pharmacokinetic evaluation of pixantrone for the treatment of non-Hodgkin's lymphoma.* Expert Opinion on Drug Metabolism & Toxicology, 2011. **7**(11): p. 1441-1448.

158. Mimeault, M., et al., *Improvement of cytotoxic effects induced by mitoxantrone on hormone-refractory metastatic prostate cancer cells by co-targeting epidermal growth factor receptor and hedgehog signaling cascades.* Growth Factors, 2007. **25**(6): p. 400-416.

159. Chen, C.Y., et al., *Isoobtusilactone A Sensitizes Human Hepatoma Hep G2 Cells to TRAIL-Induced Apoptosis via ROS and CHOP-Mediated Up-regulation of DR5.* Journal of Agricultural and Food Chemistry, 2012. **60**(13): p. 3533-3539.

160. Tzung, S.P., et al., *Antimycin A mimics a cell-death-inducing Bcl-2 homology domain 3.* Nat Cell Biol, 2001. **3**(2): p. 183-91.

161. Cossarizza, A., et al., *A NEW METHOD FOR THE CYTOFLUOROMETRIC ANALYSIS OF MITOCHONDRIAL-MEMBRANE POTENTIAL USING THE J-AGGREGATE FORMING LIPOPHILIC CATION 5,5',6,6'-TETRACHLORO-1,1',3,3'-TETRAETHYLBENZIMIDAZOLCARBOCYANINE IODIDE (JC-1).* Biochemical and Biophysical Research Communications, 1993. **197**(1): p. 40-45.

162. Deisabella, P., et al., *TOPOISOMERASE-II DNA CLEAVAGE STIMULATION, DNA-BINDING ACTIVITY, CYTOTOXICITY, AND PHYSICOCHEMICAL PROPERTIES OF 2-AZA-ANTHRACENEDIONE AND 2-AZA-OXIDE-ANTHRACENEDIONE DERIVATIVES.* Molecular Pharmacology, 1995. **48**(1): p. 30-38.

163. Evison, B.J., et al., *Pixantrone can be activated by formaldehyde to generate a potent DNA adduct forming agent.* Nucleic Acids Research, 2007. **35**(11): p. 3581-3589.

164. *Search of: Pixantrone - List Results - ClinicalTrials.gov*. 2013/03/31/21:51:13; Available from: http://clinicaltrials.gov/ct2/results?term=Pixantrone&Search=Search.

165. *BBR 2778 for Relapsed, Aggressive Non-Hodgkin's Lymphoma (NHL) - Full Text View - ClinicalTrials.gov*. 2013/03/31/21:51:52; Available from: http://clinicaltrials.gov/ct2/show/study/NCT00088530?term=Pixantrone&rank=2.

166. Salvatorelli, E., et al., *The Novel Anthracenedione, Pixantrone, Lacks Redox Activity and Inhibits Doxorubicinol Formation in Human Myocardium: Insight to Explain the Cardiac Safety of Pixantrone in Doxorubicin-Treated Patients.* Journal of Pharmacology and Experimental Therapeutics, 2013. **344**(2): p. 467-478.

167. Proudfoot, N.J., A. Furger, and M.J. Dye, *Integrating rnRNA processing with transcription.* Cell, 2002. **108**(4): p. 501-512.

168. Ayala, A., et al., *Effect of oxidative stress, produced by cumene hydroperoxide, on the various steps of protein synthesis - Modifications of elongation factor-2.* Journal of Biological Chemistry, 1996. **271**(38): p. 23105-23110.

169. Poukkula, M., et al., *Rapid turnover of c-FLIP short is determined by its unique C-terminal tail.* Journal of Biological Chemistry, 2005. **280**(29): p. 27345-27355.

170. Dohi, T., et al., *An IAP-IAP complex inhibits apoptosis.* Journal of Biological Chemistry, 2004. **279**(33): p. 34087-34090.

171. Zhao, J., et al., *The ubiquitin-proteasome pathway regulates survivin degradation in a cell cycle-dependent manner.* Journal of Cell Science, 2000. **113**(23): p. 4363-4371.

172. Moon, D.O., et al., *Verrucarin A sensitizes TRAIL-induced apoptosis via the upregulation of DR5 in an eIF2 alpha/CHOP-dependent manner.* Toxicology in Vitro, 2013. **27**(1): p. 257-263.

173. Yamaguchi, H. and H.G. Wang, *CHOP is involved in endoplasmic reticulum stress-induced apoptosis by enhancing DR5 expression in human carcinoma cells.* Journal of Biological Chemistry, 2004. **279**(44): p. 45495-45502.

174. Rutkowski, D.T., et al., *Adaptation to ER stress is mediated by differential stabilities of pro-survival and pro-apoptotic mRNAs and proteins.* Plos Biology, 2006. **4**(11): p. 2024-2041.

175. Society, A.C., *Cancer Facts & Figures 2011*, 2011, American Cancer Society: Atlanta.

176. Lockhart, A.C., M.L. Rothenberg, and J.D. Berlin, *Treatment for pancreatic cancer: current therapy and continued progress.* Gastroenterology, 2005. **128**(6): p. 1642-54.

177. Hezel, A.F., et al., *Genetics and biology of pancreatic ductal adenocarcinoma.* Genes Dev, 2006. **20**(10): p. 1218-49.

178. Farrow, B., D. Albo, and D.H. Berger, *The role of the tumor microenvironment in the progression of pancreatic cancer.* J Surg Res, 2008. **149**(2): p. 319-28.

179. Hartel, M., et al., *Desmoplastic reaction influences pancreatic cancer growth behavior.* World J Surg, 2004. **28**(8): p. 818-25.

180. Mahadevan, D. and D.D. Von Hoff, *Tumor-stroma interactions in pancreatic ductal adenocarcinoma.* Molecular Cancer Therapeutics, 2007. **6**(4): p. 1186-1197.

181. Masamune, A. and T. Shimosegawa, *Signal transduction in pancreatic stellate cells.* Journal of Gastroenterology, 2009. **44**(4): p. 249-260.

182. Wagner, M., et al., *Curative resection is the single most important factor determining outcome in patients with pancreatic adenocarcinoma.* Br J Surg, 2004. **91**(5): p. 586-94.

183. Yeo, C.J., et al., *Pancreaticoduodenectomy for cancer of the head of the pancreas. 201 patients.* Ann Surg, 1995. **221**(6): p. 721-31; discussion 731-3.

184. Joergensen, M.T., N. Brunner, and O.B.S. De Muckadell, *Comparison of Circulating MMP-9, TIMP-1 and CA19-9 in the Detection of Pancreatic Cancer.* Anticancer Research, 2010. **30**(2): p. 587-592.

185. Shields, M.A., et al., *Pancreatic cancer cells respond to type I collagen by inducing Snail expression to promote membrane type 1-matrix metalloproteinase dependent collagen invasion.* Journal of Biological Chemistry.

186. Lee, J.K., et al., *NADPH oxidase promotes pancreatic cancer cell survival via inhibiting JAK2 dephosphorylation by tyrosine phosphatases.* Gastroenterology, 2007. **133**(5): p. 1637-1648.

187. Ozawa, F., et al., *Effects and expression of TRAIL and its apoptosis-promoting receptors in human pancreatic cancer.* Cancer Lett, 2001. **163**(1): p. 71-81.

188. Sanlioglu, A.D., et al., *High TRAIL death receptor 4 and decoy receptor 2 expression correlates with significant cell death in pancreatic ductal adenocarcinoma patients.* Pancreas, 2009. **38**(2): p. 154-60.

189. Matsuzaki, H., et al., *Combination of Tumor Necrosis Factor-related Apoptosis-inducing Ligand (TRAIL) and Actinomycin D Induces Apoptosis Even in TRAIL-resistant Human Pancreatic Cancer Cells.* Clinical Cancer Research, 2001. **7**(2): p. 407-414.

190. Khanbolooki, S., et al., *Nuclear factor-kappaB maintains TRAIL resistance in human pancreatic cancer cells.* Mol Cancer Ther, 2006. **5**(9): p. 2251-60.

191. Sahu, R.P., et al., *The role of K-ras gene mutation in TRAIL-induced apoptosis in pancreatic and lung cancer cell lines.* Cancer Chemother Pharmacol, 2011. **67**(2): p. 481-7.

192. Hylander, B.L., et al., *The anti-tumor effect of Apo2L/TRAIL on patient pancreatic adenocarcinomas grown as xenografts in SCID mice.* J Transl Med, 2005. **3**(1): p. 22.

193. Rajeshkumar, N.V., et al., *A combination of DR5 agonistic monoclonal antibody with gemcitabine targets pancreatic cancer stem cells and results in long-term disease control in human pancreatic cancer model.* Mol Cancer Ther, 2010. **9**(9): p. 2582-92.

194. Dangi-Garimella, S., et al., *Collagen regulation of let-7 in pancreatic cancer involves TGF-[beta]1-mediated membrane type 1-matrix metalloproteinase expression.* Oncogene.

195. Provenzano, P.P., et al., *Engineering Three-Dimensional Collagen Matrices to Provide Contact Guidance during 3D Cell Migration*. Current Protocols in Cell Biology. 2001: John Wiley & Sons, Inc.

196. Apte, M.V., et al., *Pancreatic stellate cells are activated by proinflammatory cytokines: implications for pancreatic fibrogenesis.* Gut, 1999. **44**(4): p. 534-541.

197. Schneiderhan, W., et al., *Pancreatic stellate cells are an important source of MMP-2 in human pancreatic cancer and accelerate tumor progression in a murine xenograft model and CAM assay.* Journal of Cell Science, 2007. **120**(3): p. 512-519.

198. Brenner, C. and S. Grimm, *The permeability transition pore complex in cancer cell death.* Oncogene, 2006. **25**(34): p. 4744-4756.

199. Adams, J.M. and S. Cory, *The Bcl-2 apoptotic switch in cancer development and therapy.* Oncogene, 2007. **26**(9): p. 1324-1337.

200. An, J., et al., *Overcoming the radioresistance of prostate cancer cells with a novel Bcl-2 inhibitor.* Oncogene, 2006.

201. Gugliucci, A., et al., *Mitochondria are direct targets of the lipoxygenase inhibitor MK886. A strategy for cell killing by combined treatment with MK886 and cyclooxygenase inhibitors.* J Biol Chem, 2002. **277**(35): p. 31789-95.

202. Szeto, H.H., *Cell-permeable, mitochondrial-targeted, peptide antioxidants.* Aaps J, 2006. **8**(2): p. E277-83.

203. Sen, N., et al., *Camptothecin-induced imbalance in intracellular cation homeostasis regulates programmed cell death in unicellular hemoflagellate Leishmania donovani.* Journal of Biological Chemistry, 2004. **279**(50): p. 52366-52375.

204. Yeung, B.H.Y., D.C. Huang, and F.A. Sinicrope, *PS-341 (bortezomib) induces lysosomal cathepsin B release and a caspase-2-dependent mitochondrial*

permeabilization and apoptosis in human pancreatic cancer cells. Journal of Biological Chemistry, 2006. **281**(17): p. 11923-11932.

205. Rojewski, M.T., et al., *Depolarization of mitochondria and activation of caspases are common features of arsenic(III)-induced apoptosis in myelogenic and lymphatic cell lines.* Chemical Research in Toxicology, 2004. **17**(1): p. 119-128.

206. Rackham, O., et al., *A gold(I) phosphine complex selectively induces apoptosis in breast cancer cells: Implications for anticancer therapeutics targeted to mitochondria.* Biochemical Pharmacology, 2007. **74**(7): p. 992-1002.

207. Musacchio, T., et al., *PEG-PE Micelles Loaded with Paclitaxel and Surface-Modified by a PBR-Ligand: Synergistic Anticancer Effect.* Molecular Pharmaceutics, 2009. **6**(2): p. 468-479.

208. Gao, Y., et al., *Targeted Nanoassembly Loaded with Docetaxel Improves Intracellular Drug Delivery and Efficacy in Murine Breast Cancer Model.* Molecular Pharmaceutics, 2008. **5**(6): p. 1044-1054.

209. Torchilin, V.P., *Targeted polymeric micelles for delivery of poorly soluble drugs.* Cellular and Molecular Life Sciences, 2004. **61**(19-20): p. 2549-2559.

210. Torchilin, V.P., et al., *Immunomicelles: Targeted pharmaceutical carriers for poorly soluble drugs.* Proceedings of the National Academy of Sciences of the United States of America, 2003. **100**(10): p. 6039-6044.

211. Yoo, H.S. and T.G. Park, *Folate receptor targeted biodegradable polymeric doxorubicin micelles.* Journal of Controlled Release, 2004. **96**(2): p. 273-283.

212. White-Gilbertson, S.J., et al., *Oxidative Stress Sensitizes Bladder Cancer Cells to TRAIL Mediated Apoptosis by Down-Regulating Anti-Apoptotic Proteins.* Journal of Urology, 2009. **182**(3): p. 1178-1185.

213. Kamat, A.M., et al., *Curcumin Potentiates the Antitumor Effects of Bacillus Calmette-Guerin against Bladder Cancer through the Downregulation of NF-kB and Upregulation of TRAIL Receptors.* Cancer Research, 2009. **69**(23): p. 8958-8966.

214. Johnson, T.R., et al., *The proteasome inhibitor PS-341 overcomes TRAIL resistance in Bax and caspase 9-negative or Bcl-xL overexpressing cells.* Oncogene, 2003. **22**(32): p. 4953-4963.

215. Coghlan, A., *Cheap, safe drug kills most cancers.* New Scientist, 2007. **193**(2587): p. 13-13.

216. Bonnet, S., et al., *A mitochondria-K+ channel axis is suppressed in cancer and its normalization promotes apoptosis and inhibits cancer growth.* Cancer Cell, 2007. **11**(1): p. 37-51.

217. Administration, F.a.D. *Press Announcements > FDA approves Zytiga for late-stage prostate cancer*. 2013/04/09/18:56:15; Available from: http://www.fda.gov/NewsEvents/Newsroom/PressAnnouncements/ucm253055.htm.

218. Administration, F.a.D. *About the Center for Drug Evaluation and Research > Cabazitaxel*. 2013/04/09/20:02:50; Available from: http://www.fda.gov/AboutFDA/CentersOffices/OfficeofMedicalProductsandTobacco/CDER/ucm216214.htm.

219. de Bono, J.S., et al., *Prednisone plus cabazitaxel or mitoxantrone for metastatic castration-resistant prostate cancer progressing after docetaxel treatment: a randomised open-label trial.* Lancet, 2010. **376**(9747): p. 1147-1154.

APPENDIX A

IDENTIFICATION OF MITOCHONDRIA DAMAGING AGENTS USING A PARALLEL SCREEN OF ANTINEOPLASTIC DRUGS

INTRODUCTION

Mitochondria represent key components in the intrinsic apoptotic pathway. An important step in this process involves the mitochondrial permeability transition which represents a "point of no return" in the execution of cellular apoptosis [198]. This loss of mitochondrial integrity results in the release of pro-apoptotic proteins (e.g. cytochrome-c, SMAC/DIABLO, and apoptosis inducing factor) from the mitochondria into the cytoplasm, leading to the activation of execution caspases and ultimately apoptosis [198]. Traditional chemotherapeutics typically induce genomic DNA damage in order to trigger apoptosis signaling in cancer cells; while DNA-damaging chemotherapeutics have been relatively successful either by themselves or in combination therapies [41, 76], many studies indicate that the over expression of anti-apoptotic proteins is responsible for overcoming the pro-apoptotic signal triggered by these chemotherapeutics and is partly responsible for less effective treatments and increased cellular resistances [44, 77, 199]. For instance, the anti-apoptotic protein, Bcl-2 prevents the mitochondrial pore opening resulting in the resistance of cancer cells to chemo/radiation therapy [78, 200]. Consequently, therapeutic strategies that directly damage the mitochondrial and induce cellular apoptosis are attractive since they can bypass resistance mechanisms that act upstream of the mitochondria to prevent mitochondrial pore opening and apoptosis (e.g. p53 mutation / knockdown, over-expression of bcl-2, etc.) [75, 83, 201, 202].

The large negative potential gradient (approximately -160 mV) across the mitochondrial membrane [82] drives the mitochondrial accumulation of positively charged amphipathic molecules. Additionally, cancer cells possess a higher potential difference (-200 to 220

mV) across mitochondrial membranes compared to non-malignant cells, which accounts for some inherent selectivity of this therapeutic approach. In time, the localization of these molecules results depolarization of the mitochondrial membrane. This in turn leads to the membrane permeability transition and ultimately the release of pro-apoptotic proteins from the mitochondria resulting in apoptosis [83]. By monitoring changes in the mitochondrial membrane potential (MMP), we can assess the effect of different treatment options at depolarizing the mitochondrial membrane. In addition to changes in the membrane potential and the related increase in pro-apoptotic proteins, mitochondrial health can also be evaluated by monitoring several other factors including reactive oxygen species (ROS), pH, and concentrations of ATP, calcium, and potassium [203, 204].

This appendix describes the parallel screening of fifty-five FDA-approved chemotherapeutic drugs used to identify agents that demonstrate the ability to cause direct damage to the mitochondria of prostate, pancreatic, and breast cancer cells. Mitochondrial health was assessed my monitoring changes in the mitochondrial membrane potential using the fluorescent dye, JC-1. Drugs were first screened at a concentration of 20 μM using PC3-TR prostate cancer cells. Drug candidates that demonstrated mitochondrial depolarizing activity were rescreened at a concentration of 50 μM. A total of five potential mitochondria depolarization agents were identified from the screen. Of these leads, only mitoxantrone showed consistent depolarization activity. To maximize the therapeutic potential of mitoxantrone to depolarize/damage

mitochondria, we have incorporated the drug into micellular-based, drug delivery systems.

METHODS

Cell Culture Techniques

Two human prostate cancer cell lines (PC3, and PC3-TR), two human pancreatic cancer lines (MIAPaCa2, and BXPC-3), and one human breast cancer line (MDA-MB-231) were used in the current study. PC3-TR (TR: TRAIL resistant) [101] cells were a generous gift from Dr. Aria Olumi at the Massachusetts General Hospital in Boston, MA. Cells were grown in 75 cm^2 Corning cell culture flasks with RPMI 1640 tissue culture media supplemented with 10% Fetal Bovine Serum and 1% penicillin / streptomycin (10000 units/mL penicillin G and 10000 μg/mL streptomycin) at 37°C with 5% CO_2.

Reagent/Drug Preparation

The Johns Hopkins Chemical Compound Library (JHCCL) [102] was purchased from The Johns Hopkins University School of Medicine. The library contains a total of 1514 FDA- and foreign-approved drugs. The anti-neoplastic plate (plate #1) consists of 55 FDA-approved approved anti-cancer drugs and was employed in the screen for identifying mitochondria depolarizing agents. Stock solutions of the drugs included in the library were supplied as 10 mM aliquots solubilized in either DMSO or water. For expanded dose-response experiments, additional mitoxantrone were purchased from Sigma. All solutions were prepared to ensure that the final solvent (DMSO or water) concentration in cell treatments would be less than 1% (v/v) to limit non-specific activity.

Mitochondrial Depolarization Experiments

Cells were plated in black, clear-bottom 96 well plates at a density of 8,400 cells/well and incubated at 37°C with 5% CO_2 for approximately 24 hours. Cells were then incubated with 6.39 µM of JC-1 dye (Sigma) for 1-1.5 hours after which the cell culture media was removed and refreshed. Drug solutions were then added to the dye-treated cells; a set of control wells were treated with 1% (v/v) of the solvent alone to serve as a live control although, there was no difference between the cells treated with 1% solvent (water and DMSO) and cells with no treatment. After the final treatment, fluorescent measurements were immediately taken using the Biotech Synergy 2 Multi-Detection Microplate Reader for green fluorescence (Ex. 485/40, Em. 528/20) and red fluorescence (Ex. 485/40, Em. 590/35). Following the fluorescence measurement, cells were incubated at 37°C with 5% CO_2 and were periodically removed to take readings at various time points.

Analysis of the JC-1 fluorescent data was carried out in order to determine changes in the MMP of the treated cells compared to the live control cells. First the ratio of red fluorescent intensity/green fluorescent intensity was calculated for each well. The average R/G ratio for the live control cells was calculated and the remaining R/G ratios were normalized against this value. This is done in order to account for the decrease in the R/G ratio caused by the dye. A second normalization was then performed for each treatment against itself at the 0 hour reading (i.e. all R/G ratios measured in a given well were divided by the R/G ratio in that well at the 0 hour time point). This normalization is done so comparisons between data can be easily made since at the 0 hour time point, all wells will give a normalized value of 100%.

Statistical Analyses

All experiments were performed in at least triplicate. Data are presented as the mean ± one standard deviation. Standard deviation of a data set was calculated based on experimental variation. ANOVA was performed using the t-test function in Microsoft Excel.

RESULTS AND DISCUSSION

In this study, a library fifty-five FDA- and foreign-approved antineoplastic drugs from the Johns Hopkins Clinical Compound Library (JHCCL) was screened in order to identify drugs that caused direct mitochondrial damage to prostate and pancreatic cancer cell lines. PC3-TR (TR: TRAIL resistant) human prostate cancer cells were used in the primary screening, since little work studying mitochondrial depolarization had been done in the cell line and because the cells are representative of cancer that posses inherent resistance to apoptosis.

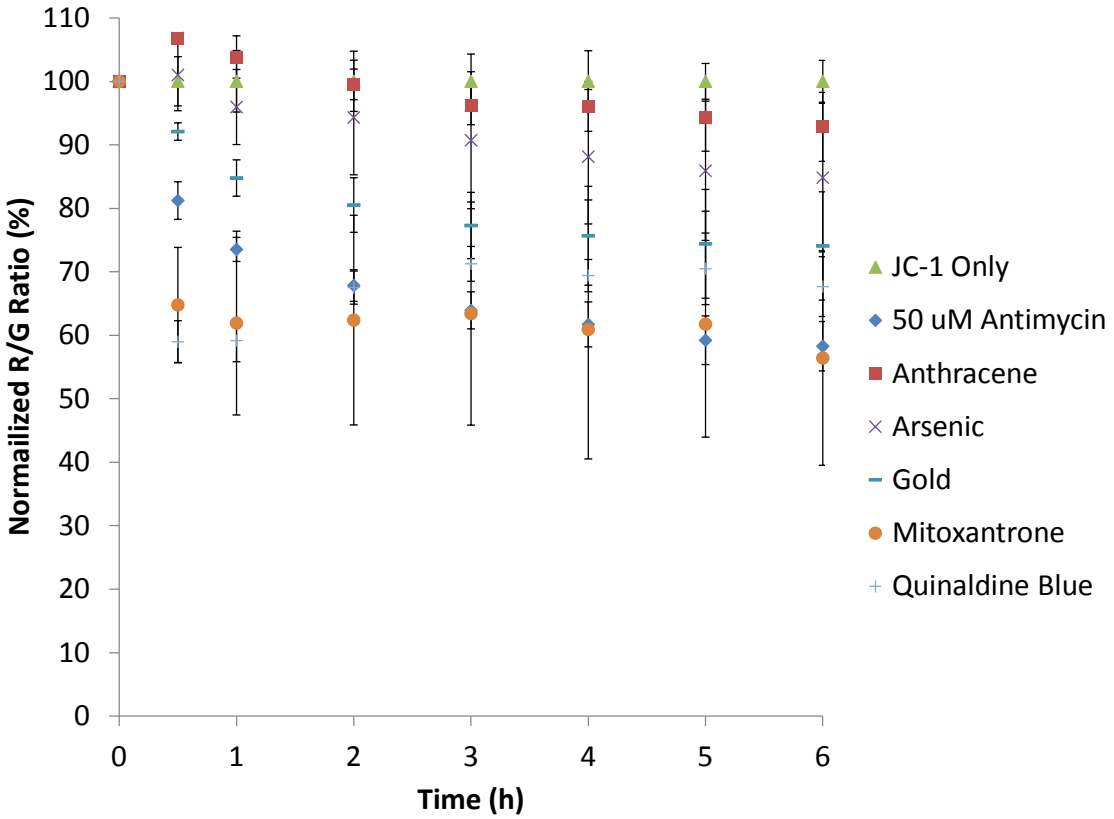


Figure A.1 50 µM screening of the John Hopkins Clinical Compound Library for mitochondrial depolarization activity. 53 antineoplastic drugs were screened at a 20 µM concentration and those that showed a depolarizing effect were retested at 50 µM.

Screening and Identification of Mitochondria Depolarization Agents from a Library of FDA-Approved, Antineoplastic Drugs. The library of fifty-five, FDA-approved, antineoplastic drugs was initially screened using a drug concentration of 20 μM (data not shown). The drug concentration was kept low in order to limit the cytotoxicity of the drugs since the goal of the screen is to identify drugs that induce mitochondrial damage and that do not outright kill the cells due to their primary effects (e.g. nucleoside). This initial 20 μM screen identified five drugs that appeared to induce mitochondrial depolarization: Anthracene, arsenic trioxide, gold sodium thiosulfate, mitoxantrone, and quinaldine blue. In general, the loss of MMP caused by these drugs was low to moderate so, in order to confirm their depolarizing activities, the drugs were tested at a concentration of 50 μM as shown in **Figure A.1**. These data shows that arsenic, gold, mitoxantrone, and quinaldine blue all cause a reduction in the R/G ratio and that anthracene initially shows a small increase in the R/G ratio but at later time points showed a very small loss of membrane potential.

Of these drug candidates, mitoxantrone was of particular interest due to the fact that our previous studies had identified the drug as a potent TRAIL sensitizer and we had also elucidated the mechanisms by which TRAIL-sensitization occurred. Of the other drugs identified, both arsenic and gold have been shown to have a depolarization effect [205, 206]. Anthracene has not been previously shown to have depolarizing activity, but its limited efficacy at both 20 μM and 50 μM restrict its use in additional experiments. To the best of our knowledge, quinaldine blue has not been previously identified as a mitochondria depolarizing agent and so it and mitoxantrone were selected for additional

characterization via expanded dose range experiments. However, it was during these additional experiments that the behavior of quinaldine blue was found to be quite erratic; in some experiments the drug had a depolarizing effect while in others treatments caused an increase in membrane potential. It is for this reason that work with quinaldine blue was suspended and our focus on became identifying methodologies that could be used to selectively deliver mitoxantrone to malignant cells and provide an opportunity for the drug to induce mitochondrial depolarization.

Depolarization Study of Mitoxantrone-Loaded Micelles. Due to the elevated, negative membrane potential of cancer cells, it is expected that cationic mitochondria damaging agents should have some selectivity toward malignant cells. However, since mitoxantrone is a genotoxic compound, it is important to protect healthy cells from non-specific activity. To this end our studies shifted from drug discovery to drug delivery and identifying a suitable delivery system for mitoxantrone. Such a system should be able to maintain the efficacy of the mitoxantrone treatment while providing a backbone from which targeting bodies can be attached for the treatment of malignant cells.

Polyethylene glycol- phosphoethanolamine (PEG-PE) based micelles have previously been used to encapsulate a wide variety of drugs including antineoplastic compounds like paclitaxel [207] and docetaxel [208]. In general, PEG-PE micelles are used for encapsulating drugs with low solubility in water [209] but what is more relevant to the current study is that the micelles have been shown to increase the efficacy of encapsulated drugs when conjugated with targeting molecules that help to selectively

delivery the drugs to the area of affliction [210, 211]. These previous results suggested that PEG-PE micelles could be used to encapsulate mitoxantrone and that these mitoxantrone-loaded micelles could then be delivered to cancer cells. The studies detailing these studies are the subject of an article titled "Sensitizing cancer cells to TRAIL-induced death by micellar delivery of mitoxantrone." The article is currently undergoing revisions for submission into *Nanomedicine-UK*. These studies have shown that PEG-PE micelles with different end functionalities, can be loaded with mitoxantrone and separated from empty micelles using size exclusion chromatography. Characterization of these mitoxantrone-loaded micelles includes size and zeta potential measurements using dynamic light scattering, confirmation of mitoxantrone encapsulation using NMR and confocal microscopy, and loading and stability measurements calculated using the standard adsorption curve generated for known concentrations of the drug. These studies represent a significant amount of effort but most of this work was done by my colleague and will be detailed in the published document. However, the focus of that article is on the mitoxantrone-encapsulated micelle's ability to retain their TRAIL-sensitizing activity. These studies focus on the study of the mitochondrial depolarizing activity of the drug-loaded micelles.

The depolarization efficacy of mitoxantrone-loaded micelles was evaluated and compared to the performance of mitoxantrone alone, of empty micelles, and of a free mixture of the drug and empty micelles in PC3-TR cells (**Figure A.2**). In these experiments measurements were only taken at the initial 0 hour time point and after 6 hours since our kinetic studies suggested that the depolarization effects of mitoxantrone

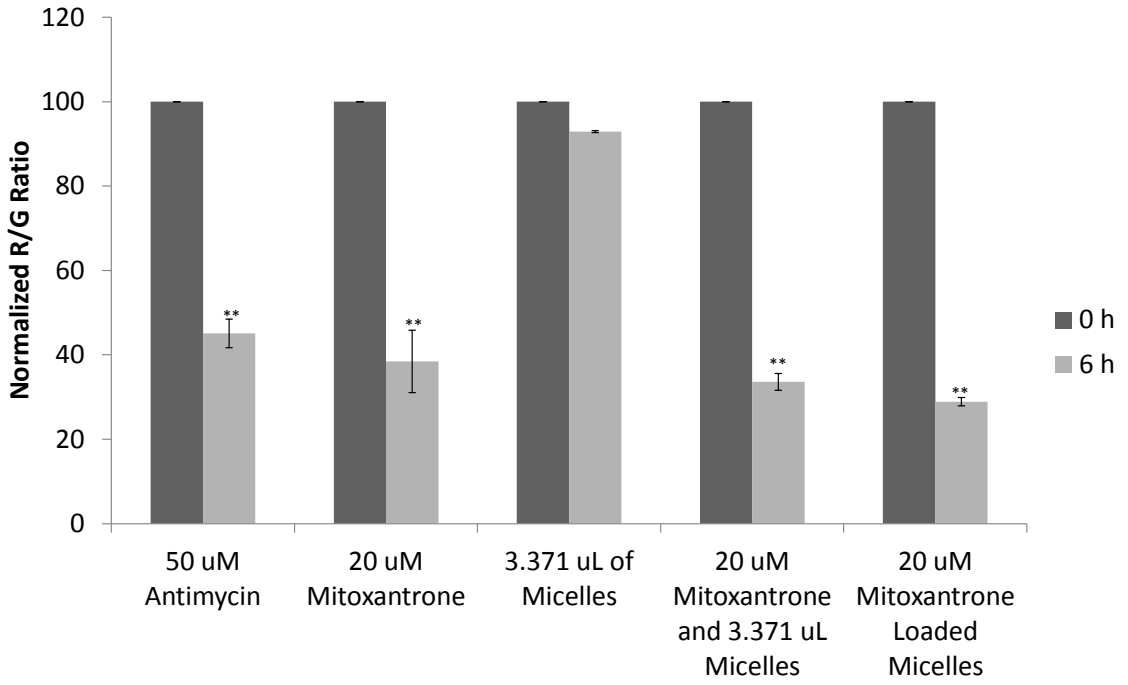


Figure A.2 Mitochondrial depolarization studies of mitoxantrone-loaded PEG-PE micelles in PC3-TR prostate cancer. Cells were treated with 20 μM of free mitoxantrone, 20 μM of mitoxantrone encapsulated in micelles, and an equivalent volume of the empty micelles both as a single agent and in a mixture with 20 μM of the drug. Asterisks (**) indicate p-values of < 0.01 when comparing the 0 hour and 6 hour data.

equilibrated after 6 hours and there is only a small reduction in the cell viability. These results showed that mitoxantrone, mitoxantrone-loaded micelles, and the free mitoxantrone/empty micelle mixture all caused a significant decrease in the normalized R/G fluorescent ratio when compared to the 0 hour reading. Additionally, all three treatments appear to have the same effect and after 6 hours the treatments show an approximate 60-70% decrease in the R/G ratio suggesting an overall loss of MMP. The empty micelle control showed an approximate 8% decrease in the R/G ratio. Although the 8% difference is not statistically significant here, it is likely that the empty micelles are having a depolarizing effect on the cells since at higher concentrations, the empty micelles do cause a significant reduction in the R/G ratio (not shown). Additionally, this

depolarizing effect of empty micelles explains why the free mitoxantrone/empty micelle mixture and the mitoxantrone loaded micelles show a slightly higher loss in the R/G ratio as compared to the mitoxantrone alone treatments. Taken together, these results suggest that the mitochondrial depolarizing activity of mitoxantrone is maintained after it is encapsulated into PEG-PE micelles and that there is application of the micelles as a delivery vehicle for the drug. Our lab has been able to form carboxy, amine, and methoxy-terminated, mitoxantrone-loaded micelles all of which provide their own advantages for the linking of various targeting, imaging, or sensitization agents. The micelles provide the backbone for a drug delivery system that can carry mitoxantrone and potentially transport the drug to an afflicted area while limiting the drug's exposure to healthy tissue.

CONCLUSIONS

In the current study, fifty-five FDA-approved antineoplastic drugs were screened in order to identify chemotherapeutic compounds that initiated loss of mitochondrial membrane potential. At the concentrations tested, the screen identified mitoxantrone as a depolarization agent and confirmation studies showed that the drug consistently decreased the membrane potential over a wide variety of concentrations and in different prostate, pancreatic, and breast cancer cell lines. The concentrations of reactive oxygen species were also measured in order to verify the mitochondria damaging activity of the drug and to better understand the kinetics of the drug's reaction upon treatment. Finally, our studies have shown that mitoxantrone can be encapsulated in PEG-PE micelles without loss of activity and that these micelles provide potential vehicle for targeted drug delivery.

APPENDIX B

ADDITIONAL COMBINATION TREATMENT EXPERIMENTS IN ALTERNATE CELL LINES AND USING ALTERNATE DRUGS

INTRODUCTION

In addition to the combination screening experiments conducted using the John's Hopkins Clinical Compound Library (JHCCL), additional combination treatment experiments were conducted using drugs that were approved by the FDA after the JHCCL had already been assembled and other drugs that show promise as chemotherapeutic agents but that have not been approved for use by the FDA. In addition combination treatments were also carried out in a murine bladder cancer cell line. The results of these different combinatorial studies are complied and discussed in this appendix.

Cell Culture Techniques

Three human prostate cancer cell lines (PC3, PC3-TR, and 22Rv1) and one murine bladder cancer line (MB49) were used in this study. PC3-TR (TR: TRAIL resistant) [101] cells were a generous gift from Dr. Aria Olumi at the Massachusetts General Hospital in Boston, MA. Cells were grown in 75 cm^2 Corning cell culture flasks with RPMI 1640 tissue culture media supplemented with 10% Fetal Bovine Serum and 1% penicillin / streptomycin (10000 units/mL penicillin G and 10000 μg/mL streptomycin) at 37°C with 5% CO_2.

Reagent/Drug Preparation

All reagents and drugs used in this study were reconstituted in either deionized water, ethanol, or DMSO depending on solubility. TRAIL was purchased from R&D Systems and reconstituted in PBS at a 10 μg/mL stock concentration in 50 μL aliquots to prevent multiple freeze/thaw cycles. Solutions were prepared to ensure that the final solvent concentration in cell treatments would be less than 1% (v/v) to limit non-specific activity.

Single Agent and Combination Treatments

Cells were plated in 96 well plates at a density of 10,000 cells/well and incubated at 37°C and 5% CO_2 for approximately 24 hours. For single-agent treatments, cells were exposed to 0-100 μM (mitoxantrone, mithramycin, cabazitaxel, and abiraterone) or 0-10 mM (dichloroacetic acid) treatments for 2 and/or 24 hours at which point the media was refreshed, and cell viability was determined using the MTT (3-(4,5-dimethylthiazolyl-2) -2,5-diphenyltetrazolium bromide) assay. For sequential combination treatments, cells were first treated with a sensitizer drug

candidate for 2 and/or 24 hours. The media was then removed, replaced with fresh serum-containing media, and the cells were treated with 10 ng/mL TRAIL. Cells were incubated for an additional 24 h after which, viability measurements were carried out using the MTT assay.

Determination of Cell Viability

Cell viability was assessed using the MTT cell proliferation assay (ATCC CA#30-1010k). Following addition of the MTT reagent (3 h at 37^{o}C), cells were treated with a lysis buffer from the kit and kept at room temperature in the dark for at least two hours in order to carry out complete lysis and to solubilize the MTT product. The absorbance of each well was measured using a Biotech Synergy 2 Multi-Detection Microplate Reader at 570 nm. Each experiment included a set of blank wells (media only), a live control (no treatment) and a dead control (0.5 μL of MTT lysis buffer). Fractional cell viability was calculated as: (OD of sample – OD of dead control)/(OD of live control – OD of dead control) where OD is the optical density. Percentage cell viability was calculated by multiplying the fractional viability by 100. Data are plotted as percentage reduction in cell viability compared to control (untreated cells) in which, a 0% value on the graph means 100% viability and 100% value on the graph means 0% viability.

Statistical Analyses

Screening experiments were carried out in duplicate and expanded dose responses with identified leads were performed at least in triplicate. Data are presented as the mean ± one standard deviation. The standard deviation of each set was calculated based on the variation between experiments. ANOVA was performed using the t-test function in Microsoft Excel. Analysis of

the single-agent treatment was performed in order to determine whether or not a drug had a significant effect when compared to the live (untreated) control. Efficacies of sensitization were determined by comparing the decrease in cell viability following combination treatments (i.e. drug in combination with TRAIL) to the reduction in cell viability as a consequence of the additive effect of single-agent treatments (drug alone + 10 ng/mL TRAIL alone).

RESULTS AND DISCUSSION

Combination Treatment Studies in MB49 Bladder Cancer Cells. The research described up to this point, has focused on using combination therapy techniques on treating prostate, breast, and pancreatic cancer cells. However, bladder cancer represents the fourth most common cancer in men and it is estimated that over 55,000 new cases were diagnosed in 2012 [1]. Fortunately, in many instances of bladder cancer, tumors are superficial and non-invasive. Typically these tumors are removed via transurethral resection and the afflicted is area is treated using intravesical therapy [212]. Such treatments are enticing for our purposes because it allows for the direct delivery of the drug to the afflicted area without needing to develop systems for targeted delivery. Based on our successful studies with sensitizer drug/TRAIL combination treatments in other malignant lines, we became interested in determining if these combination therapies would also be effective in bladder cancer cells.

Does response studies for TRAIL-combination therapies were evaluated in MB-49 murine bladder cancer cells using mitoxantrone and mithramycin. Both of these drugs were found to be effective in sensitizing several malignant cell lines to TRAIL-mediated apoptosis (**Figures 2.7, 2.8, 2.12, 2.13**). Mitoxantrone/TRAIL combination studies at 2 and 24 hours are shown in **Figure B1**. These results indicate that there is a significant loss of viable cells when comparing single-agent mitoxantrone to combination treatments of mitoxantrone and TRAIL for both treatment times tested, although there are treatment concentrations for both conditions that do not exhibit a statistically significant difference (primarily due to large variation between replicates). In the case of the 2 hour treatments

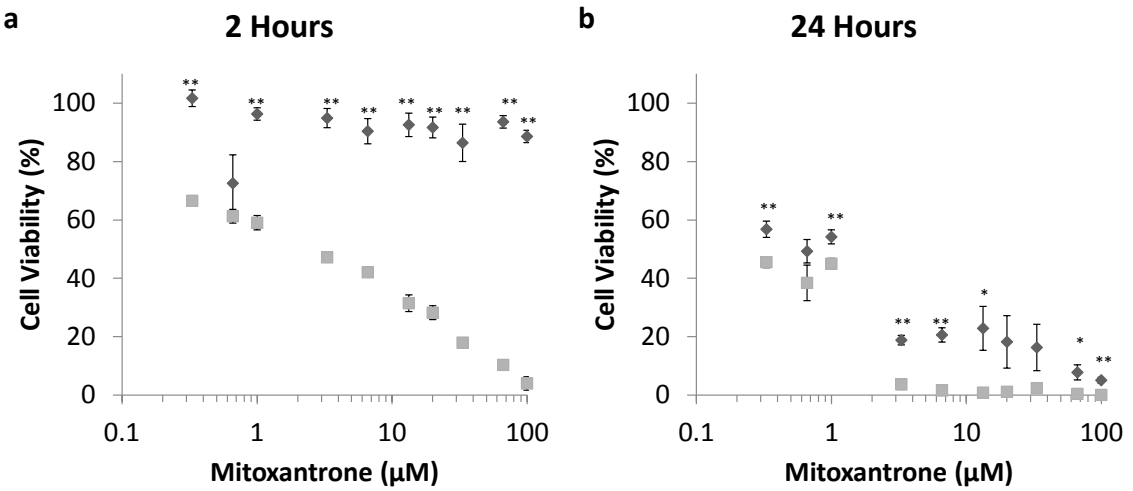


Figure B.1 Kinetic dose response for mitoxantrone in MB49 murine bladder cancer cells. Cells were treated with mitoxantrone for (a) 2 hours, and (b) 24 hours. For single-agent treatments (dark grey diamonds) the cell viability was assessed following the mitoxantrone treatments. For combination treatments (light grey squares), 10 ng/mL of TRAIL was applied for 24 hours following the initial mitoxantrone treatments. Comparisons were made between the single agent and combination treatments; asterisks (*) and (**) indicate p-values < 0.05 and <0.01, respectively. Data are presented on a logarithmic scale for x-axes in the plots.

(**Figure B1a**), single agent mitoxantrone has little to no effect on cell viability with the LC_{50} value being difficult to determine since the highest concentration treatment (100 μM) only shows a 12% reduction in viability. However, mitoxantrone/TRAIL combination treatments all show large increases in cell death as compared to the single agent treatments (with the exception of the 0.66 μM treatment); single agent TRAIL only produced a 2.6% loss in cell viability so it appears that the mitoxantrone/TRAIL treatments act synergistically. The LC_{50} value for the combination treatments drops to about 3.3 μM and the viability linearly to about 4% following the 100 μM treatments. The greatest difference in cell viability between the single agent and combination treatments is 84% at the 100 μM treatment condition. The 24 hour treatment results (**Figure B.1b**) indicate that the single agent mitoxantrone treatments is effective at reducing cell viability over this time period with the LC_{50} value found to be between 0.66 and 1 μM for these

treatments. For the 24 hour combination treatments the LC_{50} value was found to be approximately 0.2 μM. While the 24 hour treatments do indicate that there is synergy between the mitoxantrone and TRAIL treatments, the overall effect is much less than the activity seen in the 2 hour treatments as is evident by the relatively small change in the LC_{50} value. This is also confirmed by the fact that the largest significant decrease in cell viability between the single agent and combination treatments is 22% (6.6 μM) as compared to the 88% decrease seen after the 2 hour treatments. These results are important because they further demonstrate the importance of the kinetic response of mitoxantrone/TRAIL combination treatments. The results also indicate that mitoxantrone and TRAIL is effective at reducing the viability of bladder cancer in-vitro.

Mithramycin/TRAIL combination studies at 24 hours are shown in **Figure B2**. These results indicate that there is no significant loss of viable cells when comparing single-agent mithramycin treatments to combination treatments with 10 ng/mL TRAIL. These results are somewhat surprising considering that mithramycin showed synergy in all the cell lines tested previously and exhibited some of the highest synergistic activity in those experiments. However, additionally experiments need to be conducted to understand if the kinetics of treatment can improve the activity of the drugs; the combination treatments with mitoxantrone in this line showed higher efficacy when the sensitizing drug was applied for less time. It is possible that similar circumstances may exist for mithramycin. The fact that the combination treatments seems to be ineffective also provides an interesting opportunity to better understand the mechanism behind mithramycin's TRAIL sensitization activity. By identifying characteristics that differ between the MB49 cells and the other cells tested it may be possible to determine

what effect mithramycin has in other cells that it does not have in MB49 cells. It should be noted that although recombinant human TRAIL is used in all the combination studies, the drug has been previously shown to be effective in murine cell lines [213, 214] although the effect of the drug is not well characterized in the MB49 line specifically.

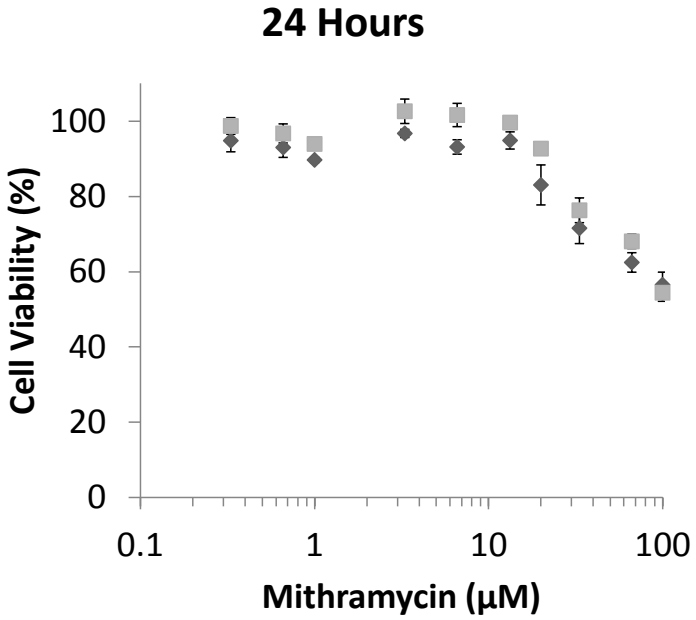


Figure B.2 Kinetic dose response for mithramycin in MB49 murine bladder cancer cells. Cells were treated with mithramycin for 24 hours. For single-agent treatments (dark grey diamonds) the cell viability was assessed following the mithramycin treatments. For combination treatments (light grey squares), 10 ng/mL of TRAIL was applied for 24 hours following the initial mithramycin treatments. Comparisons were made between the single agent and combination treatments; asterisks (*) and (**) indicate p-values < 0.05 and <0.01, respectively. Data are presented on a logarithmic scale for x-axes in the plots.

Evaluation of the TRAIL-Sensitization Activity of Additional Therapeutic Compounds. In addition to the drugs screened in the JHCCL, results were collected for compounds that were not included in the library. Two of these drugs were only recently approved by the FDA as cancer therapeutics. The other compound is not approved by the FDA, but it has been shown to be a

promising chemotherapeutic agent in laboratory experiments and has also attracted significant media attention as a "cheap" and "safe" chemotheraputic option [215]. This compound, called dichloroacetic acid (DCA) was initially found to be effective at selectively killing cancer cells and was shown to reduce tumor growth in animal models [216]. It has been shown to inhibit pyruvate dehydrogenase kinase (PDK) which in turn disrupts glycolysis. Since cancer cells express increased glycolysis, the loss of PDK forces the cells to shift to energy production using oxidative phosphorylation. Since the mitochondria is the "point of no return" for apoptosis, restoring function to the organelle allows it to identify the cells as damaged, and induce apoptosis. Since healthy cells would not be identified as dangerous or damaged the treatments would be cancer cell selective [216]. Since the compound was found to selectively target malignant cells and because its mechanism of action involves the induction of apoptosis we were interested in testing the drug in combination with TRAIL to see if DCA had any sensitization properties (**Figure B.3**). Treatments were carried out in PC3-TR prostate cancer cells using 0 to 10 mM DCA concentrations (24 hour treatments). The results indicated that the single-agent DCA and combination treatments with 10 ng/mL TRAIL did not show any significant difference in their activities. Overall the effect of the treatments seemed somewhat limited with most treatments falling around a 20-30% reduction in cell viability. This suggests that higher

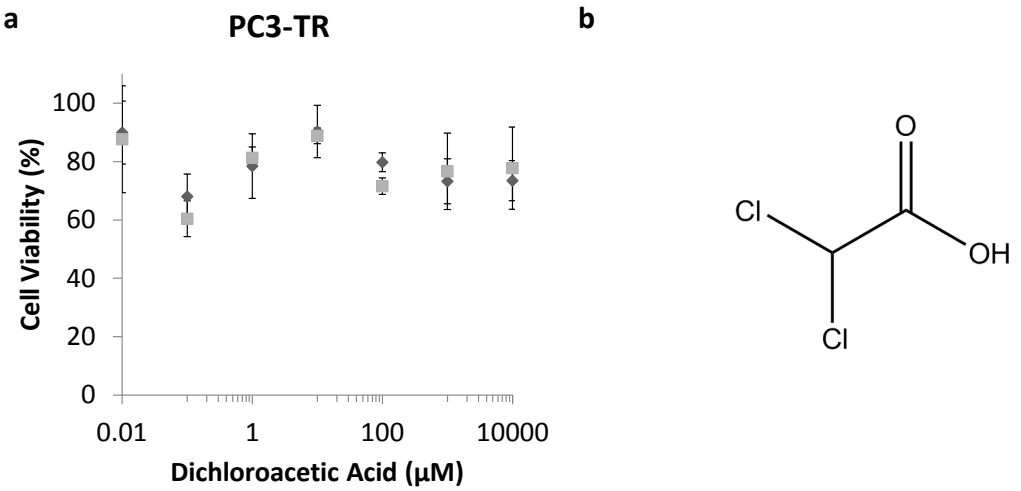


Figure B.3 (a) Dose response for dichloroacetic acid (DCA) in PC3-TR human prostate cancer cells. Malignant cells were treated with DCA for 24 hours. For single-agent treatments (dark grey diamonds) the cell viability was assessed following the initial treatments. For combination treatments (light grey squares), 10 ng/mL of TRAIL was applied for 24 hours following the initial DCA treatments. Comparisons were made between the single agent and combination treatments; asterisks (*) and (**) indicate p-values < 0.05 and <0.01, respectively. Data are presented on a logarithmic scale for x-axes in plots. (b) Chemical structures of DCA.

concentrations of the drug need to be tested to determine which concentrations of the drug can cause higher reductions in cell viability. However, at the concentrations tested there are no indications that DCA is sensitizing the PC3-TR cells to TRAIL-mediated apoptosis.

Additionally, two drugs recently approved by the FDA as chemotherapeutics were also tested for their TRAIL-sensitization activity. Abiraterone was approved for use by the FDA in April 2011 for the treatment of last stage prostate cancer [217]. The drug works by suppressing the production of testosterone through the inhibition of 17 α-hydroxylase/C17,20 lyase (CYP17A1). The second drug, Cabazitaxel, was approved for use by the FDA in June 2010 for the treatment of metastatic hormone-refractory prostate

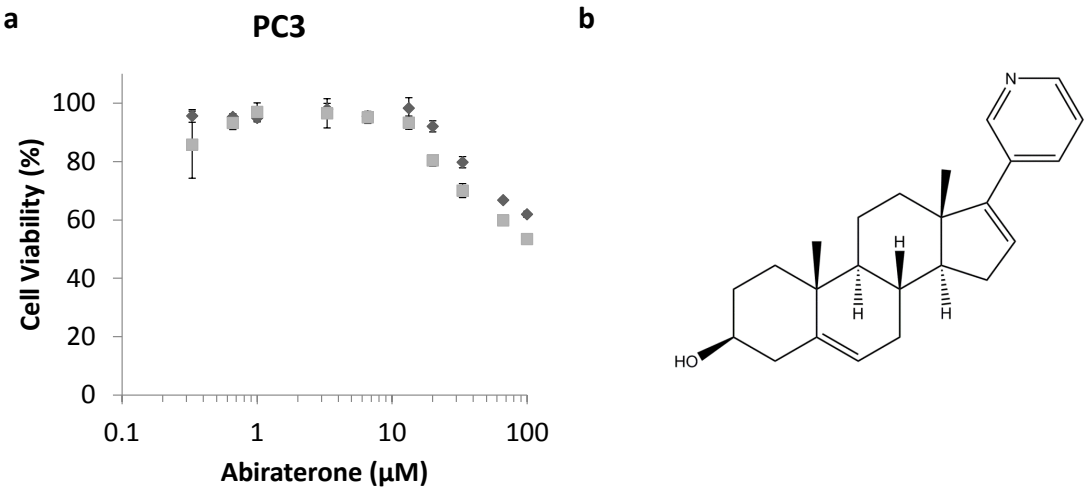


Figure B.4 (a) Dose response for abiraterone in PC3 human prostate cancer cells. Malignant cells were treated with abiraterone for 24 hours. For single-agent treatments (dark grey diamonds) the cell viability was assessed following the initial treatment. For combination treatments (light grey squares), 10 ng/mL of TRAIL was applied for 24 hours following the initial treatments. Comparisons were made between the single agent and combination treatments; asterisks (*) and (**) indicate p-values < 0.05 and <0.01, respectively. Data are presented on a logarithmic scale for x-axes in plots. (b) Chemical structures of abiraterone.

cancer in combination with prednisone [218]. The drug binds to tubulin and prevents the formation of microtubules which in turn limits cell mitosis [219]. Dose response studies for abiraterone/TRAIL combination studies in PC3 prostate cancer cells are shown in **Figure B.4**. The results of these studies show that the combination treatments reduce cell viability slightly more than the single agent abiraterone, but when taking the effect of single agent TRAIL (approximately 12%) this difference is not significant. These results suggest that abiraterone is not effective as a TRAIL-sensitizing agent. Additional experiments evaluating the effects of changing the treatment times or concentrations of abiraterone can be studied, but at this time there is little indication that would suggest these experiments would show TRAIL-sensitization activity either.

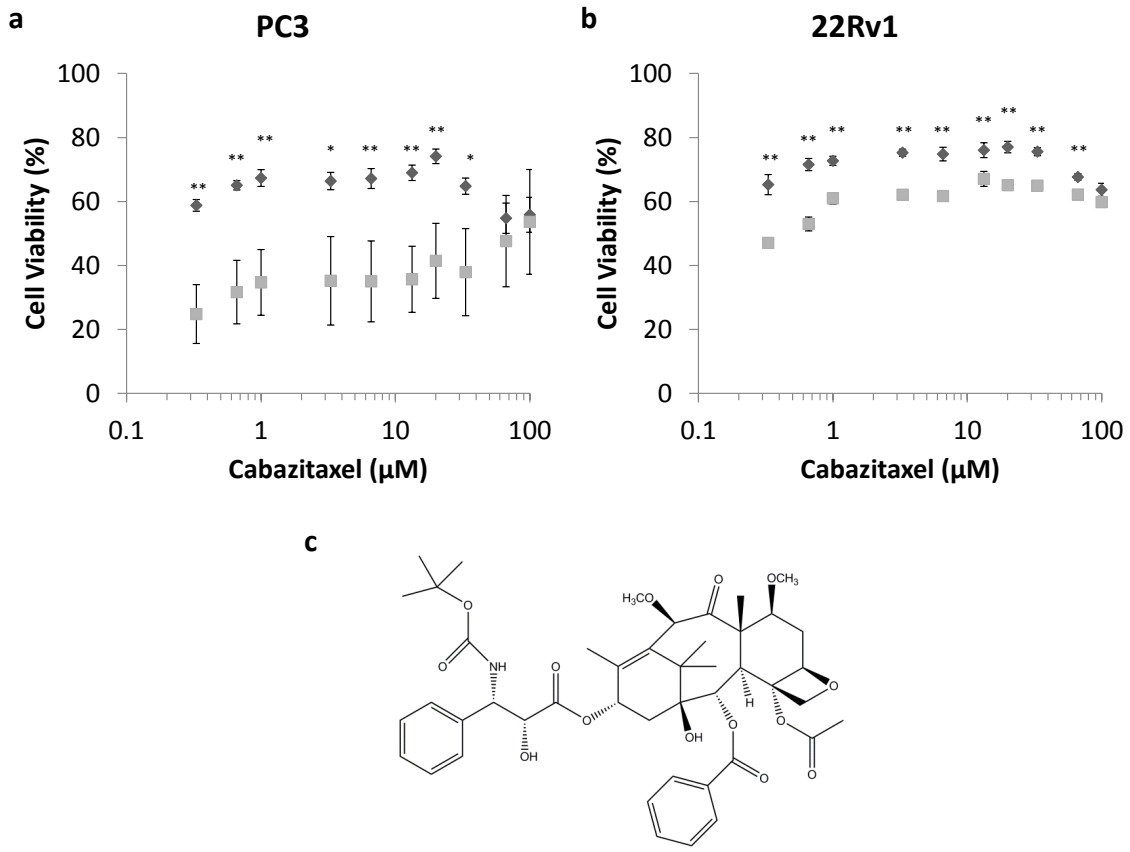


Figure B.5 Dose response for cabazitaxel in (a) PC3 and (b) 22Rv1 human prostate cancer cells. Malignant cells were treated with cabazitaxel for 24 hours. For single-agent treatments (dark grey diamonds) the cell viability was assessed following the initial treatments. For combination treatments (light grey squares), 10 ng/mL of TRAIL was applied for 24 hours following the initial cabazitaxel treatments. Comparisons were made between the single agent and combination treatments; asterisks (*) and (**) indicate p-values < 0.05 and <0.01, respectively. Data are presented on a logarithmic scale for x-axes in plots. (c) Chemical structures of cabazitaxel.

Dose response studies for cabazitaxel/TRAIL combination studies in PC3 and 22Rv1 prostate cancer cells are shown in **Figure B.5**. These results indicate that there is a significant loss of viable cells when comparing single-agent cabazitaxel to combination treatments of cabazitaxel and TRAIL for in both PC3 (**Figure B.5a**) and 22Rv1 cells(**Figure B.5b**). For PC3 cells, the cell viability of single agent cabazitaxel treatments actually appears to increase with increasing cabazitaxel concentration in a trend that holds over 2 independent experiments. Cell viability

then begins to decrease at concentrations above 20μM. While these results have been shown to be reproducible, the actual viabilities measured between these readings mainly stay between 60-70% (i.e. the amount the cell viability increases is relatively small) and it would be necessary to test lower and higher concentrations of the drug to determine if the trends seen in these initial experiments hold true. More importantly, the experiments show that the cell viability of combination treatments are significantly reduced, compared to the single agent treatments; this suggests cabazitaxel has some TRAIL-sensitization activity. The largest difference between the cell viabilities of the single agent and combination treatments is 35% (0.33 μM). However, it is difficult to do a LC_{50} analysis for these studies because the combination treatment experiments also indicate that viability increases with increasing cabazitaxel concentrations. In fact there is a 25% increase in cell viability between the 0.33 μM and the 100 μM treatments. These results, while unexpected, still indicate that there is synergy between the cabazitaxel and TRAIL for 0.33-33.3 μM treatments. Treatments in the 22Rv1 cells (**Figure B.5b**) showed similar behavior to the results seen in the PC3 line. In this cell line, both the single agent and combination treatments showed increases in cell viability with increasing concentrations up to about 33.3 μM. However, this cell line also showed a significant difference in cell viability when comparing single agent and combination treatments for all concentrations tested with the exception of 100 μM. The largest difference between these treatment methods was 18% which is significant considering the single agent TRAIL treatments showed almost no loss of viability. Taken together, these results suggest that cabazitaxel is able to moderately sensitize prostate cancer cells to TRAIL. To our knowledge these are the first studies done to show this and while there are aspects of these treatments that need to be evaluated more fully (e.g. the increase in cell viability with increasing concentration), these initial results are promising.

CONCLUSIONS

In the current study mitoxantrone and mithramycin combination treatment experiments were carried out in the MB49 murine bladder cancer cell and the effect of an additional three compounds were evaluated in various prostate cancer cell lines. These studies indicated that mitoxantrone/TRAIL combination treatments did synergistically enhance cell death in MB49 cells, but that the effect appears to be heavily influenced by the treatment kinetics. These studies also indicated that mithramycin/TRAIL combination treatments were not effect in MB49 cells. Dichloroacetic acid, abiraterone, and cabazitaxel were tested in combination with TRAIL to determine if any of these compounds could sensitize prostate cancer cells to TRAIL. The results of these studies indicated that both dichloroacetic acid and abiraterone were ineffectual as TRAIL-sensitizing agents. However, cabazitaxel/TRAIL combination treatments were shown have synergy in both PC3 and 22Rv1 prostate cancer cells. Overall these studies have demonstrated the therapeutic potential of mitoxantrone and TRAIL in bladder cancer, and have also identified cabazitaxel as a new candidate for additional optimization/mechanistic studies.

BIOGRAPHICAL SKETCH

Education:

Ph.D., Chemical Engineering, Arizona State University, Tempe, AZ: 2013
GPA: 3.89/4.0

B.S., Chemical Engineering, New Mexico Institute of Mining and Technology, Socorro, NM: 2008
Minor: Chemistry
GPA: 3.74/4.0

Publications:

(*)Corresponding Author

2013 **Taylor, D.,** Jayaraman, A. Rege, K.(*) "Mechanistic Investigation of the TRAIL-Sensitization Activity of Mitoxantrone." To be submitted 06 / 2013.

2013 Grandi, T.S.P., Potta, T., **Taylor, D.J.,** Tian, Y. (*), Johnson, R.H., Meldrum, D.R., Rege, K(*). "Sensitizing cancer cells to TRAIL-induced death by micellar delivery of mitoxantrone." ***Nanomedicine-UK, 2013,*** **in revision**.

2012 Ramos J., **Taylor, D.**, Rege, K.(*) "Gold Nanoparticle Mediated Photo-Chemotherapy." ***J. Nanomedicine and Nanotechnology*** **2012, 3:e125.**

2012 Labiano, A., Dai, M., **Taylor, D.**, Young, W., Epps III, T.H., Rege, K., Vogt, B.D(*). "Slow release kinetics of mitoxantrone from ordered mesoporous carbon films." ***Microporous and Mesoporous Materials*** **2012, 160, 143-150**

2012 Kim, J., **Taylor, D.,** Agrawal, N., Wang, H., Kim, H., Han, A., Rege, K.(*), Jayaraman, A.(*) "A programmable microfluidic cell array for combinatorial drug screening." ***Lab on a Chip*** **2012, 12:10, 1813-22. (Selected for Highlights of the journal)**

2011 **Taylor, D.J.,** Parsons, C.E., Han H., Jayaraman, A., Rege, K.(*) "Parallel screening of FDA-approved antineoplastic drugs for identifying sensitizers of TRAIL-induced apoptosis in cancer cells." ***BMC Cancer*** **2011, 11:470. (Highly Accessed)**

2011 Barua, S., Ramos J., Potta, T., **Taylor, D.,** Huang H., Montanez, G., Rege, K.(*) "Discovery of cationic polymers for non-viral gene delivery using combinatorial approaches." ***Combinatorial Chemistry & High Throughput Screening*** **2011, 14:10, 908-24.**

Conference Presentations:

2012 **Taylor, David J**. "Mechanistic Investigation of the TRAIL-Sensitization Activity of Mitoxantrone." American Institute of Chemical Engineers, Pittsburgh, Pennsylvania.

2012 **Taylor, David J**. "Lead Identification, Optimization, and Characterization of Novel Cancer Treatment Strategies Using Repositioned Drugs." American Institute of Chemical Engineers, Pittsburgh, Pennsylvania (Poster).

2011 **Taylor, David J**. "Identification of Mitochondria Damaging Agents Using Parallel Screening." American Institute of Chemical Engineers, Minneapolis, Minnesota.

2010 **Taylor, David J**. "Microfluidic Cancer Cell Array based Parallel Screening of Combination Chemotherapeutic Drug Treatments for Prostate Cancer." American Institute of Chemical Engineers, Salt Lake City, Utah.

Awards:

2011-2013	Arizona ARCS Foundation Fellowship
2011	Six Sigma Green Belt
2008-2009	Arizona State Dean's Fellowship
2008, 2005, 2004	Pell Grant
2005-2008	New Mexico Lottery Scholarship
2004-2008	New Mexico Tech Presidential Scholarship